Processes of alluvial sedimentation in the Eocene Hyalite Peak volcanics, Absaroka-Gallatin volcanic province, Southwest Montana
by Margaret M Hiza

A thesis submitted in partial fulfillment of the requirements for the degree of Master of Science in Earth Sciences
Montana State University
© Copyright by Margaret M Hiza (1994)

Abstract:
Eocene Hyalite Peak volcanics in the Gallatin Range, southwest Montana, consist of 1,800 m of sedimentary sequences and intercalated andesitic lava flows.

Lithofacies in the deposits, categorized based on texture, grain size, and fabric indicate that the processes of transport, grain support, and deposition of the sequences varied greatly. Sedimentary fabrics exhibit textures which record a broad continuum of flow transitions between streamflow, hyperconcentrated flow and debris flow processes produced by variation in the ratio of sediment to water. Variability in the amount of , clast-support and types of grading in Hyalite Peak sequences were produced primarily by coarse-grained debris flow, variable stages of non-cohesive transitional flow, and hyperconcentrated flow. Key features in volumetrically minor deposits contain depositional fabrics which indicate they were produced and transported directly by eruptive activity. Deposits produced from pyroclastic flows and surges contain a large component of pumice and glass shards produced as juvenile pyroclastic material. Other near-vent deposits contain volcanic bombs and agglutinate. Together, sedimentary sequences within the Hyalite Peak volcanics exhibit fabrics and textures commonly described as volcaniclastic deposits found in modem volcanic settings.

Utilizing recent improvements in knowledge of sedimentation in modern volcanic systems, well exposed sequences of Eocene Hyalite Peak volcaniclastic strata are described in detail, and the processes which induced their formation are for the first I time characterized. Features within these deposits suggest that volcanic activity was I phreatic or phreatomagmatic, induced by groundwater-magma interaction. The variation I of lithofacies types in Hyalite Peak sequences indicate that deposition was produced through a broad range of transitions between processes of eruption and sedimentation which took place on the flanks of stratovolcanoes and near small localized vent sources.
j

PROCESSES OF ALLUVIAL SEDIMENTATION IN THE EOCENE HYALITE PEAK VOLCANICS, ABSAROKA-GALLATIN VOLCANIC PROVINCE, SOUTHWEST MONTANA

by

Margaret M. Hiza

A thesis submitted in partial fulfillment
of the requirements for the degree

of

Master of Science

in

Earth Sciences

MONTANA STATE UNIVERSITY
Bozeman Montana

November 1994

N 378
H6425

APPROVAL

of a thesis submitted by

Margaret M. Hiza

This thesis has been read by each member of the thesis committee and has been found to be sastisfactory regarding content, English usage, format, citations, bibliographic style, and consistency, and is ready for submission to the College of Graduate Studies.

1-11-95
Date

James Schmitt
Chairperson, Graduate Committee

Approved for the Department of Earth Sciences

1-11-95
Date

Head, Department of Earth Sciences

Approved for the College of Graduate Studies

2/1/95
Date

Graduate Dean

STATEMENT OF PERMISSION TO USE

In presenting this thesis in partial fulfillment of the requirements for a master's degree at Montana State University, I agree that the Library shall make it available to borrowers under rules of the Library.

If I have indicated my intention to copyright this thesis by including a copyright notice page, copying is allowable only for scholarly purposes, consistent with "fair use" as prescribed in the U.S. Copyright Law. Requests for permission for extended quotation from or reproduction of this thesis in whole or in parts may be granted by the copyright holder.

Signature James Schmitt

Date 1-11-95

ACKNOWLEDGEMENTS

I would like to extend my warmest thanks to the members of my committee, Jim Schmitt, Dave Lageson and Steve Custer for their help in editing this thesis, and for their continual support and encouragement. Research was partially funded by the Donald L. Smith memorial scholarship, the Geological Society of America, and the American Association of Petroleum Geologists, to whom I am grateful. Additional research funding was provided through a National Science Foundation Fellowship without which the completion of this thesis would have been impossible. I would also like to thank my children, Aidan, Robert, and Shondiin Redsteer, for their understanding and moral support.

TABLE OF CONTENTS

	Page
ABSTRACT	xi
INTRODUCTION	1
Geologic Setting	2
METHODS	6
TERMINOLOGY	11
Pyroclastic Processes	11
Epiclastic Processes	15
SEDIMENTOLOGY	19
General Character of the deposits	19
Coarse-Grained Lithofacies	19
Summary of Coarse-grained Lithofacies	43
Sandy Lithofacies	45
Fine-Grained Lithofacies	48
LITHOFACIES ASSOCIATIONS	51
Lithofacies Association 1: Streamflow Facies	53
Lithofacies Association 2: Matrix-Supported Debris Flow	54
Lithofacies Association 3: Clast-Supported Debris-Flow	55
Lithofacies Association 4: Debris Avalanche and Volcanic Breccia	57
Lithofacies Association 5: Pyroclastic Flow, Fall, and Surge	58
LITHOFACIES SEQUENCES AND DESCRIPTION OF STRATIGRAPHIC SECTIONS	60
Lithofacies Sequences at Antelope Butte	60
Lithofacies Sequences at Eight Mile Canyon	65
Lithofacies Sequences at Palisade Mountain	70
Lithofacies Sequences at Silken Skein Falls	76
Lithofacies Sequences at Flanders Mountain	79
Lithofacies Sequences at Windy Pass	84

TABLE OF CONTENTS- Continued

Page

CHARACTERISTICS OF THE DEPOSITIONAL SETTING 86

Characteristics of Eruptive Activity 86
Characterization of Alluvial Sequences 93

REFERENCES CITED 96

APPENDICES 105

Appendix A - Table 4.
Distribution of Coarse-Grained Lithofacies 106

Appendix B - Measured Sections 111
Antelope Butte Measured Section I 111a
Antelope Butte Measured Section II 126
Eight Mile Canyon Measured Section I 131
Eight Mile Canyon Measured Section II 142
Palisade Mountain Measured Section I 147
Palisade Mountain Measured Section II 152
Silken Skein Falls Measured Section 157
Flanders Mountain Measured Section 160
Windy Pass Measured Section 165

LIST OF TABLES

Table | Page

1. Thickness of individual stratigraphic locations and their location by Township and Range 7
2. Summary of Coarse-Grained Lithofacies 43
3. Lithofacies Associations and Types of Processes 52
4. Relative Abundances of Coarse-Grained Lithofacies (Appendix A) 107

LIST OF FIGURES

Figure Page

1. Generalized map showing the distribution of Eocene volcanic rocks..... 3
2. Schematic cross section showing stratigraphic relations in the northern Gallatin Range..... 5a
3. Typical outcrop exposures of volcaniclastic sequences of Hyalite Peak volcanics..... 6
4. Map of field area showing location of measured sections..... 8
5. Sketch of outcrop face in Eight Mile Canyon showing flattened and aligned tuff and pumice clasts with dense blocky glass and lithic fragments..... 12
6. Sketch of outcrop face showing clasts which exhibit radial prismatic jointing..... 12
7. Sketch of idealized non-welded pyroclastic flow components..... 13
8. Schematic diagram showing transitions between flow processes..... 18
9. Sketch showing textures typical of Gmpv lithofacies..... 21
10. Sketch showing textural features of Gms lithofacies..... 23
11. Sketch showing textural features of Gcms lithofacies..... 25
12. Sketch showing textural features of Gmsn lithofacies..... 26
13. Sketch showing textural features of Gmsi lithofacies..... 27
14. Sketch showing textural features of Gmci lithofacies..... 29
15. Sketch showing textural features of Gmp lithofacies..... 31
16. Sketch showing textural features of Gmpi lithofacies..... 33
17. Sketch showing textural features of tabular deposits of Gm lithofacies..... 34
18. Sketch showing textural features of tabular deposits of Gmw lithofacies..... 35
19. Sketch showing textural features of Gmwt lithofacies..... 36

LIST OF FIGURES - continued

Figure Page

20. Sketch showing textural features of Gmcn lithofacies..... 37
21. Sketch showing textural features of Gmcin lithofacies..... 39
22. Sketch showing textural features of GmLa lithofacies..... 40
23. Sketch showing textural features of Gl lithofacies..... 41
24. Sketch showing textural features of Gt lithofacies..... 42
25. Illustration of sedimentary structures and grain-size characteristics of sandy lithofacies..... 46
26. Photograph of Fsc lithofacies deposit..... 49
27. Lithofacies Association 1, representing streamflow deposition..... 53
28. Lithofacies Association 2, representing matrix- supported debris flow deposition (MSDF)..... 54
29. Lithofacies Association 3, representing deposition from clast-supported debris flow (CSDF)..... 56
30. Lithofacies Association 4, representing deposition from debris avalanches, flow front breccia, vent breccia and debris flows (DAVB)..... 58
31. Lithofacies Association 5, representing deposition from pyroclastic flow, fall, and surge (PFFS)..... 59
32. Photo of Gm lithofacies unit at Antelope Butte Section I..... 61
33. Generalized stratigraphic sections showing sequence of lithofacies associations in Antelope Butte Section I..... 63
34. Generalized stratigraphic sections showing sequence of lithofacies associations at Antelope Butte Section II..... 64
35. Photograph of diabase clast within a Gms unit at Eight Mile Canyon..... 65
36. Generalized stratigraphic sections showing sequence of lithofacies associations at Eight Mile Canyon Section I..... 66

LIST OF FIGURES - Continued

Figure Page

37. Units of Gmsi lithofacies at Eight Mile Canyon..... 67

38. Generalized stratigraphic sections showing sequence of lithofacies associations at Eight Mile Canyon Section II..... 68

39. Gt lithofacies at the base of Palisade Mountain Section I..... 71

40. Generalized stratigraphic sections at Palisade Mountain showing sequence of lithofacies associations..... 72

41. Illustration of sequence of probable events leading to the deposition of sequences at Palisade Mountain..... 74

42. Photo of deposit of Gms lithofacies at Palisade Mountain..... 75

43. Detailed sketch of portions of measured section at Silken Skein Falls showing location of accretionary lapilli within the deposits..... 78

44. Silken Skein Falls and Flanders Mountain stratigraphic sections generalized to show relationship between lithofacies associations..... 80

45. Photo showing fragments of volcanic glass with alteration rims in Gmp deposit at Flanders Mountain..... 81

46. Sketch illustrating vertical and lateral relationships in upper portion of Flanders Mountain measured section..... 83

47. Windy Pass measured section, generalized to show relations between lithofacies associations..... 85

48. Schematic diagram illustrating interactive processes within a volcanic setting..... 87

49. Map showing paleocurrents in study area, as well as possible vent sources..... 90

ABSTRACT

Eocene Hyalite Peak volcanics in the Gallatin Range, southwest Montana, consist of 1,800 m of sedimentary sequences and intercalated andesitic lava flows. Lithofacies in the deposits, categorized based on texture, grain size, and fabric indicate that the processes of transport, grain support, and deposition of the sequences varied greatly. Sedimentary fabrics exhibit textures which record a broad continuum of flow transitions between streamflow, hyperconcentrated flow and debris flow processes produced by variation in the ratio of sediment to water. Variability in the amount of clast-support and types of grading in Hyalite Peak sequences were produced primarily by coarse-grained debris flow, variable stages of non-cohesive transitional flow, and hyperconcentrated flow. Key features in volumetrically minor deposits contain depositional fabrics which indicate they were produced and transported directly by eruptive activity. Deposits produced from pyroclastic flows and surges contain a large component of pumice and glass shards produced as juvenile pyroclastic material. Other near-vent deposits contain volcanic bombs and agglutinate. Together, sedimentary sequences within the Hyalite Peak volcanics exhibit fabrics and textures commonly described as volcaniclastic deposits found in modern volcanic settings.

Utilizing recent improvements in knowledge of sedimentation in modern volcanic systems, well exposed sequences of Eocene Hyalite Peak volcaniclastic strata are described in detail, and the processes which induced their formation are for the first time characterized. Features within these deposits suggest that volcanic activity was phreatic or phreatomagmatic, induced by groundwater-magma interaction. The variation of lithofacies types in Hyalite Peak sequences indicate that deposition was produced through a broad range of transitions between processes of eruption and sedimentation which took place on the flanks of stratovolcanoes and near small localized vent sources.

INTRODUCTION

Processes of alluvial sedimentation in regions of active volcanism are unique and unparalleled: rapid mobilization of sediment and water occurs episodically and in large volumes. As a result, debris flow and hyperconcentrated flood flow deposits tend to be numerous and extensive (Smith, 1986). Since the eruption of Mount St. Helens in 1980, a wealth of information has been collected pertaining to mechanisms of sediment transport in modern volcanic terranes (Harrison and Fritz, 1982; Fisher and others, 1987; Pierson, 1985; Brantley and Waitt, 1988). Studies at Mount St. Helens, Mayon Volcano in the Phillipines, Nevado del Ruiz in Colombia, and in other modern volcanic settings demonstrate that volcanically produced sediment tends to be coarse-grained and far traveled (Pierson and Scott, 1985; Lowe and others, 1986; Pierson and others, 1990). Volcanically induced debris flows may lack the cohesion which has been generally accepted as the mechanism which imparts mobility to the large clasts found within their deposits (Scott, 1988; Walton and Palmer, 1988; Arguden and Rudolfo, 1990). Without cohesion, mobility and grain support result from dilatant flow, which is produced in part by dispersive pressure. During eruptive phases, pyroclastic flows and surges can mobilize large amounts of sediment, initiating catastrophic debris flows. Associated steam and hot air can impart mobility and decrease viscosity in the resulting sediment gravity flows (Arguden and Rodolfo, 1990). Flow transformations between these debris flows and hyperconcentrated flood flow are common occurrences (Pierson and Scott, 1985; Major and Scott, 1988). Factors such as these make processes of sedimentation within volcanic terranes incomparable to those of other fluvial systems.

Depositional processes characteristic of volcanic settings have not been accounted for in conventional fluvial facies models. Smith (1987) refined facies codes to include hyperconcentrated flood flow deposits which result from periods of high discharge common in volcanic settings, but which are also less frequently found in arid alluvial fan sequences. Other types of coarse-grained volcaniclastic deposits have been subdivided into separate facies by Fritz and Harrison (1985), Waresback and Turbeville (1990), Palmer and Walton (1990), and Borrero and Naranjo (1990), but are still described with general facies codes.

The purpose of this study is to utilize recent improvements in the knowledge of volcanically-influenced terrestrial sedimentation derived from modern systems to characterize the types of alluvial processes that were active in the Eocene Hyalite Peak Volcanics of the northern Gallatin Range, Montana. Consisting of predominantly andesitic lava flows, these strata also include a large volume of alluvial deposits. Even though the Hyalite Peak Volcanics are well exposed, stratigraphic sections have only been generally described by Chadwick (1969). Facies were defined based upon description of lithologic units within measured sections, and used to interpret processes of transportation, grain support, and deposition. Used to describe and interpret these deposits, it is hoped that they can be applied generally to volcaniclastic sequences found elsewhere. Vertical and lateral relations between facies were also examined in order to distinguish the types of depositional sequences present and to interpret sequences of events which may have occurred.

Geologic Setting

Two belts of eruptive centers active during Eocene time are located in southwestern Montana and northwestern Wyoming. Chadwick (1970) named them the eastern and western Absaroka belts and distinguished them from each other by chemical whole rock analysis, noting that samples from eruptive centers of the eastern belt had higher K_2O:SiO_2 ratios. The resulting deposits, which are thought to have been emplaced on the flanks of stratovolcanoes, extend northwestward from the southeastern part of the Absaroka Range through the Gallatin Range (Figure 1). These volcanic and volcaniclastic rocks have been included within the Absaroka Volcanic Supergroup (Smedes and Prostka, 1972) which is divided stratigraphically into the Washburn, Sunlight, and Thorofare Creek Groups. The Absaroka Volcanic Supergroup is now considered part of the Absaroka-Gallatin volcanic province, indicating more clearly that the rocks extend beyond the Absaroka Range (Chadwick, 1970). The oldest and northernmost volcanic sequences are of the Washburn Group. Located in the Gallatin and Beartooth Ranges, the Washburn Group is characterized by near-vent lava flows, autoclastic flow breccias, mudflows, avalanche debris, and tuff deposits which grade laterally into and interfinger with well-bedded, reworked volcanic conglomerate, volcanic siltstone and sandstone, and ash-fall tuff (Smedes and Prostka, 1972).

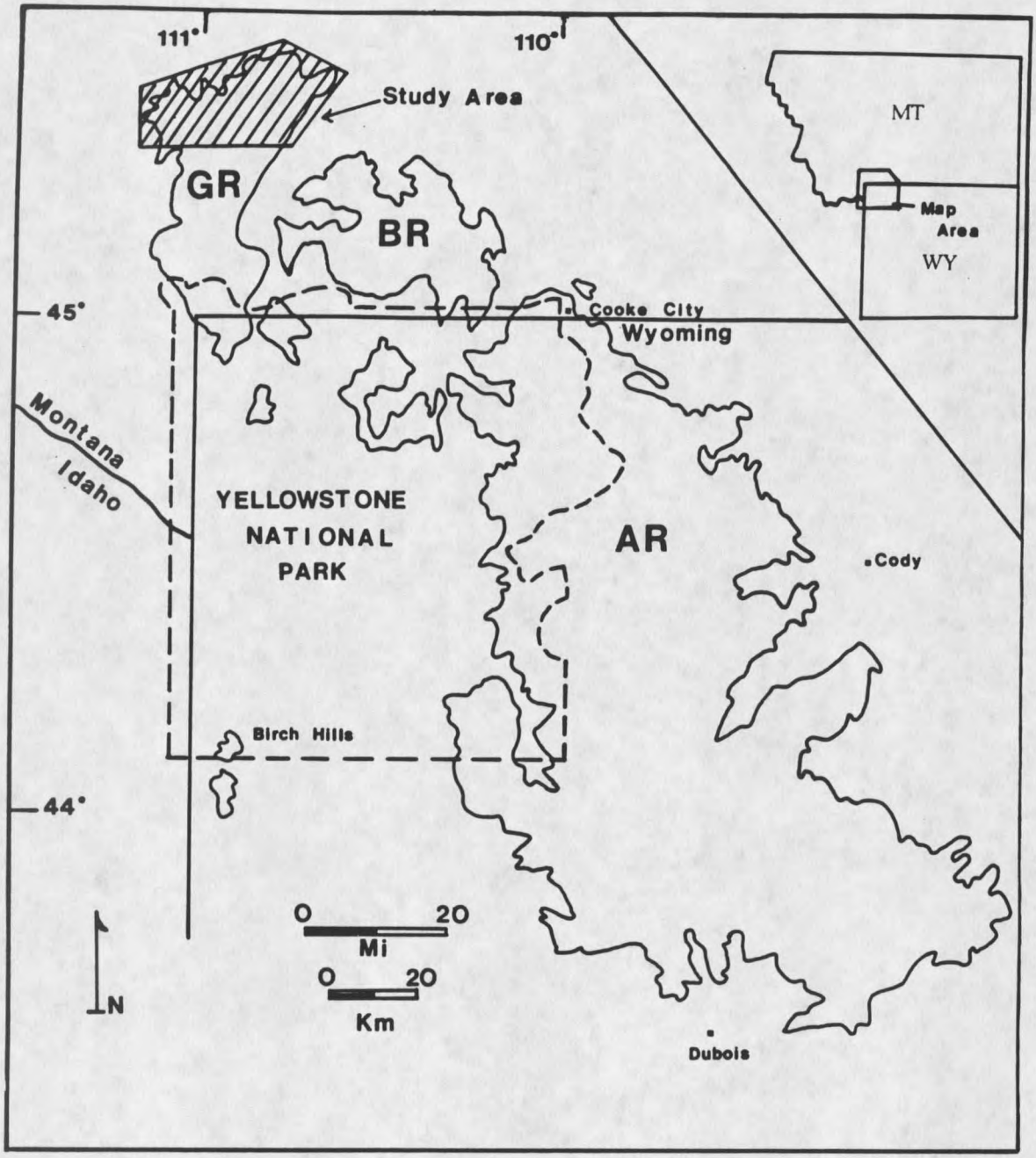


Figure 1. Generalized map with solid line showing the distribution of Eocene volcanic and volcaniclastic rocks belonging to the Absaroka-Gallatin volcanic province. Mountain ranges containing these deposits include the Absaroka Range (AR), the Gallatin Range (GR), and the Beartooth Range (BR). Location of the study area is shaded.

This study focuses on deposits within the northern Gallatin Range. Igneous centers in the northern Gallatin Range erupted predominantly andesitic lavas which have been intruded locally by dacite stocks and plugs. The Big Creek stock, a dacite intrusion which cuts across both northern volcanic sequences, has been dated at 49.5 $\pm$ 1.5 ma, by K/Ar whole rock analysis (U.S. Gelogical Survey, J.D. Obradovich, in Chadwick, 1969).

Initial Eocene volcanism in the Gallatin Range is recorded by the Golmeyer Creek Volcanics, a 600 m thick sequence of interbedded hypersthene-andesite flows and flow breccias and minor epiclastic sedimentary rocks which have no correlative units elsewhere (Smedes and Prostka, 1972). These deposits rest on top of an erosional surface developed on Archean metamorphic and igneous rocks. Early dacite intrusions are represented by clasts found within the Golmeyer Creek volcaniclastic units (Chadwick, 1969). Golmeyer Creek deposits were extensively eroded prior to the eruption of younger volcanics and pinch out to the northwest.

The Hyalite Peak Volcanics, which are widespread and unconformably overlie the Golmeyer Creek Volcanics, also in places rest directly on an irregular pre-Eocene topographic surface (Iddings and others, 1894; Peale, 1896; McMannis and Chadwick, 1964). Deformed Precambrian metamorphic rocks and folded Paleozoic and Mesozoic sedimentary beds impart an estimated 650 m of relief to the pre-volcanic topography (Chadwick, 1984). Eocene volcanic deposits filled in paleovalleys, but many units are subhorizontal, dipping 10 to 12° southeast due to regional tilting toward the Yellowstone River Valley (Figure 2). The Hyalite Peak volcanics consist of a 700 to 1100 m thick sequence of interbedded augite-hypersthene andesite flows and flow breccia which are interbedded and interfinger with volcaniclastic sequences. Lenses of a fluvial conglomerate containing well-rounded pre-Hyalite Peak clasts of Precambrian quartzite, Paleozoic and Mesozoic clasts, along with volcanic clasts from an unknown source are locally found at the base. Volcaniclastic intervals within the Hyalite Peak Volcanics have thicknesses from a few tens to hundreds of meters, and constitute approximately 40% of the unit as a whole. Sedimentary sequences at several locations contain upright, buried trees and stumps. Epiclastic deposits were described by Chadwick (1969) as being characterized by crude stratification with poor sorting and angular clasts, and containing boulders more than 2 m in diameter from unknown sources.

This study focuses on deposits within the northern Gallatin Range. Igneous centers in the northern Gallatin Range erupted predominantly andesitic lavas which have been intruded locally by dacite stocks and plugs. The Big Creek stock, a dacite intrusion which cuts across both northern volcanic sequences, has been dated at 49.5 $\pm$ 1.5 ma, by K/Ar whole rock analysis (U.S. Gelogical Survey, J.D. Obradovich, in Chadwick, 1969).

Initial Eocene volcanism in the Gallatin Range is recorded by the Golmeyer Creek Volcanics, a 600 m thick sequence of interbedded hypersthene-andesite flows and flow breccias and minor epiclastic sedimentary rocks which have no correlative units elsewhere (Smedes and Prostka, 1972). These deposits rest on top of an erosional surface developed on Archean metamorphic and igneous rocks. Early dacite intrusions are represented by clasts found within the Golmeyer Creek volcaniclastic units (Chadwick, 1969). Golmeyer Creek deposits were extensively eroded prior to the eruption of younger volcanics and pinch out to the northwest.

The Hyalite Peak Volcanics, which are widespread and unconformaby overlie the Golmeyer Creek Volcanics, also in places rest directly on an irregular pre-Eocene topographic surface (Iddings and others, 1894; Peale, 1896; McMannis and Chadwick, 1964). Deformed Precambrian metamorphic rocks and folded Paleozoic and Mesozoic sedimentary beds impart an estimated 650 m of relief to the pre-volcanic topography (Chadwick, 1984). Eocene volcanic deposits filled in paleovalleys, but many units are subhorizontal, dipping 10 to 12° southeast due to regional tilting toward the Yellowstone River Valley (Figure 2). The Hyalite Peak volcanics consist of a 700 to 1100 m thick sequence of interbedded augite-hypersthene andesite flows and flow breccia which are interbedded and interfinger with volcaniclastic sequences. Lenses of a fluvial conglomerate containing well-rounded pre-Hyalite Peak clasts of Precambrian quartzite, Paleozoic and Mesozoic clasts, along with volcanic clasts from an unknown source are locally found at the base. Volcaniclastic intervals within the Hyalite Peak Volcanics have thicknesses from a few tens to hundreds of meters, and constitute approximately 40% of the unit as a whole. Sedimentary sequences at several locations contain upright, buried trees and stumps. Epiclastic deposits were described by Chadwick (1969) as being characterized by crude stratification with poor sorting and angular clasts, and containing boulders more than 2 m in diameter from unknown sources.

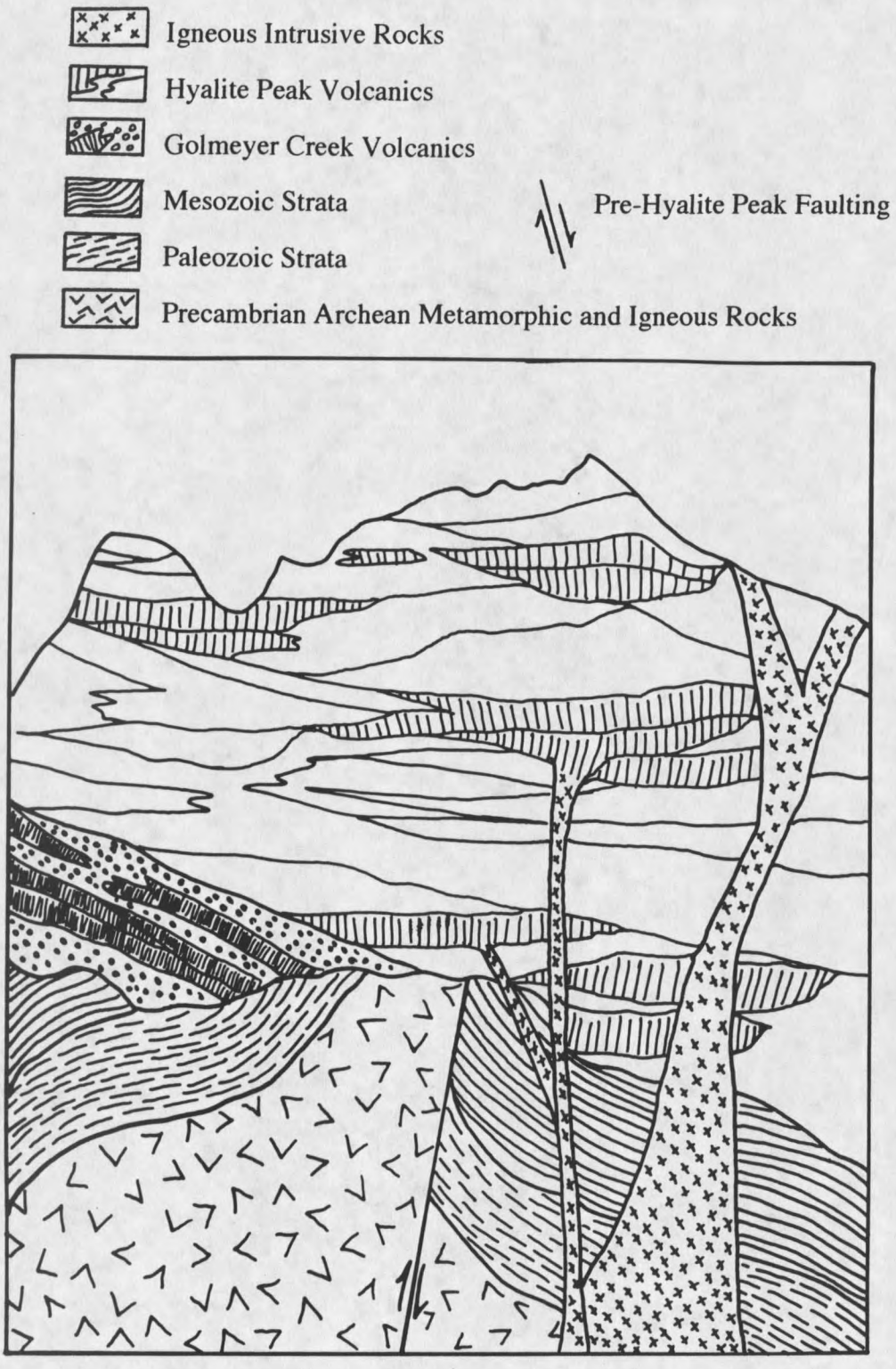


Figure 2. Schematic cross section showing stratigraphic relations in the northern Gallatin Range, southwest Montana. Actual thickness of the deposits is not represented.

METHODS

Outcrops selected for study are primarily within the Fridley Peak 15' quadrangle mapped by Chadwick (1982) and Garnet Mountain 15' quadrangle mapped by McMannis and Chadwick (1964). Additional stratigraphic sections were studied at Antelope Butte, located due west of Pine Creek. These two geologic quadrangles, and the addition of generally described stratigraphic sections by Chadwick (1969), served as a foundation for preliminary field reconaissance during the summer of 1990. Appropriate areas in which to concentrate further study were also selected on the basis of accessibility and the amount of climbable outcrop exposure. Although excellent exposures of Hyalite Peak volcaniclastic sequences exist, many are inaccessible crumbly vertical cliffs located several miles from the nearest road. A typical outcrop exposure is shown in Figure 3.

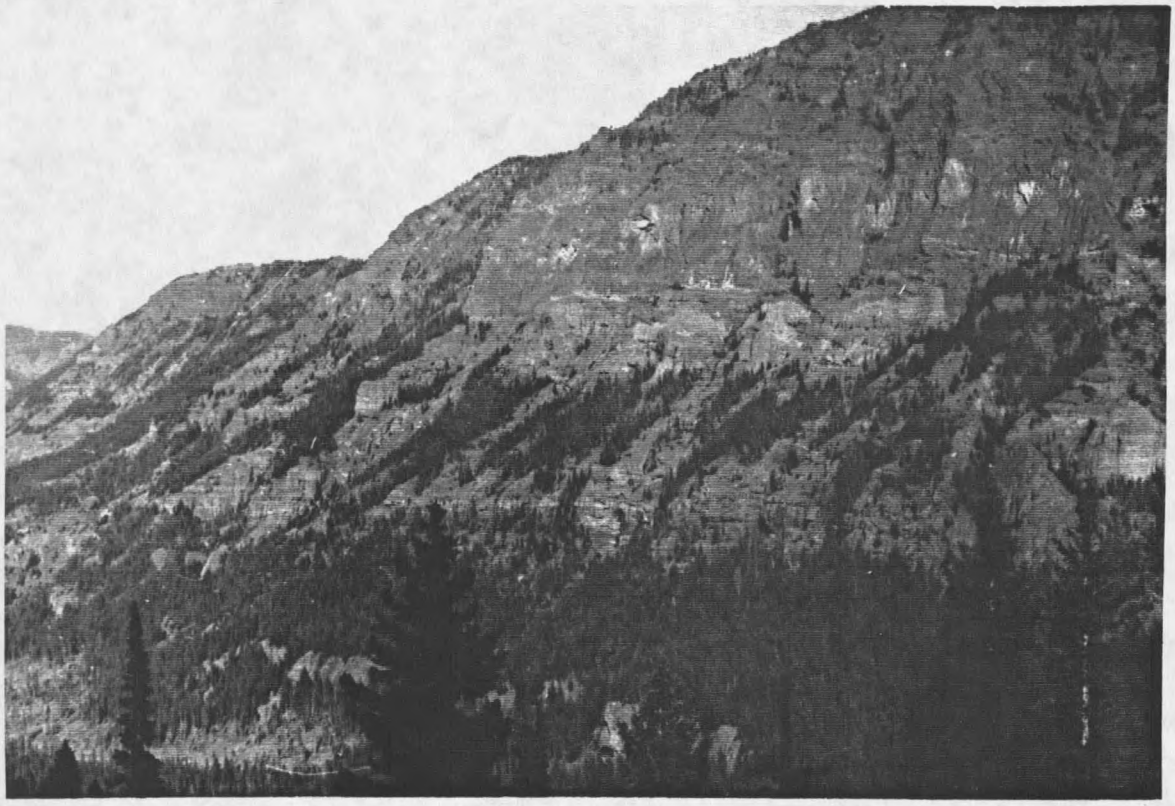


Figure 3. Typical outcrop exposures of volcaniclastic sequences of Hyalite Peak volcanics. Photograph is of the east wall of Hyalite Canyon.

Field investigations were conducted during the summers of 1990 and 1991, beginning in mid-July and lasting until mid-September due to the persistence of snowcover at higher elevations. Nine stratigraphic sections were described from six separate areas. A total of 1,056 m of strata was measured using a Brunton compass and tape (Table 1). All stratigraphic columns measured are considered partial sections. Their locations are shown in Figure 4. Contacts between the Eocene volcanics and older units below are covered and their locations inferred. The upper limit of stratigraphic measurement was determined by the limit of the outcrop and is either an upper erosional surface or the face of a cliff. Due to extreme lateral discontinuity of stratigraphic units as well as the disjointed nature of the outcrops, determination of the relative stratigraphic position of measured sections was not possible. Detailed mapping and petrographic and geochemical analysis of lava flows to determine their lateral continuity are necessary steps to understanding the stratigraphy of the area, and are beyond the scope of this thesis.

Table 1. Thickness of individual stratigraphic sections and their location by Township and Range.

Location Name	Section number	Thickness measured	T&R Coordinates.
Windy Pass	I	41.5 m	SW 1/4, Sec 22 T 6 S, R 5 E
Silken Skein Falls	I	51.5 m	SW 1/4, Sec 2 T 5 S, R 6 E
Palisade Mountain	I	167.1 m	SE 1/4, Sec 24
	II	58.9 m	T 4 S, R 6 E
Flanders Mountain	I	70.0 m	NW 1/4, Sec 35 T 4 S, R 6 E
Eight Mile Canyon	I	185.3 m	NW 1/4, Sec 36 T 4 S, R 6 E
	II	72.8 m	SE 1/4, Sec 31, T 4 S, R 8 E
Antelope Butte	I	44.3 m	NW 1/4, Sec 13, T 4 S, R 8 E
	II	364.3 m	SW 1/4, Sec 12, T 4 S, R 7 E

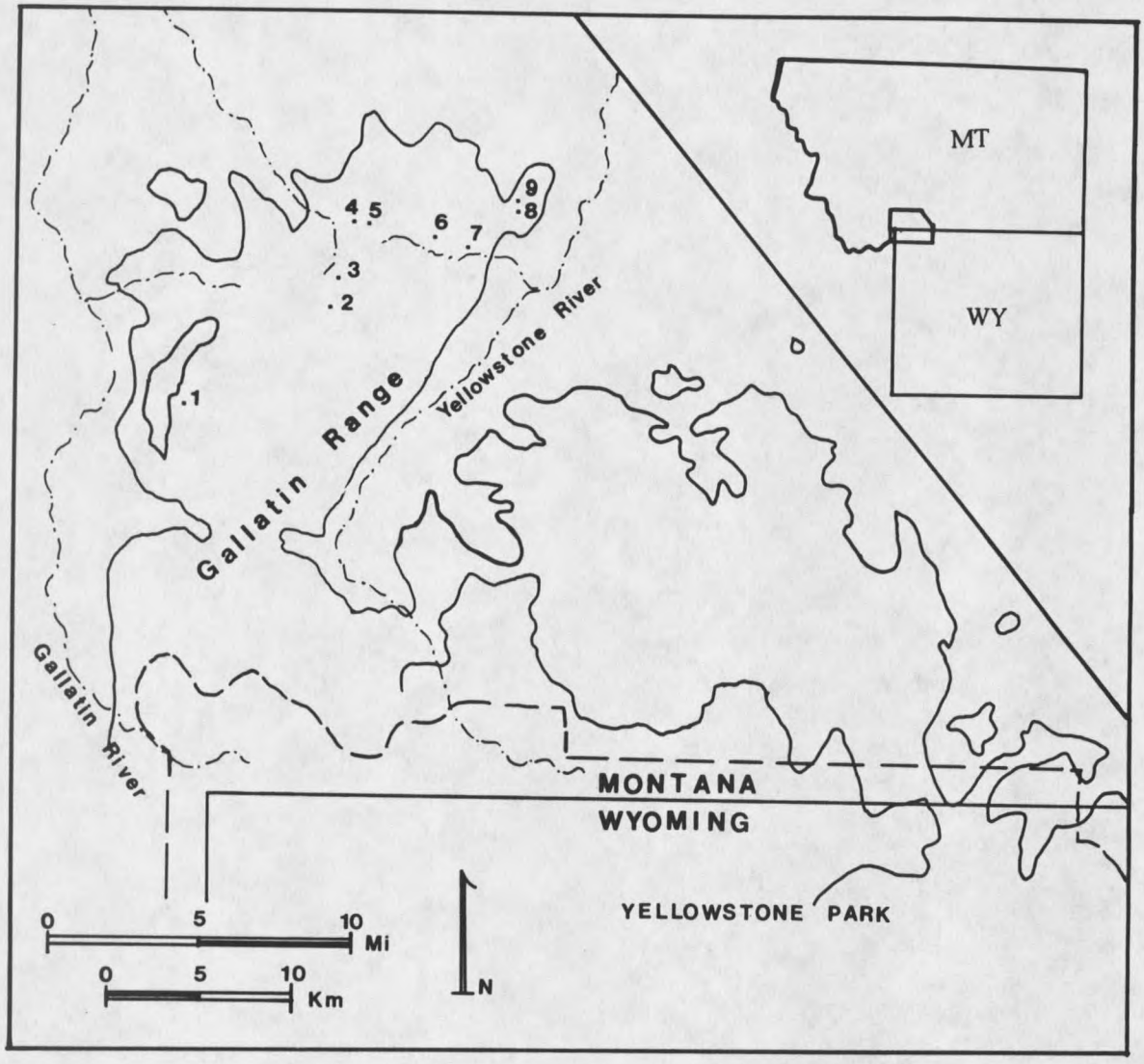


Figure 4. Map of field area showing the location of the following measured sections: 1) Windy Pass, 2) Silken Skein Falls, 3) Flanders Mountain, 4 and 5) Palisade Mountain (I and II), 6 and 7) Eight Mile Canyon (I and II), 8 and 9) Antelope Butte (I and II).

Stratigraphic column descriptions include bed thickness, thickness variability, stratigraphic contacts, and the overall texture and fabric of units, including vertical and lateral variability of lithofacies. Although rare, paleocurrent indicators such as imbrication, cross bedding, and channel orientation are also included. Lateral facies relationships are key features used in understanding and interpreting depositional processes and are not always preserved in vertical columns. Therefore, when sketching vertical columns, notes were made regarding lateral relationships between deposits as well as the geometry and continuity of the units themselves.

Select samples were taken for petrographic analysis to aid in determination of depositional processes. Sample petrography included observations of grain size, fabric, and matrix lithology. The presence of glassy rims, unabraided phenocrysts, amount of glass present, and degree of fragmentation and rounding of grains were noted.

Lithofacies codes used to describe units within these sections are based upon classification methods of Miall (1978), with additional modifications used to describe grain size, fabric and texture. Stratigraphic units were initially described and categorized using Miall's standard lithofacies codes. Many additional subdivisions were made within units classified as Gm facies due to the notable variety of coarse-grained deposits. Other subdivisions were made based upon the types of sedimentary structures present and variations in grading due to clast density. Separate lithofacies units were distinguished based on differing grain size, or by the presence of erosional surfaces. Each unit may be considered a single deposit, but may not be the unique product of an individual event. Because of recent observations of sedimentation processes at Mount St. Helens, it is clear that individual lithologic units with contrasting textural fabrics may be the product of one event, or may be the result of separate pulses or depositional phases during a larger event or series of events (Harrison and Fritz, 1982).

Sedimentologic and hydrodynamic interpretation of lithofacies was based on standard lithofacies models of Schultz (1984), Rust (1978), and Miall (1978). Because the response of systems to episodic, volcanically induced sediment loads has not been accounted for in popular facies models, this work has been augmented by recent studies in modern volcanic settings by Harrison and Fritz (1982), Pierson and Scott (1985), Freundt and Schmincke (1986), Brantley and Waitt (1988), Mellors and others (1988), Arguden and Rodolfo (1990), Fisher (1990), and Pierson (1981, 1991), as well as recent work in volcaniclastic sedimentary rocks by Fritz and Harrison (1985), Smith (1986, 1987), Palmer and Walton (1990), Borrero and Naranjo (1990), Waresback and

interpretations. Vertical and lateral relationships between lithofacies were analyzed as architectural elements within a three-dimensional framework (Miall, 1985, 1988) in order to determine sequences of events and to reconstruct the depositional setting.

TERMINOLOGY

Volcaniclastic deposits consist of clastic aggregates of volcanic grains which originate from various fragmentation and depositional processes (Fisher, 1961). Pyroclastic processes resulting directly from the force of an eruption are commonly associated with epiclastic processes, which involve the weathering and erosion of emplaced material. Determination of which processes resulted directly from volcanic activity during sedimentation provide critical information on the geological setting of the basin and source area. Terms used to discriminate between different types of processes vary in usage from author to author, and are often subject to debate. In order to distinguish between these processes, the context in which they are used herein must be clearly defined.

Pyroclastic Processes

Tephra deposited directly as fall-out from an eruption column is herein referred to as *ash-fall* (< 2 mm) or *pumice-fall* or *lapilli-fall* (> 2 mm), depending upon particle size and type. The use of the term "air-fall" deposits is abandoned in favor of the above terms which describe these types of deposits more completely.

Pyroclastic flows are hot, dry flows of volcanic debris (Wilson, 1980). Mobility is imparted by hot air and gas, the explosive force of an eruption, and by the force of gravity. Gas fluidization of fine particles within the flows acts as a transporting medium similar to water in mudflows (Sparks, 1976). Pyroclastic flows move in a dominantly laminar fashion, with the deposit of the flow retaining the same fabric as the flow itself (Fisher, 1986). Their deposits are typically coarse-grained, poorly sorted, and although generally massive, they are often graded. Pyroclastic flow deposits may closely resemble debris flow deposits, especially in regions of uneven paleotopography where increased turbulence aids in incorporation of lithic clasts from the substrate into the flow (Buesch, 1992). They can sometimes be distinguished by evidence that they were once hot, such as the presence of clasts which appear to be flattened or to have flowed after deposition (Figure 5). Eutaxitic texture and fiamme, which are collapsed, melted pumice fragments, are similar to these features, but are textures produced by a higher degree of welding,

which can be exhibited to varying degrees (Peterson, 1979; Branney and Kokelaar, 1992). Other evidence of deposition of hot material are clasts containing radial prismatic joints formed by cooling (Smith and Lowe, 1991)(Figure 6). In addition, deposits may sometimes exhibit density segregation of clasts. This segregation consists of normally graded lithic concentration zones below inversely graded pumice concentration zones (Sparks and others, 1973; Freundt and Schminkce, 1986). This type of grading has not been described in debris flows, and has been considered a common fabric in non-welded pyroclastic flows (Figure 7). Although pyroclastic flows are high particle concentration flows, density segregation may occur because the flow has a lower yield strength than debris flows (Sparks, 1976).

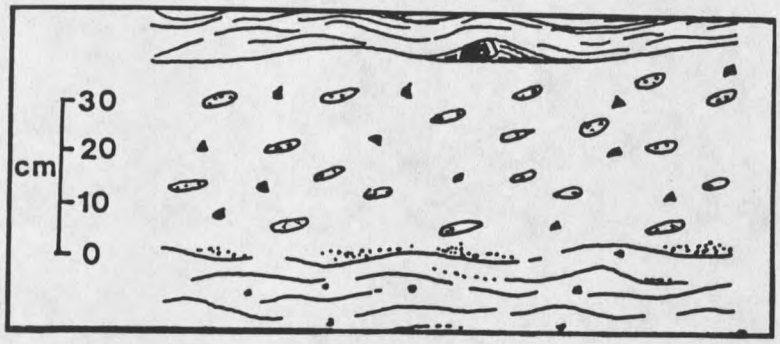


Figure 5. Sketch of outcrop face in Eight Mile Canyon showing flattened and aligned tuff and pumice clasts with dense blocky glass and lithic fragments. These are interbedded with thin, wavy ash strata and laminae. In this outcrop, flattened pumice are dense and poorly vesicular, but retain their pumiceous texture.

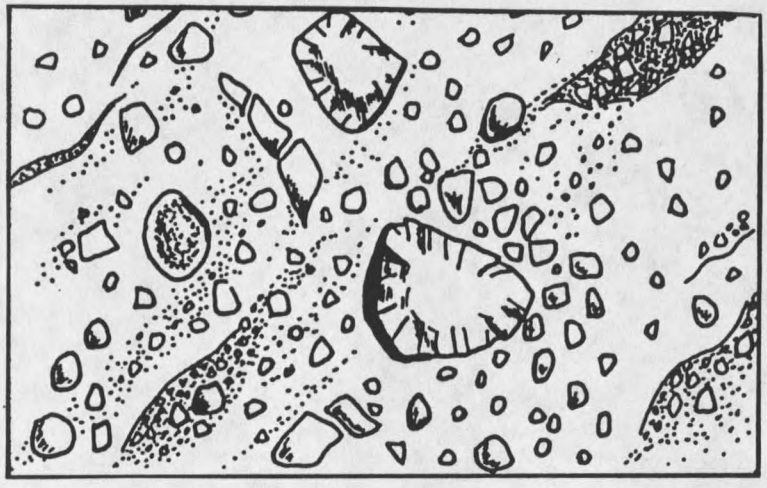


Figure 6. Sketch of outcrop face showing clasts which exhibit radial prismatic jointing. This characteristic develops as a result of in situ cooling and thermal contraction. Clasts which contain these joints are not easily transported or reworked without fragmentation.

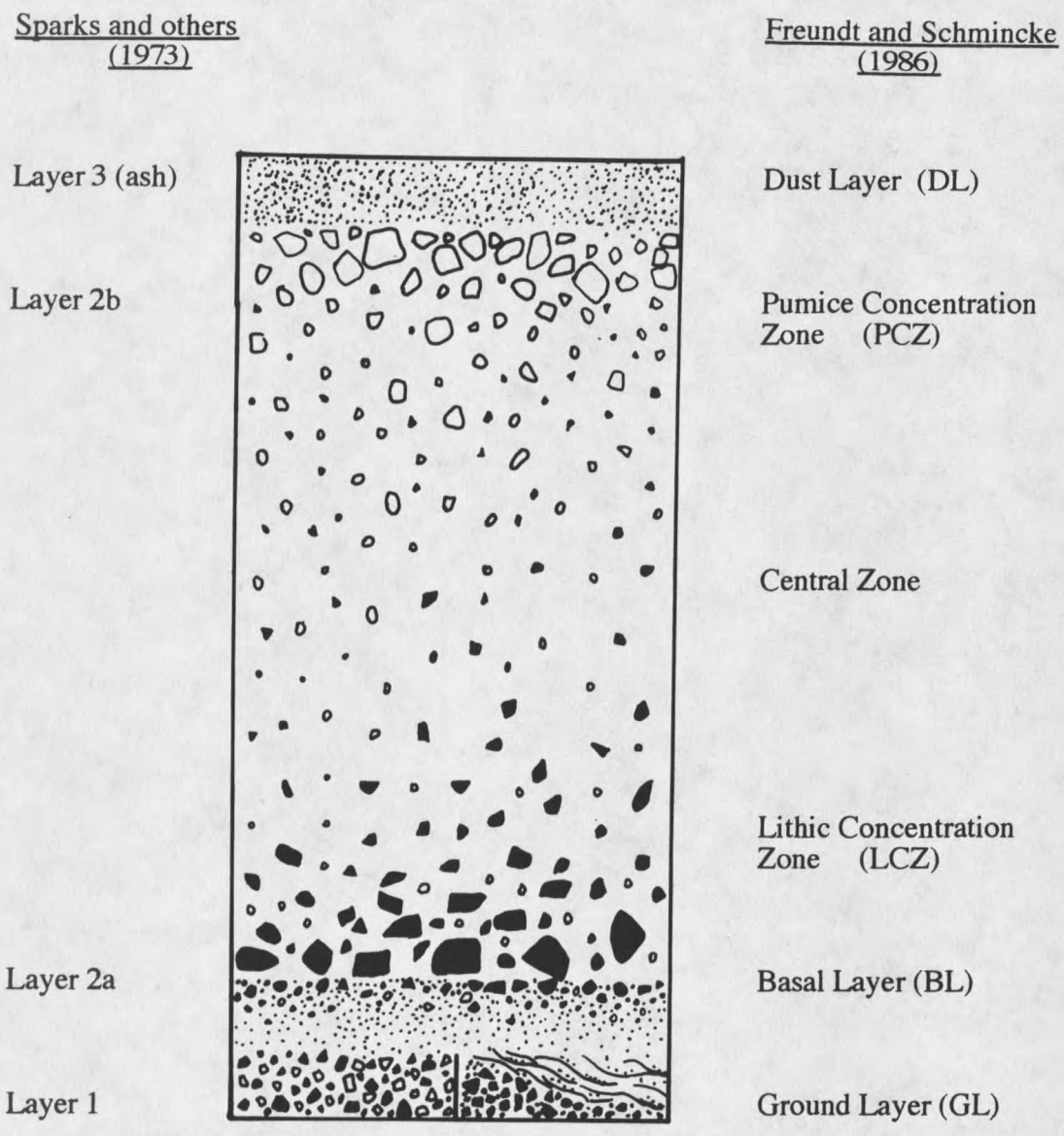


Figure 7. Sketch of idealized non-welded pyroclastic flow components with structural and compositional designations from Sparks and others (1973), and Freundt and Schmincke (1986). Sparks and others (1973) interpret layer 2 (a and b) as one flow unit, which is considered to be the main body of the pyroclastic flow by Freundt and Schmincke (1986). This central portion of the deposit exhibits normal grading of dense clasts at the base with inverse grading of less dense pumice above.

Pyroclastic surges are low-concentration mixtures of volcanic particles, water, and expanding gases in a turbulent gravity flow (Cas and Wright, 1987; Valentine, 1987; Carey, 1991). Surges may originate by eruption column collapse, lava dome collapse, lateral blasts, or as ash clouds generated by dense pyroclastic flows (Valentine, 1987). Associated with eruptions of basaltic to andesitic magma as well as more silicic varieties, surges can be an important component in volcaniclastic sequences (Carey, 1991) and are intimately associated with pyroclastic flows (Fisher and Schmincke, 1984). Deposits characteristically may be planar, massive, or may exhibit dune-form or wave-like bedding structures.

Two types of surges can be recognized in the depositional record: *dry surges* consisting of particles and superheated steam, and *wet surges* originating from the interaction between magma and subsurface water incorporated into the flow (Sheridan and Wohletz, 1983; Fisher and Schmincke, 1984). Dry surge deposits can be widespread, and generally consist of sand size pyroclasts in well-bedded layers with low angle cross stratification. These are distinctly different than wet surge deposits found only in the vicinity of a vent, and commonly consisting of thin subparallel layers of vesiculated ash (Dellino and others, 1990).

Surge deposits can also be subdivided genetically, distiguished primarily on the basis of vertical and lateral relationships to pyroclastic flow deposits, but also on the basis of thickness and types of stratification. These subdivisions include base surges, ground surges, ash cloud surges, and blast surges (Wright and others, 1980; Fisher, 1990). *Base surges* and *ground surges* usually precede pyroclastic flows, forming at the base of an eruption column, and therefore deposits usually underly pyroclastic flow deposits. *Ash cloud surge* deposits may grade laterally into pyroclastic flow deposits, or be located above them because they form from a less dense, more turbulent cloud above and in front of the flow. *Blast surges* form explosively, and may be extremely hard to distinguish in the geologic record. As with pyroclastic flows, blast surges may also incorporate, transport, and deposit accidental material from the substrate due to increased turbulence caused by flowing over an uneven surface (Fisher, 1990)

During volcanic eruptions, pyroclastic flows and surges can be produced alone or in close association with each other. Resulting deposits may show a wide range of variety due to particle-concentration variability. The diversity of deposits found in regions of active volcanism are also closely related to process interaction. Pyroclastic flows and surges have the ability to generate other types of sediment gravity flows. In November, 1985, Nevado del Ruiz, Colombia erupted with pyroclastic flows and surges

that interacted with snow and ice, triggering debris flows which killed more than 23,000 people (Pierson and others, 1990).

Epiclastic Processes

The term *lahar* is an Indonesian word used as a general designation for deposits originating on the slopes of a volcano. It is a useful term when referring in general to volcaniclastic deposits formed by any process on the flanks of a volcano, as the term was originally applied, especially if the process of deposition is not known. Although it was initially applied to deposits generated by any process (van Bemmelen, 1949) the definition of *lahar* has varied greatly with use. It may now include any volcaniclastic deposits resulting from flows mobilized by water (Crandell, 1971; Crandell and Mullineaux, 1973). Others have suggested restriction of the term to deposits from water-mobilized flows containing not less than 80% sediment by weight (Beverage and Culbertson, 1964; Pierson and Scott; 1985; Major and Scott, 1988). Whether or not a flow is mobilized by water alone, or by water and hot air, may be difficult to determine from deposits. Ambiguity in interpretation is especially difficult in the case of hot lahars, or wet pyroclastic surges which are sometimes transformed into volcanic debris flows as they move downslope. In addition, weight percentages of a sediment/water mixture are difficult to apply to ancient deposits. As a result, the term *lahar* is now only applied to a process rather than a deposit (Smith and Lowe, 1991). Because this term may include or exclude a wide range of flow phenomena, and because more specific terms referring to flows of volcaniclastic materials exist, this term will not be used herein.

Sediment concentration-based definitions of flow processes are not directly applicable to the geologic record. However, different sediment/water ratios result in different flow processes, and the resulting deposits exhibit different fabrics. Specific types of flows of volcaniclastic material mobilized by water result from differing ratios of sediment to water during flow (by weight %). *Streamflow* has less than 40% sediment by weight, *hyperconcentrated flow* 40-80% sediment by weight, and *debris flow* greater than 80% (Beverage and Culbertson, 1964). Coarse-grained material, such as clay-poor, fresh volcanic debris, may require a greater sediment concentration for the transition of one process to another (Pierson and Costa, 1987).

Streamflow (< 40% sediment by weight) is the turbulent flow of a Newtonian fluid (Smith, 1986). Newtonian fluids do not posess shear stength, and exhibit a linear

relationship between shear stress and the rate of strain (Costa, 1988). Sediment, as a separate component within the flow, is suspended in water by the transfer of energy from moving water to rolling and saltating particles. Resulting deposition of entrained sediment occurs in a grain-by-grain fashion (Smith and Lowe, 1991). Dilute streamflow deposits are sub-rounded to well rounded, and characterized by the presence of cross-bedded sands and moderately to well sorted gravel with a sandy matrix which may be massive, horizontally bedded or cross-bedded, and associated with lenses and thin beds of sand.

As the sediment concentration in a flow increases, gradual changes in flow properties take place. Entrained sediment remains in suspension longer than in normal streamflow, and sediment transport rates increase (Costa, 1988). Flows begin to support debris by dampened turbulence, bouyancy, and dispersive pressure, and fall into the category of *hyperconcentrated flow* (40-80% sediment concentration). This type of flow generally occurs during periods of high discharge. Deposits are, for the most part, sand to granule-sized, but may contain outsized clasts. If present, low-density pumice and organic matter may be concentrated in the upper part of individual units. Many of the deposits are ungraded or exhibit distribution nomal grading. Cross-bedding and ripple cross-lamination are absent. Fine-grained units tend to be horizontally stratified, possibly as a result of bedform migration (Smith and Lowe, 1991). Normal grading suggests that flow is turbulent enough for differential settling of individual granules and pebbles. Gravel may sometimes exhibit long-axis imbrication, also as a result of turbulence (Smith, 1986).

Debris flows contain more than 80% sediment by weight. Flow is mostly laminar, although it can be partially turbulent on steep slopes. Deposition occurs en masse, because solid and liquid components move together as a coherent flow. Resulting deposits exhibit grading and fabric which are imparted by flow mechanisms while the flow was in motion. Debris flows are ideally considered to be cohesive flows which exhibit internal strength and resistance to shear. Resulting deposits are ideally described as matrix-supported with poorly sorted clasts floating in a poorly sorted matrix. These qualities are attributed to sediment gravity flows with a cohesive matrix containing some amount of clay. However, many volcanic debris flows are clay poor (Fisher and Schminke, 1984; Smith, 1986; Smith and Lowe, 1991) because they form by the mobilization of fresh debris on the steep flanks of volcanoes. Many are coarse-grained and clast-rich, containing a low percentage of fine material which is mostly ash. Coarse-grained debris flows have higher internal pore pressure which acts as a bouyant force on

large boulders and facilitates flow on low gradient slopes (Pierson, 1981). Shear resistance is imparted by grain to grain collisions in a non-cohesive fashion. Because internal strength is common to debris flows, they are capable of transporting clasts 3 m or more in diameter. Large in both volume and discharge, volcanically derived debris flows tend to travel large distances. Resulting deposits are often poorly sorted and may have inverse or inverse-to-normal grading. They are commonly clast-supported although the degree of clast support may vary.

Debris avalanches are considered a dominant mechanism in the evolution of volcanoes (Palmer and others, 1991). They may be triggered by volcanic eruptions such as the May 8, 1980 eruption at Mount St. Helens (Voight and others, 1981). Avalanche debris is derived from the collapse of a volcanic edifice, and may introduce large amounts of sediment to an alluvial system, triggering debris flows. Because volcanic regions are seldom arid, debris flows are commonly diluted with water to hyperconcentrated flow by traveling down stream channels.

Transitional stages between debris flow and hyperconcentrated flow processes are a reflection of the gradual variations in sediment/water concentration common in volcanic settings (Figure 8). Hyperconcentrated flow may also transform to debris flow by incorporating loose sediment into the flow or by the loss of water infiltrating into the substrate. Water-mobilized flow processes depend upon the concentration of sediment in water, abundance of clay minerals, and grain-size distribution of the flow (Smith and Lowe, 1991).

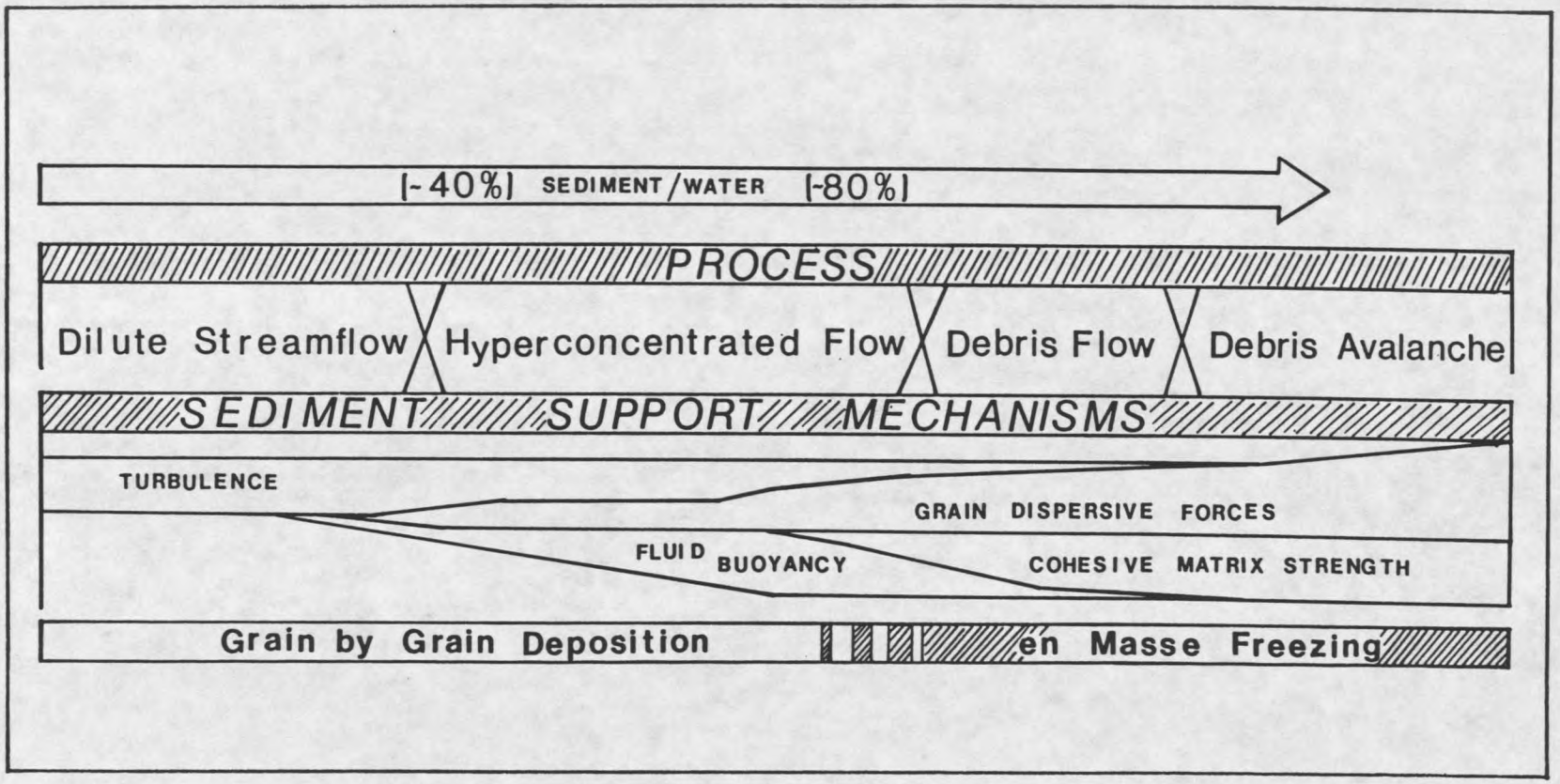


Figure 8. Schematic diagram showing transitions between flow processes with a variable sediment to water ratio and illustrating sediment support and depositional mechanisms. The degree of importance of each type of mechanism is indicated by bar thickness (after Smith and Lowe, 1991).

SEDIMENTOLOGY

General Character of the Deposits

Volcaniclastic sequences within the Hyalite Peak Volcanics have a similar overall appearance from outcrop to outcrop. However, upon examination of structures and fabric, they appear quite distinct from one another. Most of the deposits studied are tabular within the mesoscopic scale of the observation (distances of 10 m across), but thin or thicken laterally over distances of 30 to 50 m and appear to be more wedge-shaped when exposures are more extensive. Bed thickness varies from 5 cm to almost 70 m, but are more commonly from 0.5 to 2.0 m thick. Contacts between deposits are characteristically sharp, nonerosional and planar. Deposits rarely fill channels and channel fill is not peculiar to any one type of lithofacies. Individual units may grade laterally from one lithofacies to another. Internal boundaries within units can be sharp even though they are difficult to trace laterally. Non-volcanic clasts within these units are rare, variable in size, and can be found at the base of a stratigraphic section or up to 250 m above it. Although the deposits are predominantly coarse-grained, consisting mostly of angular to subangular gravel with clasts which are more than 98% volcanic in origin, they display a variety of patterns in grading, grain-size distribution, and distribution of clast lithologies which are used to categorize them as separate lithofacies.

Coarse-Grained Lithofacies

Gravel, Massive, Poorly-Sorted, Volcanic (Gmpv):

Variable from clast to matrix support both vertically and laterally, units contain gravel which may be very angular to subrounded. Locally, some clasts are flattened or distorted and have very delicate outlines indicating that they may have flowed after deposition, others are fragmented in a "jigsaw" fashion, such that adjacent particles can

be visually restored into one clast. Clasts are in some cases monolithologic throughout the entire unit, and some units have localized areas within them which are monolithologic. More commonly clast types vary, consisting of cauliflower bombs of basalt or andesite, scoria, rimmed volcaniclastic boulders, petrified logs, and other various volcanic and non-volcanic lithologies. Matrix color is variable, with a streaked appearance, changing from grey, yellow, orange, and brick red to brown within a single unit. Matrix consists of silt with variable amounts of angular coarse sand. Some units have regions or blotches of a specific color (dark grey, red, or orange) which have a single lithology or group of lithologies different than the area surrounding these regions. Units are massive, and tend to be very poorly sorted, containing clasts up to 3 m in diameter or more. They may be tens of meters thick without any apparent stratigraphic breaks and laterally continuous within the limits of the outcrop exposure (tens of meters). The distinct textural characteristics of this lithofacies are illustrated in Figure 9.

Although this lithofacies is comprised of only eight individual units, they make up a large portion of measured section thickness and volume. The average unit thickness is 21.74 m. The thickest unit (69.3 m) of this lithofacies is located at Antelope Butte, and is the thickest unit of any lithofacies described herein. Even though this unit is more than 200 m above the base of the measured section, it contains boulders of Precambrian phyllite, and Paleozoic oolitic, fossiliferous and silty limestone, and limestone conglomerate. Some limestone clasts within this unit are up to a meter in diameter. It also contains rounded andesite boulders with radial prismatic joints. The upper surface of the deposit is irregular and undulatory. Other units of this lithofacies type are located in measured sections at Palisade Mountain. Although they share the same basic characteristics, they contain clasts which are only of volcanic or volcaniclastic origin. Clasts are predominantly very angular and fragmented, although some are rounded and scoriacious. Large boulders within the units at Palisade Mountain are volcaniclastic blocks >3 m in diameter. Some have discoloration rims and appear to be altered. Where exposed, units at Palisade Mountain have planar upper and lower contacts, but many of these dip sharply to the south.

Interpretation: Gmpv facies deposits resemble those resulting from both hot and cold debris avalanches and brecciated lava flows. Although some units of this lithofacies are clearly the result of one process in particular, other units exhibit characteristics which could have resulted from their combination. The debris avalanche matrix facies of Crandell and others, (1984) is described as an unsorted unstratified mixture of volcanic clasts, in which additional clasts as a secondary component, may be incorporated from the

ground surface during movement (Palmer and others, 1991). Matrix facies may also include shattered tree trunks (Voight and others, 1983). It is likely that moving avalanche debris plucked out surface materials, including timber, which are found in the deposit at Antelope Butte. Thicknesses exceeding 50 m are described by Crandell and others (1984) in debris avalanche deposits of Mt. Shasta, which is consistent with extreme thickness of some units of Gmpv lithofacies. Wavy pressure ridges and wrinkles perpendicular to flow (Endo and others, 1989) and hummocky upper surfaces (Crandell and others, 1984) found in some debris avalanche deposits are consistent with irregular upper contacts of deposits of this lithofacies. Flat upper surfaces of some of these deposits may be due to post-depositional erosion by fluid flow succeeding the debris avalanche as described by Endo and others (1989). Debris avalanches may also contain vari-colored monolithologic patches caused by incomplete mixing of avalanche material (Ui, 1983) which are considered in some cases to be brecciated megaclasts (Glicken, 1991). Vari-colored stripes or ridges within the deposits are described by Endo and others (1989) from a modern debris avalanche as layers of elongate deposits which parallel flow direction. These features are characteristic of deposits of this lithofacies found at Palisade Mountain.

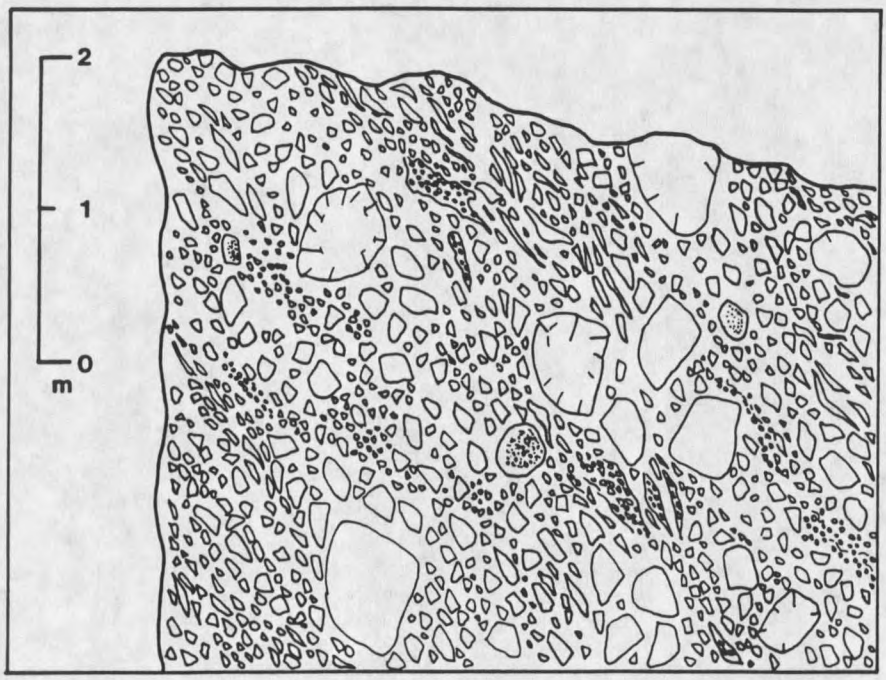


Figure 9. Sketch showing textural features typical of Gmpv (gravel, massive, poorly-sorted, volcanic) lithofacies. These units are not common, but make up a large volume of the deposits because of individual unit thickness, which averages more than 20 m.

Some of the Gmpv lithofacies deposits contain strong evidence that they were deposited as hot material. Some units of this lithofacies contain bread-crusted clasts, clasts with radial prismatic jointing, and distorted clasts with delicate outlines. Eruptive activity may have triggered debris avalanches which then incorporated hot pyroclastic material into the resulting deposits. Alternatively, some of the deposits of this lithofacies may contain some component of pyroclastic lag deposits similar to those deposited on crests of irregular hills of debris avalanche deposits at Mount St. Helens (Rowley and others, 1981). Lithic clasts within these deposits may originate from the upper volcano flanks, be incorporated into an avalanche from the disrupted dome and vent filling material, or torn directly from the sides of the vent during explosion and collapse of a volcanic edifice. Metamorphic amphibolite clasts derived from great depth were incorporated into the pyroclastic material at Mount St. Helens during the 1980 eruption (Rowley and others, 1981). Similarly, Gmpv deposits at Antelope Butte contain large limestone and phyllite clasts 250 m above the base of the measured section, and an unknown greater distance above the base of the volcanic pile deposited there. These clasts may be derived from disruption of prevolcanic deposits brought to the surface as shallowly derived xenoliths during an eruptive phase.

Monolithologic units of Gmpv lithofacies are interpreted to be autoclastic flow breccia which results from fragmentation by mechanical friction of a viscous lava flow, gaseous explosion during movement of lava, or gravitational crumbling of spines or domes (Fisher and Schmincke, 1984). Paleomagnetic drill sampling of Gmpv lithofacies may be helpful in determining how hot units or portions of this lithofacies may have been during deposition.

Gravel, Matrix-Supported (Gms):

This facies consists of massive or structureless matrix-supported gravel in which both clasts and matrix are characterized by very poor sorting (Rust, 1978). Clasts are angular to rounded. Matrix consists of silt and fine to coarse sand with minor clay. Textural characteristics typical of this lithofacies are illustrated in Figure 10. Units within this lithofacies, at Eight Mile Canyon and Windy Pass, typically have white subrounded tuff and pumice fragments of granule to cobble size intermixed with angular clasts of grey, purple, red and black andesite, and light grey dacite. The matrix is typically

pink, weathering to orange and grey, and is comprised of silt, biotite, and minor amounts of poorly-sorted fine to coarse angular sand. In contrast, units of this lithofacies located at Antelope Butte and Flanders Mountain are predominantly tan to grey-brown with a silty matrix of more than 50% poorly-sorted sand. The same clast types are present, but white tuff is less abundant. Units at Antelope Butte also contain rare clasts of non-volcanic green siltstone, and commonly have petrified fragmented wood at the base. At Palisade Mountain this lithofacies is characterized by units containing very angular clasts, and white tuff is rare. Pumice is absent, with the exception of one subrounded clast 20 cm in diameter. Individual beds from all locations average 1.21 m thick, although some located at Antelope Butte are as thin as 0.05 m. Most units within this lithofacies are tabular, although a small number of the units at Windy Pass and Eight Mile Canyon have a channel-fill geometry.

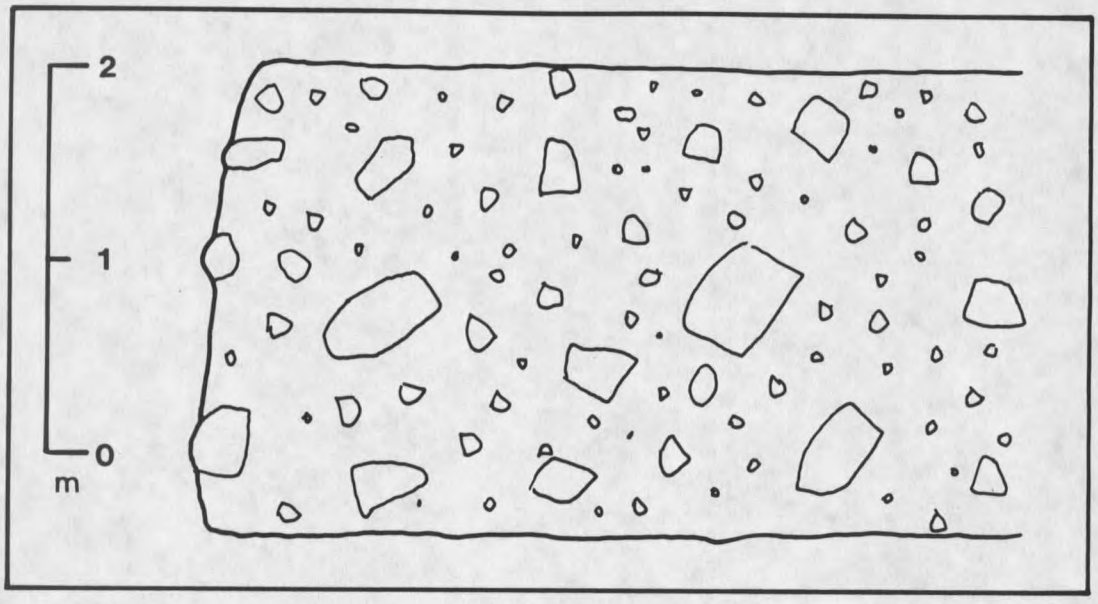


Figure 10. Sketch showing typical textural features of Gms (gravel, matrix-supported) lithofacies. This lithofacies comprises a small percentage of described deposits. Average thickness = 1.2 m.

Interpretation: This lithofacies is interpreted as having characteristics indicative of debris flow or pyroclastic flow deposition. Poorly-sorted matrix and clasts indicate that deposits resulted from non-Newtonian, non-turbulent, laminar flow, with deposits resulting from en masse freezing of sediment (Smith, 1986). A matrix-supported fabric implies that the flows were cohesive and that matrix strength and bouyancy were

dominant mechanisms during transport (Lowe, 1979). Units of this lithofacies containing large pumice clasts (>4 cm) are more likely to be pyroclastic flows than those without pumice. However, some pyroclastic flows are lithic rich, with little or no pumice (Buesch, 1992). Textural and structural criteria available to distinguish non-welded pyroclastic flow deposits from debris flow deposits are often non-exsistent (Sparks and others, 1973, Sparks, 1976). Paleomagnetic sampling may distinguish hot pyroclastic flows from cold pumice-rich debris flows. However, flow temperature within some pyroclastic flows has been estimated to be less than 200° C (Freundt and Schmincke, 1986).

Distinct lithologies found within debris flows of this lithofacies are indicative of distinct source areas in which the source rock may have higher amounts of fine-grained materials, including clay derived from hydrothermal alteration or surficial weathering. Clay content as low as 3% can be critical in determining the matrix strength and cohesive properties of a debris flow (Rodine and Johnson, 1976).

Gravel, Clast-Supported at Base, Transitional to Matrix-Supported in Upper Part (Gcms):

The upper portion of units of this lithofacies is matrix-supported and clast poor overall, generally with less than 15% clasts, even though clasts are sometimes clustered together with tangential contacts. The lower portion of these units is clast rich, and clast-supported toward the base. Units of Gcms lithofacies typically contain sub-rounded to angular clasts which are less than 10 cm in diameter, poorly sorted and non-graded. In some cases the base of the unit contains rip-up clasts from the unit below (Figure 11). The matrix consists of silt and poorly sorted fine to coarse sand. Units classified as part of this lithofacies are rare, occurring only at Antelope Butte. Generally, they average 2 m in thickness with a tabular geometry and sharp planar or erosional bases.

Interpretation: A matrix-supported fabric is indicative of deposition from a cohesive debris flow (Miall, 1977; Lowe, 1979) or a pyroclastic flow (Freund and Schmincke, 1986) However, a clast rich basal fabric which may include rip up clasts from lower units indicates that the flow was eroding and entraining material from the substrate. Bulking of the flow through addition of loose or eroded material implies that the flow was partially turbulent. This could result from a non-plug phase or more fluid pulse within the flow, an increase in velocity due to an increase in slope, or the breaching of an obstruction. Although characteristics of the deposits imply turbulence or increased

fluidity, they are still indicative of laminar flow processes. The lack of normal grading of clasts within units of the Gcms lithofacies indicates that particles were not deposited individually as they dropped out of suspension from within a fluid; instead, the flow "froze in place", preserving a fabric characterizing flow processes rather than depositional processes.

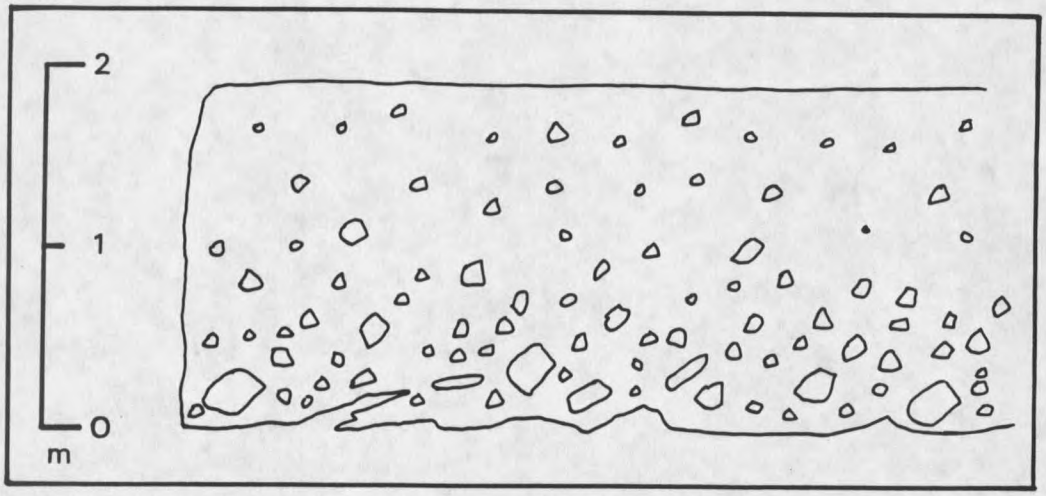


Figure 11. Textural features typical of Gcms lithofacies (gravel, clast-supported at base, transitional to matrix-supported in upper part). These units are described from deposits at Antelope Butte. Average thickness = 1.9 m.

Gravel, Matrix-Supported, with Clast-Supported Normally Graded Base (Gmsn):

The upper portion of units of this lithofacies is matrix-supported and typically contains pebbles or granules with outsized clasts up to 10 cm. Units are transitional to clast-support at the base, with an average clast size of 5 to 10 cm at the bottom of the normally graded portion (Figure 12). Clasts are subangular to rounded, and larger clasts up to 30 cm in diameter are rare. The matrix consists of silt with variable amounts of poorly-sorted fine to coarse sand. Observed units do not occur widely, and descriptions are restricted to those found at Antelope Butte and Eight Mile Canyon. Units tend to be thin, with an average thickness of less than 0.5 m. Contacts between units tend to be sharp and planar.

Interpretation: Although units of Gmsn lithofacies have a matrix-supported fabric, clasts within the upper part are typically small (< 3 cm in diameter). The characteristics of these deposits are interpreted as resulting from deposition during conditions of hyperconcentrated flow rather than debris flow. Particle entrainment is more likely due

to dampened turbulence of a viscous fluid combined with dispersive pressure. Traction transport of clasts is likely reflected by the base of the unit. Normal grading indicates that larger clasts were deposited first: deposition took place in a progression from larger to smaller rock fragments in a grain-by-grain fashion as the flow lost energy. Progressive deposition of clasts may have been the result of flow dilution. Alternatively, deposition may have resulted from a decrease in flow discharge, possibly by partial obstruction of the flow or decreasing gradient. The thinness of the deposits may be an indication of fluidity of the flow, or indicate that channelized flow occurring upslope lost energy as it was transformed to unconfined flow. Normal grading within the flow indicates that the flow was not deposited en masse; however, a transition to matrix support within the upper part of the deposit also implies that flow was not fully turbulent.

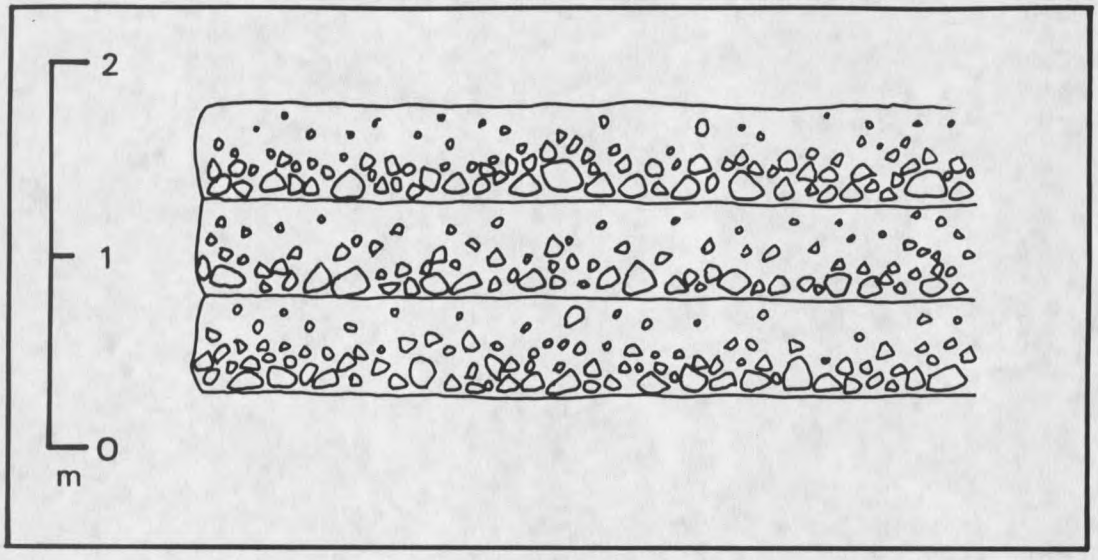


Figure 12. Textural features typical of Gmsn lithofacies (gravel, matrix supported with clast-supported, normally-graded base). Deposits of this lithofacies are found at Antelope Butte and Eight Mile Canyon. Average thickness = 0.5 m.

Gravel, Matrix-Supported at Base,
Inversely-Graded to Clast-Supported (Gmsi):

Units of this lithofacies exhibit an upward transition from a matrix- to clast-supported fabric. The amount of clast support is variable; the upper clast-supported portion typically encompasses the upper 10% to 60% of the unit. Matrix consists primarily of silt with small, but variable amounts of angular, poorly-sorted, fine to coarse

sand. Units may sometimes be inversely-graded, or rarely exhibit inverse to normal grading with the normally-graded upper portion being clast-supported (Figure 13). Clasts tend to be small and angular. Maximum clast size for units observed is 40 cm, but large clasts are more commonly from 5 to 10 cm in diameter. They usually consist of small, rounded, granule to pebble size tuff fragments, and angular red, black and purple andesite and light grey dacite. The upper part of the units commonly exhibit an increase in the proportion of non-tuffaceous to tuffaceous clasts. Unit color varies with matrix color and may be pink, tan, or light grey. The matrix in deposits of this lithofacies at Silken Skein Falls contains euhedral hornblende phenocrysts. Units of this lithofacies are commonly wedge-shaped, occasionally with undulating lower contacts.

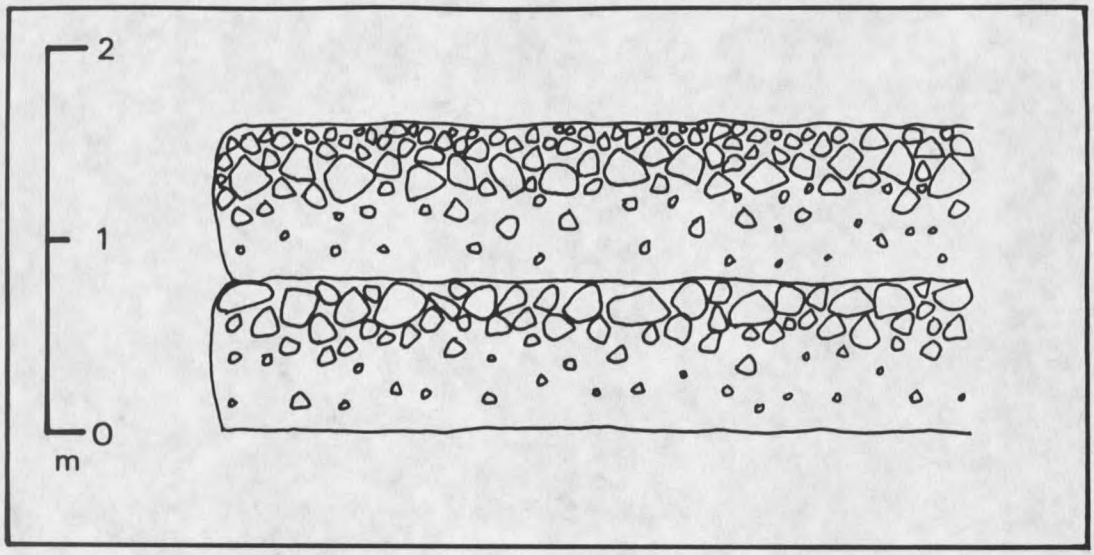


Figure 13. Sketch showing textural fabric typical of Gmsi lithofacies (gravel, matrix-supported at base, inversely-graded to clast-supported). Units of this lithofacies are found at Antelope Butte, Eight Mile Canyon and Silken Skein Falls. Average thickness = 0.8 m.

Interpretation: Gmsi lithofacies is interpreted as resulting from deposition by debris flows or pyroclastic flows. Alternatively, deposition may have resulted from a combination of debris flow and hyperconcentrated flow. A matrix-supported depositional fabric results from laminar cohesive processes (Lowe, 1979; Smith, 1986). Clast-supported normal grading found at the top of some units may be caused by segregation within the flow; the upper portion may have been less dense and more fluid than the matrix-supported lower portion. Because the lower portion was dense and viscous, it acted as a barrier to fluid migration. Density stratification within modern pyroclastic

flows is common, and is attributed to topographic controls. The matrix-supported lower portion of the beds, which is increasingly clast rich toward the upper surface, may also form by a number of debris flow processes. These include clast bouyancy in a viscous flow, shear within the flow along any horizon due to vertical changes in flow velocity, and by kinetic sieving. Kinetic sieving is a process resulting from particle agitation, allowing small clasts to pass downward through the interstices between larger clasts that, as a result, migrate upward during flow movement (Middleton, 1970). Alternatively, if the base of the debris flow were diluted to hyperconcentrated flow, larger clasts would drop out, being deposited and left behind the flow. This would probably cause the lower part of the flow to initially exhibit normal grading, but eventually the clasts from the lower half could completely drop out, resulting in a flow devoid of clasts in the lower portion, as in the "transition facies" of Scott (1988).

Gravel, Clast-Supported with Inverse Coarse-Tail Grading (Gmci):

Units of this lithofacies are inversely graded. Outsized clasts at the top of units are common, and typically 0.5 to 1.0 m in diameter, but can be 2.0 to 3.0 m in diameter and often protrude into units above. Large clasts at the top of units are commonly from 10 to 50 cm in diameter, grading upward from granule sized clasts above a fine-grained base which is usually 10 to 20 cm thick. These distinctive texural characteristics are illustrated in Figure 14. Smaller clasts tend to be very angular, with increased rounding proportional to grain size. Boulders are usually subrounded. Elongate clasts from cobble to boulder size commonly exhibit subhorizontal alignment. The matrix consists of silt and very poorly sorted, fine to coarse sand in variable proportions, with silt commonly constituting 20 to 50% of the matrix (based on visual estimates). Angular pebbles and matrix are usually well intermixed throughout individual units. Bed thicknesses average 1.2 m, and rarely are more than 3.5 m or less than 0.5 m. Grading tends to be more gradual in thicker units. Individual units appear tabular for tens of meters, but thin and thicken laterally over greater distances. The same unit may appear tabular or wedge-shaped depending upon the viewing perspective. Contacts between units are commonly planar and are often sharp.

This lithofacies is extremely common, being the most abundant in number of individual units as well as constituting the greatest thickness of measured section. In units studied at Eight Mile Canyon and Antelope Butte clasts of white tuff and pumice

common to other lithofacies units are rare, whereas black, grey and red andesite clasts are common. Units of these lithofacies at Flanders Mountain and Silken Skein Falls commonly contain pumice granules and petrified logs and fragments of wood. Some of the wood is not petrified, and is either carbonized or charred. Trunks of trees which are often not petrified are buried upright within units of this lithofacies at Flanders Mountain and at Silken Skein Falls. In some of these units, fragments of black, friable wood are commonly associated with fluid escape structures located immediately above them or sometimes surrounding them. Lower in the measured sections at both locations, fine-grained units of this lithofacies are a distinctive yellow-brown and are palagonitized. The matrix of units of this lithofacies at Silken Skein Falls contain euhedral phenocrysts of hornblende and plagioclase.

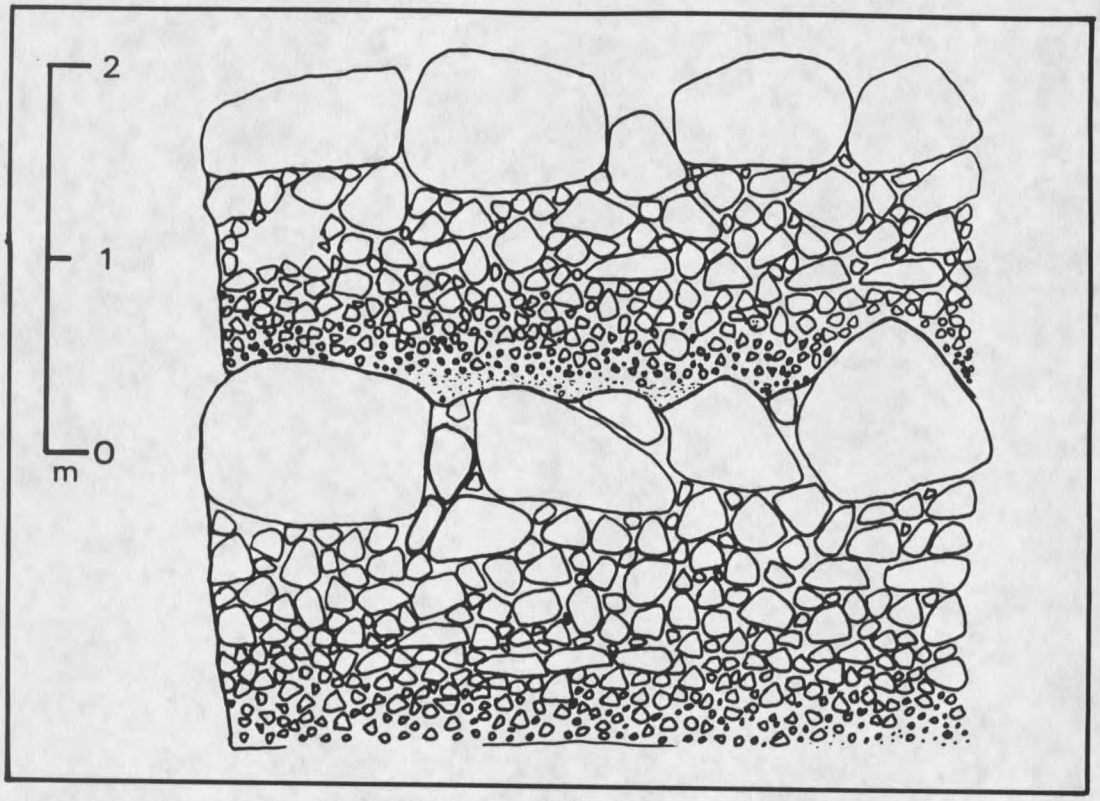


Figure 14. Sketch of typical texture of Gmci lithofacies (gravel, clast-supported with inverse coarse-tail grading). Units of this lithofacies are widespread and numerous, found within measured sections at Silken Skein Falls, Flanders Mountain, Eight Mile Canyon and Antelope Butte. Average thickness = 1.2 m.

Interpretation: Deposits classified as Gmci lithofacies units are interpreted as resulting from deposition by non-cohesive debris flows. In coarse-grained sediment gravity flows that contain little clay, cohesion plays a minor role in imparting strength to

the flow. Instead, pore pressure between clasts and clast bouyancy become important factors (Pierson, 1981), enabling coarse-grained flows to transport large clasts at the top of the flow. Inverse grading within these deposits is formed by a combination of processes. When particles of mixed grain size are sheared together, larger grains drift to the zone of least shear strain, which is the free surface (Naylor, 1980). Agitated, small particles pass through the interstices between larger particles by kinetic sieving (Middleton, 1970). In addition, dispersive pressure, caused by interparticle collisions may cause inverse grading in cohesionless flows because of its increased effect on larger particles. Because shearing within a flow decreases upward, inverse grading throughout an individual unit is possible, but is more pronounced at the base. Shearing may take place at any horizon due to zones of changing velocity within a flow, as in cases where the flow moves over an obstruction. Rotation of elongate particles occurs in velocity gradients (Naylor, 1980) due to differences in shear velocity, and may result in orientation of elongate clasts parallel to flow. The base of the deposits, where shear is greatest, are fine-grained and consist mostly of sand and pebbles. Shearing may cause clast migration upward into the flow. Alternatively, because the bottom of the flow is a basal zone of intense shear causing a marked decrease in strength (Hampton, 1975), it may be unable to transport large clasts, which would drop out of the base of the flow.

Units of this lithofacies at Silken Skein Falls show evidence that they may have been deposited while hot. This implies that they may be pyroclastic flow deposits. Palagonitization of lower units at Silken Skein Falls and Flanders Mountain implies that steam may have increased hydration of volcanic glass within these deposits. Textural differences include a thicker fine-grained basal shear zone, and zones below upper bedding surfaces which do not have clearly defined inverse grading, but are more massive. It is possible that steam acted to enhance clast mobility and that bouyancy reduced the amount of kinetic sieving and shearing between clasts. Deposits of Gmci lithofacies exhibit characteristics indicative of cohesionless, coarse-grained sediment gravity flows which, because of internal strength, have the ability to transport clasts > 2 m. Internal fabric of the deposits suggest that they undergo shear along different horizons during laminar flow movement, and are therefore interpreted as resulting from debris flow or pyroclastic flow deposition.

Gravel, Massive, Poorly-Sorted (Gmp):

Units of this lithofacies are clast-supported, with no internal structure or fabric evident. Clasts and matrix both are typically very poorly-sorted. Clasts are commonly subangular to subrounded; larger clasts tend to be more rounded and may be 1 m in diameter or larger. Typical textural features of this lithofacies are illustrated in Figure 15. Units of this lithofacies can be either matrix poor or matrix rich, with matrix consisting of silt and fine- to coarse-grained very poorly sorted sand. Units of this lithofacies are widespread and present within every measured section, except Palisade Mountain. Clasts commonly are of durable types, consisting of black, red, and dark grey andesite and light grey dacite, with rare volcanic bombs and vesicular andesite or basalt. Some units of this lithofacies measured at Antelope Butte contain andesite clasts with radial prismatic jointing. Units of this lithofacies may be up to 13 m thick, but are generally between 1 and 6 m. Upper surfaces of bedding contacts may be planar or irregular; lower contacts are commonly planar.

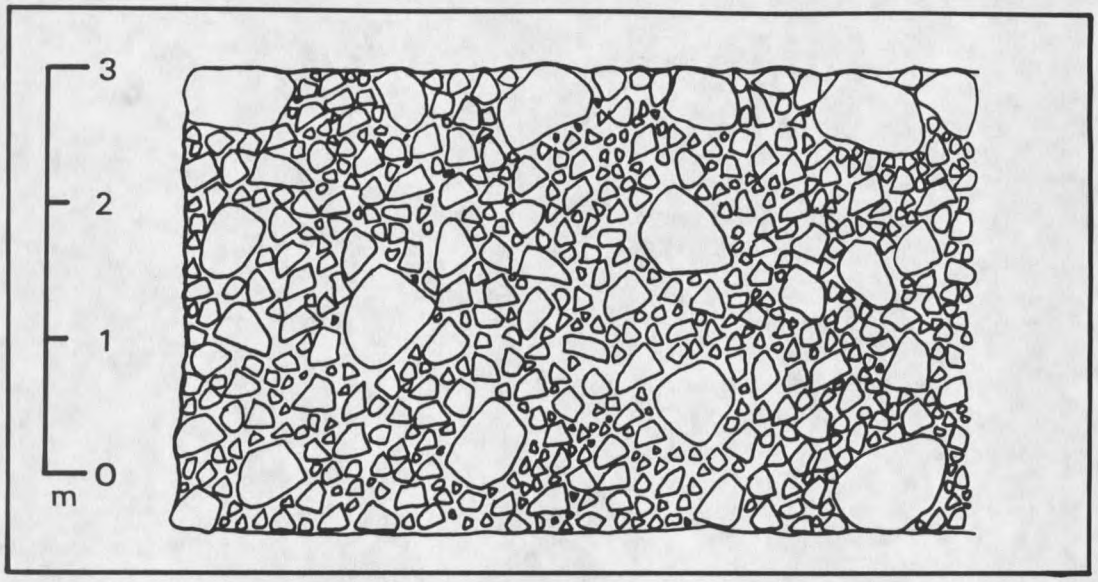


Figure 15. Sketch of textural features of Gmp lithofacies (gravel, massive, poorly-sorted) illustrating a matrix-poor deposit. Deposits of this lithofacies are common, widespread, and may be matrix-rich or matrix-poor. Average thickness = 3.6 m.

Interpretation: Gmp lithofacies are interpreted as pyroclastic lag deposits, or as a result of deposition from debris flows through a variety of processes. Medial facies deposits of non-welded pyroclastic flows commonly contain lithic clasts not present in

the distal facies, which are assumed to have dropped out during flow movement (Fisher, 1986; Freund and Schmincke, 1986). Extremely poor sorting indicates that differential movement between clasts was not likely. However, because clasts with radial prismatic jointing are present in some of the units of this lithofacies, there may have been enough heat to impart mobility (Arguden and Rudolfo, 1990). Steam in the interstices between fine particles in these units, along with water, could cause flow dilation, acting as part of the matrix which would eventually dissipate, resulting in deposition of a unit with a clast-supported fabric. Conversely, variability in the degree of clast support and percentage of matrix may be a reflection of differences among debris flow processes, or may also be due to the amount of interstitial fluid dilating and mobilizing the debris flow which drains away subsequent to flow deposition. Pierson (1985) described poorly-sorted, non-stratified debris flow deposits, resulting from the 1980 eruption of Mount St. Helens, which were thin relative to flow depth. A clast-supported fabric may also result from deposition of a clast-rich zone of laminar plug flow within a debris flow that "freezes" in place. Alternatively, deposits of this lithofacies may result from debris flow levee deposition: during movement of a debris flow, clasts positioned at the flow front and sides were pushed aside of the advancing plug, leaving clast-supported, poorly sorted deposits. Gmp lithofacies deposits probably result from a variety of debris flow depositional processes. Individual deposits may have been produced by a combination of these processes, or by any single process mentioned above.

Gravel, Massive, Poorly-Sorted, Imbricated (Gmpi):

Units of this lithofacies are clast-supported. Although generally massive, deposits may exhibit discontinuous subhorizontal stratification and grading, often variable within lateral distances of less than 2.0 m. Units of this lithofacies often exhibit subtle distribution inverse grading, and generally contain a higher percentage of matrix towards the base. Clasts up to 30 cm in diameter often exhibit imbrication in the long axis direction. Textural characteristics of this lithofacies are illustrated in Figure 16. The matrix usually consists of poorly-sorted, fine to coarse sand with less than 50% silt. Units are variable in thickness and often wedge-shaped, pinching-out laterally. Lower contacts may be undulatory or planar. Units of this lithofacies at Silken Skein Falls, where it is most abundant, contain glass fragments with alteration rims. Occasionally they contain

white pumice fragments, euhedral phenocrysts of hornblende and plagioclase, and charred pieces of wood.

Interpretation: Units of Gmpi lithofacies exhibit a large degree of variability reflecting differences between debris flow and hyperconcentrated flow depositional processes, and represent a transitional phase between the two. Alternatively, some units of this lithofacies may be pyroclastic flow deposits. Inverse grading within many of the units indicates that pore pressure, bouyancy, dispersive pressure and internal shear may have been interactive processes within the moving flow. Clasts which are imbricated in the long axis direction result from flow turbulence. In deposits such as those at Silken Skein Falls, which may also have been hot, turbulence may be accompanied by increased bouyancy of clasts, increased mobility of flows, and flow dilation (Arguden and Rudolfo, 1990). This may account for deposition of clasts exhibiting long axis imbrication which are 0.5 m long or more.

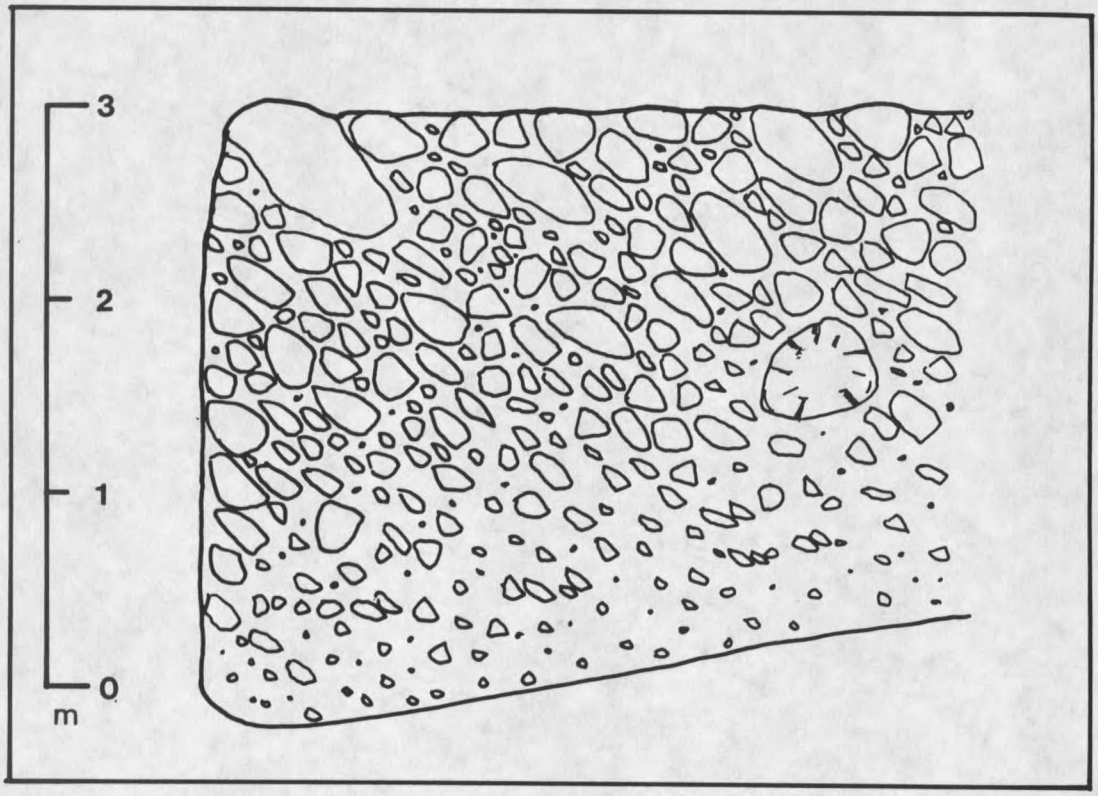


Figure 16. Sketch of textural features typical of Gmpi lithofacies (gravel, massive, poorly-sorted, imbricated). Units of this lithofacies are widespread. Average thickness = 3.3 m.

Gravel, Massive (Gm):

Units of this lithofacies are clast-supported and ungraded, with a matrix of poorly to moderately sorted, fine to medium sand (Miall, 1977). Characteristics of this lithofacies are illustrated in Figure 17. Deposits of Gm lithofacies generally have subrounded to rounded clasts in greater quantities than other lithofacies types, although some have abundant angular clasts. Clasts are generally moderately sorted. Average clast size is sometimes variable laterally. However, maximum clast size never exceeds 1.0 m. Units of this lithofacies are widespread and are found in all of the measured sections with the exception of Palisade Mountain I. Although beds vary widely in thickness, they are more commonly between 0.5 and 2.0 m thick with an average thickness of 1.2 m and are either tabular or have a channel cross section geometry. In Antelope Butte measured section I, units of this lithofacies contain well-rounded Precambrian quartzite clasts.

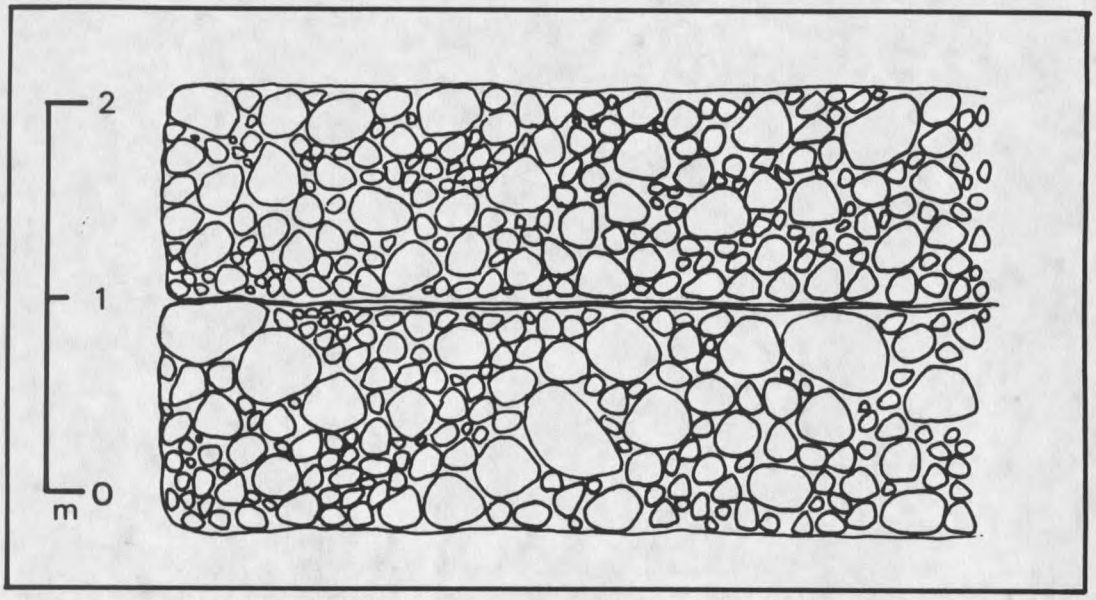


Figure 17. Sketch of textural features typical of tabular deposits of Gm lithofacies (gravel, massive). Deposits of this lithofacies are not numerous, but are widespread, found in each area where measured sections were described. Average thickness = 1.2 m.

Interpretation: Units of Gm lithofacies are interpreted as longitudinal bar deposits (Miall, 1977) which accumulated during conditions of normal streamflow. Deposits of Gm lithofacies accumulated by clast-by-clast accretion over lag deposits or channel

obstructions (Miall, 1977); sand and pebbles subsequently become trapped within the clast framework as velocity decreases. This process is not conducive to development of well-developed stratification in the deposits, which is absent from units of Gm lithofacies observed within the measured sections.

Gravel, Massive, Well-Sorted (Gmw):

Units of this lithofacies are clast-supported and ungraded. Clasts are commonly angular to subangular and may be monolithologic, usually consisting of durable lithologies. Clast size is fairly constant, averaging of 4 to 6 cm in diameter, with a maximum diameter of 10 cm. Units are generally devoid of granules and pebbles and contain a low percentage of matrix (<15%) which consists of silt and poorly-sorted fine to medium sand. Units are thin and tabular, but occasionally are found within channel-shaped bodies (Figure 18). From 0.05 to 2.0 m thick, they average 0.5 m in thickness.

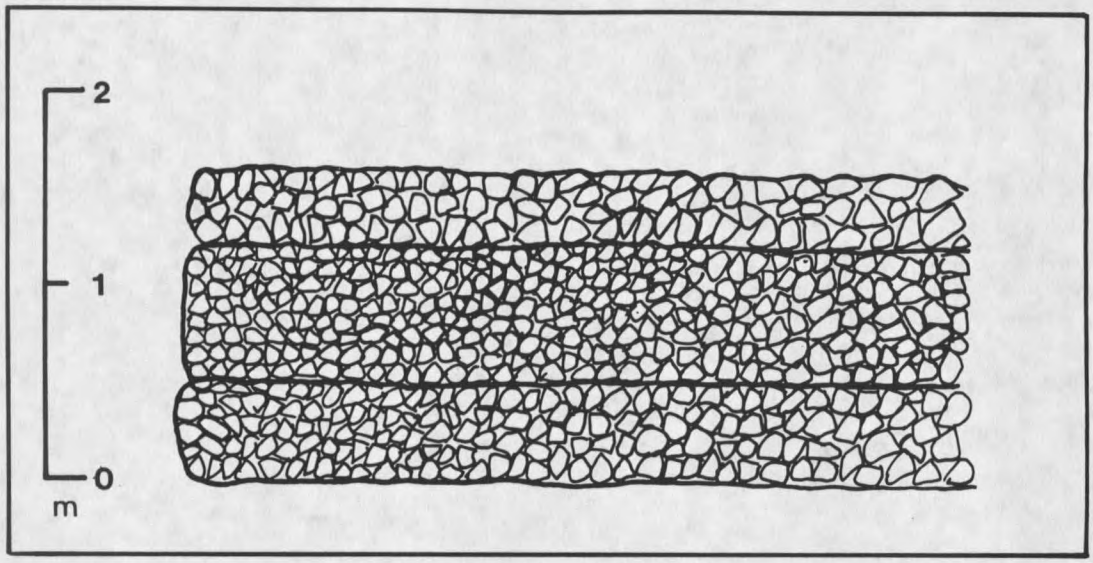


Figure 18. Sketch of typical textural features of tabular deposits of Gmw lithofacies (gravel, massive, well-sorted). Deposits of this lithofacies are found at Windy Pass, Silken Skein Falls, Flanders Mountain and Antelope Butte. Average thickness = 0.5 m.

Interpretation: Lithofacies Gmw is interpreted as having formed during flow dilution. Deposition of a fairly constant, well-sorted clast size is an indication of the inability of a flow to continue to transport clasts within that size range. Clast deposition

could have been the result of waning flow energy, but that hypothesis seems unlikely. Rather than leveling off at a slightly lower, but fairly constant value, decreasing flow energy tends to be pronounced and would probably result in the deposition of clasts from more than one size range. It is more likely that clast size sorting would result from flow dilution, causing a decreased but fairly constant amount of flow viscosity, bouyancy and dispersive pressure. Because clasts within these deposits rarely exceed 10 cm, they may originate as basal clasts from pyroclastic flows or from diluting inversely graded debris flows. It is also possible that, as hyperconcentrated flow becomes increasingly more diluted by available water, deposition of clasts within a particular size range could take place.

Gravel, Massive, Well-Sorted Tephra (Gmwt):

These units are clast-supported and sometimes graded. This lithofacies consists almost exclusively of angular pumice lapilli from 1 to 3 cm in diameter, although they also contain small angular lithic fragments which are 2 to 5 mm in diameter . Units are from 4 to 15 cm thick and are extremely matrix poor (Figure 19). Units of this lithofacies are extremely rare, found only within the Windy Pass measured section.

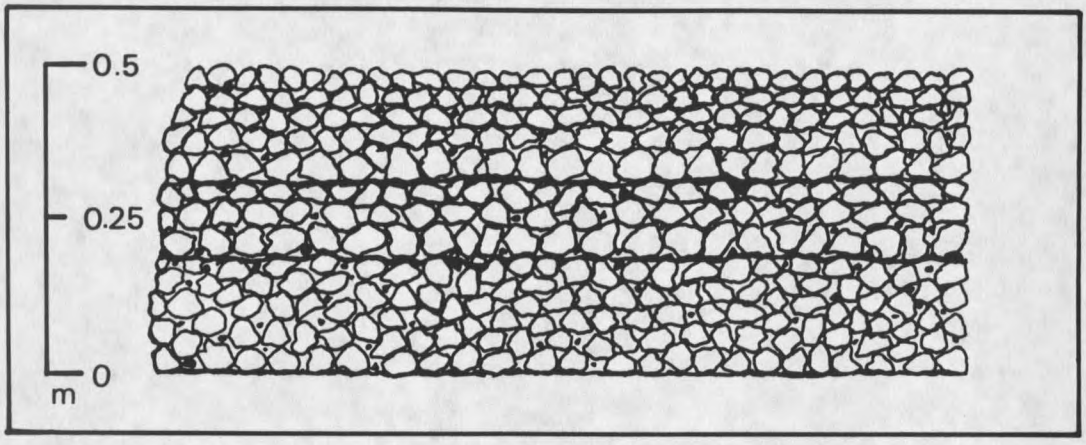


Figure 19. Sketch of textural features of Gmwt lithofacies. Units of this lithofacies are found at Windy Pass. Average thickness = 0.1 m.

Interpretation: Units of this lithofacies are considered lapilli-fall tuff. These thin units are devoid of matrix and consist of delicate angular pumice which would not

withstand transport within a flow. In addition, they are well-sorted, probably as a result of fall-out from an eruption column.

Gravel, Massive, Clast-Supported, with Normal Coarse-Tail Grading (Gmcn):

Clasts in units of this lithofacies may be angular to subrounded, are rarely as large as 0.5 m in diameter, and consist primarily of durable flow rock lithologies. Units generally contain a low percentage of matrix (<20%) which is poorly-sorted and consists of silt and fine to coarse sand. Beds are commonly tabular within the limits of outcrop exposure; however, rare units are wedge-shaped or lenticular in lateral exposures of tens of meters. Average thickness is 1.3 m, but is variable within measured sections; measured beds are from 0.1 to 3.4 m thick. General textural characteristics of this lithofacies are illustrated in Figure 20.

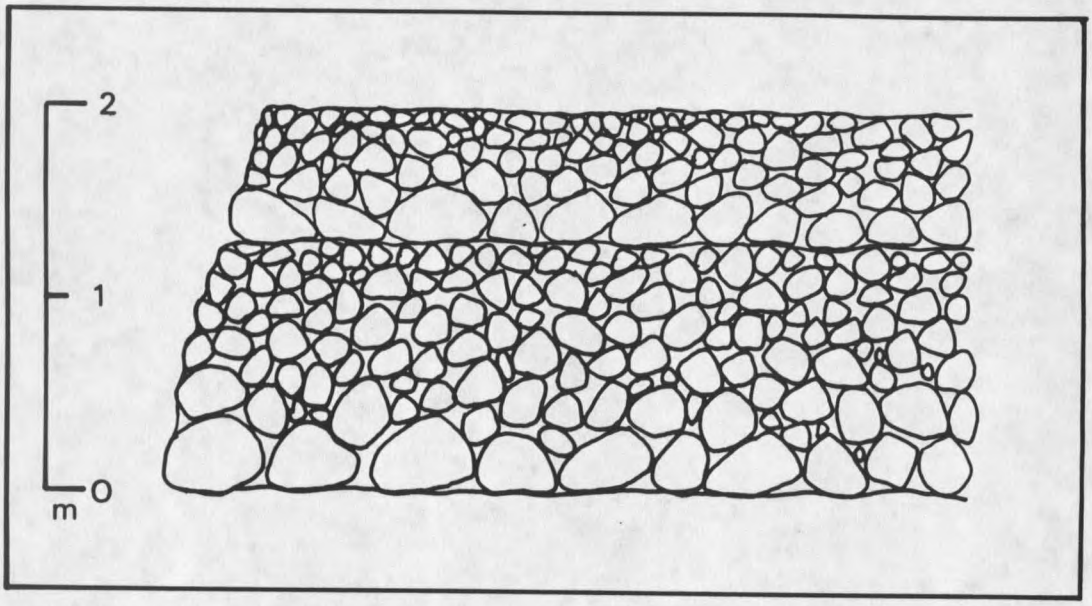


Figure 20. Sketch of typical textural features of Gmcn lithofacies (gravel, massive, clast-supported, with normal coarse-tail grading). Deposits of this lithofacies are found at Windy Pass, Flanders Mountain, Eight Mile Canyon, and Antelope Butte. Average thickness = 1.3 m.

Interpretation: Lithofacies Gmcn is interpreted as having formed as a result of rapid energy loss during hyperconcentrated flow or streamflow conditions. Normal

grading of clasts indicates clast-by-clast deposition caused by progressively decreasing flow energy. Rapidly decreasing energy may have a number of causes: it may be due to constricted flow or decreasing gradient accompanied by a decrease in flow velocity, or as a result of channelized flow transforming to unconfined flow. These deposits closely resemble the descriptions of whaleback bar deposits of Scott (1988), which formed during recession flow of peak flood stages at Mount St. Helens during the May 1980 eruption. These deposits may also result from decreasing flow energy in passing pyroclastic flows causing dense lithic clasts to be deposited.

Gravel, Massive, Clast-Supported, with Inverse to Normal Coarse-Tail Grading (Gmcin):

Some units of this lithofacies exhibit crude horizontal stratification. Clasts may be angular to subrounded, commonly consisting of durable flow rock lithologies. General textural characteristics of this lithofacies are illustrated in Figure 21. Rare units contain clasts which exhibit long axis imbrication. Maximum clast size rarely exceeds 30 cm, and is commonly less than 10 cm. The matrix is poorly-sorted, consisting of silt and fine to coarse sand. Units of this lithofacies are rare, but where they occur they are thin and tabular, generally with sharp, planar contacts. Commonly less than 1.0 m thick, the average thickness of individual beds is 0.4 m.

Interpretation: Deposits which exhibit characteristics of Gmcin lithofacies are interpreted as having formed from flows in which a vertical variation of fluid density existed. Inverse grading may have been caused by basal shear, active within the lower part of the flow. The upper part of the flow may have been more fluid, with larger clasts at the base of the normally graded upper section being transported above a more dense and viscous lower half which acted as a barrier to fluid migration. The relative thinness of deposits as well as clast imbrication may have resulted from flow fluidity. The depositional fabric of this lithofacies indicates that flows which resulted in Gmcin depositional fabric were probably debris flows, or pyroclastic flows, which contain a vertical gradient in fluid density and viscosity. A gradient in fluid content may have resulted from a transition of hyperconcentrated flow to debris flow through sediment bulking. Increased shearing within the base of the flow, induced by roughness of the substrate, may also have contributed to the formation of this depositional fabric.

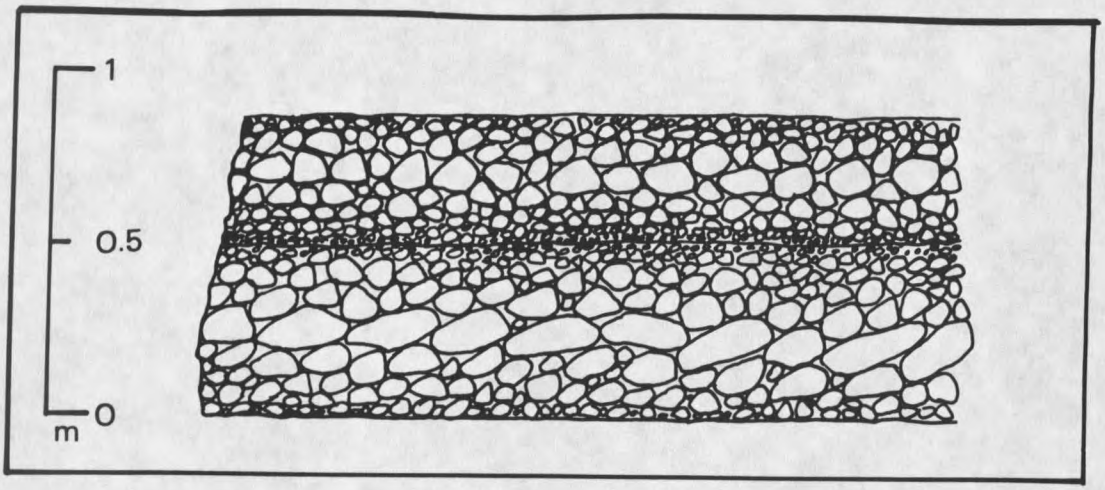


Figure 21. Sketch of textural features of Gmcin lithofacies (gravel, massive, clast-supported, with inverse to normal coarse-tail grading). Deposits of this lithofacies are found at Antelope Butte, Eight Mile Canyon, and Silken Skein Falls. Average thickness = 0.4 m.

Gravel, Massive, with Pumice Lapilli (GmLa):

Clast support in units of this lithofacies is variable. Deposits of GmLa lithofacies commonly exhibit coarse-tail grading. The central portions of units usually contain a higher portion of matrix along with small (< 2 cm) lithic clasts and clasts of less dense vesicular pumice and lapilli. Clasts which are primarily subangular to subrounded tuff which rarely exceed 20 cm in diameter, and are commonly inversely graded or may be concentrated within the upper 10 to 15 cm of an individual bed. Clasts of more dense and durable andesite flow rock, if present, are angular to subangular and normally graded in the lower portion of the unit (Figure 22). Matrix consists of silt with very little sand. Units measured at Windy Pass, where this lithofacies is most common, have a light pink to light tan matrix. Bed contacts are commonly planar, but may also be gradational. Units of this lithofacies are not widespread; where they do occur they are commonly thin and tabular. Average thickness of individual units is 0.4 m.

Interpretation: Units of GmLa lithofacies are interpreted as pyroclastic flow deposits. The fabric of the units suggests conditions of dampened turbulent to laminar flow. In pyroclastic flows, low density laminar flow allows sinking of clast lithologies of greater density (Sparks, 1976), such as flow rocks of andesite and dacite produced a

normally graded fabric. However, the fluid is viscous and dense enough to buoyantly support less dense lithologies of pumice and tuff fragments. This leads to inverse grading in the upper part of a bed, probably due to deposition from a concentrated upper layer. Differences in grading between clasts of differing densities within units of GmLa lithofacies were perhaps caused by gravity segregation from gas-mobilized fine particles in an inflated density flow (Sparks, 1976; Pierson, 1985). This suggests that the flow was less viscous and more turbulent than a cohesive debris flow which, because of greater shear strength, would transport clasts in a laminar fashion, regardless of density contrasts. The units of this lithofacies show a striking similarity to deposits from small volume pyroclastic flows described at Laacher See (Freundt and Schmincke, 1986). The systematic differences in grading of different density clast types are characteristic of the main body of a pyroclastic flow (layer 2b deposits) of an idealized ignimbrite eruption (Sparks and Walker, 1973; Sparks, 1976; Carey, 1991).

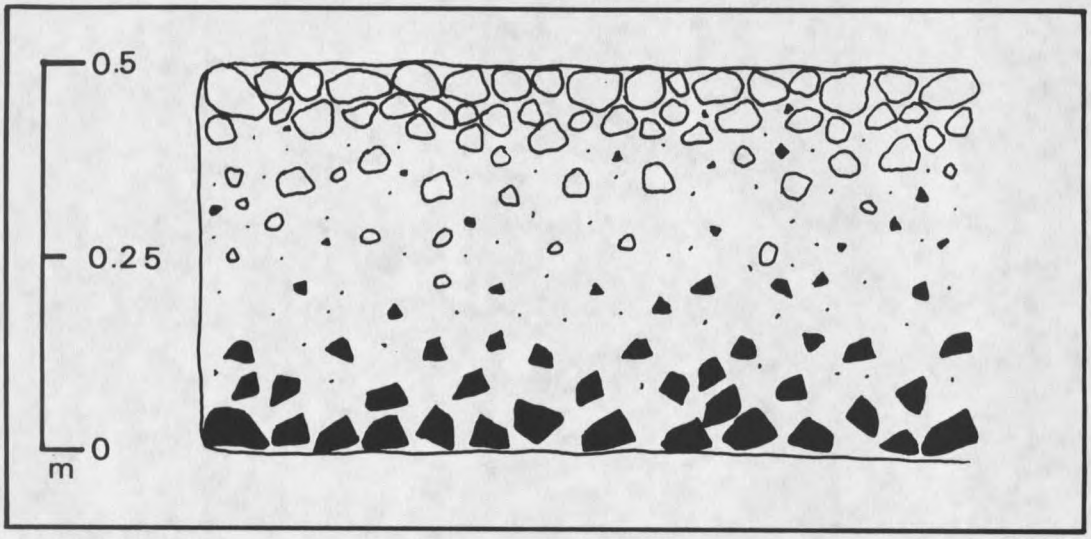


Figure 22. Sketch of textural features of GmLa lithofacies (gravel, massive, with pumice lapilli). Deposits of this lithofacies are found at Eight Mile Canyon and Windy Pass. Average thickness = 0.4 m.

Gravel, with Low-Angle Stratification (Gl):

Units of this lithofacies are stratified and interbedded with medium to coarse angular sand in troughs at angles < 10°. Stratification of gravel is inclined at low angles

to subtle gradational tabular unit boundaries, illustrated in Figure 23. Clasts are predominantly rounded to subrounded and often less than 10 cm in diameter. Commonly units are light tan to yellow-tan, although they contain clasts and sand of variable lithologies. The average thickness of these units is 0.7 m. Units of this lithofacies are rare, occurring primarily at Silken Skein Falls and Antelope Butte.

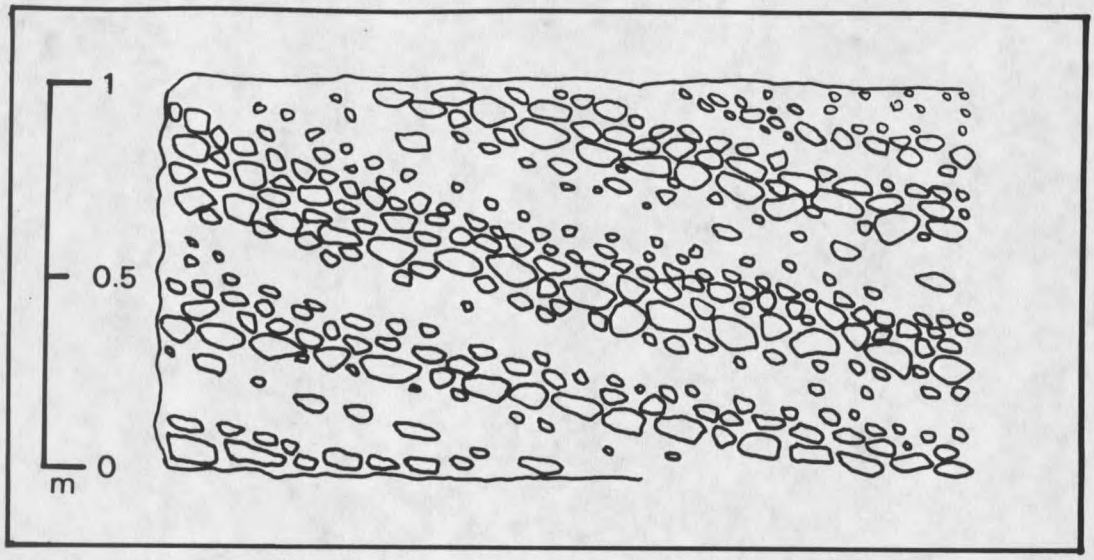


Figure 23. Sketch of textural features typical of Gl lithofacies (gravel, with low-angle stratification. Deposits of this lithofacies are found at Antelope Butte , Eight Mile Canyon and Silken Skein Falls. Average thickness = 1.9 m.

Interpretation: Lithofacies Gl is interpreted as deposits which form during conditions of high discharge during normal streamflow (Miall, 1985). Clasts are deposited in a grain-by-grain fashion on the surface of a streambed, forming thin, diffuse gravel sheets (Hein and Walker, 1977). These sheets may travel as a traction carpet along the stream-bed interface, becoming stationary during lower energy flow conditions. Low angle inclination of gravel deposits result from conformation of diffuse sheets to the streambed morphology.

Gravel, with Trough Cross-Stratification (Gt):

Units of this lithofacies are clast-supported (Miall, 1977). Maximum clast size is less than 10 cm. Troughs are 20 to 80 cm deep and 0.5 to 1.0 m wide (Figure 24). Units

of this lithofacies are rare, occurring only at Antelope Butte and Palisade Mountain. Units within measured section I at Antelope Butte have gradational contacts. There the clasts are predominantly rounded to subrounded and of variable lithologies including black, grey, and red andesite, granule-sized white tuff, limestone, brown chert, and red, pink, and grey quartzite. Matrix consists of angular and pebbly coarse sand. In contrast, units of this lithofacies within measured section I at Palisade Mountain consist entirely of white to light grey dacite. Clasts and sand within the unit are very angular, regardless of size. Where exposed at Palisade Mountain, contacts are sharp and planar .

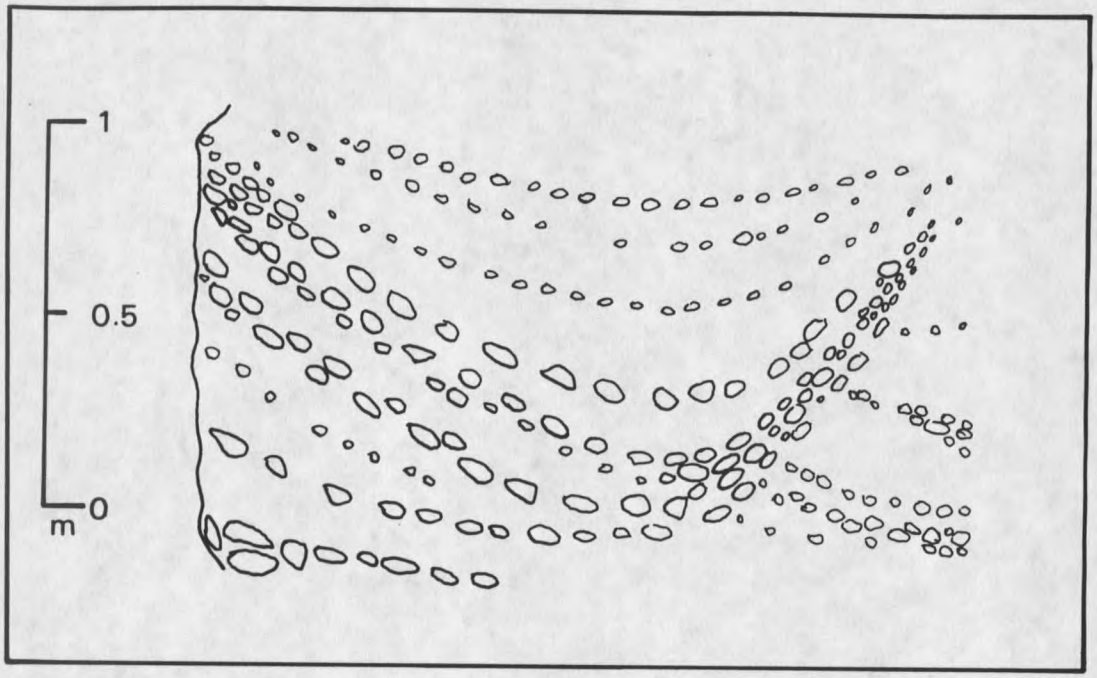


Figure 24. Sketches of textural features typical of Gt lithofacies (gravel with trough cross-stratification). Illustration shows textures typical of deposits of this lithofacies at Antelope Butte I.

Interpretation: Facies Gt is interpreted as being formed by turbulent transport and grain-by-grain deposition. During conditions of normal streamflow, small shallow channels are scoured as a result of separation eddies which form in the lee of an advancing gravel bar, dune or sand wave (Miall, 1977). These are subsequently filled by sand and gravel with stratification parallel to the scoured surface. All units of this designated lithofacies are thought to have been deposited by streamflow except for the unusual outcrop at Palisade Mountain. Because the unit of this lithofacies contains

angular fragmented dacite with rare clasts of Precambrian gneiss, it is interpreted as a pyroclastic surge deposit. Cross-bedding in surge deposits also results because of the formation of dune or sand wave bedforms during turbulent transport (Waters and Fisher, 1971; Wohletz and Sheridan, 1979). Although cross-bedding in surges is usually at lower angles and more subtle than those formed during streamflow, higher angle cross-stratification can occur as a result of particle-to-bed cohesion in wet surges (Valentine, 1987) or as a shadow effect caused by surface irregularities (Fisher, 1990).

Summary of Coarse-grained Lithofacies

Utilizing the hydrodynamic interpretation of volcaniclastic coarse-grained lithofacies, several genetic interpretations can be made for many of the deposits. This is especially true for deposits in which volcanism has played a major role in deposition, because hot air and gas or water may be the transporting medium. Many of the water-laid coarse-grained lithofacies have textures which cannot be attributed to deposits typically left by normal streamflow, idealized debris flow, or deposition from hyperconcentrated flow conditions. Transitional stages in flow density and the type of flow generate a broad spectrum of depositional textures which are reflected in the large number of lithofacies types. A summary of coarse-grained lithofacies and interpretation of associated depositional processes are listed below in Table 2.

Table 2. Summary of Coarse-Grained Lithofacies

Lithofacies Code	General Features	Genetic Interpretation
Gmpv	Gravel, massive, poorly-sorted, volcanic	debris avalanche, flow front breccia, pyroclastic lag
Gms	Gravel, matrix-supported	laminar flow as pyroclastic flow or debris flow
Gcms	Gravel, clast-supported at the base transitional to matrix-support in the upper portion	partially turbulent transitional flow

Table 2. Summary of Coarse-grained Lithofacies (continued)

Lithofacies Code	General Features	Genetic Interpretation
Gmsn	Gravel, matrix-supported with clast-supported, normally graded base	dampened turbulence as hyperconcentrated flow
Gmsi	Gravel, matrix-supported at the base, inversely graded to clast-supported upper portion	Transitional flow, laminar debris flow with basal shear or dilution
Gmci	Gravel, clast-supported with inverse coarse-tail grading	Coarse-grained, non-cohesive, laminar debris flow
Gmp	Gravel, massive, poorly-sorted	dilatant laminar flow debris flow plug or levee deposits
Gmpi	Gravel, massive, poorly-sorted, imbricated	partially turbulent dilatant transitional flow
Gm	Gravel, massive	clast-by-clast accretion during streamflow
Gmw	Gravel, massive, well-sorted	debris flow, hyperconcentrated flow, or pyroclastic flow lag
GmLa	Gravel, massive, with inversely graded pumice in upper portion, normally graded lithic base	laminar pyroclastic flow
Gl	Gravel with low-angle stratification	clast-by-clast deposition during high discharge turbulent streamflow
Gt	Gravel with trough cross-stratification	clast-by-clast deposition during turbulent streamflow
Gmwt	Gravel, massive, with well-sorted tephra	deposition as eruption fall-out

Sandy Lithofacies

Sand, Trough Cross-Stratified (St)

This lithofacies occurs very rarely, and is only included in the measured section II at Antelope Butte. Trough cross-sets are commonly from 5 to 20 cm deep and 15 to 40 cm wide (Figure 25). The sand is poorly-sorted, and fine- to medium-grained, containing subangular grains of biotite, hornblende, volcanic glass, chert and quartz.

Interpretation: Units of this lithofacies are interpreted as forming during normal streamflow conditions within the deeper portions of active channels (Miall, 1985). Cross-stratification forms as a result of dune bedform migration during Newtonian flow. Although high-angle trough cross-stratification may sometimes form in wet surges, observed units of this lithofacies exhibit features consistent with formation from streamflow deposition.

Sand In Erosional Scours (Se):

Units of this lithofacies occur in lenticular bodies (Figure 25). The sand is fine- to coarse-grained, poorly to moderately-sorted, angular to subrounded, and may be pebbly. Grains include variable amounts of biotite, hornblende, volcanic glass and quartz.

Interpretation: This lithofacies is interpreted as sand deposited within erosional scours during conditions of normal streamflow (Rust, 1978). Scours are formed during high discharge streamflow by erosional turbulent eddies, or in areas of flow separation around obstructions in gravely streambeds. They are filled by sand which is suspended by turbulence during periods of high discharge, which drops out of suspension during waning flow conditions.

Sand, Horizontally Stratified (Sh)

Units of this lithofacies consist of fine to coarse sand, often with pebbles and granules. Stratification within units may also exhibit normal or inverse grading (Figure 25). The sand is generally poorly sorted, often composed of biotite,

hornblende, quartz, plagioclase and volcanic glass which may be altered. Pebbles and granules are commonly rounded pumice or angular to subrounded andesite, basalt and dacite. Units may also fine or coarsen laterally (within distances of 1 to 2 m). Thin units (< 20 cm) are discontinuous over distances of 1 to 5 m. This lithofacies is not always deposited horizontally, but may dip to conform to pre-existing topographic features. Grading and stratification in dipping units is identical to those deposited horizontally. These deposits pinch and swell moderately, thickening against obstructions, but are laterally continuous. In thicker portions, they locally exhibit subtle cross-stratification. Rare deposits at Silken Skein Falls contain armored lapilli. Units of this lithofacies are widely occurring, being the most common fine-grained lithofacies.

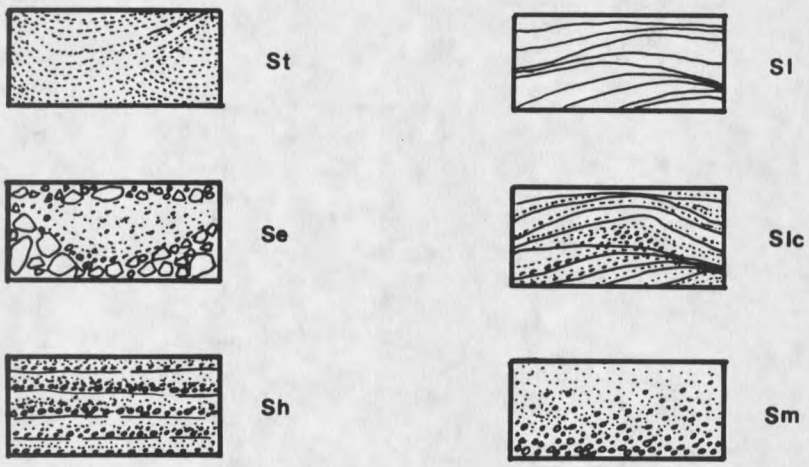


Figure 25. Illustration of sedimentary structures and grain-size characteristics of sandy lithofacies: St, trough cross-stratified sand; Se, sand in erosional scours; Sh, horizontally stratified sand; Sm, massive sand; Sl, low-angle cross-stratified sand; and Slc, coarse-grained low-angle cross-stratified sand.

Interpretation: Lithofacies Sh may be deposited under turbulent flow conditions, or under conditions of dampened turbulence (Smith and Lowe, 1991). Deposition of horizontally stratified sand may result from the migration of low

amplitude bedforms during streamflow or hyperconcentrated flow (Cheel, 1990; Smith and Lowe, 1991). This fabric was originally described from normal streamflow facies as resulting from planar bed flow (Miall, 1985) usually forming under shallow upper flow regime conditions. Stratified sand deposited during planar bed flow is usually fine to medium-grained, whereas deposits resulting from hyperconcentrated flow may in some cases be very coarse-grained. Units of this lithofacies are also characteristic of medial or distal surge facies which form under conditions of turbulent flow (Wohletz and Sheridan, 1979). Deposits which conform to surface irregularities and those containing predominantly pumice and glass, or palagonitic volcanic glass and armored lapilli are interpreted as surge deposits.

Sand, Massive (Sm)

This lithofacies consists of pebbly sand, usually medium to coarse-grained. It occurs in units from 10 cm to 1 m thick, which are sometimes normally graded (Figure 25). Deposits of this lithofacies are often poorly-sorted, consisting of subangular to subrounded grains of predominantly lithic volcanic fragments and volcanic glass, which is sometimes strongly palagonitized. Rare units contain rounded granule-sized pumice.

Interpretation: Deposits of this lithofacies probably result from rapid deposition from suspension during conditions of hyperconcentrated flow (Smith, 1986). Alternatively, some massive beds may be medial facies surge deposits (Wohletz and Sheridan, 1979). Units of this lithofacies which may be surge deposits contain large amounts of altered volcanic glass, mafic phenocrysts, and rounded pumice. Deposition of massive beds can result during transition from highly-fluidized turbulent flow to non-turbulent planar flow (Valentine, 1987), or as a surge becomes more concentrated towards the base (Wohletz and Sheridan, 1979).

Sand, Low-Angle Cross-Stratified (Sl)

Deposits of this lithofacies consist of fine sand with low-angle cross-stratification of less than 10° (Figure 25). This lithofacies occurs in thin units (5 to 20 cm) and has only been found at the Antelope Butte locality of sections I and II.

Interpretation: Low-angle stratification in fine-grained deposits is indicative of turbulent streamflow deposition of upper flow regime antidunes or scour fill (Miall, 1985). Upper flow regime conditions are associated with deposition of fine-grained sand. Antidune bedforms, which generate deposits of fine-grained sand at low angles, are restricted to formation under conditions of shallow flow depths and high flow velocity conditions (Allen, 1985).

Sand, Low-Angle Cross-Stratified, Coarse-Grained (Slc)

Slc lithofacies is comprised of fine to coarse sand, often containing pebble-sized pumice lapilli, with low-angle cross-stratification of less than 10° (Figure 25). Finer-grained units of this lithofacies are usually thin (< 0.5 m), may become coarse-grained laterally (within 1-2 m), and exhibit crystal-poor, thin laminae interstratified with coarse sand-sized crystal-rich layers. Thicker units (> 0.5 m) contain large amounts of rounded pumice and rare angular, dense lithic fragments which may be imbricated. Units are usually tabular but may thicken locally to fill topographic depressions.

Interpretation: Units of this lithofacies are interpreted as the result of pyroclastic surge deposition of dunes, sometimes called sand-waves. Migration of this type of bedform is facilitated through particle support by turbulent flow. Turbulent suspension is supplied by interstitial gas in a low density, expanded mixture which is driven by gravitational energy (Wilson, 1988; Carey, 1991). Sand-wave cross-stratification in surge deposits have been described as proximal to medial pyroclastic surge facies by Wohletz and Sheridan (1979).

Fine-Grained Lithofacies

Fine-Grained, Silt and Clay (Fsc)

These units consist of horizontally laminated layers of silt and mud, or massive layers which become more clay-rich upward. Thicker units (> 10 cm) are commonly

laminated towards the upper surface and exhibit thin vari-colored stripes. Lower contacts usually grade into sandy facies (Figure 26). Deposits of this lithofacies locally contain organic debris including twigs, pine needles and leaf impressions.

Interpretation: This lithofacies results from deposition of fine sediment from suspension from waning floods, overbank deposits and restricted ephemeral ponds (Miall, 1977, 1978).

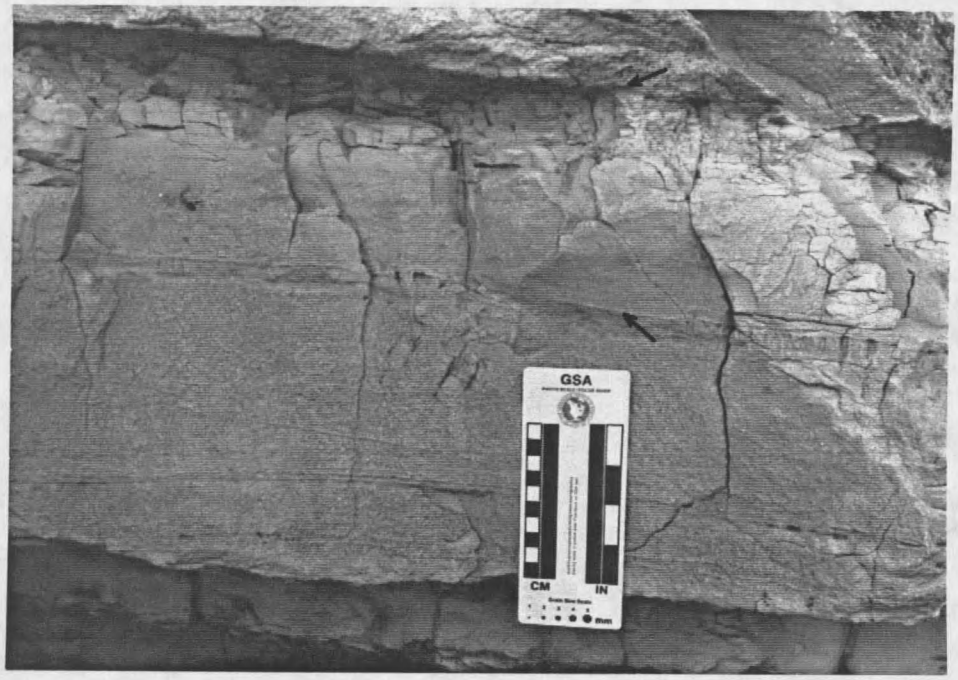


Figure 26. Fsc lithofacies deposit (between arrows) overlying Sl facies unit at Antelope Butte II.

Fine-Grained, Laminated, Wavy (Flw)

This lithofacies consists of clay- to silt-sized particles in thin deposits with laminations which are sometimes wavy in appearance. Deposits of this lithofacies are usually vitric, white or light pink, and generally from 1 to 2 cm thick. Thicker units (>5 cm) are rare and may contain granule- to pebble-sized tuff fragments which are commonly flattened. Although thin, they are usually laterally continuous across an outcrop exposure (tens of meters).

Interpretation: This lithofacies consists of lithified ash, probably deposited as ash-fall. Flattened tuff lapilli were probably aggregates of ash which distorted upon impact or during flow movement (Branney and Kokelaar, 1992; Schumacher and Schmincke, 1991). Some units of this facies which are finely laminated may have been deposited from dilute pyroclastic surges (Fisher and Schmincke, 1984). Although continuous across a single exposure these units have not been traced from exposure to exposure due to the disjoint nature of the outcrop.

LITHOFACIES ASSOCIATIONS

Coarse-grained lithofacies comprise 98% of the stratigraphic thickness and 75% of the depositional units within measured sections of Hyalite Peak volcaniclastic sequences. They are listed in Appendix A, Table 4, in order of relative abundance. Some lithofacies units are much more common than others. Fine-grained and sandy lithofacies tend to be much thinner and much less abundant. This may be partly due to preservability and volume of the lithofacies unit, rather than the relative frequency or duration of a process or processes which produce a particular lithofacies. Some types of lithofacies may be underrepresented because of deposition in areas subject to erosion and reworking, and finer-grained units have a tendency to be more easily eroded. In order to characterize processes active within a depositional setting, all types of lithofacies regardless of relative abundance, should be studied carefully.

Even though distinct differences in fabric and texture distinguish lithofacies and indicate separate depositional mechanisms, these may not always be the product of a unique process. This is equally true for fine- and coarse-grained textures. In volcanic settings, process interaction is the driving force which leads to deposition: volcanic eruptions introduce pyroclastic material, spur avalanches, and cause the breaching of crater lakes, all of which demand adjustments within the local alluvial system. As a result, relationships between lithofacies, both vertically and laterally, become extemely important in deciphering processes of deposition. Because of the large degree of process interactions and transitions which must take place, it becomes nearly impossible to distinguish exact depositional processes utilizing isolated lithofacies.

Grouping lithofacies into lithofacies associations provides clearer insight into the relative occurrence of different processes, as well as how these processes may relate to one another. Because of the large number and variation in lithofacies occurrences, Markov chain analysis was attempted in order to decipher any common lithologic transitions in successions of depositional units (Miall, 1973). However, the results showed that the spatial occurrence of lithofacies types do not reveal any statistically significant relationships. Therefore, lithofacies associations are not based upon the common spatial associations of a group of lithofacies. Instead, associations are primarily based on groups of lithofacies with similar genetic interpretations. Units

are grouped which commonly result from a particular process. For example, lithofacies Gm is grouped with St and Gt, because all commonly are associated with streamflow deposits. Secondly, they are grouped by closely associated processes with clear evidence of process transitions. These groups of lithofacies grade from one to another, such as Gms and Gmsn (Table 3). Resulting groups sometimes have common lithofacies because similar depositional fabrics may form from similar hydrodynamic conditions found in both epiclastic and pyroclastic processes (lithofacies such as Gms and Sh). Some lithofacies do not clearly fall into any lithofacies associations because they may represent a transitional phase associated with process interaction (such as Gmpi). These types of deposits are also listed in Table 3, but are grouped into lithofacies associations with which they are most commonly found. Lithofacies associations grouped according to genetic process help to delineate process interactions, and serve as an aid in interpreting the relative occurrence of these processes.

Table 3. Lithofacies Associations and Types of Processes. (Lithofacies followed by * are indicative of phase transitions or process interactions.)

Lithofacies Association	Associated Process	Lithofacies
LA1 SFF	Streamflow facies	Gm, St, Gt, Gl, Se, Sh, Sm, Fsc
LA 2 MSDF	Cohesive, matrix-supported debris flow transitional to hyperconcentrated flow and streamflow	Gms, Gmp, Gmsi*, Gmsn*, Gcms*, Sm, Sh, Sl, Fsc
LA 3 CSDF	Clast-supported debris flow transitional to hyperconcentrated flow and streamflow	Gmci, Gmp, Sh, Gmcin*,Gmpi*, Gmw*, Gm, Sm,
LA 4 DAVB	Debris avalanche, flow and vent breccia, and debris flow	Gmpv, Gms, Gmp
LA 5 PFFS	Pyroclastic flow, fall and surge, with associated lag deposits	GmLa, Gms, Gmsn, Slc, Gmwt, Flw, Gt*, Gmcn*

Lithofacies Association 1:
Streamflow Facies (SFF)

Deposits of this lithofacies association may include units of Gm,St, Gt, Gl, Se, and Sh. Units of Gm lithofacies occur widely and are commonly interbedded with Se and Sh facies units. In order of abundance, units of Gl, Gt and St facies may also be interbedded with lithofacies Gm or with each other, but in no particular order (Figure 27). Gravel tends to be subrounded to rounded, and occasionally contains rare clasts of Precambrian quartzite and gneiss. Sand within these units is fine to coarse and generally poorly sorted. Units of these lithofacies are thin and tabular and comprise a volumetrically minor component of the volcaniclastic sequences.

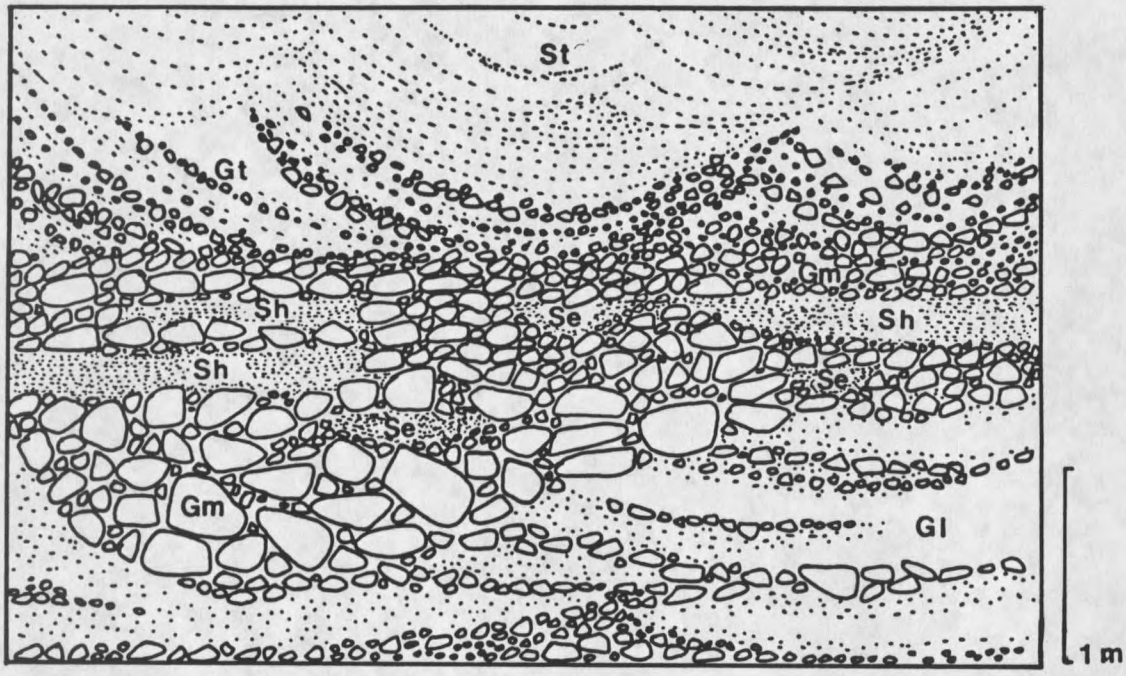


Figure 27. Lithofacies Association 1: Gm, Gt, Gl, St and Sh lithofacies, representing streamflow deposition (SFF).

Interpretation: These units are considered deposits resulting from normal streamflow conditions. The overall geometry of these units, together with the scarcity of cross-bedding, implies that for the most part streamflow took place in poorly confined, shallow braided channels. Few deep channels existed for migrating dune bedforms to develop (facies St). The complexly interstratified nature of the preserved

lithofacies is a reflection of fluctuating streamflow discharge. Massive conglomerates (facies Gm) may be longitudinal bar deposits. During waning flow, sand lenses were probably deposited by filling erosional scours, and stratified sand was deposited on shallow bar tops (Miall, 1985).

Lithofacies Association 2:
Matrix-Supported Debris Flow (MSDF)

Deposits which are categorized as matrix-supported debris flow facies may include Gms, Gmsn, Gmsi, Gcms, Gmp, Gmw, Sl, Sm and Fsc. Lithofacies Gms occurs in tabular units of variable thickness (20 cm to 3 m). Units of this lithofacies may grade laterally into several thin (20 to 40 cm) repetitive units of Gmsn lithofacies, or thick (>1 m) Gmsi lithofacies. It is also interbedded with tabular units of Gmsn, Gmcs and Gmsi lithofacies, and normally graded Sm facies, any one of which commonly grade upward into units of Fsc lithofacies. Units of Sm and Gmsn lithofacies often have erosional planar bases and contain rip-up clasts from the units below (Figure 28). As with other lithofacies associations, these lithofacies are generally not all found deposited together at one outcrop, or in one depositional interval .

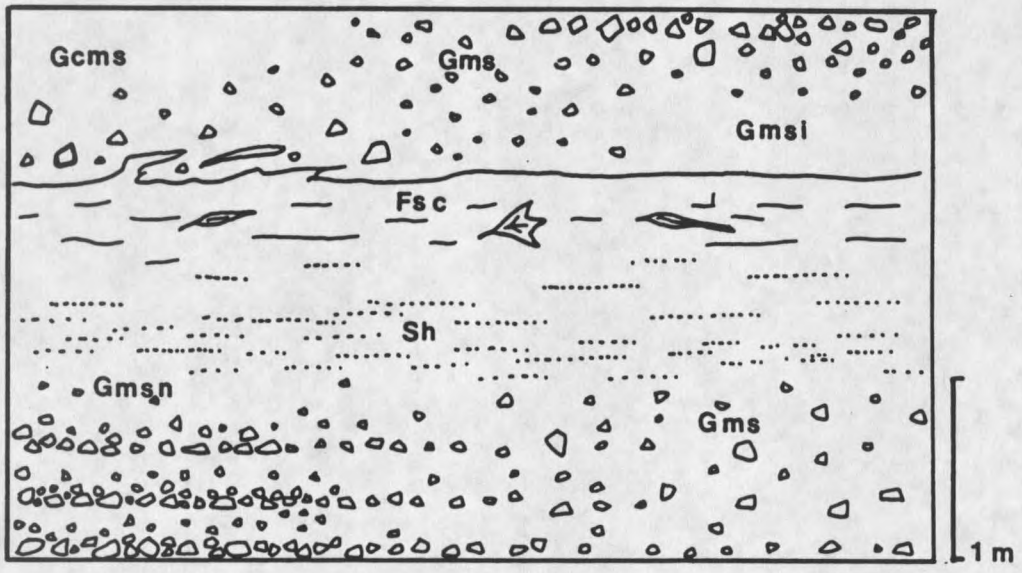


Figure 28. Lithofacies Association 2: Gms, Gmsi, Gmsn, Sm, and Fsc representing deposition from matrix-supported cohesive debris flow transitional to hyperconcentrated flow (MSDF).

Interpretation: These units represent cohesive matrix-supported debris flows and dilution to hyperconcentrated flow, as well as deposits of transitional stages of flow between the two. Units of Gms may become more dilute at the base, clasts in the bottom of the flow may drop out, and a transition represented by Gmsi lithofacies occurs. Because a single Gms unit may grade laterally into several thinner Gmsn units, these may represent a single flow undergoing increased internal shear as a result of incomplete mixing during flow dilution. Alternatively these units may represent deposition after increased dilution to hyperconcentrated flow, especially units of this lithofacies with erosional bases which are often interbedded with Sl lithofacies. Massive, normally graded sand was deposited from hyperconcentrated flow, represented by units of Sm, which may have formed from dilution of flows represented by Gmsn lithofacies. Decreasing viscosity would cause gravel at the base of the flows to drop out, depositing interbedded units of Gmw lithofacies. Conversely, fine-grained sandy hyperconcentrated flow may have incorporated sediment, including gravel-sized clasts during an increase in flow energy, perhaps due to an increase in flow gradient. Resulting deposits would be represented by the association of Gcms and Sm lithofacies units. Numerous rip-up clasts and flame structures within Sm facies suggest rapid deposition of successive units. Deposition of these units is followed by Fsc lithofacies suggesting that water ponded on top of and behind deposits of Sm and Gms lithofacies which probably acted as dams, inhibiting water flow.

Lithofacies Association 3:
Clast-Supported Debris Flow (CSDF)

Lithofacies categorized as clast-supported debris flow facies may include Gmci, Sh, Sm, Gmp, Gmcin, Gmpi, Gm, and Se. In measured sections where lithofacies Gmci is common, it forms tabular to wedge-shaped bodies commonly from 1 to 3 m thick, and 30 to 50 m wide. It is frequently overlain or underlain by thin (< 20 cm) units of Sh or Sm. Clast shadows or faint cross-bedding within the sandy units are locally found adjacent to outsized clasts protruding from the coarse-grained units. Some Gmci units grade downward into Sm units. These unit packages typically interfinger and repeat. Gmp and Gm lithofacies form a minor component within these sequences and are interbedded with them (Figure 29). Gmci units may grade laterally into Gmp deposits within the face of an outcrop (10 m).

Interpretation: These deposits are characteristic of clast-supported debris flow and hyperconcentrated flood-flow deposition. Debris flow deposition is represented by facies Gmci and Gmp, which are deposits resulting from dilatant non-cohesive flow. Debris flow deposits interlayered with hyperconcentrated flow deposits implies that the debris flow fronts and tails were diluted by streamwater. This dilution transformation process may be one of the primary mechanisms by which hyperconcentrated flow is produced (Pierson and Scott, 1985; Smith 1986). Gmcin units are most likley a transition from hyperconcentrated flow to debris flow. The amount of coarse-grained material within deposits of this transitional facies is probably due to the lack of fines available. Hyperconcentrated flood-flow deposition preceding or following deposition of debris flows are represented by lithofacies Sm and Sh. These units may be thin (<10 cm) because flows were deposited over a broad flat surface. Interbedded Gm, Sh and Se units represent reworking of these deposits by normal streamflow.

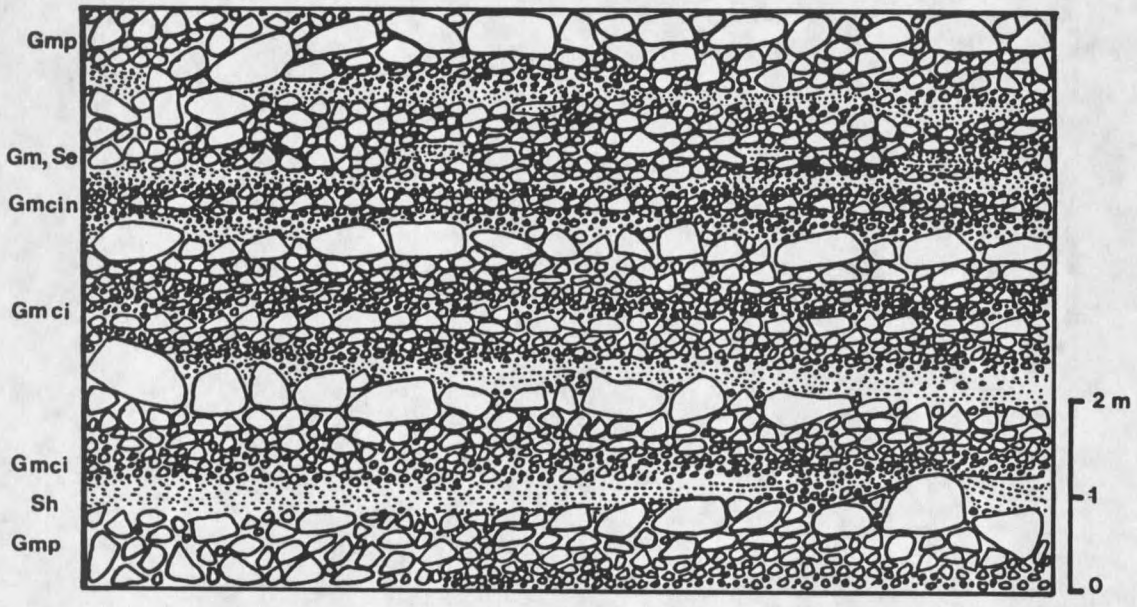


Figure 29. Lithofacies Association 3: Facies Gmci, Sh, Sm, Gmp, and Gm representing deposition from clast-supported debris flow, hyperconcentrated flow, and streamflow (CSDF).

Several Gmci units may repeat without the presence of other lithofacies units between them. There may be several reasons for this. Streamflow dilution may have been lacking in flows which deposited these units. Although these flows are mobilized by water and travel down depressions which may contain water, they are associated with large volume discharges of sediment. As a result they may also flow across the dry surfaces of terraces or alluvial fans. These surfaces are rich in loose debris, which would lead to flow bulking rather than flow dilution. In addition, basal erosion by successive debris flows may have taken place. As flows move down-slope they may become partly turbulent, especially at the base, and may erode the upper portion of previous deposits. Fine-grained deposits of hyperconcentrated flood-flow facies are easily eroded if they have been recently deposited, are poorly indurated, or lack a vegetated covering. It is also possible that a debris flow event may have several pulses within it which are represented by the deposition of successive units. Witnessed eruptive events at Mount St. Helens, during May 1980, indicate that debris flows triggered by pyroclastic flows on the crater rim, coalesced after traveling downstream and into a major drainage system. They then traveled as succeeding pulses within a continuous flow (Pierson, 1985). Finally, Gmci lithofacies which are not clearly associated with streamflow or hyperconcentrated flow facies may be lithic-rich pyroclastic flow deposits similar to those at Galeras Volcano in Colombia. These are described as clast-supported and inversely-graded with little or no juvenile pyroclastic component. Pyroclastic flow deposits of this type are the result of phreatic eruption sequences which involve the clearing of vent material from the volcano (Cavalache V. and Williams, 1992).

Facies Association 4:
Debris Avalanche and Volcanic Breccia (DAVB)

Deposits of this lithofacies association may include units of Gmpv, Gms, and Gmp. Thick Gmpv deposits (5 to 30 m) are irregular in thickness and have dipping planar to undulatory contacts. Interbedded Gms and Gmp lithofacies are generally tabular in appearance, but pinch out up-dip (Figure 30). Commonly Gms and Gmp show a subtle lateral gradation from one to the other. Gms and Gmp deposits associated with Gmpv facies tend to have very angular clasts and are often transitional between clast and matrix support.

Interpretation: These deposits represent flow front breccia and avalanche debris, breccia ejected from and associated with volcanic vents, and associated debris flow activity. Debris flows were probably triggered by avalanche activity (Palmer and others, 1991), or may have resulted from mobilization of large amounts of saturated debris avalanche material (Smith and Lowe, 1991). Debris flow fabrics imply that the flow deposition resulted from cohesive plug flow and flow levee development.

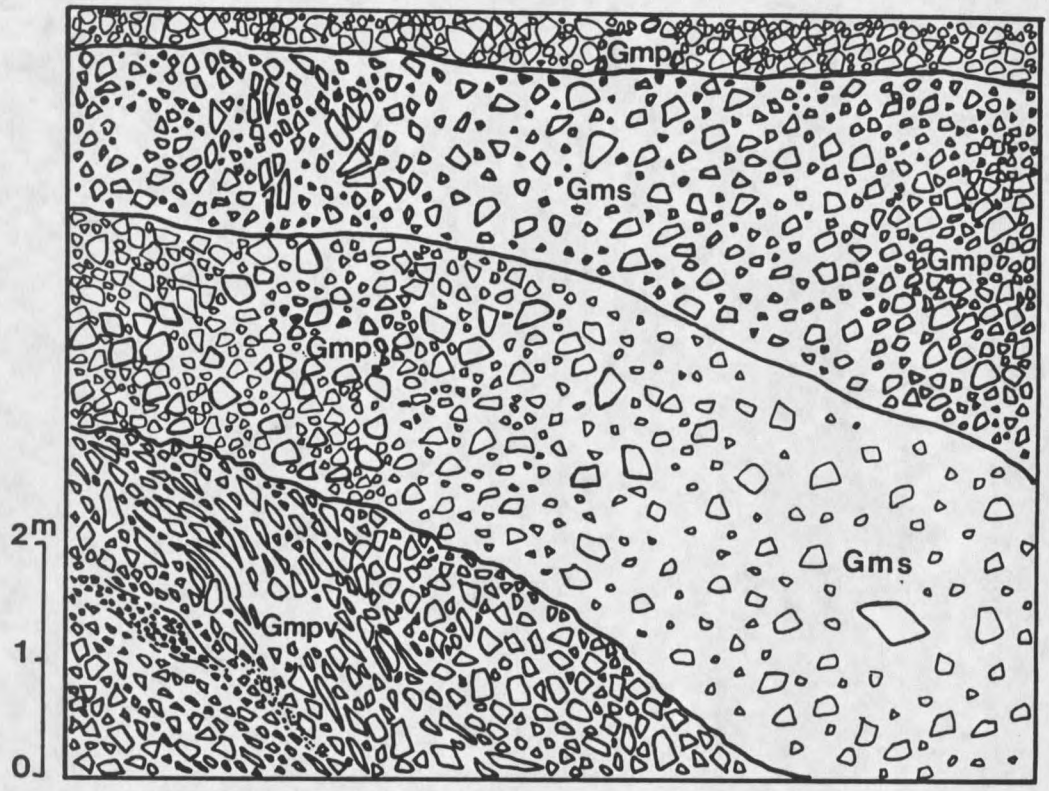


Figure 30. Lithofacies Association 4: Gmpv, Gms and Gmp deposits representing deposition from debris avalanches, flow front breccia, vent breccia and debris flows (DAVB).

Lithofacies Association 5:
Pyroclastic Flow, Fall, and Surge (PFFS)

Deposits of this lithofacies association may include units of GmLa, Slc, Gms, Gmwt, Flw, and Gmcn lithofacies. GmLa units occur in thin tabular bodies from 0.5 to 1.5 m thick, which are intercalated with 3.0 to 5.0 m thick units of tephra-rich Gms, and 10 to 20 cm thick Gwt lithofacies (Figure 31). Gms lithofacies occasionally fill U-

shaped channels cut into units of Slc facies. Rare Slc lithofacies occur in thick units (3.5 m) at the base of the sequence with low-angle, long-wavelength cross beds. Gmcn units are sometimes located at the base of GmLa units.

Interpretation: This sequence of units is thought to have been deposited from multiple small volume pyroclastic flows and fall. GmLa and Gms represent the main body of a pyroclastic flow; Gmcn units associated with them represent lag deposits deposited as clasts drop out from associated pyroclastic flows. Gmwt are lapilli-fall tephra, deposited from eruption clouds, commonly on top of pyroclastic flow sequences. These deposits are considered multiple units because of interbedded fall-out units. Slc deposits are more likely to be ash-cloud surge deposits rather than base surge deposits because they are relatively thick and have a large volume of rounded pumice lapilli (Wright and others, 1980). These surges probably preceded and were buried by subsequent pyroclastic flow deposits.

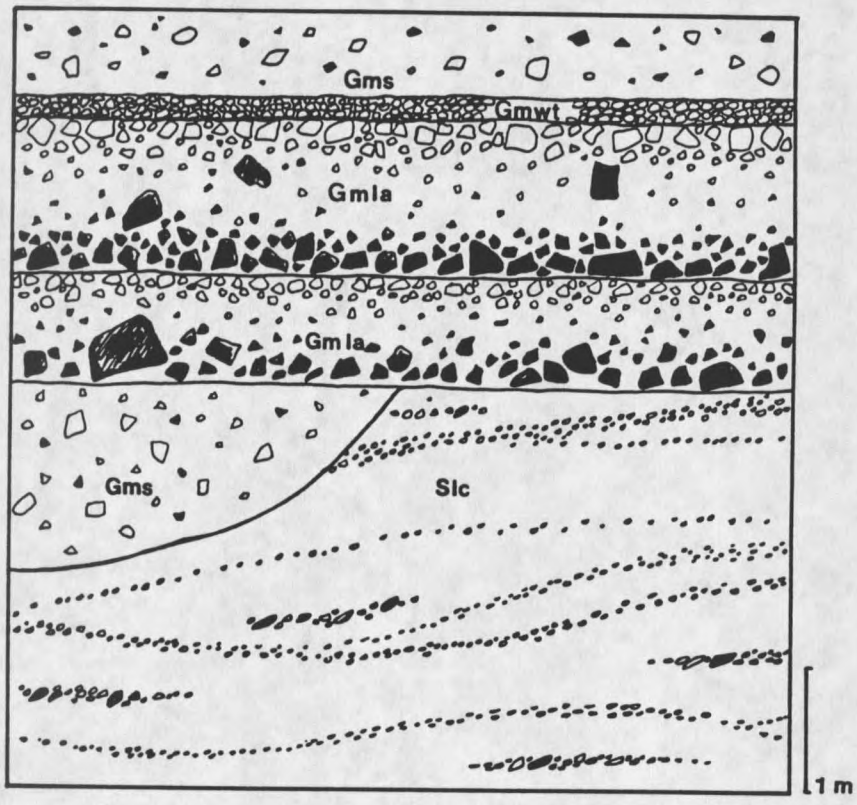


Figure 31. Lithofacies Association 5: GmLa, Gms, Gmcn, Gmwt, and Slc representing deposits from pyroclastic flow, fall, and surge (PFFS).

LITHOFACIES SEQUENCES AND DESCRIPTION OF STRATIGRAPHIC SECTIONS

Hyalite Peak volcaniclastic sequences display a wide range of chaotic variation in lateral and vertical stratigraphic relationships. In order to understand these relationships and to piece together the sequence of events that created them, lithofacies associations are grouped into sequences based on measured stratigraphic sections. Although lithofacies associations are discernable within measured sections, they are greatly generalized. Lithofacies such as Gmp and Sh do not occur uniquely within a single lithofacies association, but occur sporadically within many of them. Lithofacies such as Gm, Gmcn and Gmw, are more frequently found within a particular lithofacies association. However, they are not exclusive to any association in particular and occur widely within any group of lithofacies sequences. Therefore, the interpretation of lithofacies associations, their order and abundance is based upon the presence of lithofacies unique to a particular association and the spatial occurrence of adjacent lithofacies belonging to the same lithofacies association. Variation in lithofacies associations and sequences are the product of interplay between different volcanic and sedimentologic processes. Differences in lithofacies sequences and the types of associations within them become more pronounced over the distances between measured section localities, and may also be caused by the distribution of multiple source areas within the region of study.

Lithofacies Sequences at Antelope Butte

The base of both sections measured at the Antelope Butte locality have deposits characteristic of streamflow (lithofacies association 1: SFF), and contain rare trough cross-bedded sandstones (St). Units of Gm, Gt, Gl, Sh and additional St lithofacies units are present, but in no particular order of appearance. Although trough cross-set paleocurrents are difficult to measure accurately from these outcrops, they roughly indicate flow to the southwest (S 60° W). These units are light tan to buff-colored and consist primarily of volcanic detritus, but also contain rare rounded clasts of Precambrian quartzite. Units are tabular, with the exception of one channel-shaped

Gm unit (Figure 32). These lithofacies are sporadically interbedded with tabular deposits debris flow facies. These are primarily deposits of matrix-supported debris flow facies, including Gms, Gcms, Gmsn, Fsc, and normally graded Sm lithofacies. Many of these units contain rounded granule- to pebble-sized pumice fragments. Units of Sm commonly grade upward into Fsc lithofacies which contain abundant fossilized plant material and rounded granule to pebble-sized pumice fragments.



Figure 32. Photo of Gm lithofacies unit at Antelope Butte Section I with rare channel-shaped geometry. Below Gm lithofacies is a deposit of Gl lithofacies, which is covered at the base.

Antelope Butte section II is 320 m thicker than section I. The lower portion of section II is shown with section I in Figure 33. Both measured sections exhibit an upward shift from domination by streamflow facies to alternating matrix-supported and clast-supported debris flow and hyperconcentrated flow facies with numerous units of Gmp lithofacies in section II. The clast content of debris flow facies deposits is primarily volcanic (99%), and includes basalt, porphorytic and glassy andesite, dacite, and grey and black striped vitrophyre. The appearance of Gmp lithofacies becomes increasingly common from 60 to 150 m above the base of section II, in conjunction with deposition represented by lithofacies association 4: debris avalanche, flow front breccia and debris flow deposition (DAVB). Two units of Gmpv are 170 m

above the base of section II (Figure 34). The uppermost Gmpv unit is extremely thick (70 m). Its color varies from brick red to grey and black in long, inclined streaks. This unit is primarily mafic in composition although it contains some dacite clasts, and approximately 5% non-volcanic clasts including rare meter-sized boulders of limestone. It also contains abundant cauliflower bombs, scoria, agglutinate, and prismatically jointed basalt and andesite clasts.

Deposited on the uneven upper surface of the Gmpv unit are deposits of Gms, Gmsn and Gmsi with clear lateral gradations from one to the other, representing matrix-supported debris flow facies. These units contain clasts which are primarily composed of andesite, basalt and granule-sized rounded white tuff. Above this sequence, 280 m above the base of the section, are more lithofacies representing matrix-supported debris flow processes. They are numerous repetitive units of Gmcin and Gmsn lithofacies interbedded with units of Gmp, Gmsn, and thin fine-grained interbeds of Sl lithofacies. Found sporadically within matrix supported debris flow facies are rare units of Slc and Sh lithofacies containing thin (3 to 5 cm) crystal-rich and crystal-poor layers with abundant granule-sized tuff. One Slc unit 320 m from the base of the section contains outsized clasts in block sags. The upper portion of the measured section (325 m from the base) is characterized by clast-supported facies, represented by the presence of tabular deposits of Gmpi lithofacies containing prismatically jointed clasts together with numerous stacked deposits of Gmcin facies.

The presence of lithofacies association 1 at the base of the Antelope Butte sections represents deposition from channelized streamflow which becomes increasingly interrupted up-section by debris flow and hyperconcentrated flow deposition. Although paleocurrents indicate that streamflow may be to the southwest, there are not enough paleocurrent indicators to be statistically accurate. As streamflow deposits become rare, deposits of debris avalanche, vent and flow breccia facies appear which indicate the advent of proximal volcanic activity, or the renewal of it. Paleozoic boulders and agglutinate within the avalanche facies were probably ejected from a nearby vent, as were the volcanic blocks in Slc deposits. Slc lithofacies at Antelope Butte, which are deposits resulting from pyroclastic surge, are deformed by the impact of ejected blocks of volcanic debris and are typical of near vent deposits resulting from hydromagmatic activity (Heiken, 1971). Gmp deposits which contain prismatically jointed clasts are probably pyroclastic flow deposits rich in dense lithic fragments.

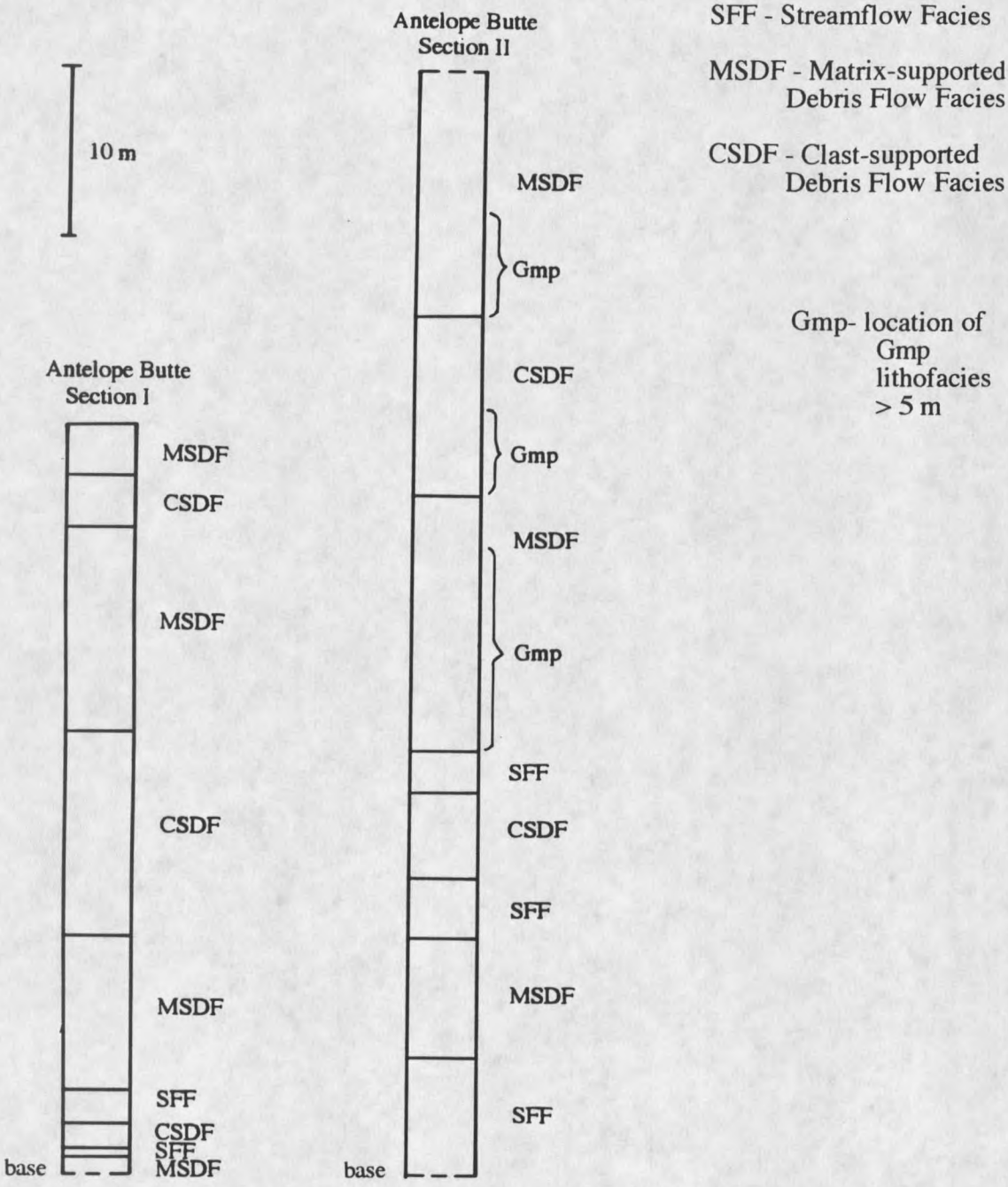


Figure 33. Generalized stratigraphic sections showing the sequence of lithofacies associations in Antelope Butte Section I and the lower portion of Antelope Butte Section II.

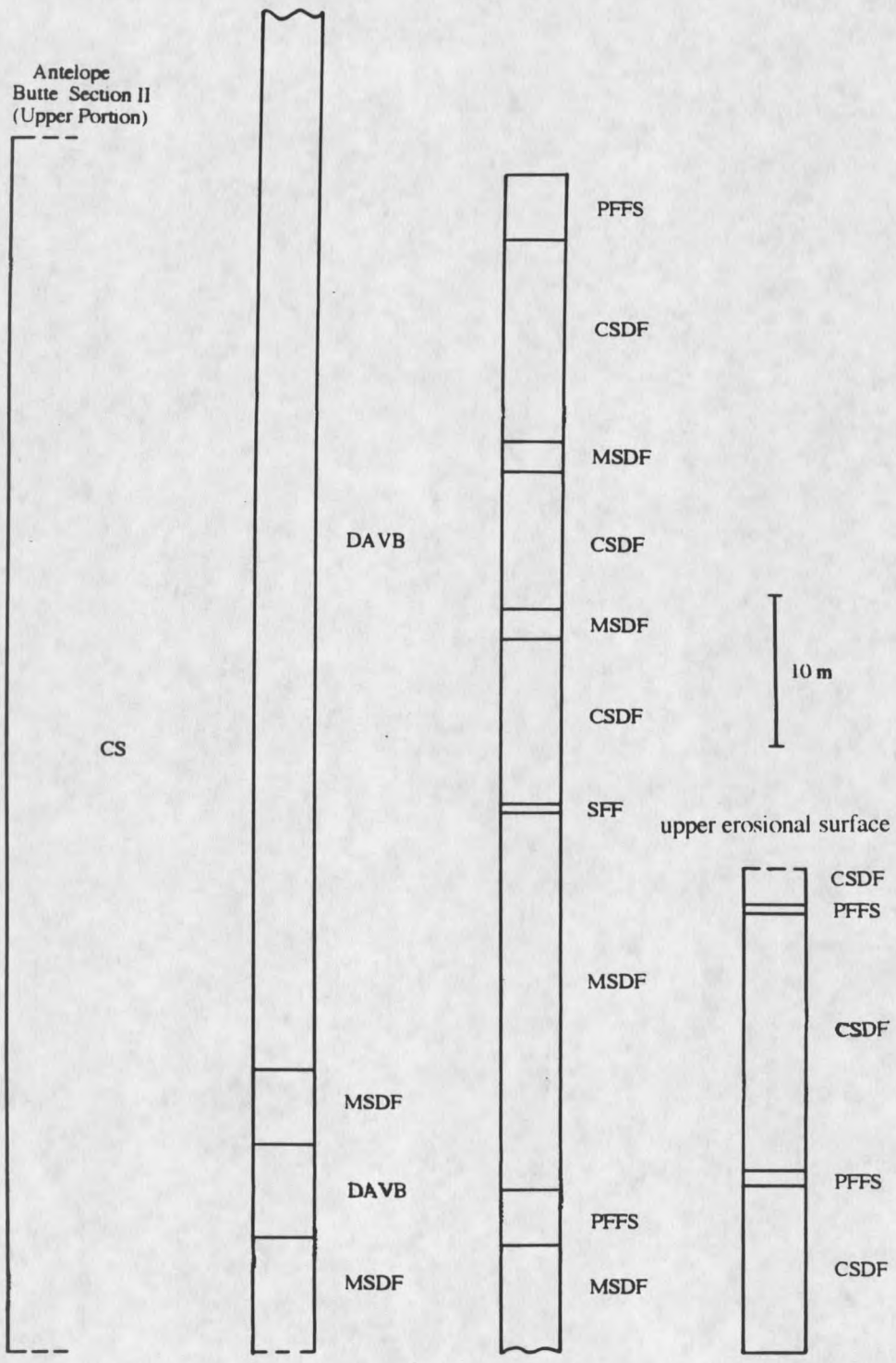


Figure 34. Generalized sketch of showing lithofacies associations in upper portion of sequence at Antelope Butte Section II. CS- Covered Slope; SFF- Streamflow Facies; MSDF-Matrix-Supported Debris Flow Facies; CSDF- Clast-Supported Debris Flow Facies; DAVB- Debris Avalanche and Volcanic Breccia Facies; PFFS- Pyroclastic Flow, Fall and Surge Facies.

Lithofacies Sequences at Eight Mile Canyon

The base of Eight Mile Canyon Section I is characterized by numerous Gms units which contain large (10 to 30 cm) subangular clasts of pumice and white fine-grained tuff. Clasts of other volcanic lithologies are present, but generally are not as large. A thin (40 cm) tabular unit at the base of the section contains flattened, horizontally aligned pumice and white ash with small (< 1 cm) glass fragments. Rare accidental clasts of diabase (> 20 cm) within these deposits may be derived from diabase intrusions located to the north (Figure 35). Additionally, the long axis of a channel containing a Gms deposit is oriented S 20° E. Units of Gmsi and Gmw and Gmcin are interbedded with Gms deposits, but are not as numerous. Flw lithofacies appears as thin interbeds from 1.0 to 30 cm thick between many of these units.

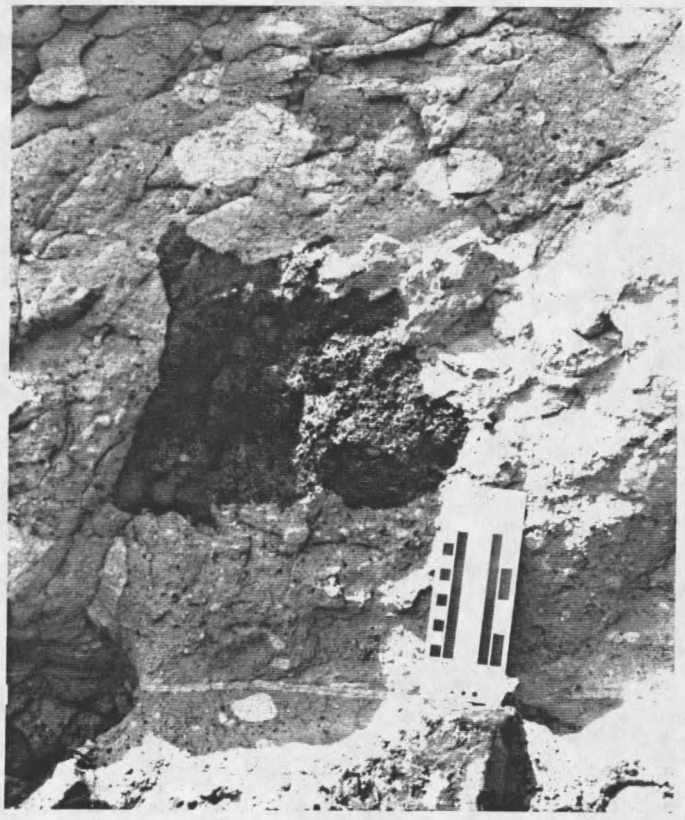


Figure 35. Photograph of diabase clast within a Gms unit at Eight Mile Canyon. Note that the basal contact of the unit contains a thin white deposit of Flw lithofacies.

Above these units and approximately 30 to 45 m from the base of the section, there is a transition to units characteristic of lithofacies association CSDF: deposits characteristic of clast-supported debris flow and hyperconcentrated flow (Figure 36). Deposits of Gmci lithofacies are repetitive and numerous, dominating exposures both vertically and laterally. Interbedded deposits of Sh contain clast shadows which indicate flow to the southeast. Deposits of Flw facies are still common but less numerous, and thin to 1 to 3 cm. Clasts of pumice and tuff are rare. Units contain clasts of more durable volcanic lithologies, which are predominantly basalt and andesite.

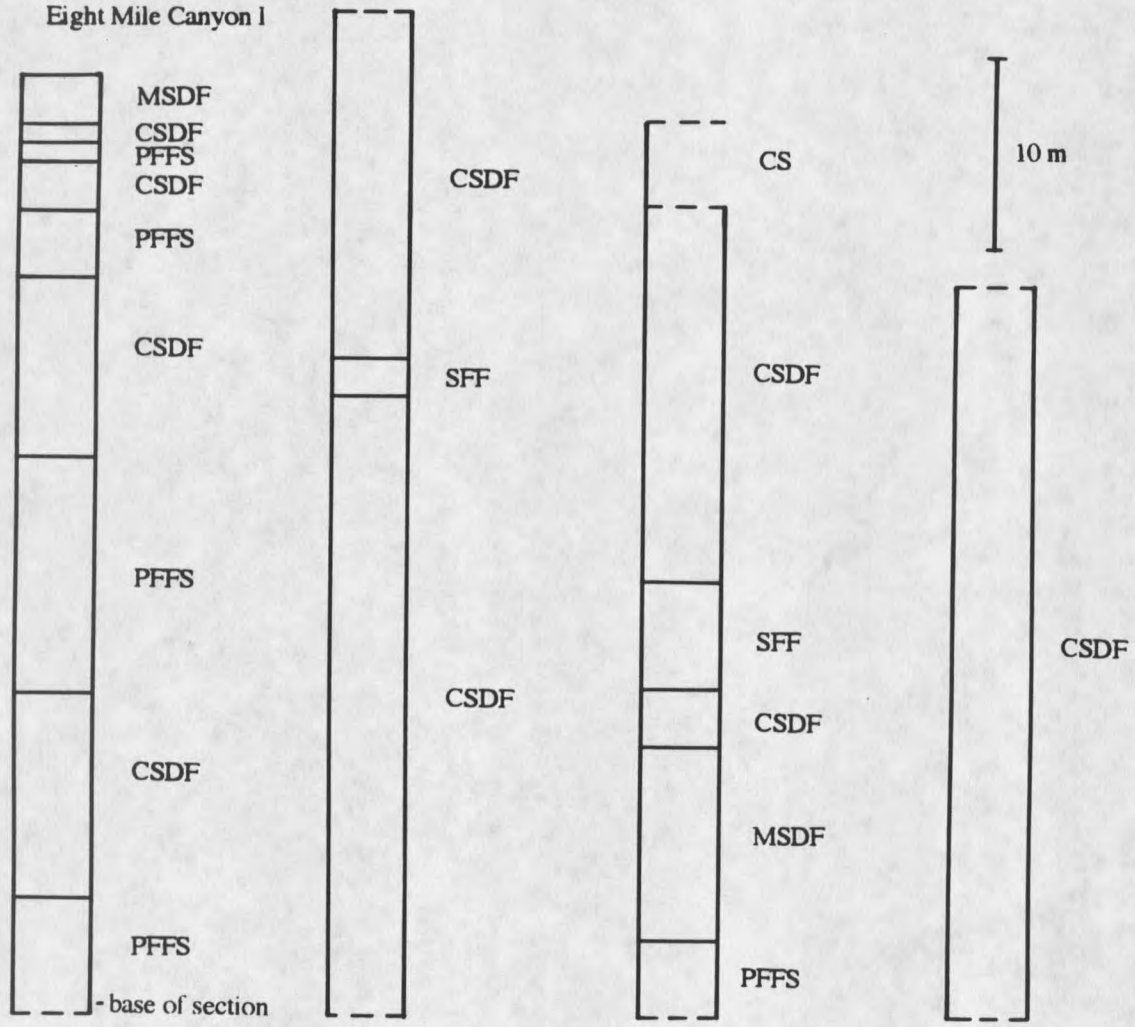


Figure 36. Eight Mile Canyon Section I, generalized to show locations and transitions between lithofacies associations. SFF-Streamflow Facies; MSDF-Matrix-Supported Debris Flow Facies; CSDF-Clast-Supported Debris Flow Facies; PFFS-Pyroclastic Flow, Fall and Surge Facies; CS-Covered Slope.

A second transition occurs approximately 100 m from the base of the section, where deposits of Gmsi and Gmw predominate. These units are interbedded with thin fine-grained deposits which are similar to GmLa, but generally lack well-developed dense lithic normal grading at the base. Exposures of Gms, Gmsi and GmLa lithofacies contain blocky fragments of dense black glass throughout the units (Figure 37). Numerous subangular pumice lapilli are concentrated toward the top of each unit. This succession of deposits representing various facies associations is overlain by lithofacies association 4 (CSDF) containing numerous deposits from clast-supported debris flows. Channels incised into deposits of Gms, Gmw, and Flw facies are filled with units of Gm facies, and several meters of streamflow facies deposits alternate with clast-supported non-cohesive debris flow deposits in this portion of the measured section. The uppermost 60 m of section consists of numerous tabular units of Gmci, Sh, and Sm interbedded with Gm and Gmp units. Gmci deposits within this part of the section may contain angular boulders of andesite up to 3 m in diameter.

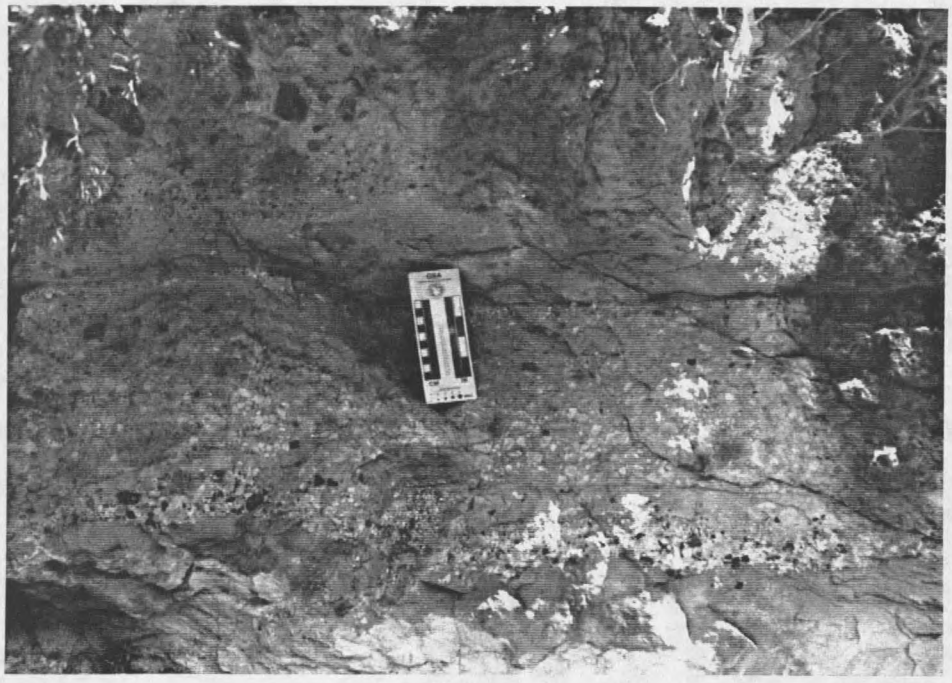


Figure 37. Units of Gmsi lithofacies at Eight Mile Canyon which contain rounded white pumice and black angular fragments of volcanic glass. Notice clasts of black volcanic glass in upper left corner.

Eight Mile Section II is not as thick as Section I (65 m). It consists predominantly of units characteristic of lithofacies association 4: clast-supported debris flow deposits, interbedded with streamflow facies deposits. Numerous units of Gmci are interbedded with lithofacies Sm and Sh (Figure 38). Trough cross-bedding resulting from diluted flow over outsized clasts consistently indicates a southeast flow direction at more than one bedding horizon (S 20° E to S 30° E). These units are sporadically interbedded with units of Gm, Gmp, Gmw and Gmcin.

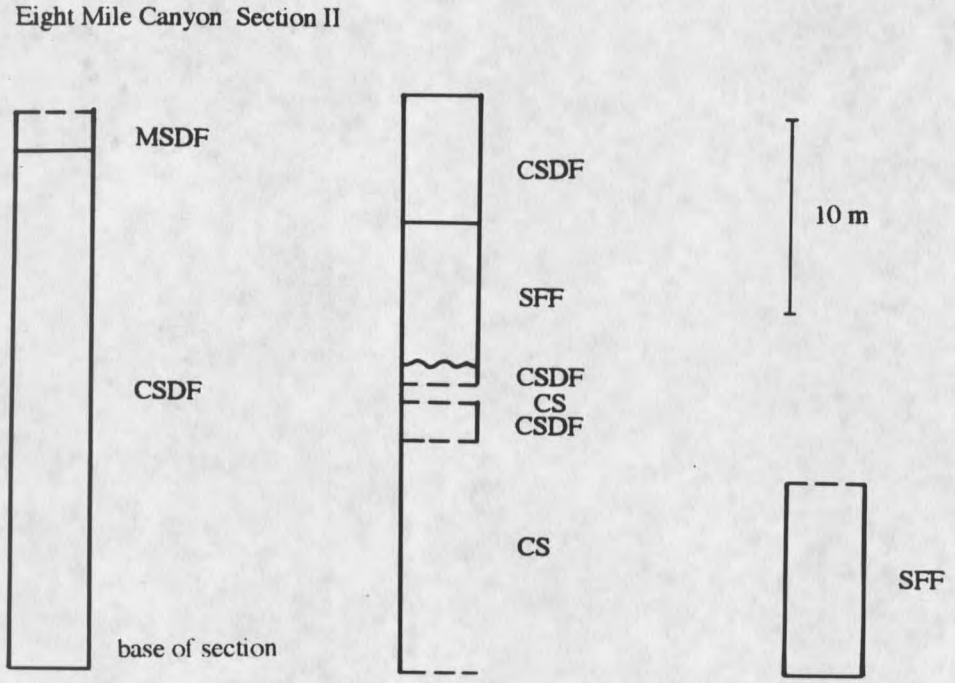


Figure 38. Eight Mile Canyon Section II, generalized to show relations between lithofacies associations; CSDF-Clast Supported Debris Flow Facies; SFF-Streamflow Facies; MSDF-Matrix-Supported Debris Flow Facies; CS-Covered Slope.

The Eightmile Canyon measured sections I and II contain evidence that pulses of eruptive activity somewhere to the north were the source of the deposits. The base of section I contains units of Gms facies which are probably pyroclastic flows. Flattened pumice, numerous layers of ash, some of which may be thin deposits of dilute surges, and large subangular pumice and tuff clasts are evidence that the deposits were the direct result of volcanic activity. Thin Flw facies interbedded with Gmci facies may represent deposition from ash clouds associated with debris flows

which are triggered by pyroclastic flows and surges (Pierson, 1985). This would explain the lack of lateral continuity of these ash layers which do not appear at other outcrops. Alternatively, some of these layers could be ash cloud surges associated with pyroclastic flows which lack juvenile pyroclastic material.

Pyroclastic flow facies become gradually less frequent up-section, replaced by numerous deposits resulting from streamflow, debris flow and hyperconcentrated flow. This trend is present in both measured sections. Above these deposits (95 m from the base of the section), a second pulse of volcanic activity is recorded in the deposits of Eight Mile Canyon Section I. GmLa and Gmsi units within this measured section may result from deposition of pyroclastic flows. Dense lithic clasts in pyroclastic flows, which are often normally graded in the base of the flow, are known to drop out during flow transport, imparting subsequent flow deposits with a fine-grained base (Sparks, 1976). Distal pyroclastic flow facies at Laacher See Volcano, 5 to 10 km from the source, are characteristically fine-grained and lack a lower concentration zone of dense lithic clasts (Freundt and Schmincke, 1986). In addition, Gms and GmLa units at Eight Mile Canyon contain a high percentage of blocky glass fragments, characteristic of deposits which result from phreatomagmatic activity (Heiken, 1974).

Both measured sections at Eight Mile Canyon contain a large number of deposits characteristic of clast-supported debris flow and hyperconcentrated flow facies. Many of these units are considered clast-supported debris flows rather than pyroclastic flows lacking juvenile material because they are closely associated with Gm lithofacies. At section I, the transition from pyroclastic flow facies to streamflow and debris flow facies is marked by the presence of channels filled with Gm lithofacies, indicating that material deposited during eruptive activity was being reworked by streamflow. Streamflow deposits are thin, probably because reworked material was actively transported away from the source. The difference in facies types between the two measured sections at Eight Mile Canyon is most likely to be a reflection of the thickness of the sections measured, although differences may also be a function of conditions relating to deposition.

Lithofacies Sequences at Palisade Mountain

Measured Section I at Palisade Mountain consists of debris avalanche, vent and flow breccia facies with minor pyroclastic flow, fall and surge facies (DAVB and PFFS). The base of Measured Section I at Palisade Mountain contains a very unusual light grey outcrop of trough cross-stratified gravel (Gt) which consists almost exclusively of angular fragmented dacite with rare fragments of Precambrian gneiss and quartzite (Figure 39). Troughs within the unit indicate that direction of flow was to the southeast (S 20° to S 50° E). This unit is deposited on and thins across discontinuous deposits of an eroded monolithologic Gmpv unit and lava flow. A Gmpv unit overlies the Gt deposit. The contact between the units is steeply dipping northeastward into the face of the outcrop. This unit has rare clasts of variable volcanic lithologies, but consists predominantly of andesite and scoria and dips steeply below a thick Gms lithofacies unit. This Gms unit thickens into the hillside 15 m above the base of the section (to the northeast), and is heterogenously welded and altered along fractures. Clasts within it consist of brecciated blocks (> 1 m) of intermediate composition and smaller variable volcanic lithologies including welded ash and very large (0.5 m) blocks of dense pumice. The uppermost unit is deposited on the planar upper surface of the Gms deposit. It is a very thick (30 m) deposit of Gmpv lithofacies. Clasts within this unit consist primarily of angular dacite and andesite. It weathers into pinnacle shaped exposures, with cliffs on all sides.

Palisade Mountain Section II is located uphill and 800 m to the southeast of Section I. This section consists of basal Gm and Se streamflow facies, above which are deposits characteristic of debris avalanche facies (DAVB). Gmpv, Gmp, and Gms deposits are interbedded and grade laterally from one to another in the lower part of the section. Gms deposits are rare and are not present in the upper part of the measured section. With the exception of basal streamflow facies units, most of the deposits are very similar lithologically and texturally to the uppermost unit in Palisade Mountain Section I (Figure 40). Units are wedge-shaped and thicken dramatically southward. Upper surfaces of deposits lower in the section are roughly planar and also dip southward. They consist of fragmented intermediate composition rocks. Deposits higher in the section have uneven upper surfaces and tend to be much thicker. Zones within the units in the upper portion of the measured section have deformed clasts which appear to have flowed after deposition. Patches within some of these units are

of various shades of orange and red. Clasts and matrix within these zones are monolithologic.



Figure 39. Gt lithofacies at the base of Palisade Mountain Section I. This unit is composed almost exclusively of angular fragments of light grey dacite.

The outcrop of Gt lithofacies at the base of Section I is unusual because it consists of only one volcanic lithology in which even sand sized grains are extremely fragmented. It also contains clasts of non-volcanic lithologies stratigraphically below the volcanic sequences which are not commonly found within them. This unit is interpreted as an explosion breccia and may have resulted from the destruction of a dacite dome. Deposited from a surge, it has been preserved within a local topographic depression, resulting in preservation of the portion of the unit with a cross-bedded texture. Precambrian clasts within the unit are probably derived from vent walls. Features of units stratigraphically above this and to the south are probably also related to different activities and stages of dome growth.

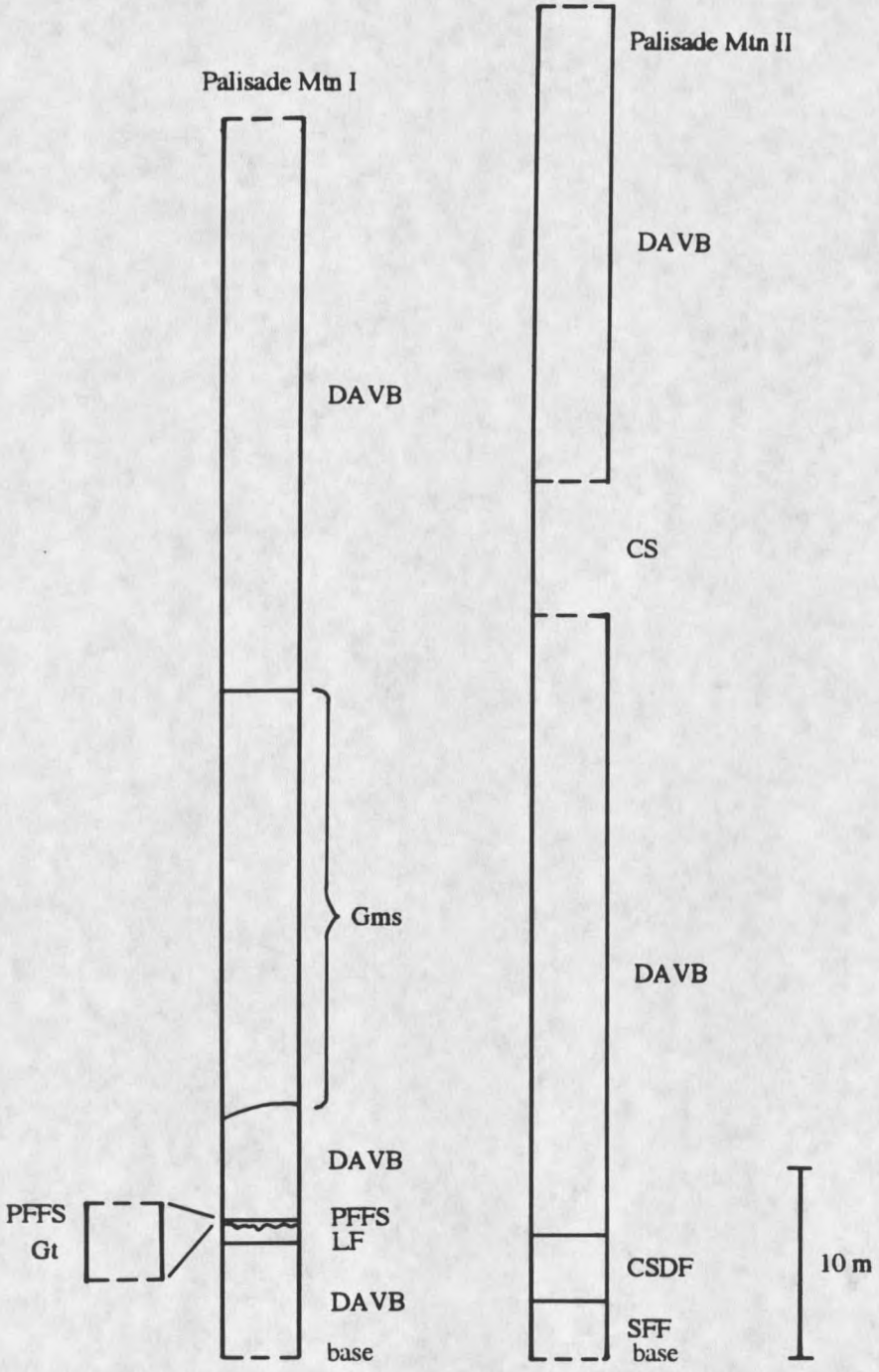


Figure 40. Palisade Mountain measured sections I and II, generalized to show relations between lithofacies associations. Lateral changes in unit thickness in section I and location of Gms matrix-supported vent facies are also shown; DAVB- Debris Avalanche and Volcanic Breccia Facies; PFFS - Pyroclastic Flow, Fall and Surge Facies; CSDF - Clast-Supported Debris Flow Facies; SFF - Streamflow Facies.

Avalanche activity may have triggered explosive decompression of magma beneath the surface (Figure 41). This would account for the numerous avalanche deposits which thicken southward from Palisade Mountain Section I toward the locality of Palisade Mountain Section II and beyond. New gas-rich magma brought to the surface, could result in lava flows and deposits of Gmpv flow breccia (Heiken and Wohletz, 1987). Associated ash cloud surges may have been dilute, leaving a thin veneer of deposits, as well as thicker deposits preserved in topographic depressions that contain lithologies of underlying strata blasted from the vent. In some places surge deposits may not have been preserved as subesequent explosive activity widened the vent and probably blew away proximal deposits. The Gms unit above Gmpv flow breccia and thin ash deposits is interpreted as vent fill which has been altered by fumarolic activity (Figure 42). Associated avalanche debris deposits above this indicates that dome growth and avalanche activity continued, probably from a related proximal vent and may have been similar to recent witnessed activity at Santiaguito volcano in Guatemala (Rose, 1973, 1987). Vapor phases associated with fumarolic activity from the vent are probably responsible for cementation of overlying deposits and their subsequent erosional tower-like morphology.

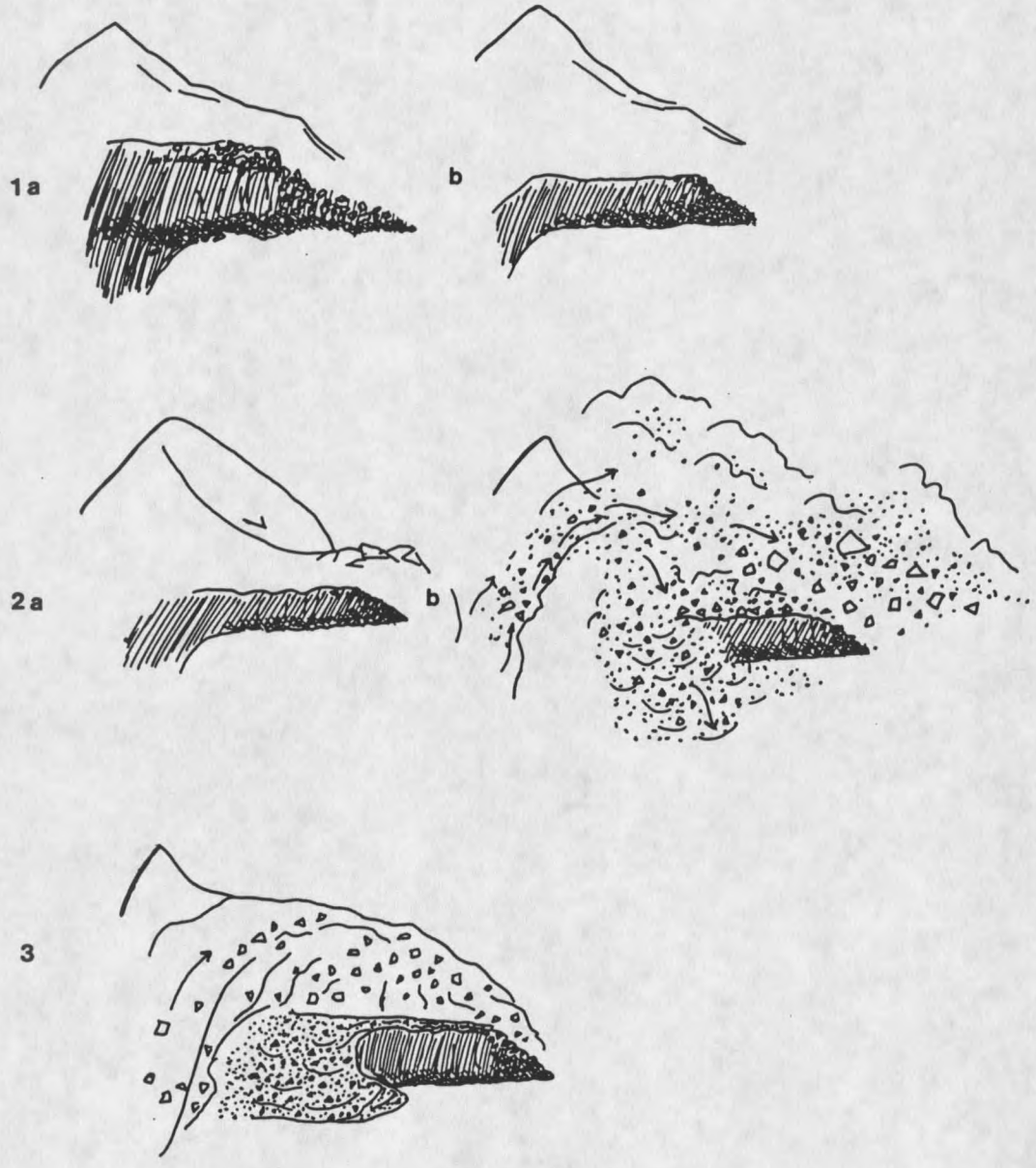


Figure 41. Illustration of sequence of probable events leading to deposition of facies sequences at Palisade Mountain. 1) Deposition of flow and vent breccia, eroded into uneven paleotopography. 2) Explosive decompression of magma by avalanche processes, leaving thin surge deposits overlying breccia which thicken laterally and become cross-bedded over surface depressions. 3) Additional vent breccia deposition, subsequently covered by deposition during a repetition of similar events, then cemented through vapor phase activity associated with vent fumaroles.

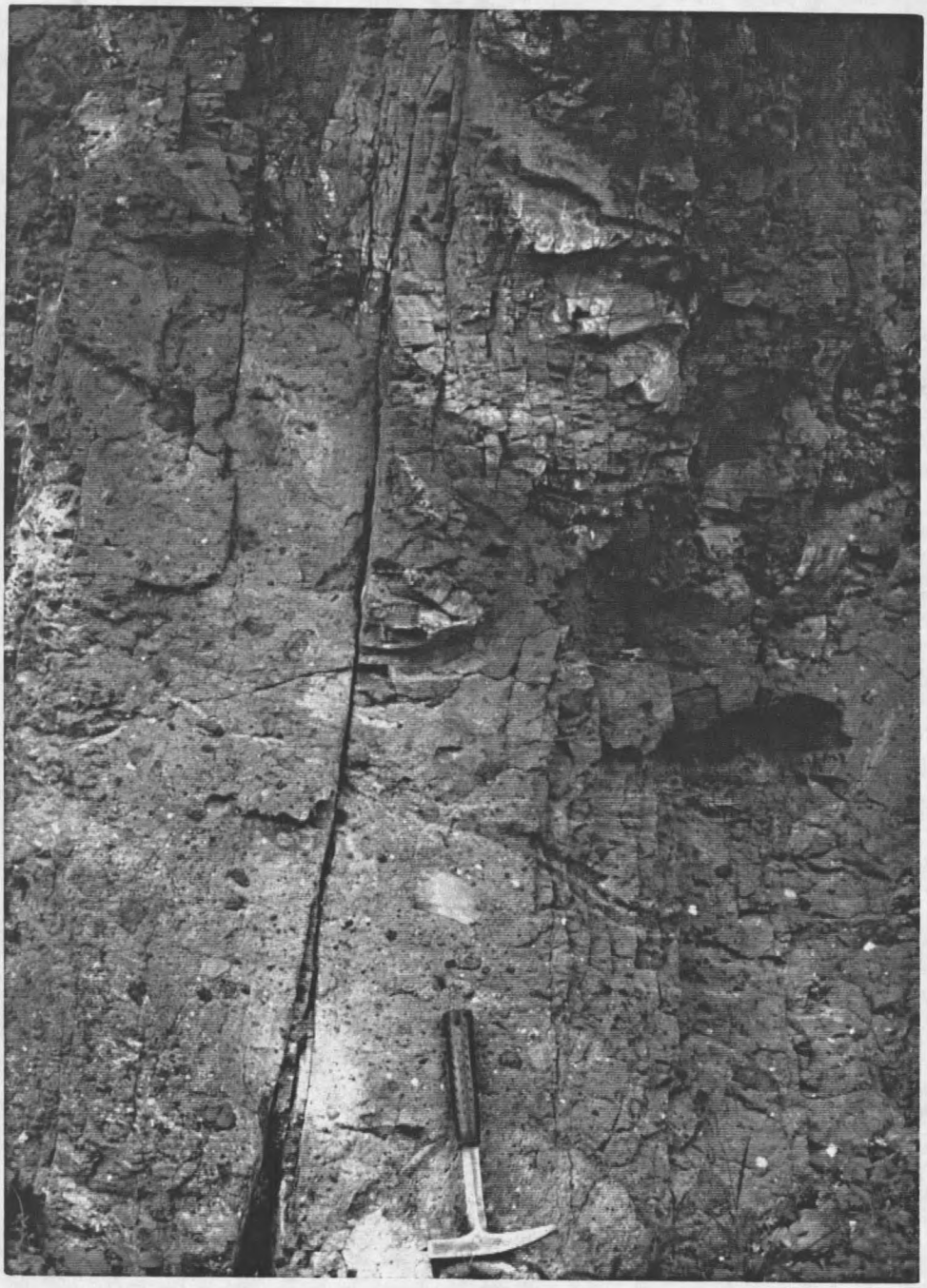


Figure 42. Photo of deposit of Gms lithofacies at Palisade Mountain. This unit is interpreted as vent facies. Note heterogenous nature of welding, alteration along fractures, and large pumice clast behind hammer.

Lithofacies Sequences at Silken Skein Falls

The base of the measured section at Silken Skein Falls contains eroded debris flow facies (Gmp) covered by thin (10 cm) tabular streamflow (Gm) deposits. Above these units, from 2 to 30 m from the base of the section, are deposits representing predominantly clast-supported debris flow facies (Gmpi, Gmp, Gmsi, Gmci, Gms, Gmw, Sh, and Sm). Gmpi facies units within the vicinity of Silken Skein Falls are commonly imbricated and uniquely contain very large clasts (50 cm) which exhibit long-axis imbrication. Imbricated clasts indicate that the direction of flow was between N 50° W and N 60° W. Concentrated in the upper and lower parts of these units are numerous pumice fragments, fragmented cauliflower bombs, fragmented pieces of volcanic glass with devitrified rims, and charred or carbonized wood fragments. Wood fragments often have gas escape structures associated with them. One unit of this lithofacies contains an upright tree stump. Many of the debris flow facies deposits, and thin interbedded units of pyroclastic flow, fall and surge facies contain a high percentage of phenocrysts in the matrix. The glassy portion in a few of the units is palagonitic, imparting them with a yellow-brown color. Gmci units at Silken Skein falls are typically finer-grained than similar units at Eight Mile Canyon, and inverse grading within these units appears to be more gradual. Interbedded Gmsi lithofacies are very similar in appearance to Gmci units, but contain a higher percentage of matrix. These units are interrupted once, 15 meters above the base of the section, by streamflow facies which are commonly thin, tabular deposits of Gl and Gm. Stratigraphically above the streamflow deposits is a unit of Sh which contains irregular lateral grading into fine and coarse portions. Overlying this deposit are Gmpi facies units, an andesitic lava flow, and repeating units of Gmci.

Three thin palagonitic units of Sh, Sm, and Gms directly overlying Gmci units (32 m from the base of the section) contain fragments of charred or carbonized wood, and armored and accretionary lapilli. Rimmed, discoidal accretionary lapilli, and cored discoidal accretionary lapilli which have long axes horizontally aligned, occur immediately above a deposit of Gms lithofacies (Figure 43). Rimmed accretionary lapilli are also found in the upper portion of this deposit. Rimmed accretionary lapilli are commonly from 8 to 10 mm in diameter; cored accretionary lapilli are larger, with long axes up to 4.5 cm and short axes of 2.5 cm. The Gms unit in which they occur is

very fine-grained and palagonitic, containing predominantly pebble-sized clasts of andesite, dacite, and vesicular ash, and large euhedral phenocrysts of black hornblende and copper-colored biotite. Fine-grained Sm deposits which directly overlie the Gms unit contain armored lapilli 7 to 8 mm and rimmed accretionary lapilli up to 10 mm in diameter. This Sm unit also contains numerous carbonized twigs. Above this, rimmed lapilli are also found in the coarse fraction of graded Sm facies units which generally underlie and are gradational into overlying Gmpi facies deposits. Above these deposits are large, cored discoidal accretionary lapilli, with short axis diameters of 2.3 cm and long axis diameters of 4.2 cm, in a fine-grained unit of Sh lithofacies. This unit is generally massive in appearance, but contains vague low angle stratification. It is gradational into the base of a deposit of Gms facies (38 m from the base of the section) which is similar in appearance to the lower Gms unit, but which contains more fragments of andesite and dacite as well as outsized clasts up to 30 cm in diameter protruding into the unit above. This unit is immediately below a thin Sh facies deposit containing flattened, granule-sized tuff lapilli, composed of light colored ash. Overlying this deposit are clast-supported debris flow facies represented by units of Gmpi and Gmci lithofacies.

The top of the measured section at Silken Skein Falls (47 m above the base) contains Gm, Se, and Sh units interbedded as streamflow facies. However, some of these units contain volcaniclastic boulders up to 1 m in diameter which contain relict bedding and appear to have undergone soft sediment deformation.

Units at the base of Silken Skein Falls indicate that deposits resulting from debris flow activity were eroded by streamflow activity which reworked deposits between events. The occasional presence of streamflow deposits probably represents periods of degradation, perhaps due to a brief period of volcanic quiescence, when agradation due to an influx of volcanic debris had ceased.

The character of the deposits between streamflow facies units changes up-section, exhibiting textures which may be attributable to heat. Carbonization of wood, which is common within the deposits, takes place at temperatures in excess of 300° C (Freundt and Schmincke, 1986). Although delicate carbonized wood can still be transported and reworked as fragments, an upright carbonized stump within one of the units suggests that carbonized wood originated from the deposits in which they are found. Studies comparing hot and cold debris flows by Arguden and Rodolfo (1990) indicate that hot flows have more internal mobility which may be imparted to the clasts by decreased friction between clasts and increased dispersive pressure due to

interstitial steam. Increased clast mobility, together with increased dispersive pressure, permits clasts to more freely orient themselves within a flow, and is reflected in depositional textures. In the deposits at Mayon Volcano, deposits from hot debris flows exhibit inverse grading which appears to be more gradual than deposits from cold debris flows from the same source (Arguden and Rudolfo, 1990). Clast imbrication, even within large clast sizes in units of Gmpi facies, as well as textural changes in inverse grading in units of Gmci and Gmsi facies, both found in deposits at Silken Skein Falls, may have resulted from a greater degree of clast mobility and increased dispersive pressure.

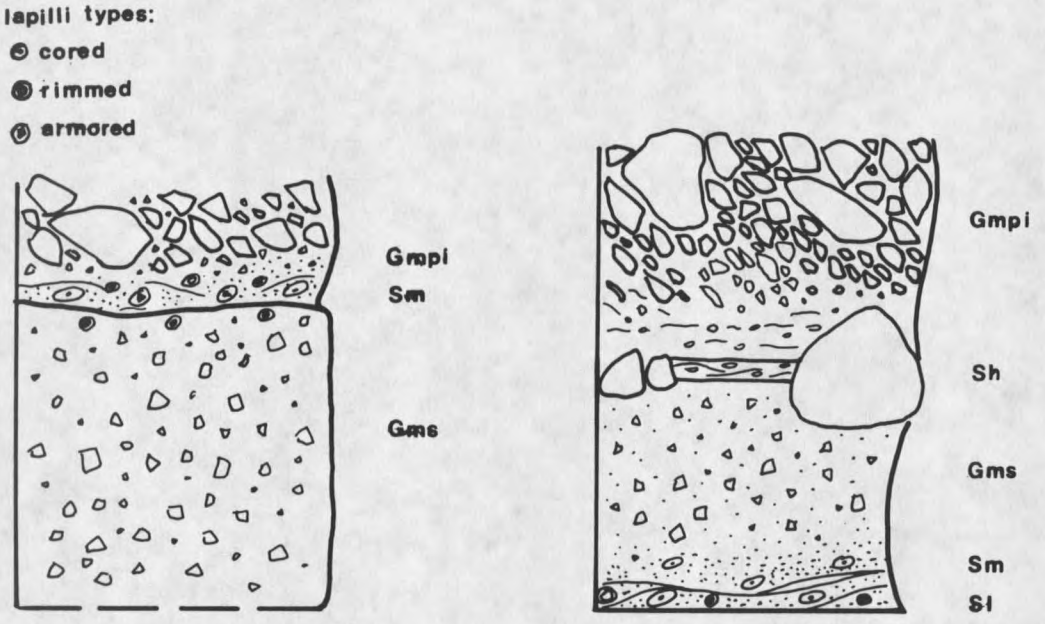


Figure 43. Detailed sketch of portions of measured section 32 m from base of Silken Skein Falls section, showing location of accretionary lapilli within the deposits.

It is likely that many of the palagonitic deposits of Sh, Sm, Gms, Gmci, Gmpi, and Gmsi are pyroclastic flows and surges with interbedded ash-fall resulting from hydromagmatic activity. Palagonitization, a process of alteration of volcanic glass, is commonly associated with hydomagmatic activity. Increased palagonitization is known to be restricted to near vent areas and occurs in the presence of hydrothermal vapor (Fisher and Schmincke, 1984). Palagonitization also occurs during low temperature weathering and diagenesis, and alone, cannot be used as a distinguishing

characteristic (Heiken, 1972). However, this degree of alteration is not widespread and is uniquely associated with deposits which contain large accretionary lapilli.

Accretionary lapilli form as moist aggregates of ash in eruption clouds; armored lapilli form when wet ash becomes plastered around a solid nucleus such as pumice or lithic fragments (Fisher and Schmincke, 1984). Cored accretionary lapilli are commonly associated with hydromagmatic-pyroclastic surge and flow deposits while rimmed accretionary lapilli result from ash-fall deposits associated with pyroclastic surges and flows (Schumacher and Scmincke, 1991). The distribution of different types of lapilli at Silken Skein Falls is a reflection of the depositional mode of the deposits. These characteristics are ascribed to similar deposits at Laacher See, which is a maar volcano (Schumacher and Schmincke, 1991). Rimmed (fall) lapilli occur in thin fine-grained units which are probably ash-cloud deposits associated with overlying pyroclastic surges and flows. They also occur in the upper portion of Gms deposits directly beneath them, most likely as a result of penetration upon impact (Schumacher and Schmincke, 1991). Cored (flow) lapilli form within pyroclastic surges and dilute pyroclastic flows (Schumacher and Schmincke, 1991). They are found at the base of a Gms deposit in a unit with low angle stratification which is consistent with this interpretation. Overall, these deposits, which are within the middle portion of the measured section at Silken Skein Falls, have characteristics similar to those found in proximity to maar volcanoes, which are the product of hydroclastic eruptive activity (Wohletz and Sheridan, 1983). The portion of the measured section above these deposits is characterized by non-cohesive, clast-supported debris flow and streamflow facies, probably deposited as proximal eruptive activity ceased.

Lithofacies Sequences at Flanders Mountain

Deposits at the base of Flanders Mountain are similar in appearance to those found in the middle of the measured section at Silken Skein Falls (Figure 44), although coarse conglomeratic units are finer-grained and thinner (<1 m). Deposits within the lower 13 m of section are yellow-brown, palagonitic, and contain a high percentage of rounded, vesicular pumice lapilli, and hornblende, biotite and plagioclase phenocrysts. Near the base of the section, Sh and Sm units have armored and accretionary lapilli which are sub-spherical to discoidal and are from 10 to 12 mm in diameter. Above these deposits are units of clast-supported debris flow facies represented by Gmci and

Gmpi lithofacies which contain numerous petrified logs; several are more than a meter long and upright.

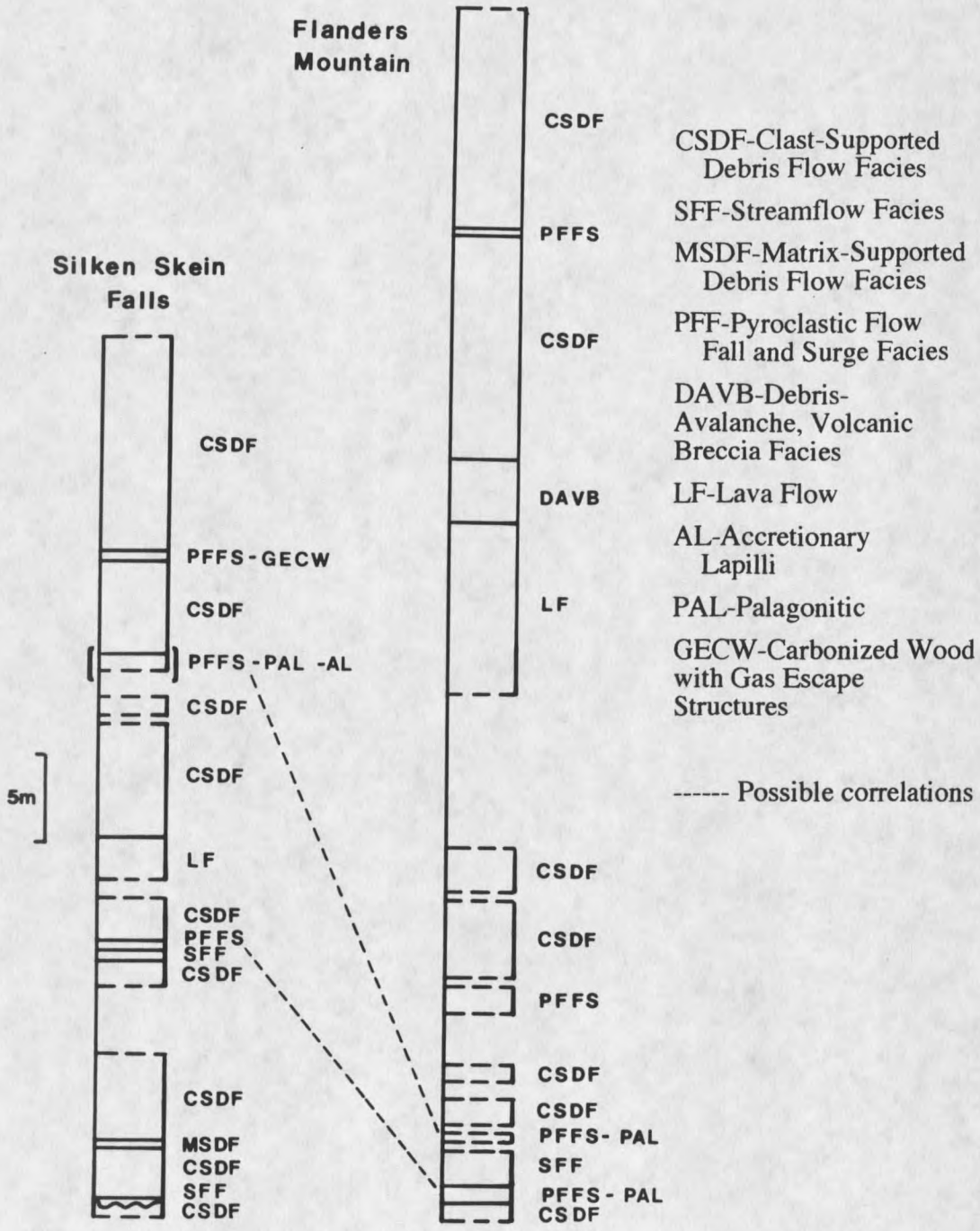


Figure 44. Silken Skein Falls and Flanders Mountain stratigraphic sections, generalized to show relationships between lithofacies associations. Location of Figure 43 is indicated by brackets.

Gmci and Gmpi units are covered by an aphanitic, glassy black lava flow that is basaltic in appearance, and a thick, bomb-rich Gmpv facies unit 40 m above the base of the section. Depositional units above the lava flow have very angular clasts, many of which are fragmented pieces of volcanic glass, commonly from 2 to 5 cm in diameter with devitrified rims (Figure 45). Directly overlying this is a Gmpi deposit containing rare large blocks of volcanic glass. It fines upward and is covered by a pumice rich unit of Slc facies. Both of these deposits indicate that paleoflow was to the northwest. Long axis imbrication of clasts in the Gmpi unit indicate that flow was N 50° W to N 55° W. Above these units are multiple tabular, but not laterally continuous Gmp deposits. These deposits are truncated by erosion in a stair-step fashion and are interbedded with Sh and Slc deposits. Truncated edges of these depositional units strike N 60° E, and dip to the north. Slc facies units are found locally where Sh facies thicken. Their distribution corresponds to changes in the dip of the surface of truncated units.



Figure 45. Fragments of volcanic glass with alteration rims in Gmp deposit at Flanders Mountain.

Deposits at the base of the section contain accretionary lapilli and are probably stratigraphically equivalent to similar deposits at Silken Skein Falls (Figure 44). Because these deposits contain smaller accretionary lapilli and are finer grained and thinner, they were likely deposited farther from the source vent. Slc and Gmpi deposits above this are interpreted as pyroclastic surge and flow deposits, with similar paleocurrent orientations. The large amount of volcanic glass indicates that volcanic activity was still hydromagmatic in nature (Heiken, 1978). This suggests that eruptive activity may have continued from the same source at a later time. Beneath these deposits and above the base of the section, are a lava flow and flow breccia which are not laterally continuous to Silken Skein Falls, and may be from a separate source.

Stacked Gmp units are interpreted as successive debris flows deposited after these eruptive phases and may not have any relation to them. They were eroded into terraces as a result of streamflow degradation, and subsequently covered and overtopped by a pyroclastic surge (Figure 46). Localized cross-bedding resulted from obstruction of the pyroclastic surge which flowed at an angle to the terrace edges, probably in a west to southwestward direction. As a whole, the sequence of deposits at Flanders Mountain indicates that local deposits were derived from multiple source areas.

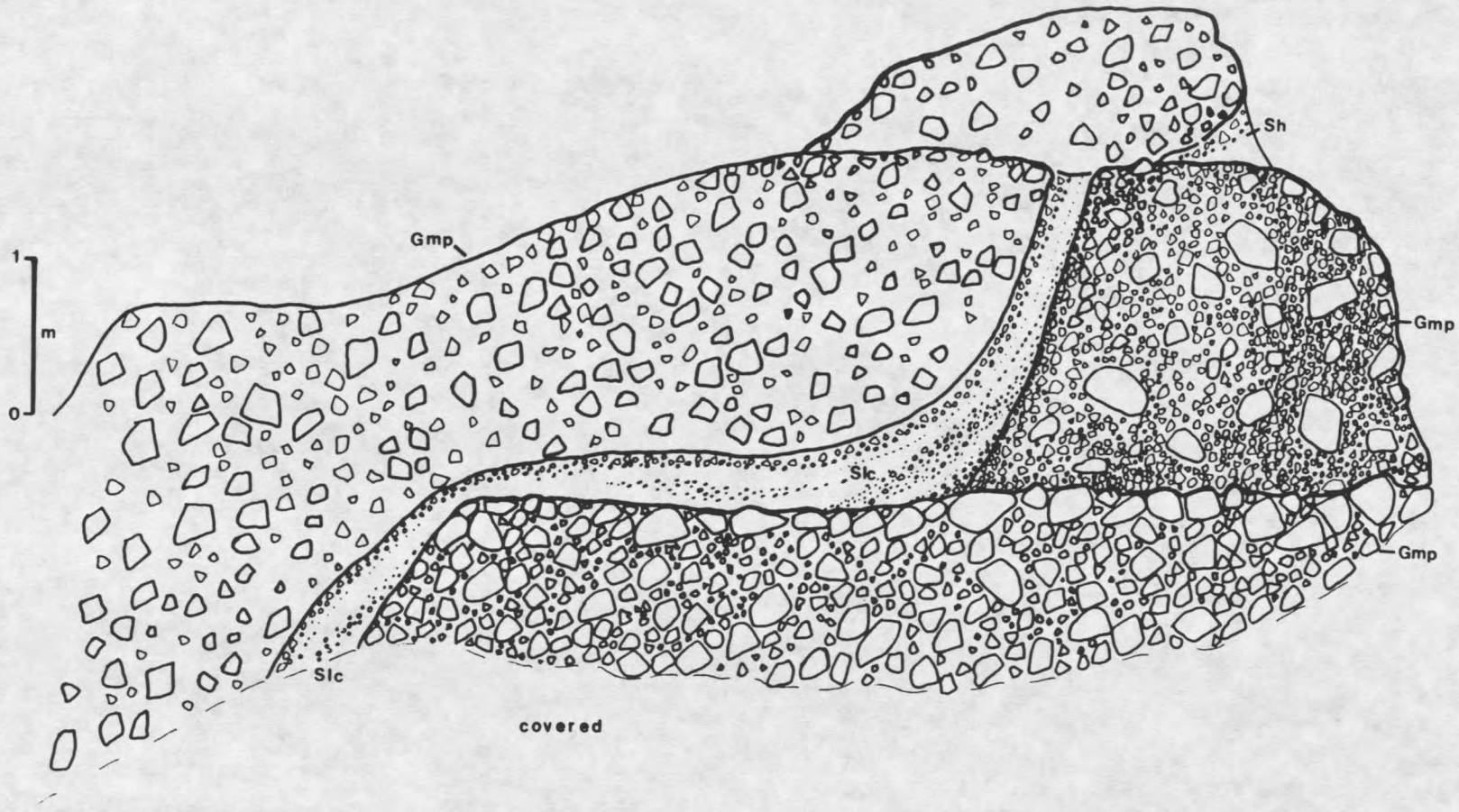


Figure 46. Sketch illustrating vertical and lateral relationships in upper portion of Flanders Mountain measured section. Sh deposit which grades laterally into Slc mantles paleoerosional surface of debris flow deposits eroded into terrace form.

Lithofacies Sequences at Windy Pass

The base of the measured section at Windy Pass contains coarse-grained lithic-rich deposits interbedded with a thin Slc facies unit located 4 m from the base. The basal Gmp facies deposit contains clasts of variable volcanic lithologies. Its upper surface is erosional and is overlain by a Gmw deposit above pinches and swells to fill erosional voids. An overlying tabular Slc deposit contains thin strata which are normally graded and pinch and swell, these are interstratified with low angle cross-beds of fine sand. A single unit of Gmci directly overlies the Slc facies deposit, and is in turn overlain by a unit of Gmpi and wedge-shaped Gmcn deposits which contain clasts of predominantly angular red and purple andesite.

Units above this, 12 m above the base of the section, are typical of pyroclastic flow and surge facies. A thick pumice-rich Sh facies deposit (7m) has U-shaped channels cut into it which contain Gms and Gm deposits. These deposits are overlain by a thick Slc facies unit with very low angle cross-bedding. Both the Slc and Sh units exhibit imbrication of dense angular lithic clasts indicating that the surges originated to the north (flow direction to S 20° E or S 22° E). Above these units are a series of tabular Gms and GmLa deposits with thin (10 to 20 cm) interbeds of Gmwt (Figure 47). The top of the measured section is an eroded deposit of Gmp which overlies an eroded uneven surface with a thin layer of orange silt which is rich in pumice fragments.

The basal Gmp deposit is considered to be a debris flow deposit that underwent subsequent erosion and non- deposition followed by a period of renewed volcanic activity. The lower Slc facies unit is overlain by coarse-grained deposits interpreted as pyroclastic flow and pyroclastic lag deposits mainly on the basis of their close association with surge deposits. The lower Slc unit is considered to have been deposited from a ground surge or base surge because it is dense and contains cross-laminations (Fisher and Waters, 1969; Wohletz and Sheridan, 1979; Fisher, 1983). Slc and Sh deposits above these units may be ash-cloud surge deposits because they are poorly compacted. Large voids between individual particles in a deposit is a characteristic common to ash-cloud surge deposits (Schumacher and Scmincke, 1991). These deposits are 4 to 6 m thick, with low angle cross-beds indicating deposition from low amplitude, long wave-length surges close to the source (Fisher, 1983; Valentine, 1987). Channels cut into the deposits could have resulted from pyroclastic

flows which are known to cut furrows into pre-existing deposits (Fisher and Schmincke, 1984). Above these units, 26 m above the base of the section are Gmwt deposits resulting from volcanic activity involving explosively ejected tephra. They consist of thin units of delicate pumice which are matrix-poor as a result of elutriation of finer particles within the eruption cloud (Fisher, 1983) Gwt units are interbedded with Gms and GmLa deposits which may have preceded or followed the explosive bursts. GmLa deposits from 25 to 31 m from the base of the section are similar to medial facies deposits at Laacher See volcano which were deposited 5 to 7 km from the source (Freundt and Schmincke, 1986). Interbedded GmLa Gms and Gwt deposits may be derived from a separate source than Slc units lower in the section. Explosive activity, commonly associated with all stages of dacite dome growth (Heiken and Wohletz, 1987), may have resulted in the deposition of pyroclastic surge and flow facies at Windy Pass. More than one possible source for these units have been mapped. Dacite plugs occur 10 km to the north (McMannis and Chadwick, 1964). Because of the limited area that these deposits cover, they are probably the result of a short dense eruption column which was not widespread. This suggests that there was a large volume of water in the erupted mixture (Sparks, 1978). The erosional surface in the upper part of the measured section (40 m above the base) is interpreted to have formed by erosion of a pyroclastic flow in which the lower normally graded dense clasts are preserved. The orange silty layer may represent an immature soil. Development of this surface indicates that eruptive activity had ceased for a time before later deposition of a debris flow across the weathered horizon.

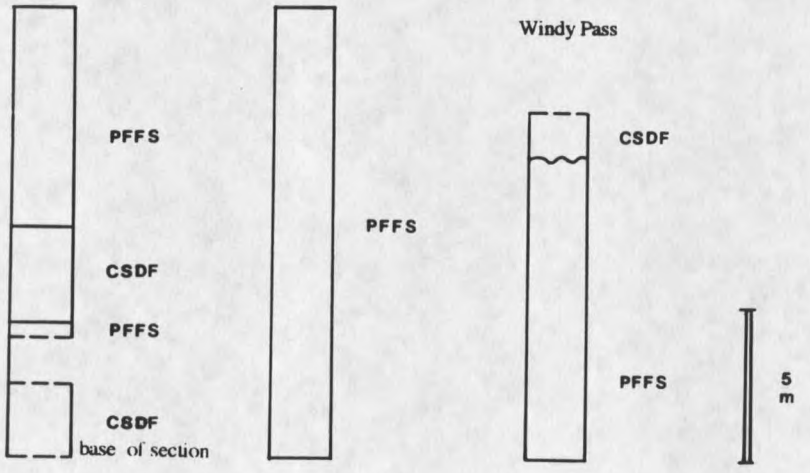


Figure 47. Windy Pass measured section, generalized to show relations between lithofacies associations. PFFS-Pyroclastic Flow, Fall and Surge Facies; CSDF-Clast-Supported Debris Flow Facies.

CHARACTERISTICS OF THE DEPOSITIONAL SETTING

Volcaniclastic sequences within the Hyalite Peak Volcanics are the product of a broad range of transitions between depositional processes. These transitions are a product of interaction between pyroclastic and epiclastic processes which induce various flow types, such as debris flows triggered by pyroclastic flows. Additional and numerous transitions in flow type are produced by changing sediment to water ratios, an inherent characteristic of areas with large fluctuations in discharge of sediment or water. Transitions in depositional processes have been documented in numerous modern volcanic settings including Mount St. Helens and Nevado del Ruiz (Pierson, 1985; Waitt, 1989; Cavalache V. and Williams, 1992). Process interactions and transitions described as typical in modern volcanic settings are also characteristic of those which produced Hyalite Peak sequences (Figure 48). They are reflected in the high degree of variation in textures and structures within the large number of lithofacies types, and the chaotic order of lithofacies sequences.

Characteristics of Eruptive Activity

A large portion (50%) of deposits within the Hyalite Peak volcaniclastic sequences which are coarse-grained, have fabrics similar to those described from Galeras volcano in Colombia which are composed predominantly of dense lithic clasts mobilized by explosive phreatic activity into pyroclastic flows (Cavalache V. and Williams, 1992). Some of the coarse-grained Hyalite Peak sequences were probably deposited in a similar fashion. Together with dense lithic material numerous deposits within Hyalite Peak sequences also contain juvenile pyroclastic material consisting of poorly vesicular pumice, cauliflower bombs, blocky glass fragments, and armored and accretionary lapilli. All of these features suggest that volcanic activity was induced by groundwater-magma interaction. Clasts which are dense, non-vesiculated and glassy suggest that magma was quenched prior to the exsolution of volatiles. Blocky shapes are indicative of breakage by thermal shock and steam explosions (Heiken, 1974; Fisher and Schmincke, 1984, Cas and Wright, 1987).

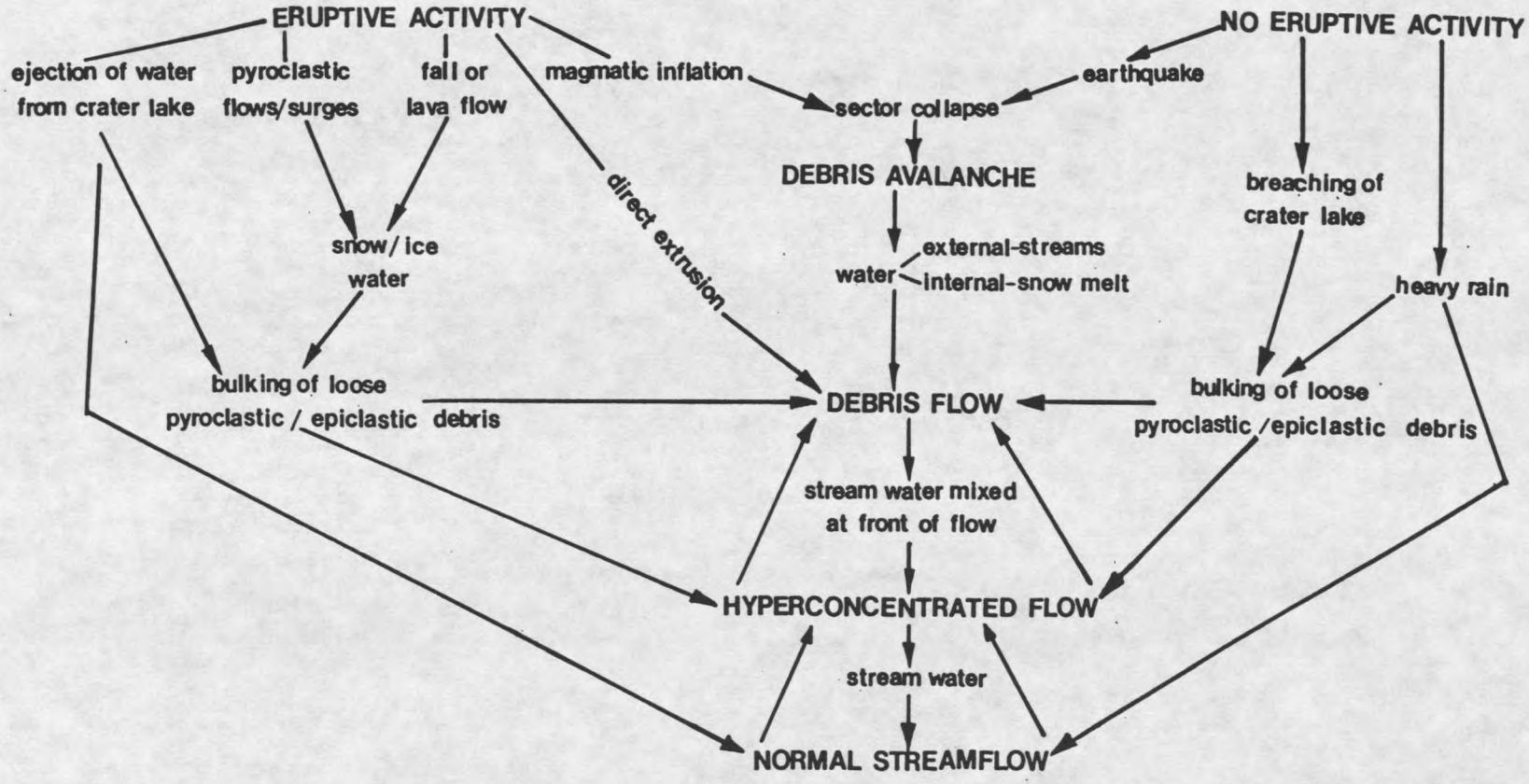


Figure 48. Schematic diagram illustrating interactive processes within a volcanic setting. Process interactions are reflected in the high degree of variation in textures and structures found within volcanically derived deposits.

Cauliflower bombs commonly have dense to slightly vesicular interiors because of low residual gas pressures associated with deposits resulting from water-magma interaction (Fisher and Schmincke, 1984). Some deposits contain accretionary lapilli, composed of concentric lapilli-sized aggregates of ash which form in ash clouds containing water or steam. They are bound together by condensed moisture and the electrostatic attraction between particles (Schumacher and Schmincke, 1991). Armored lapilli are a variety of accretionary lapilli containing crystal- or rock-fragment nuclei with ash coatings and have only been reported from volcanic settings where eruptive activity is associated with steam explosions (Fisher and Schmincke, 1984). These types of materials are found in near-vent deposits which contain a low volume of pumiceous material and ejected clasts of pre-volcanic lithologies. The few deposits clearly resulting from pyroclastic flows found at Windy Pass are similar to those described at Laacher See, Germany, that were emplaced during phreatomagmatic and vulcanian eruptive activity (Fisher, 1983; Freundt and Schmincke, 1986). Deposits at Windy Pass as well as those at Laacher See are not widespread, and probably were associated with dense, short eruption columns induced by large volumes of water within an eruption column (Sparks, 1978; Fisher, 1983). Together, these features indicate that explosive interaction between magma and water was intrinsic to the nature of eruptive activity synchronous with deposition of Hyalite Peak volcaniclastic rocks.

Different types of eruptive activity have been attributed to water-magma interactions. Hyalite Peak volcaniclastic sequences, which contain a low volume of juvenile pyroclastic material, have deposits which resemble those resulting from phreatic and phreatomagmatic eruptions. The presence of localized palagonitic deposits containing fragmental glass suggests that hydromagmatic eruptions of basaltic magma may have occurred locally. Other types of volcanic eruptions not associated with phreatic activity may have taken place, but evidence for these is lacking. The terms vulcanic and hydromagmatic have been used synonymously with phreatomagmatic by some authors (Fisher and Schmincke, 1984; Heiken and Wohletz, 1987; Cavalache V. and Williams, 1992) but are considered distinctly different by others (Williams and McBirney, 1979; Self and others, 1979; Barberi and others, 1992). Phreatic eruptions, as the term is used herein, are considered to be caused by the violent expansion of steam generated from groundwater without emission of juvenile material (Fisher and Schmincke, 1984; Barberi and others, 1992). Phreatomagmatic eruptions are caused by the explosive interaction of magma with underground aquifers and may be phreatic or hydrothermal in nature (Barberi and

others, 1992). However, it is believed that phreatomagmatic eruptions in the Hyalite Peak sequences were not related to hydrothermal activity because of the lack of extensive hydrothermal alteration.

Paleocurrent measurements, from clast imbrications, channel orientations, and sedimentary structures record sediment dispersal indicative of multiple source areas, when used in conjunction with lithofacies associations, (Figure 49). Deposits were sourced from the north at Windy Pass and Eight Mile Canyon and from the south at Flanders Mountain and Silken Skein Falls. Sequences at Eight Mile Canyon indicate that pyroclastic flows and debris flows originated from a northern source which may no longer be preserved. Surge deposits at Windy Pass probably originated from an intrusive feature 2 km to the north. This feature together with other dacite intrusions in the northwestern part of the Gallatin Range have been interpreted as extrusive domes by Shaver (1978). Domes of this type are commonly associated with explosive activity (Heiken and Wohletz, 1987). Proximal to medial facies pyroclastic flows also found within the Windy Pass measured section may have also come from one of the dacite intrusions described by Shaver (1978), in the vicinity of these deposits. Lower and medial sections of deposits at Silken Skein Falls and Flanders Mountain indicate that deposits were being shed from the south, but for the most part from a local source. Facies associations together with paleocurrent data indicate that material was derived from a combination of small localized vents and large volcanic edifices with regional sediment dispersal. Some surge deposits higher up in the section at Flanders Mountain may have originated from Point of Rocks, an area of numerous intrusive features 10 km to the southeast, which has been previously interpreted as a source for most of the volcanics (Chadwick, 1970). Preserved sequences at Antelope Butte and Eight Mile Canyon are not far to the north of the Point of Rocks intrusions. However, paleocurrent data indicate that the source for Eight Mile Canyon deposits is from the north rather than south. Antelope Butte sequences also do not show any indication that they were derived from volcanic activity originating at Point of Rocks, although it seems to be a possible source because of its proximity.

Paleocurrents indicate that there were two directions of flow: volcanic debris was transported southeastward and northwestward. These measurements illustrate some of the difficulty in interpreting provenance in volcanic settings. If paleocurrents are taken alone, without utilizing accompanying lithofacies associations, they could

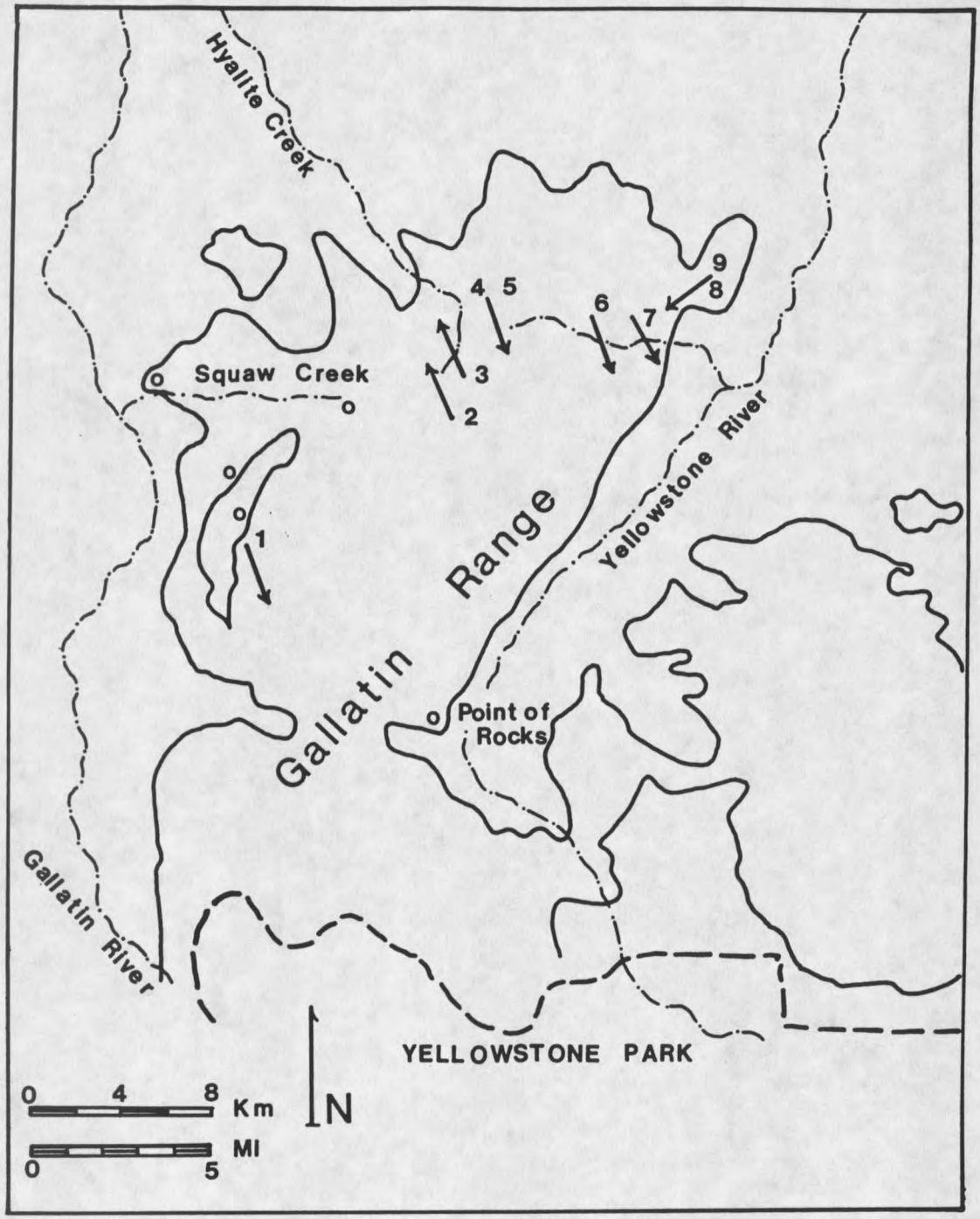


Figure 49. Map showing direction of paleocurrents in study area, as well as possible vent sources (denoted by small circle - o). Modified from base maps by McMannis and Chadwick (1964) and Chadwick (1970).

be mistakenly interpreted as resulting from two large sources rather than several localized sources. Even in the simplest of volcanic terranes, at one isolated stratovolcano, there are associated side vents forming cinder cones and domes. These features act as separate sources of debris, may eject material in different directions, and may also act to deflect paleocurrents from a central vent.

Multiple vent sources also confuse local and distal facies associations. Smedes and Protska (1972) categorized lithofacies into distal alluvial facies and proximal vent facies based on the number of interbedded lava flows, thickness of volcaniclastic debris, and degree of channelization. These assumptions are simplistic, and do not account for explosive eruptive styles which generate pyroclastic debris rather than lava flows. Hyalite Peak volcanic sequences were probably erupted from andesitic stratovolcanoes and dacitic domes, as well as maar cones or tuff rings. Some lava flows which are connected with feeder dikes originated from localized fissure eruptions, possibly located at the flanks of a central vent. This type of activity has been described as a common occurrence on the flanks of Santiaguito volcanic dome in Guatemala (Rose, 1973). Preserved lava flows in the vicinity of Hyalite Peak have exposed dikes which are interconnected with them but have no indication of relationships to a centralized vent. In addition, explosive eruptive activity at Palisade Mountain produced primary volcanic deposits consisting predominantly of pyroclastic debris and avalanche material. Many of these deposits initially thicken away from the source. Associated explosive activity, common in phreatomagmatic eruptions, may have blasted away local vent deposits. Moreover, channels cut into deposits are rare and occur in sequences which are interpreted as proximal surge deposits at Windy Pass, probably as a result of furrowing by proximal eruptions of pyroclastic flows. Other downcutting and erosion within Hyalite Peak sequences may be closely related to periods of degradation by streamflow between periods of eruptive activity, at any distance from the vent. Detailed mapping of lithofacies associations is a necessary step to aid in further understanding and characterization of this volcanic setting.

At the time of eruption, Hyalite Peak volcanic sequences and associated vents were situated in a region with primary topographic relief of as much as 600 m (2000 ft). Eruption of vent material may not have acted only to fill in paleotopographic depressions, but also resulted in localized paleorelief. Paleotopography coupled with phreatic eruptive activity, resulted in the deposition of volumes of dense lithic material in the form of pyroclastic debris where local paleotopography probably diverted the flow of erupted material in different directions. Pyroclastic flows and blast surges

probably incorporated material from the substrate when flowing over uneven surfaces, similar to the blast surge at Mount St. Helens (Fisher, 1990). This process is well documented in other pyroclastic deposits as well (Buesch, 1992). Dense materials which accumulate at the base of a pyroclastic flow, eventually decouple and flow down localized channels. An additional dense lithic component inherent in pyroclastic flows results from vent-clearing phreatic activity such as those deposited at Galeras volcano, Colombia (Cavalache V. and Williams, 1992) creating additional lag deposits which also tend to decouple from the less dense portion of the flow (Walker and others, 1981; Suzuki-Kamata and Kamata, 1990). Underlying deposits of durable lithologies are more easily preserved than overlying less dense loose deposits of ash and pumice from the dilute ash cloud most commonly associated with pyroclastic flows. Preservation of the lithic portion of pyroclastic flows in low lying areas tends to bias the depositional record to preferentially include dense, clast-supported lithic-dominated pyroclastic flows containing pre-existing volcaniclastic detritus. Numerous coarse-grained deposits in Hyalite Peak sequences and the lack of fine-grained material may be due in part to initial paleorelief coupled with these processes. These deposits may be impossible to distinguish from debris flow deposits, with the exception of Gmp and Gmpi lithofacies deposits containing clasts which are prismatically jointed, indicating that they were deposited while hot.

If hot pyroclastic flows become incorporated into localized streamflow, they transform into debris flows. In recent events as well as in the geologic record, it is extremely difficult to ascertain at which point this transformation occurred. Personal accounts of survivors engulfed in a recent lahar at Nevado del Ruiz described the mud within the flow as warm, while others were clearly burned to death (Pierson and others, 1990). Temperatures within pyroclastic flows and debris flows change as a result of common interactions and transitions between these types of flows. However, flow transitions and resulting temperature changes may not take place in a homogenous fashion, which would require complete mixing of the two flow types. The temperature of the debris flow or pyroclastic flow at the time of deposition may be impossible to deduce on the basis of depositional textures. One exception may be lithofacies Gmpi. Clearly associated and interbedded with deposits of pyroclastic origin, it has textures indicating increased clast mobility that could have been imparted by interstitial steam. Future paleomagnetic core sampling could aid in interpreting blocking temperatures of the deposits as well as any possible correlation to depositional fabric (Kent and others, 1981; Downey and Tarling, 1991) While

magnetic properties can be effective in determining emplacement temperature, recent pyroclastic flows at Laacher See have documented depositional temperatures estimated as low as 200° C (Freundt and Schmincke, 1987). Such conditions could make interpretation of paleomagnetic data difficult.

Characterization of Alluvial Sequences

Hyalite Peak volcaniclastic sequences contain numerous deposits resulting from debris flows and flows transitional to hyperconcentrated flood flow which originated from pyroclastic flows and surges, as well as avalanche debris. These types of flow transitions are ubiquitous in modern volcanic settings described from recent occurrences throughout the world: Mount St. Helens, and Mt. St. Augustine, USA; Nevado del Ruiz, Colombia; Reventator, Ecuador; Mt. Asama, Japan; Mt. Bezymianny, Soviet Union; and many others (Pierson and Scott, 1985; Lowe and others, 1986; Major and Newhall, 1989). Hyalite Peak sequences were deposited on the flanks of volcanoes and localized vents. For the most part these deposits do not exhibit fabrics associated with idealized matrix-supported debris flow facies. Lithofacies Gms with a matrix-supported fabric is rarely found within these deposits. In measured sections containing matrix-supported debris flow facies, lithofacies Gms grades into lithofacies Gmsn and Gmsi. These depositional fabrics as well as those of lithofacies Gmpi, Gmw, Gmcin, and Gcms are indicative of flow that is transitional between hyperconcentrated flow and debris flow. Lithofacies Gmsi is identical to the lahar-runout facies of Scott (1988) produced by flow dilution, although it is possible to produce similar flow fabric through more than one mechanical process. Flow transitions are also reflected by numerous interbedded debris flow and hyperconcentrated flow deposits, especially within clast-supported debris flow lithofacies containing interbedded units of Gmci and Sm or Sh. The variety of sedimentary textures and lithofacies fabrics found in Hyalite Peak volcaniclastic sequences at all of the measured sections is a reflection transition in sediment to water ratios, transition in flow processes and interaction between flow processes and volcanic activity. Numerous lithofacies with depositional fabrics and three dimensional relationships resulting from transitional processes indicate that flow transitions were a normal occurrence during periods of deposition.

Although depositional textures reflecting flow transitions are very common, there are no indications of intermittent flooding caused by the breaching of crater lakes found in some volcanic settings, with the possible exception of Sl and Gmsn units found within the measured section at Antelope Butte. Flow transitions probably occurred as a result of the introduction of large volumes of volcaniclastic material as pyroclastic flows and debris flows that mixed with streamwater as they flowed down channels. Debris in some cases was introduced into the alluvial system as avalanche material which may have contained some clay. Avalanche deposits at Palisade Mountain are closely associated with deposits of matrix-supported Gms. However, at other measured section localities, coarse-grained clast-supported debris flow facies are extremely common, and suggest that large volumes of fresh, clay-poor volcanic debris were available. The large volume of these deposits may also be a reflection of the availability of coarse-grained material in the source area.

Alluvial sequences at most of the measured sections contain interspersed, volumetrically minor deposits characterisitic of streamflow deposition. The volume of streamlaid deposits which would indicate the presence of distal valley sequences is lacking. Most of the units associated with streamflow deposition consist of thin and tabular Gm and Sh units. These were probably deposited in shallow poorly-confined channels within braided stream systems. Because deposits of streamflow lithofacies are widespread, it is believed that streams within the region were numerous even though streamflow deposits are low in volume. The sedimentary record of eruptive activity is comprised of packages of intercalated debris flow, hyperconcentrated flow, and minor pyroclastic flow and surge deposits which rapidly agraded during eruptive phases when large volumes of clastic material were introduced into the system. Streamlaid deposits are low in volume because streams acted to degrade and dissect these packages during periods of quiescence. Sequences dominated by debris flow deposits such as those in the upper part of the Flanders Mountain measured section, record deposition in local valleys and subsequent cutting of terraces by streamflow activity. In some cases debris flow deposits acted to dam stream channels and constrict localized streamflow, as indicated by the deposits at Antelope Butte. However, deposits of this type are rare.

Motion along the Deep Creek fault or other local faulting during the period of Hyalite Peak deposition was suggested by Chadwick (1969, 1982) to be preserved by the changing angle of bedding within depositional sequences. Evidence for this is lacking because angular unconformities within well-bedded deposits are found only

locally at Eight Mile Canyon, and not within other sections studied in proximity of the Deep Creek Fault. The Eight Mile Canyon unconformity more likely resulted from the failure of thick unstable sediments on steep paleoslopes which is a common occurrence in regions of volcanic activity. It is likely, however, that the location of small vents and domes within the Gallatin Range are structurally controlled. The low volume of streamlaid valley sequences, indicating local degradation of volcaniclastic debris packages, implies that deposition took place without coincident subsidence. Therefore, faulting and subsidence required in order to preserve these volcaniclastic sequences could have occurred after deposition.

Volcaniclastic material within the Hyalite Peak sequences was probably deposited on the flanks of volcanoes where material was deposited primarily as debris flows and in stages of non-cohesive transitional flow and hyperconcentrated flow. These deposits are far more coarse-grained than those described as resulting from the recent eruption of Mount St. Helens and are more similar to those recently observed at Mt. Unzen, Japan (T.C. Pierson, oral commun.). The large percentage of coarse-grained deposits described herein reflects the character of the source area, and the lack of preservation potential for fine-grained deposits which are thinner, poorly consolidated, and ash-rich and often overlie coarse-grained deposits so that erosion is likely. The coarse-grained nature of the deposits, used in conjunction with facies associations also reflects the proximity of the source. Proximal pyroclastic flow deposits are generally coarse-grained (Suzuki-Kamata and Kamata, 1990) and are probably interbedded with numerous deposits interpreted that result from coarse-grained debris flows and hyperconcentrated flow from several sources, and in some cases inundated small volcanic vents. These deposits do not show evidence that they emanated from a single central vent. Because of the lack of stratigraphic continuity, the deposits may well have been produced during different episodes of eruptive activity.

REFERENCES CITED

REFERENCES CITED

Allen, J.R.L., 1985, Principles of Physical Sedimentology: Allen and Unwin, London, 272 p.

Arguden, A.T., and Rudolfo, K.S., 1990, Sedimentologic and dynamic differences between hot and cold laharic debris flows of Mayon Volcano, Phillipines: Geological Society of America Bulletin, V. 102, p. 865-876.

Barberi, F., Bertagnini, A., Landi, P., and Principe, C., 1992, A review on phreatic eruptions and their precursors: Journal of Volcanology and Geothermal Research, v.52, p. 231-246.

Beverage, J.P., and Culbertson, J.K., 1964, Hyperconcentrations of suspended sediment: American Society of Civil Engineers, Proceedings, Hydraulics Division Journal, v. 90, no. HY6, p. 117-128.

Borrero, C.A., and Naranjo H., J.L., 1990, Casabianca Formation: a Colombian example of volcanism-induced aggradation in a fluvial basin: Journal of Volcanology and Geothermal Research, v. 41, p. 253-267.

Branney, M.J., and Kokelaar, P., 1992, A reappraisal of ignimbrite emplacement: progressive aggradation and changes from particulate to non-particulate flow during emplacement of high-grade ignimbrite: Bulletin of Volcanology, v. 54, p. 504-520.

Brantley, S.R. and Waitt, R.B. 1988, Interrelations among pyroclastic surge, pyroclastic flow and lahars in Smith Creek valley during first minutes of 18 May 1980 eruption of Mount St. Helens, USA: Bulletin of Volcanology, v. 50, p. 304-326.

Buesch, D.C., 1992, Incorporation and redistribution of locally derived lithic fragments within a pyroclastic flow: Geological Society of America Bulletin, v. 104, p. 1193-1207.

Carey, S.N., 1991, Transport and deposition of tephra by pyroclastic flows and surges, *in* Fisher, R.V., and Smith, G.A., eds., Sedimentation in Volcanic Settings: Society for Sedimentary Geology Special Publication No. 45, p. 49-57.

Cas, R.A., and Wright, J.V., 1987 Volcanic Successions, Modern and Ancient: Allen and Unwin, London, 528 p.

Cavalache V., M.L., and Williams,S.N., 1992, Lithic dominated pyroclastic flows at Galeras volcano, Colombia- An unrecognized volcanic hazard: Geology, v. 20, p. 539-542.

Chadwick, R.A., 1969, The northern Gallatin Range, Montana: Northwestern part of the Absaroka-Gallatin volcanic field: University of Wyoming Contributions to Geology, v. 8, No. 2, p. 150-166.

Chadwick, R.A., 1970, Belts of eruptive centers in the Absaroka-Gallatin volcanic province, Wyoming-Montana: Geological Society of America Bulletin, v. 81, p. 267-273.

Chadwick, R.A., 1982, Igneous geology of the Fridley Peak quadrangle, Montana: Montana Bureau of Mines and Geology, Geologic Map 31.

Chadwick, R.A., 1984, Pre-Eocene paleosurface of the Gallatin Range, southwestern Montana (abst.): Geological Society of America Program, Annual Meeting, Reno, Nevada, p. 466-467.

Cheel, R.J., 1990, Horizontal lamination and the sequence of bed phases and stratification under upper-flow-regime conditions: Sedimentology, v. 37, p. 517-529.

Costa, J.E., 1988, Rheologic, geomorphic, and sedimentologic differentiation of water floods, hyperconcentrated flows, and debris flows, in Baker, V.R., Kochel, R.C., and Patton, P.C., eds., Flood Geomorphology: New York, J. Wiley and Sons, p. 113-122.

Crandell, D.R., 1971, Post-glacial lahars from Mt. Ranier volcano, Washington: U.S. Geological Survey Professional Paper 1444, 91 p.

Crandell, D.R., Miller, C.D., Glicken, H.X., Christiansen, R.L., and Newhall, C.G., 1984, Catastrophic debris avalanche from ancestral Mt. Shasta, California: Geology, v. 12, p.143-146.

Crandell, D.R., and Mullineaux, D.R., 1973, Pine Creek volcanic assemblage at Mount St. Helens, Washington, U.S.A.: U.S. Geological Survey Bulletin 1383-A, 23 p.

Dellino, P., Frazzetta, G., and La Volpe, L., 1990, Wet surge deposits at La Fossa di Vulcano: depositional and eruptive mechanisms: Journal of Volcanology and Geothermal Research, v. 43, p.215-233.

Downey, W.S. and Tarling, D.H., 1991, Reworking characteristics of Quaternary pyroclastics, Thera (Greece), determined using magnetic properties: Journal of Volcanology and Geothermal Research, v. 46, p. 143-155.

Endo, K., Sumita, M., Machida, M., and Furuichi, M., 1989, The 1984 collapse and debris-avalanche deposits of Ontake Volcano, Central Japan, in Latter, J.H., ed., Volcanic Hazards: IAVCEI Proceedings in Volcanology 1: Springer-Verlag, Berlin Heidelberg, p.210-229.

Fisher, R.V., 1961, Proposed Classification of volcaniclastic sediments and rocks: Geological Society of America Bulletin, v. 72, p. 1409-1414.

Fisher, R.V., 1979, Models for pyroclastic surges and pyroclastic flows: Journal of Volcanology and Geothermal Research, v. 6, p. 305-318.

Fisher, R.V., 1983, Flow transformations in sediment gravity flows: Geology, v. 11, p. 273-274.

Fisher, R.V., 1986, Systems of transport and deposition within pyroclastic surges: Evidence from Mount St. Helens, Washington: EOS Transactions, American Geophysical Union, v. 67, p. 1246.

Fisher, R.V., 1990, Transport and deposition of a pyroclastic surge across an area of high relief: The 18 May 1980 eruption of Mount St. Helens, Washington: Geological Society of America Bulletin, v. 102,, p. 1038-1054.

Fisher R.V., Glicken, H.X., and Hoblitt, R.P., 1987, May 18, 1980, Mount St. Helens deposits in South Coldwater Creek, Washington: Journal of Geophysical Research, v. 92, p. 10267-10283.

Fisher, R.V., and Schmincke, H.-U., 1984, Pyroclastic rocks: Berlin, Springer-Verlag, 472 p.

Fisher, R.V., and Waters, A.C., 1969, Bed forms in base surge deposits: lunar implications: Science, v. 165, p. 1349-1352.

Freundt, A., and Schmincke, H-U., 1986, Emplacement of small-volume pyroclastic flows at Laacher See (East-Eifel, Germany): Bulletin of Volcanology, v. 48, p. 39-59.

Fritz, W.J., and Harrison, S., 1985, Early Tertiary volcaniclastic deposits of the northern Rocky Mountains, in Flores, R.M. and Kaplan, S.S., eds., Cenozoic Paleogeography of West-Central United States: Rocky Mountain Section Society for Sedimentary Geology, Denver, Colorado, p.383-402.

Glicken, H., 1991, Transport and deposition of tephra by pyroclastic flows and surges, *in* Fisher, R.V., and Smith, G.A., eds., Sedimentation in Volcanic Settings: Society for Sedimentary Geology Special Publication No. 45, p. 49-57.

Hampton, M.A., 1975, Competence of fine-grained debris flows: Journal of Sedimentary Petrology, v. 45, p. 834-844.

Harrison, S., and Fritz J., 1982, Depositional features of March 1982 Mount St, Helens sediment flows: Nature, v. 299, p.720-722.

Heiken, G.H., 1971, Tuff rings: Examples from the Fort Rock -Christmas Lake Valley Basin, south-central Oregon: Journal of Geophysical Research, v. 76, p. 5615-5626.

Heiken, G.H., 1972, Morphology and petrography of volcanic ashes: Geological Society of America Bulletin, v. 83, p. 1961-1988.

Heiken, G. H., 1974, An atlas of volcanic ash: Smithsonian Contributions to Earth Sciences, v. 12, 101 p.

Heiken, G., 1978, Characteristics of tephra from Cinder Cone, Lassen Volcanic National Park, California: Bulletin Volcanologique, v. 41, p.119-130.

Heiken G., and Wohletz, K., 1987, Tephra deposits associated with silicic domes and lava flows: *in* Fink, J.H. ed., The emplacement of silicic domes and lava flows, Geological Society of America Special Paper 212, p. 55-76.

Hein, F.J., and Walker, R.G., 1977, Bar evolution and development of stratification in the gravelly, braided, Kicking Horse River, British Colombia: Canadian Journal of Earth Sciences, v.14, p. 562-570.

Iddings, J.P., Weed, W.H., and Hague, A., 1894, Livingston folio: U.S. Geological Survey Geological Atlas of the United States, Folio no. 1.

Kent, D.V., Ninkovich, D., Pescatore, T., and Sparks, S.R.J., 1981, Paleomagnetic determination of emplacement temperature of Vesuvius AD 79 pyroclastic deposits: Nature, v. 290, p. 393-396.

Lowe, D. R., 1979, Sediment gravity flows: Their classification and some problems of application to natural flows and deposits, *in* Doyle, L.J. and Pilkey, O.H., eds., Geology of Continental Slopes: Society of Economic Paleontologists and Mineralogists Special Publication 27, p.75-82.

Lowe, D.R., Williams, S.N., Leigh, H., Connor, C.B., Gemmell, J.B., and Stoiber, R.E., 1986, Lahars initiated by the 13 November 1985 eruption of Nevado del Ruiz, Colombia: Nature, v. 324, p. 51-53.

Major, J.J., and Scott, K.M., 1988,Volcaniclastic sedimentation in the Lewis River Valley, Mount St. Helens, Washington- Processes, extent, and hazards: U.S. Geological Survey Bulletin 1383-D, 38 p.

Major, J.J., and Newhall, C.G., 1989, Snow and ice perturbation during historical volcanic eruptions and the formation of lahars and floods: a global review: Bulletin of Volcanology, v. 52, p. 1-27.

McMannis W.J., and Chadwick, R.A. 1964, Geology of the Garnet Mountain quadrangle, Gallatin County, Montana: Montana Bureau of Mines and Geology Bulletin 43, 47 p.

Mellors, R.A., Waitt, R.B., and Swanson, D.A., 1988, Generation of pyroclastic flows and surges by hot-rock avalanches from the dome of Mount St. Helens volcano, U.S.A.: Bulletin of Volcanology, v. 50, p. 14-25.

Miall, A.D., 1973, Markov chain analysis applied to an ancient alluvial plain succession: Sedimentology, v. 20, p. 347-364.

Miall, A.D., 1977, A review of the braided river depositional environment: Earth Science Reviews, v.13, p.1-62.

Miall, A.D., 1978, Lithofacies types and vertical profile models in braided river deposits: A summary, *in* Miall, A., ed., Fluvial Sedimentology: Canadian Society of Petroleum Geologists Memoir 5, p. 597-604.

Miall, A.D., 1985, Architectural-element analysis: a new method of facies analysis applied to fluvial deposits: Earth Science Reviews, v. 22, p. 261-308.

Miall, A.D., 1988, Facies architecture in clastic sedimentary basins:*in* Kleinspehn, K.L., and Paola, C., eds., Frontiers in sedimentary geology series: New perspectives in basin analysis: Springer-Verlag, p. 67-81.

Middleton, G.V., 1970, Experimental studies related to problems of flysch sedimentation, *in* Lajoie, J., ed., Flysch sedimentology in North America: Geological Society of Canada Special Paper 7, p. 253-272.

Naylor, M.A., 1980, The origin of inverse grading in muddy debris flow deposits- A review: Journal of Sedimentary Petrology, v. 50, no. 4, p. 1111-1116.

Palmer, B.A.,. Alloway, B.V., and Neall, V.E., 1991, Volcanic-debris-avalanche deposits in New Zealand- Lithofacies organization in confined, wet-avalanche flows, *in* Fisher, R.V., and Smith, G.A., eds. Sedimentation in volcanic settings: Society for Sedimentary Geology Special Publication No. 45, p.89-98.

Palmer, B.A., and Walton, A.W. 1990, Accumulation of volcaniclastic aprons in the Mount Dutton Formation (Oligocene-Miocene), Marysvale volcanic field, Utah: Geological Society of America Bulletin, v. 102, p.734-748.

Peale, A.C., 1896, Three Forks folio: U.S. Geological Survey Atlas of the United States, Folio no. 24.

Peterson, D.W., 1979, Significance of the flattening of pumice fragments in ash-flow tuffs, in Chapin C.E., and Elston, W.E., eds., Ash Flow Tuffs: Geological Society of America Special Paper 180, p.195-203.

Pierson, T.C., 1981, Dominant particle support mechanisms in debris flows at Mt. Thomas, New Zealand, and implications for flow mobility: Sedimentology, v.28, p.49-60.

Pierson, T.C., 1985, Initiation and flow behavior of the 1980 Pine Creek and Muddy River lahars, Mount St. Helens, Washington: Geological Society of America Bulletin, v. 96, p. 1056-1069.

Pierson, T. C., and Costa, J.E. 1987, A rheological classification of subaerial sediment-water flows: *in* Costa, J.E. and Wierczorek, G.F. eds., Debris Flows/Avalanches: Process, recognition, and mitigation: Geological Society of America Reviews in Engineering Geology, v. 7, p. 1-12.

Pierson, T.C., Janda, R.J., Thouret, J.C. and Borrero, C.A., 1990, Perturbation and melting of snow and ice by the 13 November 1985 eruption of Nevado del Ruiz, Colombia, and consequent mobilization, flow and deposition of lahar: Journal of Volcanology and Geothermal Research, v. 41, p. 17-66.

Pierson, T.C., and Scott, K.M., 1985, Downstream dilution of a lahar: transition from debris flow to hyperconcentrated streamflow: Water Resources Reasearch, v.21, p.1511-1524.

Rodine, J.D., and Johnson, A.M., 1976, The ability of debris, heavily freighted with coarse clastic materials to flow on gentle slopes: Sedimentology, v. 23, p. 213-234.

Rose, W.I., 1973, Pattern and mechanism of activity at the Santiaguito volcanic dome, Guatemala: Bulletin Volcanologique, v. 37, p. 73-94.

Rose, W.I., 1987, Volcanic activity at Santiaguito volcano, 1976-1984: *in* Fink, J.H., ed., The emplacement of silicic domes and lava flows, Geological Society of America Special Paper 212, p.17-28.

Rowley, P.D., Kuntz, M.A., and Macleod, N.S., 1981, Pyroclastic-flow deposits, *in* Lipman, P.W., and Mullineaux, D.R., eds., The 1980 Eruptions of Mount St. Helens: U.S.Geological Survey Professional Paper 1250, p.489-512.

Rust, B.R., 1972, Structure and process in a braided river: Sedimentology, v. 18, p. 221-246.

Rust, B.R., 1978, Depositional models for braided alluvium, *in* Miall, A., ed. Fluvial Sedimentology: Canadian Society of Petroleum Geologists Memoir 5, p. 605-625.

Scott, K.M., 1988, Origins, behavior, and sedimentology of lahars and lahar-runout flows in the Toutle-Cowlitz River system: U.S. Geological Survey Professional Paper 1447-A, 74 p.

Scott, K.M., 1989, Magnitude and frequency of lahars and lahar-runout flows in the Toutle-Cowlitz River system: U.S. Geological Survey Professional Paper 1447-B, 82 p.

Shultz, A.W., 1984, Subaerial debris-flow deposition in the Upper Paleozoic Cutler Formation, Western Colorado: Journal of Sedimentary Petrology, v. 54, p. 749-772.

Schumacher, R., and Schmincke, H-U., 1991, Internal structure and occurrence of accretionary lapilli- a case study at Laacher See Volcano: Bulletin of Volcanology, v.53, p. 612-634.

Self, S., Wilson, L., and Nairn, I.A., 1979, Vulcanian eruption mechanism: Nature, v. 277, p. 440-443.

Shaver, K.C., 1978, Chronology of dacite intrusion in the northwest end of the Absaroka-Gallatin volcanic province, Montana: Northwest Geology, v. 7, p. 20-27.

Sheridan , M. F., 1979, Emplacement of pyroclastic flows: A review: *in* Chapin C.E., and Elston, W.E., eds., Ash-flow tuffs: Geological Society of America Special Paper 180, p. 125-136.

Sheridan, M.F., and Wohletz, K.H., 1983, Hydrovolcanism: Basic considerations and review: Journal of Volcanology and Geothermal Research, v. 17, p. 1-29.

Smedes, H.W., and Prostka, H.J. 1972, Stratigraphic framework of the Absaroka Volcanic Supergroup in the Yellowstone National Park region: U.S. Geological Survey Professional Paper 729-C, 33 p.

Smith, G.A., 1986, Coarse-grained nonmarine volcaniclastic sediment: Terminology and depositional process: Geological Society of America Bulletin, v.97, p. 1-10.

Smith, G. A., 1987, The influence of explosive volcanism on fluvial sedimentation: The Deschutes Formation (Neogene) in central Oregon: Journal of Sedimentary Petrology, v. 57, p. 613-629

Smith, G.A., and Lowe, D.R., 1991, Lahars: volcano-hydrologic events and deposition in the debris flow- hyperconcentrated flow continuum, *in* Fisher, R.V., and Smith, G.A., eds., Sedimentation in volcanic settings: Society for Sedimentary Geology, Special Publication No.45, p. 59-70.

Sparks, R.J.S., 1976, Grain size variations in ignimbrites and implications for the transport of pyroclastic flows: Sedimentology, v. 23, p. 147-188.

Sparks, R.J.S., 1978, Gas release rates from pyroclastic flows: An assessment of the role of fluidization in their emplacement: Bulletin of Volcanology, v. 41, p. 1-9.

Sparks, R.J.S., Self, S., and Walker, G.P.L., 1973, Products of ignimbrite eruptions: Geology, v. 1, p. 115-118.

Sparks, R. J. S., and Walker, G.P.L., 1973, The ground surge deposit- A third type of pyroclastic rock: Nature, v. 241, p. 62-64.

Suzuki-Kamata, K., and Kamata, H. 1990, The proximal facies of the Tosu pyroclastic-flow deposit erupted from Aso caldera, Japan: Bulletin of Volcanology, v. 52, p. 325-333.

Ui, T., 1983, Volcanic debris-avalanche deposits- Identification and comparison with non-volcanic debris stream deposits: Journal of Volcanology and Geothermal Research, v. 18, p. 135-150.

Valentine, G.A., 1987, Stratified flow in pyroclastic surges: Bulletin of Volcanolgy, v.49, p. 616-630.

Van Bemmelen, R.W. 1949, Geology of Indonesia: The Hague, The Netherlands, Government Printing Office, 732 p.

Voight, B., Janda, R.J., Glicken, H., and Douglass, P.M., 1983, Nature and mechanics of the Mount St. Helens rockslide - avalanche of 18 May 1980: Geotechnique, v. 33, p. 243-273.

Voight, B., Glicken, H.X., Janda, R.J., and Douglass, P.M. 1981, Catastrophic lansdslide avalanche of May 18, *in* Lipman, P.W., and Mullineaux, D.R., eds., The 1980 Eruptions of Mount St. Helens: U.S. Geological Survey Professional Paper 1250, p.347-377.

Waitt, R.B., 1989, Swift snowmelt and floods (lahars) caused by great pyroclastic surge at Mount St. Helens volcano, Washington, 18 May 1980: Bulletin of Volcanology, v. 52, p. 138-157.

Walton, A.W., and Palmer, B.A., 1988, Lahar facies of the Mount Dutton Formation (Oligocene-Miocene) in the Marysvale volcanic field, southwestern Utah: Geological Society of America Bulletin, v. 100, p.1078-1091.

Walker, G.P.L., Self, S., and Froggatt, P.C., 1981, The ground layer of the Taupo Ignimbrite: A striking example of sedimentation from a pyroclastic flow: Journal of Volcanology and Geothermal Research, v. 10, p. 1-11.

Waresback, D.B., and Turbeville, B.N. 1990, Evolution of a Plio-Pleistocene volcanogenic alluvial fan: The Puye Formation, Jemez Mountains, New Mexico: Geological Society of America Bulletin, v.. 102, p. 298-314.

Waters, A.C., and Fisher, R.V., 1971, Base surges and their deposits: Capelinhos and Taal volcanoes: Journal of Geophysical Research, v. 94, p. 1867-1887.

Williams, H., and McBirney, A.R., 1979, Volcanology: Freeman, Cooper and Company, San Fransisco, 397 p.

Wilson, C.J., 1988, Comment on "Stratified flow in pyroclastic surges", by G.A. Valentine: Bulletin of Volcanology, v. 50, p. 350 - 351.

Wilson, C.J., 1980, The role of fluidization in the emplacement of pyroclastic flows: An experimental approach: Journal of Volcanology and Geothermal Research, v. 8, p. 231-249.

Wohletz, K., and Sheridan, M.F., 1979, A model of a pyroclastic surge, in Chapin, C.E., and Elston, W.E., eds., Ash flow tuffs: Geological Society of America Special Paper 180, p. 177-194.

Wohletz, K.H., and Sheridan, M.F. 1983, Hydrovolcanic explosions II. Evolution of basaltic tuff rings and tuff cones: American Journal of Science, v. 283, p. 384-413.

Wright, J.V., Smith, A.L., and Self, S., 1980, A working terminology of pyroclastic deposits: Journal of Volcanology and Geothermal Research, V. 8, p. 315-336.

APPENDICES

APPENDIX A
DISTRIBUTION OF COARSE- GRAINED LITHOFACIES

Table 4. Distribution of coarse-grained lithofacies (in order of unit abundance)

	Measured Section	Ave Thickness of lithofacies (m)	% thickness of measured section.	% of Gmci facies units in section
Gmci	Windy Pass	0	0	0
(0.2 -3.8 m)	Silken Skein F.	0.68	19	11
ave thickness	Palisade Mtn. I	0	0	0
1.21 m	Palisade Mtn. II	0	0	0
	Flanders Mtn.	0.64	11	10
	Eight Mile I	1.41	35	46
	Eight Mile II	0.98	31	22
	Antelope B. I	2.6	18	3
	Antelope B. II	1.46	3	9

	Measured Section	Ave Thickness of lithofacies (m)	% thickness of measured section.	% of Gmp facies units in section
Gmp	Windy Pass	2.95	8	4
(0.5-13 m)	Silken Skein F.	1.04	20	13
ave thickness	Palisade Mtn. I	0	0	0
3.64 m	Palisade Mtn. II	3.77	26	7
	Flanders Mtn.	5.00	47	9
	Eight Mile I	4.17	26	20
	Eight Mile II	1.80	14	9
	Antelope B. I	5.80	39	6
	Antelope B. II	4.34	20	31

	Measured Section	Ave Thickness of lithofacies (m)	% thickness of measured section.	% of Gm facies units in section
Gm	Windy Pass	1.70	9	5
(0.05-5.43 m)	Silken Skein F.	0.55	3	5
ave thickness	Palisade Mtn. I	0	0	0
1.18 m	Palisade Mtn. II	1.49	5	5
	Flanders Mtn.	2.00	4	2
	Eight Mile I	0.54	5	39
	Eight Mile II	2.13	41	29
	Antelope B. I	0.35	1	2
	Antelope B. II	0.87	1	13

	Measured Section	Ave Thickness of lithofacies (m)	% thickness of measured section.	% of Gms facies units in section
Gms	Windy Pass	2.18	28	13
(0.05-6.1 m)	Silken Skein F.	0	0	0
ave thickness	Palisade Mtn. I	0	0	0
1.21 m	Palisade Mtn. II	1.57	8	7
	Flanders Mtn.	0.60	1	3
	Eight Mile I	1.2	8	31
	Eight Mile II	2.00	3	3
	Antelope B. I	1.2	3	3
	Antelope B. II	0.83	4	41

	Measured Section	Ave Thickness of lithofacies (m)	% thickness of measured section.	% of Gmsn facies units in section
Gmsn	Windy Pass	0	0	0
(0.7 -1.3 m)	Silken Skein F.	0	0	0
ave thickness	Palisade Mtn. I	0	0	0
0.48 m	Palisade Mtn. II	0	0	0
	Flanders Mtn.	0	0	0
	Eight Mile I	0.1	<1	3
	Eight Mile II	0	0	0
	Antelope B. I	0.34	3	12
	Antelope B. II	0.51	4	85

	Measured Section	Ave Thickness of lithofacies (m)	% thickness of measured section.	% of Gmw facies units in section
Gmw	Windy Pass	0.35	<1	4
(0.05-2.0 m)	Silken Skein F.	0.98	11	14
ave thickness	Palisade Mtn. I	0	0	0
0.49 m	Palisade Mtn. II	0	0	0
	Flanders Mtn.	0.35	1	7
	Eight Mile I	0.32	3	57
	Eight Mile II	1.2	4	7
	Antelope B. I	0	0	0
	Antelope B. II	0.52	<1	11

	Measured Section	Ave Thickness of lithofacies (m)	% thickness of measured section.	% of Gmsi facies units in section
Gmsi	Windy Pass	0	0	0
(0.2-4.6 m)	Silken Skein F.	0.65	7	18
ave thickness	Palisade Mtn. I	0	0	0
0.83 m	Palisade Mtn. II	0	0	0
	Flanders Mtn.	0	0	0
	Eight Mile I	0.75	6	68
	Eight Mile II	0	0	0
	Antelope B. I	0	0	0
	Antelope B. II	4.0	3	14

	Measured Section	Ave Thickness of lithofacies (m)	% thickness of measured section	% of Gmpi facies units in section
Gmpi	Windy Pass	2.50	6	5
(0.20-13.2 m)	Silken Skein F.	1.68	42	45
ave thickness	Palisade Mtn I	0	0	0
3.31 m	Palisade Mtn II	3.20	5	5
	Flanders Mtn	3.50	13	10
	Eight Mile I	1.44	3	15
	Eight Mile II	0	0	0
	Antelope B. I	6.30	28	10
	Antelope B II	11.13	6	10

	Measured Section	Ave Thickness of lithofacies (m)	% thickness of measured section.	% of Gmcn facies units in section
Gmcn (0.1-3.4 m) ave thickness 1.29 m	Windy Pass	1.85	19	21
	Silken Skein F.	0	0	0
	Palisade Mtn I	0	0	0
	Palisade Mtn II	0	0	0
	Flanders Mtn	3.00	6	5
	Eight Mile I	1.19	2	16
	Eight Mile II	2.50	5	11
	Antelope B. I	0	0	0
	Antelope B II	0.82	2	47

	Measured Section	Ave Thickness of lithofacies (m)	% thickness of measured section.	% of Gmcin facies units in section
Gmcin (0.1-1.0 m) ave thickness 0.44 m	Windy Pass	0	0	0
	Silken Skein F.	1.0	8	19
	Palisade Mtn. I	0	0	0
	Palisade Mtn. II	0	0	0
	Flanders Mtn.	0	0	0
	Eight Mile I	0.49	2	38
	Eight Mile II	0.24	<1	6
	Antelope B. I	0	0	0
	Antelope B. II	0.25	<1	38

	Measured Section	Ave Thickness of lithofacies (m)	% thickness of measured section	% of GmLa facies units in section
GmLa (0.10-1.35 m) ave thickness 0.40 m	Windy Pass	0.51	11	56
	Silken Skein F.	0	0	0
	Palisade Mtn. I	0	0	0
	Palisade Mtn .II	0	0	0
	Flanders Mtn.	0.30	<1	6
	Eight Mile I	0.21	<1	38
	Eight Mile II	0	0	0
	Antelope B. I	0	0	0
	Antelope B II	0	0	0

	Measured Section	Ave Thickness of lithofacies (m)	% thickness of measured section.	% of Gmpv facies units in section
Gmpv (6.1-69.3 m) ave thickness 21.74 m	Windy Pass	0	0	0
	Silken Skein F.	0	0	0
	Palisade Mtn. I	16.86	40	50
	Palisade Mtn. II	12.4	63	38
	Flanders Mtn.	0	0	0
	Eight Mile I	0	0	0
	Eight Mile II	0	0	0
	Antelope B. I	0	0	0
	Antelope B. II	69.3	19	12

	Measured Section	Ave Thickness of lithofacies (m)	% thickness of measured section.	% of Gcms facies units in section
Gcms	Windy Pass	0	0	0
(0.82-4.5 m)	Silken Skein F.	0	0	0
ave thickness	Palisade Mtn. I	0	0	0
1.88 m	Palisade Mtn. II	0	0	0
	Flanders Mtn.	0	0	0
	Eight Mile I	0	0	0
	Eight Mile II	0	0	0
	Antelope B. I	0.82	<1	20
	Antelope B. II	2.15	2	80

	Measured Section	Ave Thickness of lithofacies (m)	% thickness of measured section.	% of Gl facies units in section
Gl	Windy Pass	0	0	0
(0.15 -1.5 m)	Silken Skein F.	0.80	2	25
ave thickness	Palisade Mtn. I	0	0	0
0.73 m	Palisade Mtn .II	0	0	0
	Flanders Mtn.	0	0	0
	Eight Mile I	0.30	<1	50
	Eight Mile II	0	0	0
	Antelope B. I	1.5	3	25
	Antelope B. II	0	0	0

	Measured Section	Ave Thickness of lithofacies (m)	% thickness of measured section.	% of Gt facies units in section
Gt	Windy Pass	0	0	0
(0.50-3.96 m)	Silken Skein F.	0	0	0
ave thickness	Palisade Mtn I	3.96	2	50
2.23 m	Palisade Mtn II	0	0	0
	Flanders Mtn	0	0	0
	Eight Mile I	0	0	0
	Eight Mile II	0	0	0
	Antelope B. I	0	0	0
	Antelope B II	0.50	<1	50

APPENDIX B
MEASURED SECTIONS

Key

Gradational contact

Unit thickness
(to nearest 0.1m)

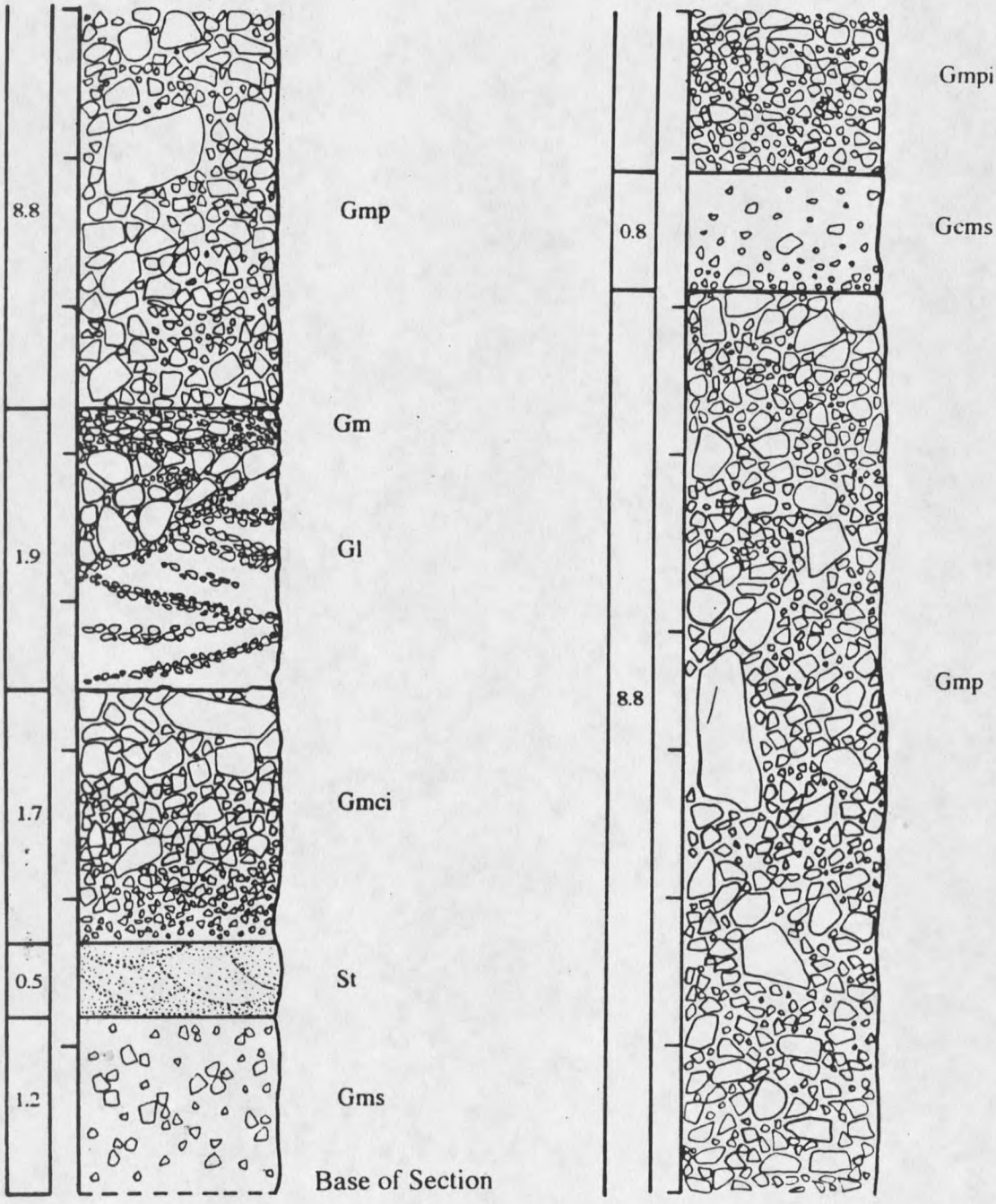
Bar distance = 1m

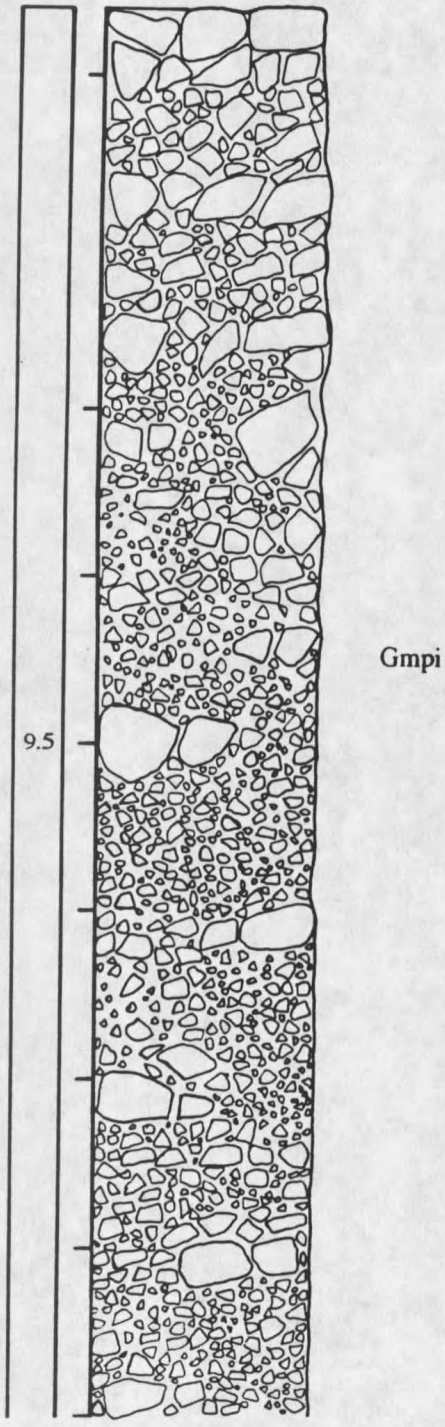
Covered contact

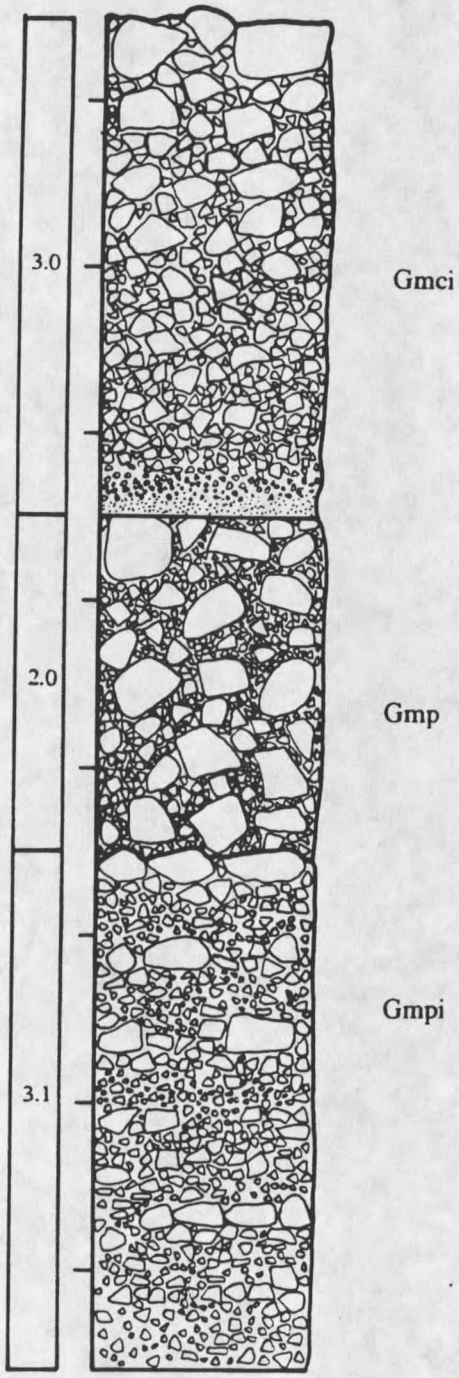
Paleocurrent - N 45° W
(from clast imbrication)

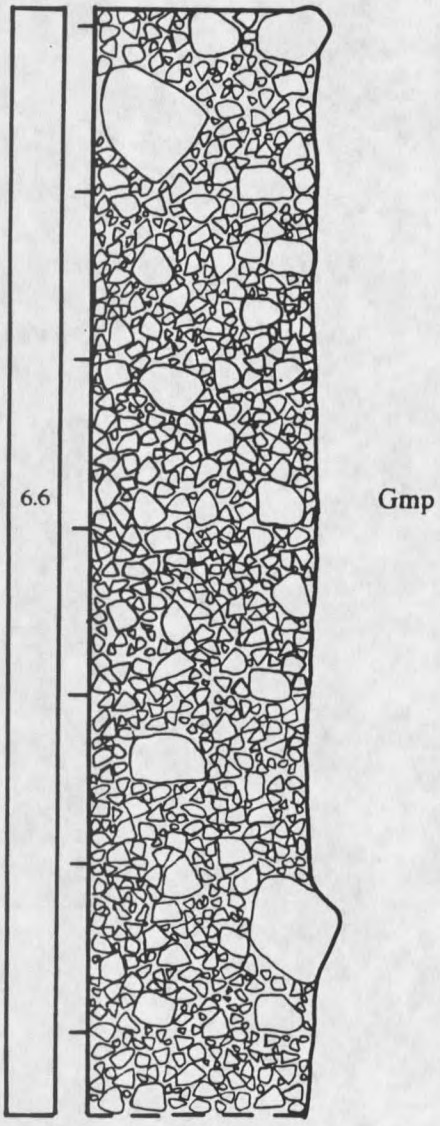
Antelope Butte Measured Section 1

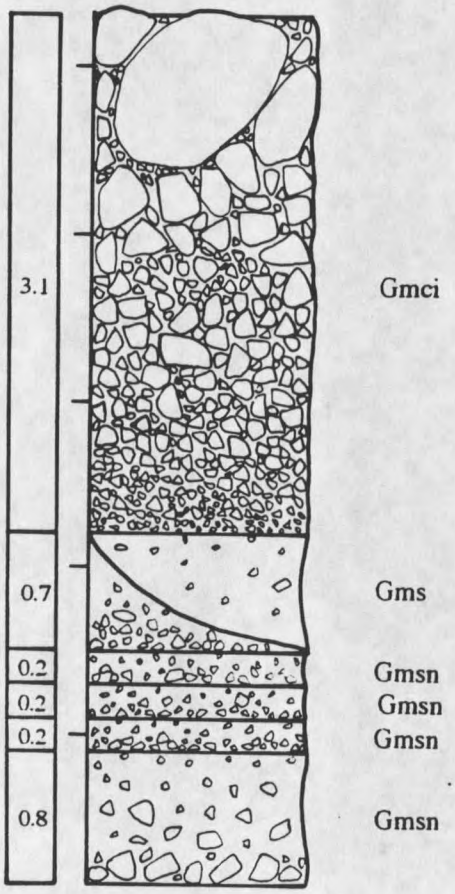
Location:
NW1/4, Sec 13, T4S, R8E

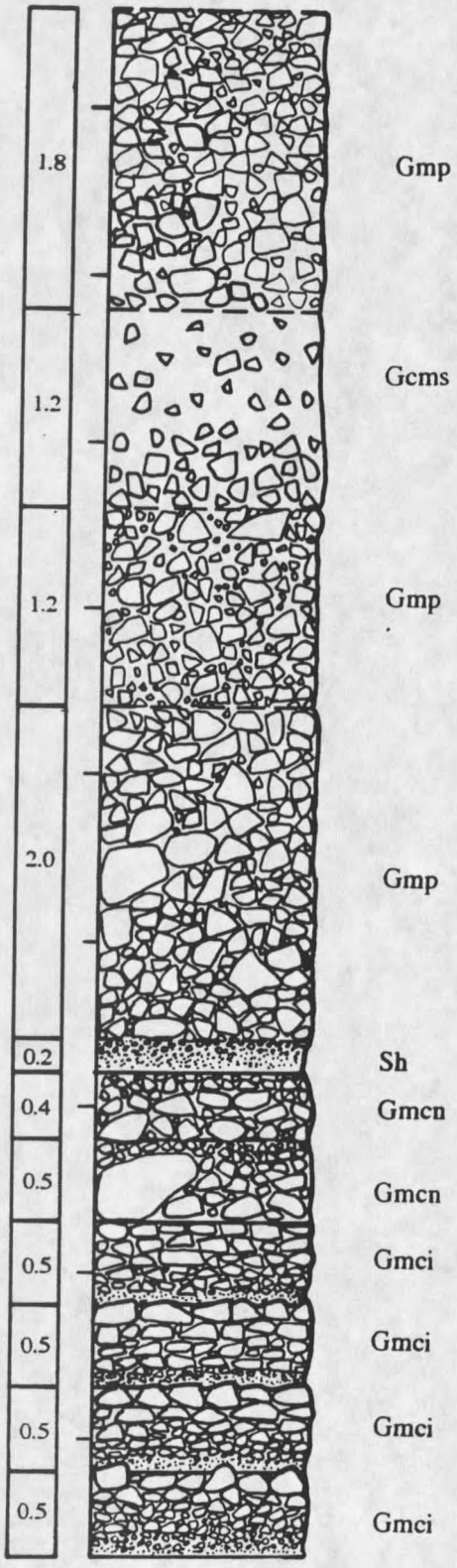


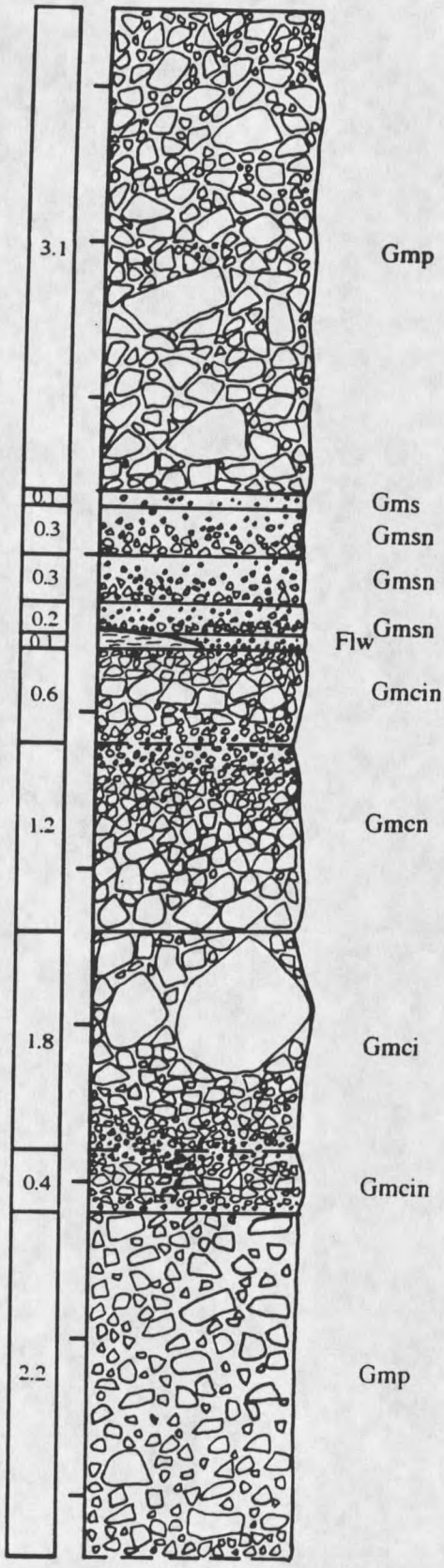

9.5
Gmpi

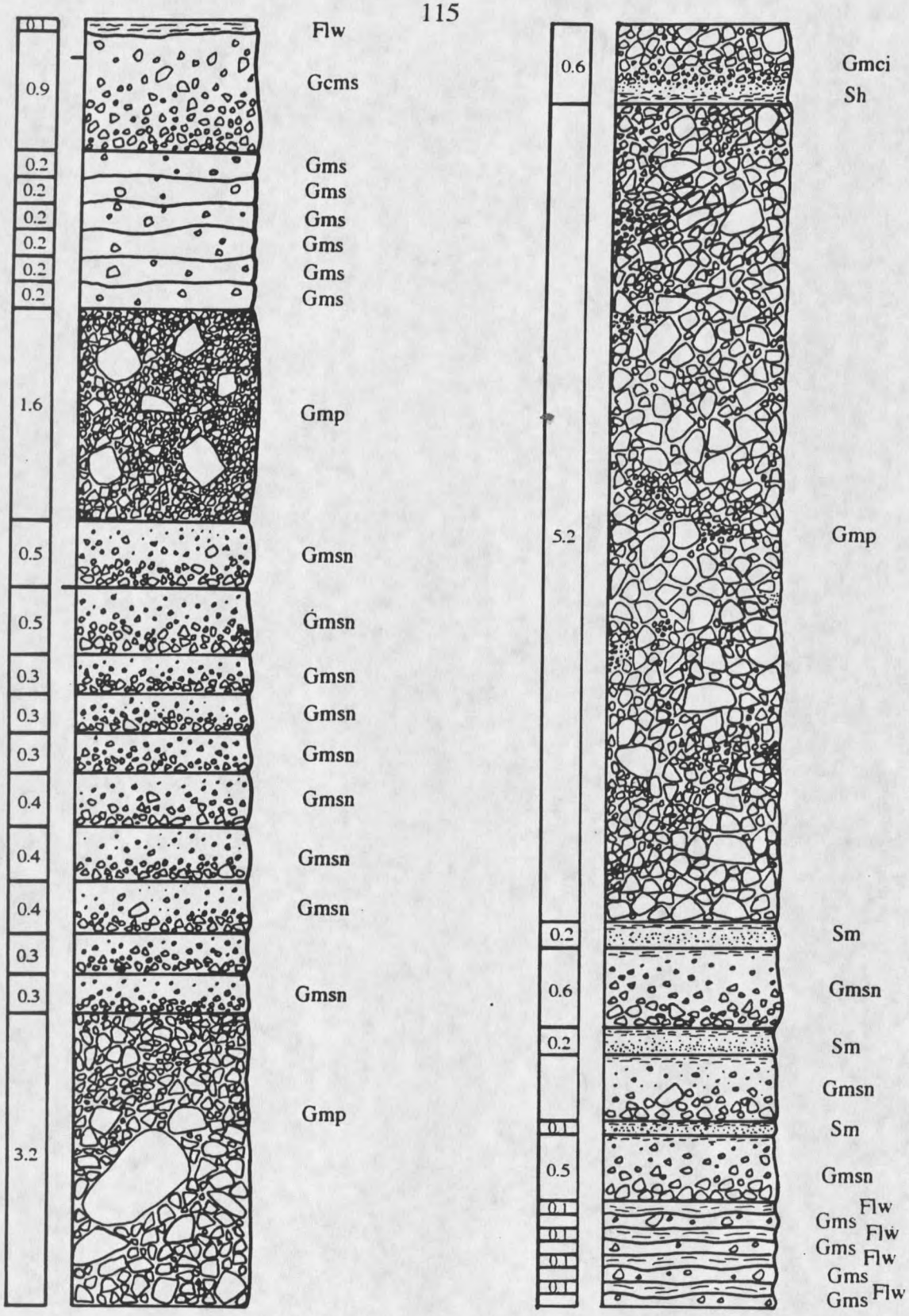

3.0
Gmci
2.0
Gmp
3.1
Gmpi

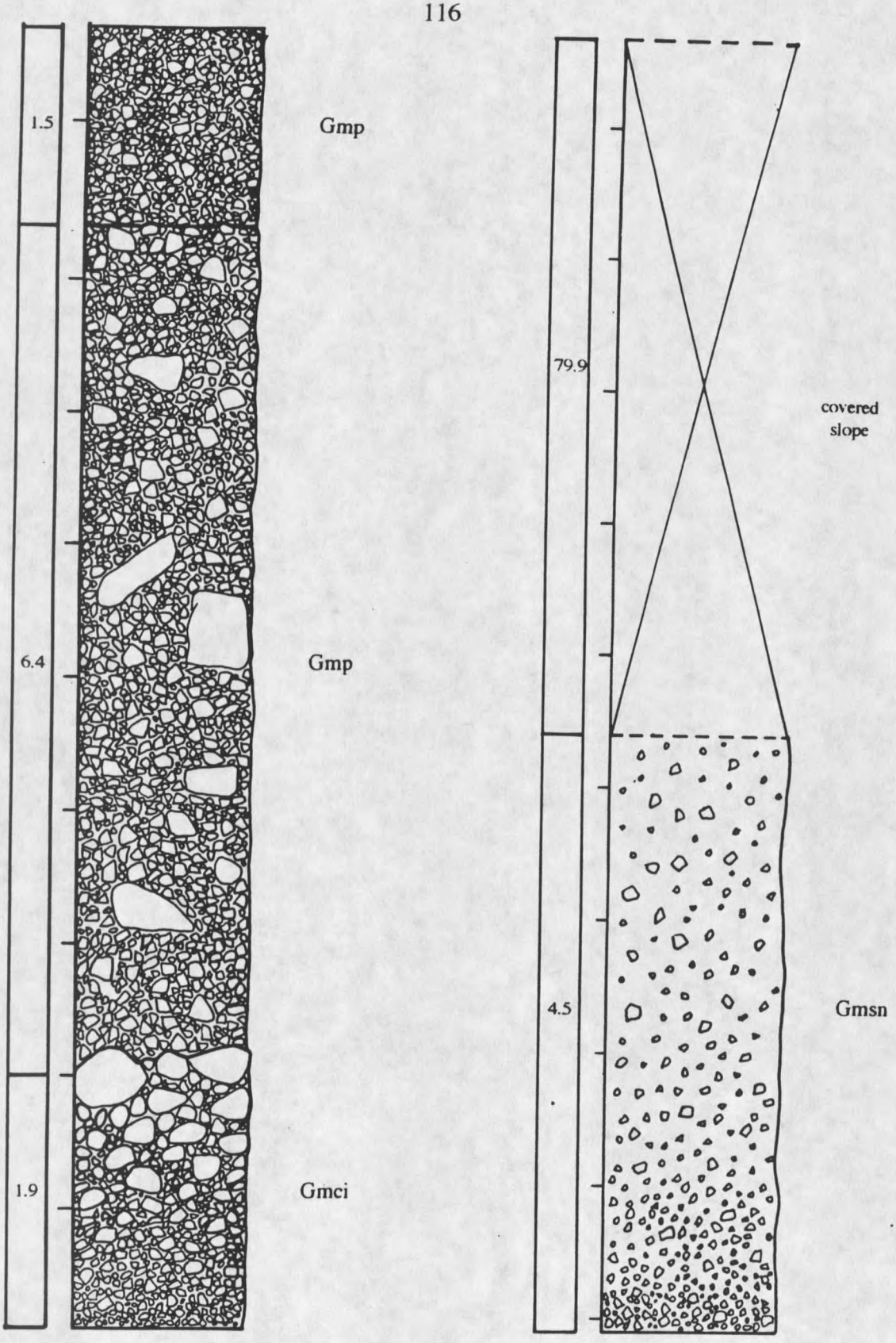

6.6
Gmp

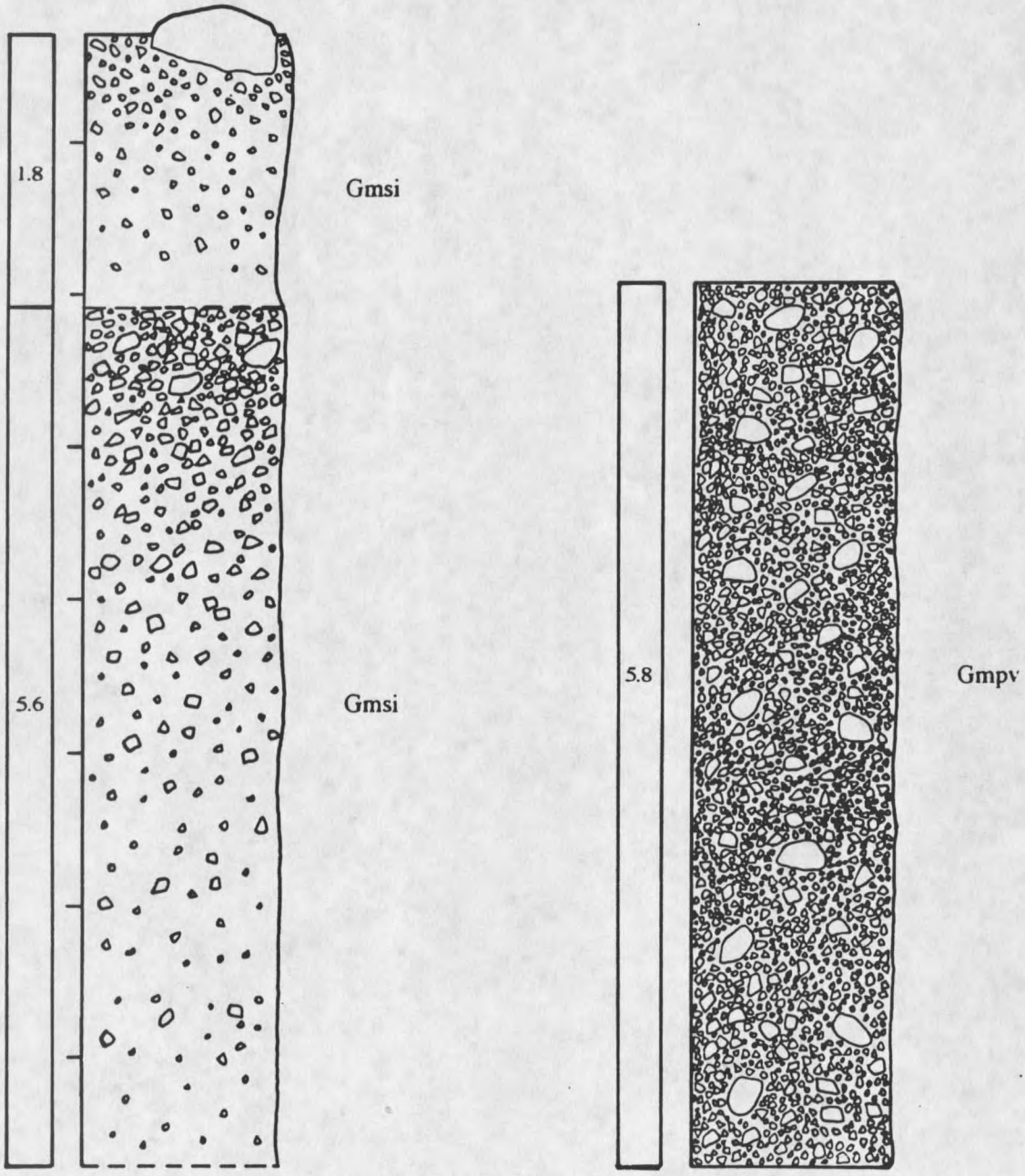

3.1
Gmci
0.7
Gms
0.2
Gmsn
0.2
Gmsn
0.2
Gmsn
0.8
Gmsn

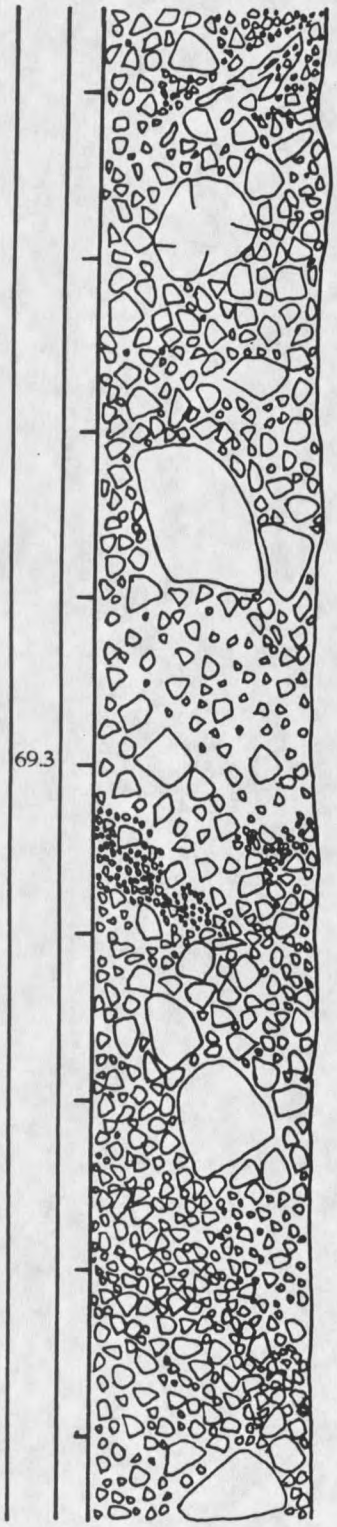

1.8
1.2
1.2
2.0
0.2
0.4
0.5
0.5
0.5
0.5
Gmp
Gcms
Gmp
Gmp
Sh
Gmcn
Gmcn
Gmci
Gmci
Gmci
Gmci

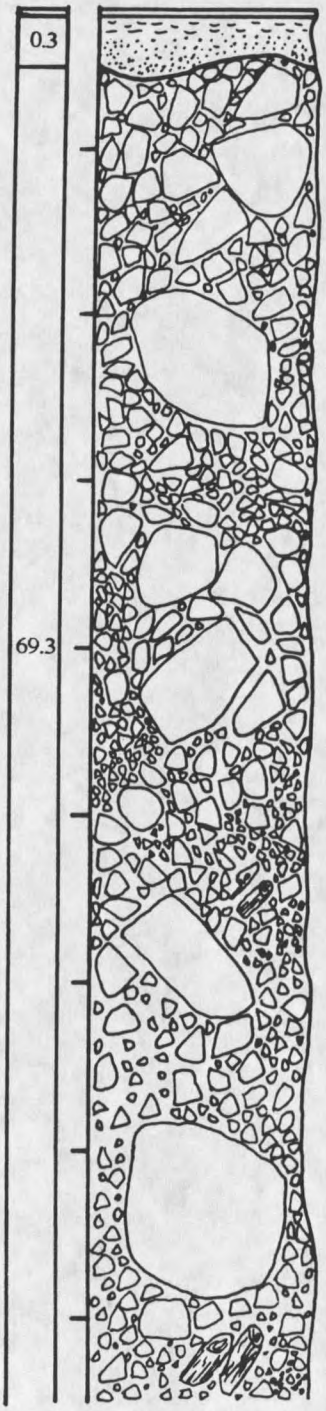

3.1
0.1
0.3
0.3
0.2
0.1
0.6
1.2
1.8
0.4
2.2
Gmp
Gms
Gmsn
Gmsn
Gmsn
Flw
Gmcin
Gmcn
Gmci
Gmcin
Gmp


0.1
0.9
0.2
0.2
0.2
0.2
0.2
0.2
1.6
0.5
0.5
0.3
0.3
0.3
0.4
0.4
0.4
0.3
0.3
3.2
Flw
Gcms
Gms
Gms
Gms
Gms
Gms
Gms
Gmp
Gmsn
Gmsn
Gmsn
Gmsn
Gmsn
Gmsn
Gmsn
Gmsn
Gmsn
Gmp
0.6
5.2
0.2
0.6
0.2
0.5
Gmci
Sh
Gmp
Sm
Gmsn
Sm
Gmsn
Sm
Gmsn
Gms Flw
Gms Flw
Gms Flw
Gms Flw


1.5
Gmp
6.4
Gmp
1.9
Gmci
79.9
covered
slope
4.5
Gmsn


1.8
Gmsi
5.6
Gmsi
5.8
Gmpv

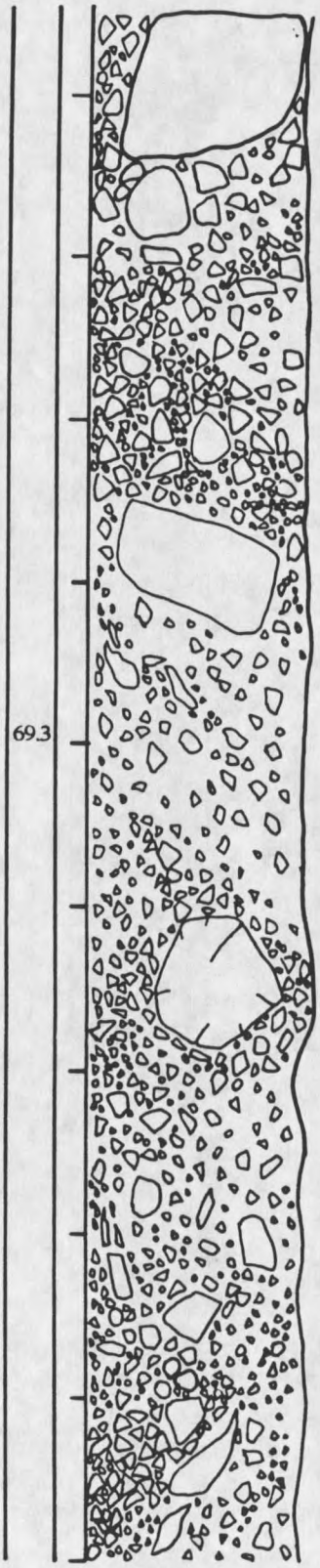

69.3
Gmpv


0.3
Sh
69.3
Gmpv

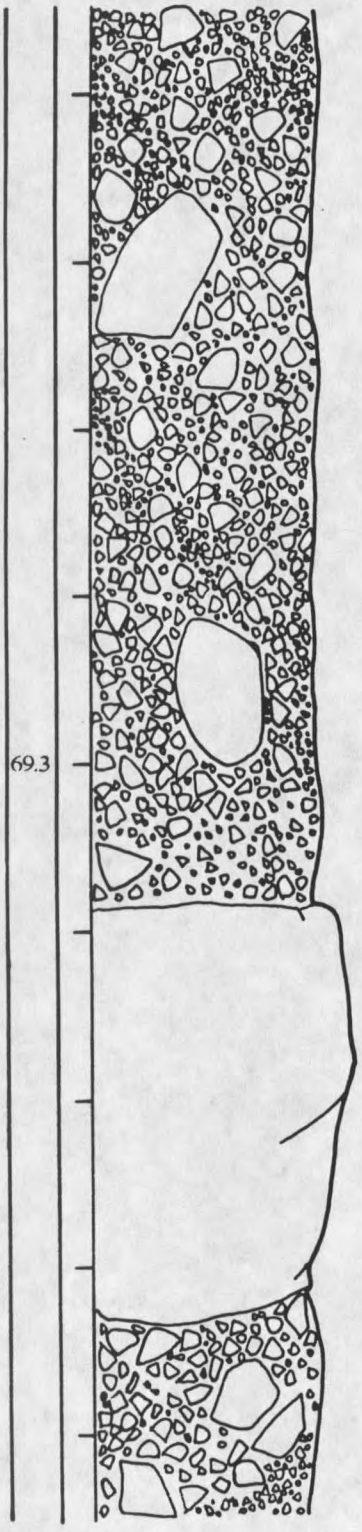


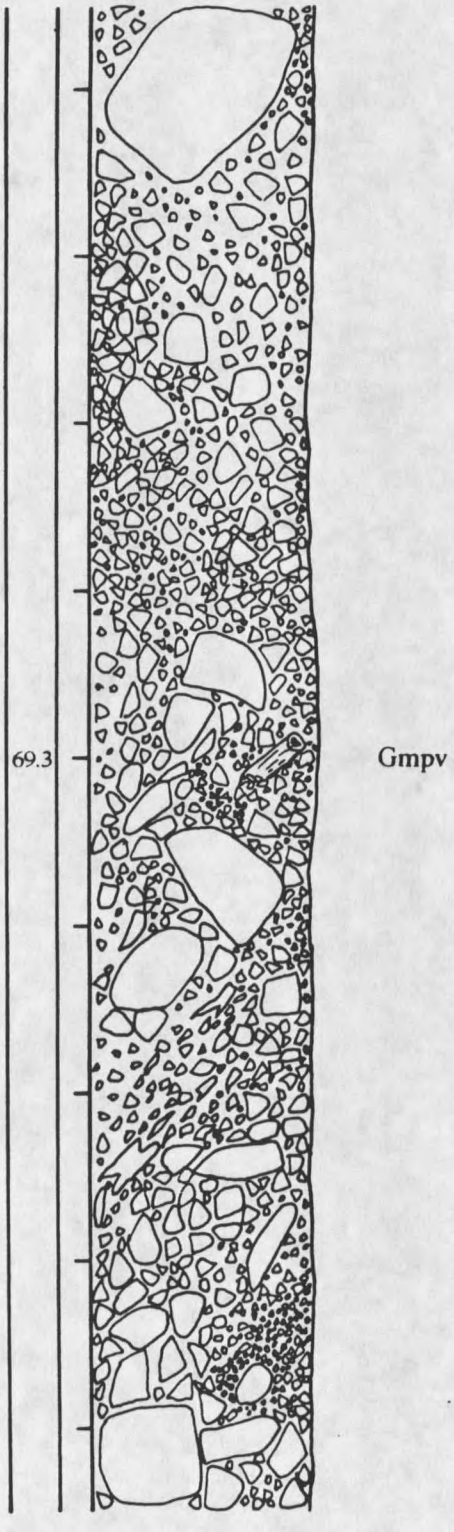
Gmpv

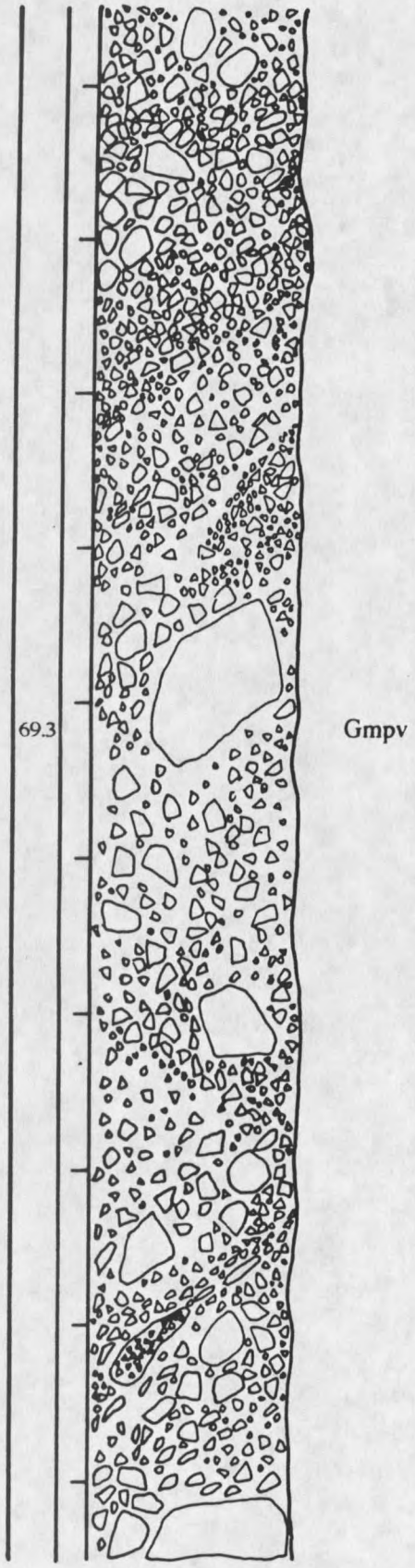
Gms

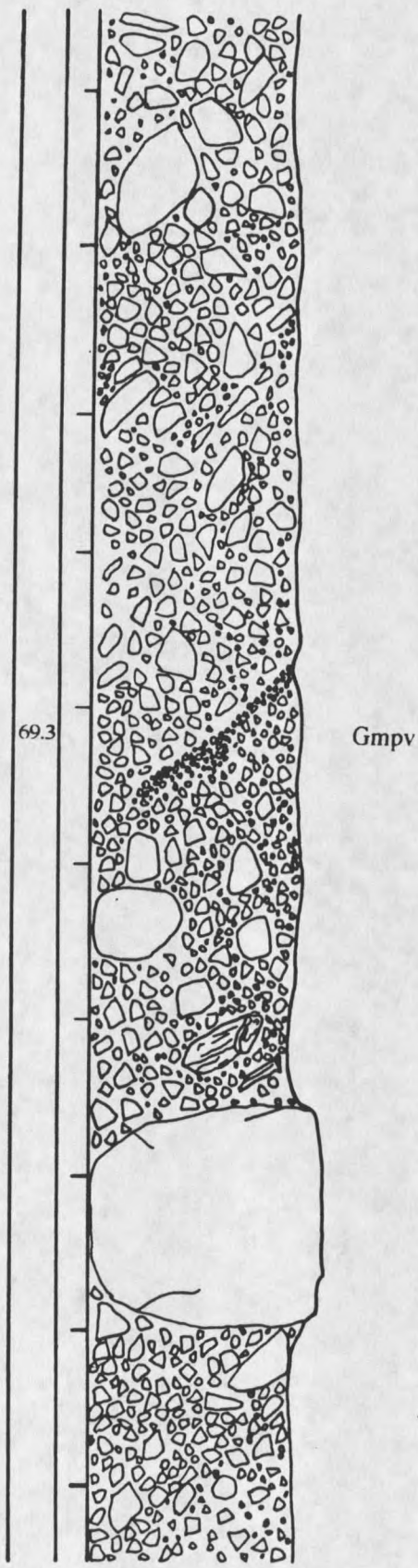


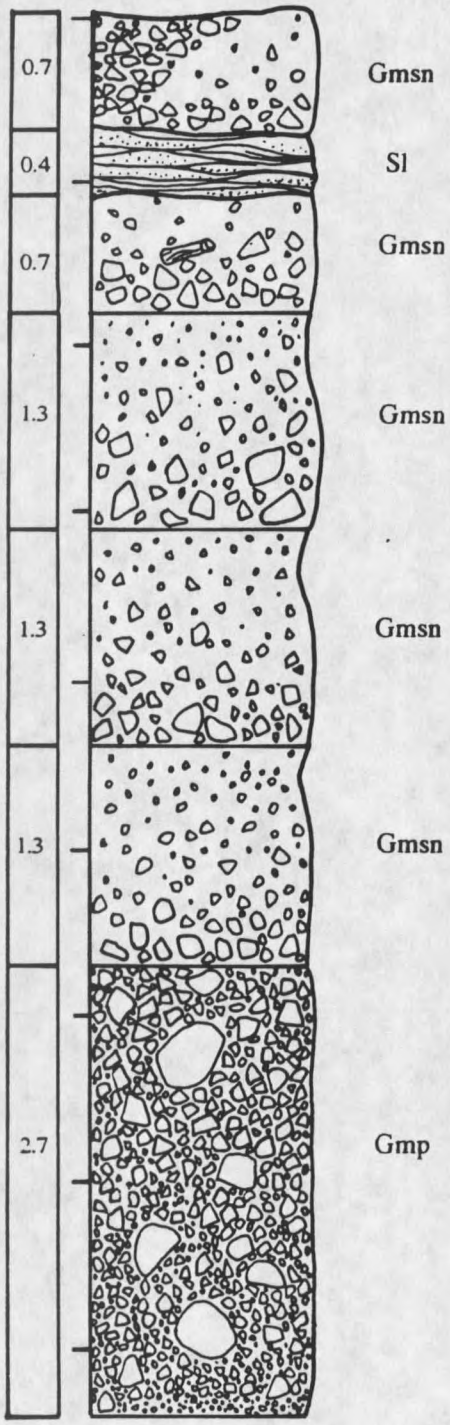
Gmpv

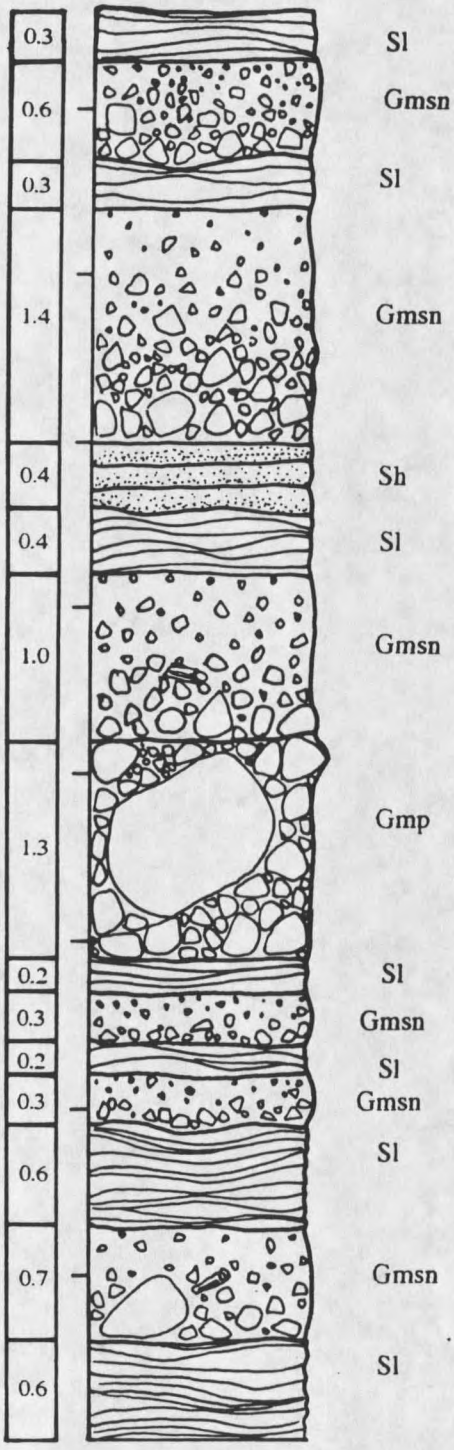

69.3
Gmpv

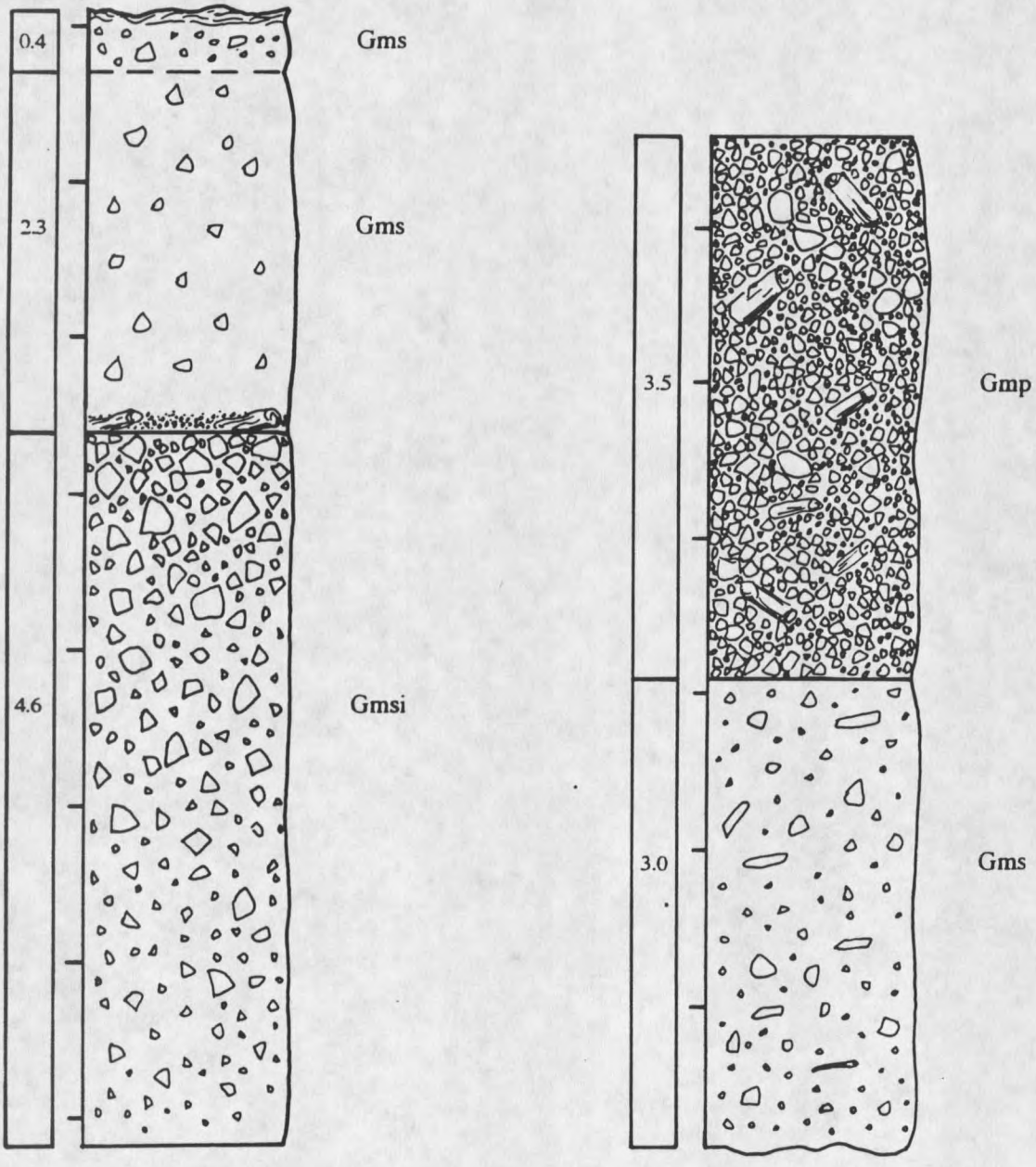

69.3
Gmpv

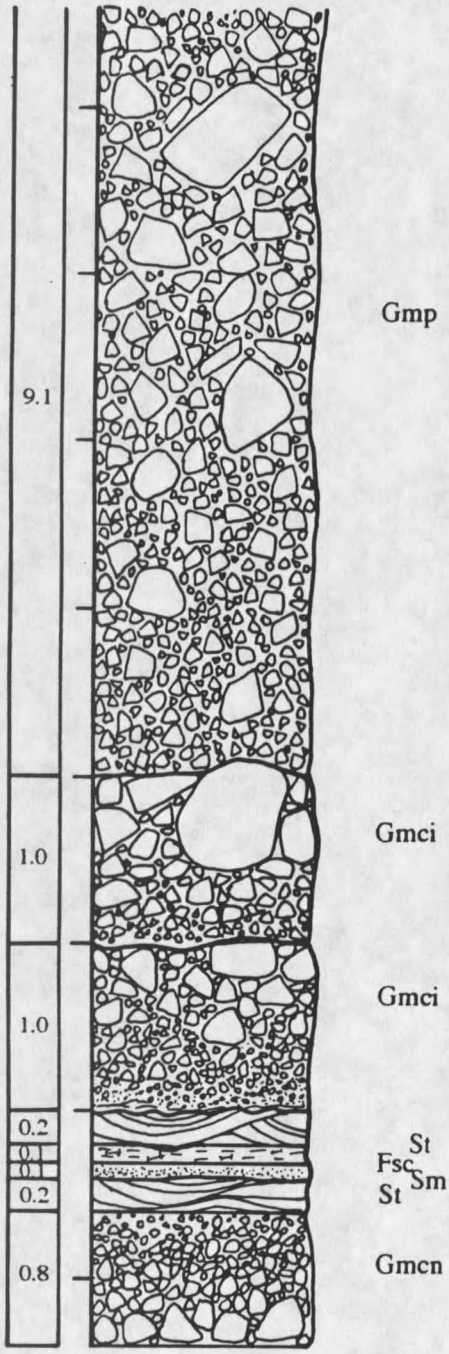

69.3
Gmpv

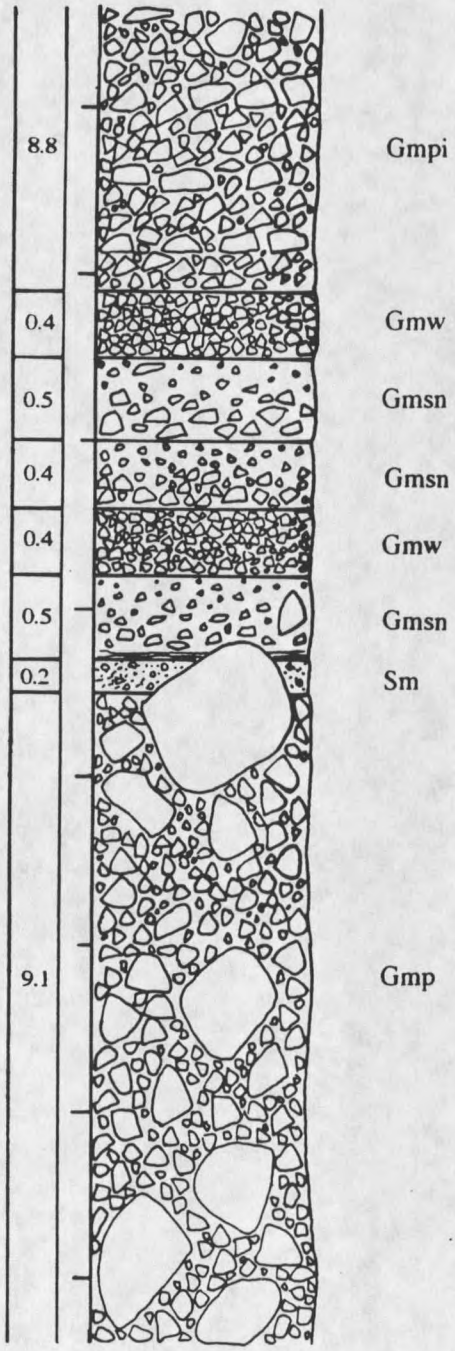

69.3
Gmpv

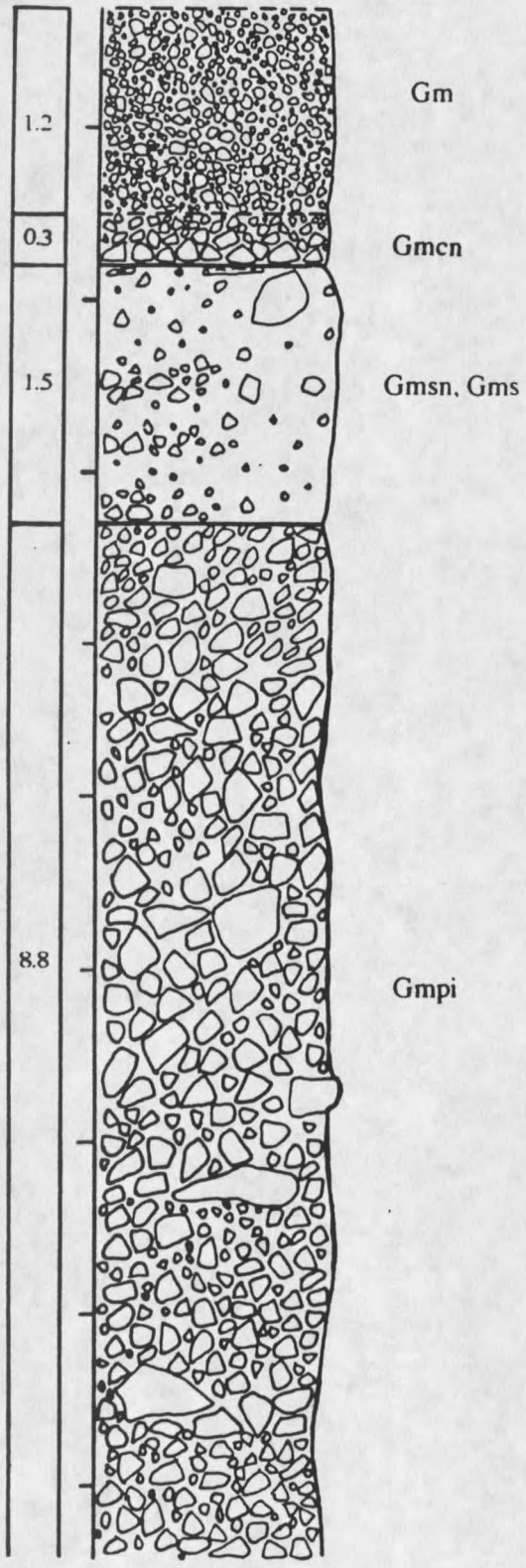

0.7
Gmsn
0.4
Sl
0.7
Gmsn
1.3
Gmsn
1.3
Gmsn
1.3
Gmsn
2.7
Gmp

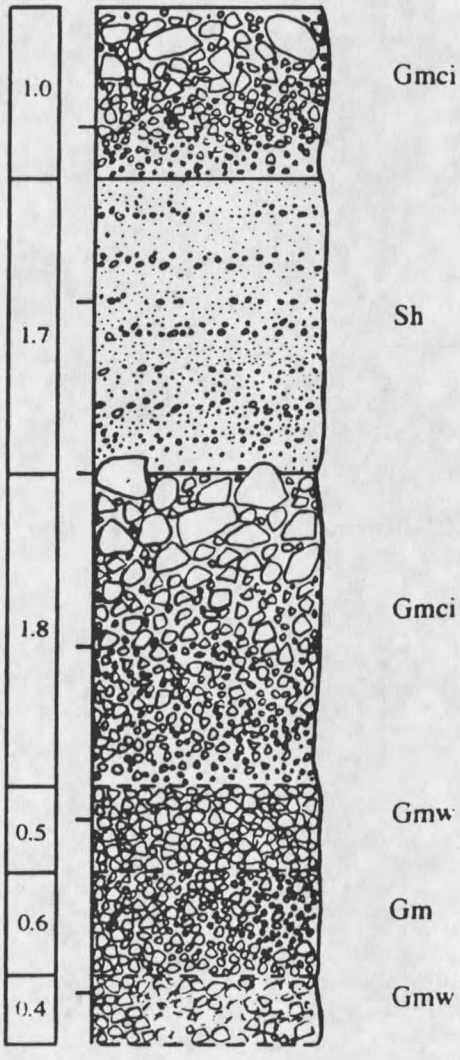

0.3
Sl
0.6
Gmsn
0.3
Sl
1.4
Gmsn
0.4
Sh
0.4
Sl
1.0
Gmsn
1.3
Gmp
0.2
Sl
0.3
Gmsn
0.2
Sl
0.3
Gmsn
0.6
Sl
0.7
Gmsn
0.6
Sl


0.4
Gms
2.3
Gms
4.6
Gmsi
3.5
Gmp
3.0
Gms


9.1
1.0
1.0
0.2
0.1
0.1
0.2
0.8
Gmp
Gmci
Gmci
St
Fsc
Sm
St
Gmcn

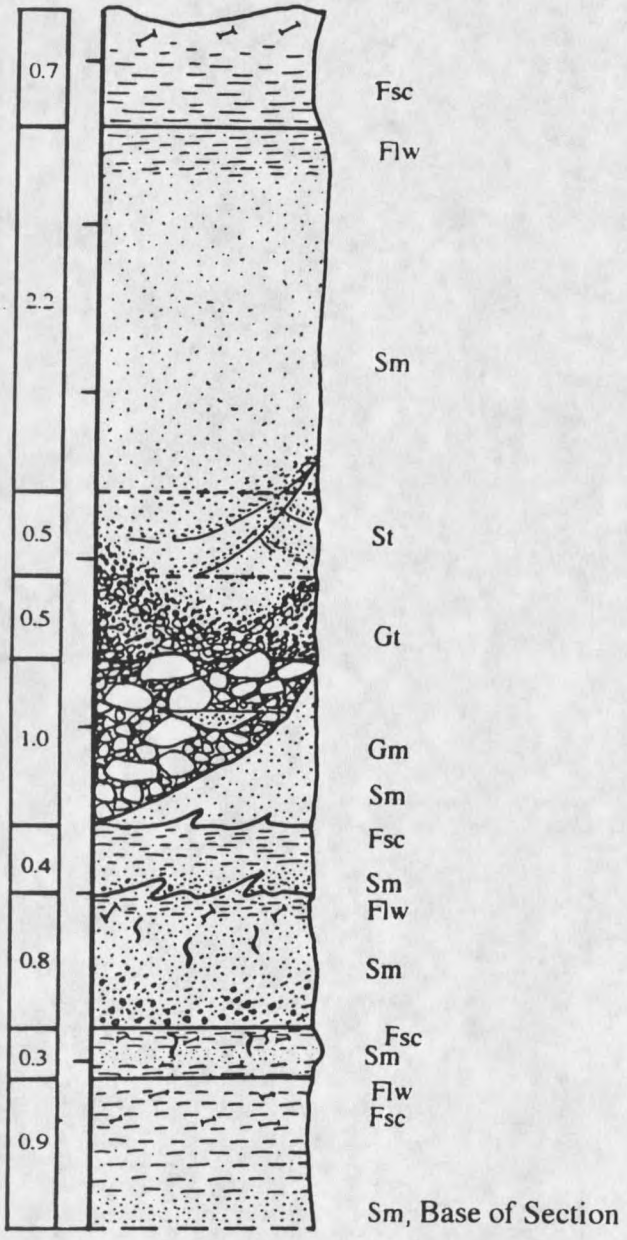

8.8
0.4
0.5
0.4
0.4
0.5
0.2
9.1
Gmpi
Gmw
Gmsn
Gmsn
Gmw
Gmsn
Sm
Gmp

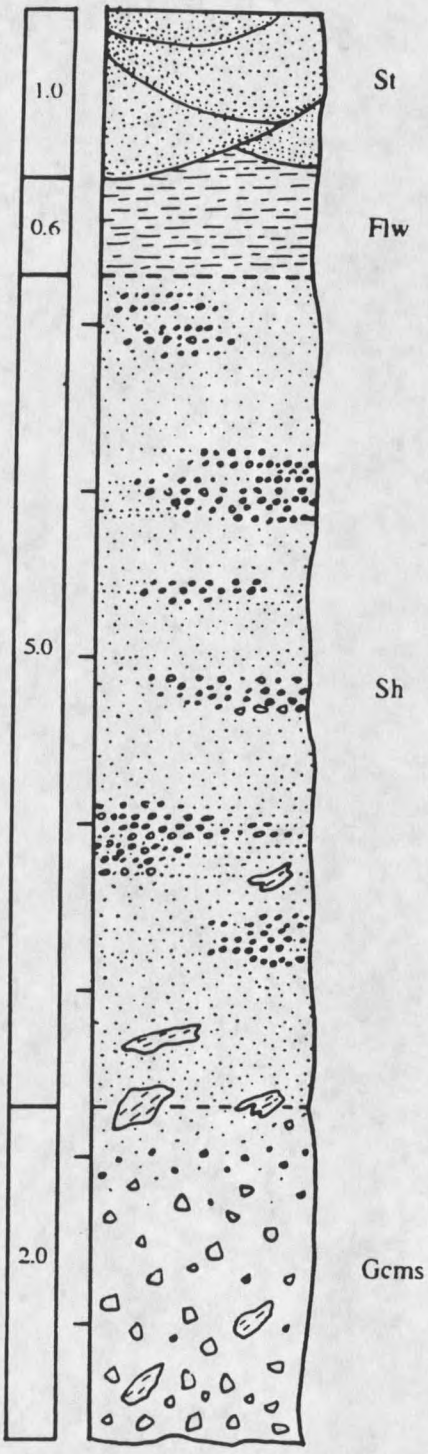

1.2
0.3
1.5
8.8
Gm
Gmcn
Gmsn, Gms
Gmpi

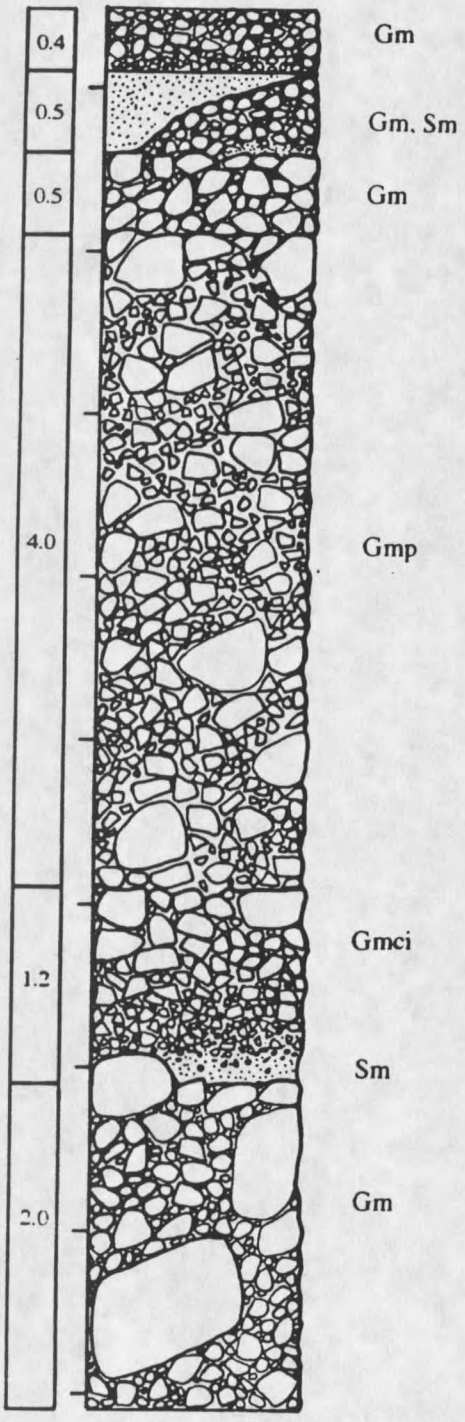

1.0
1.7
1.8
0.5
0.6
0.4
Gmci
Sh
Gmci
Gmw
Gm
Gmw

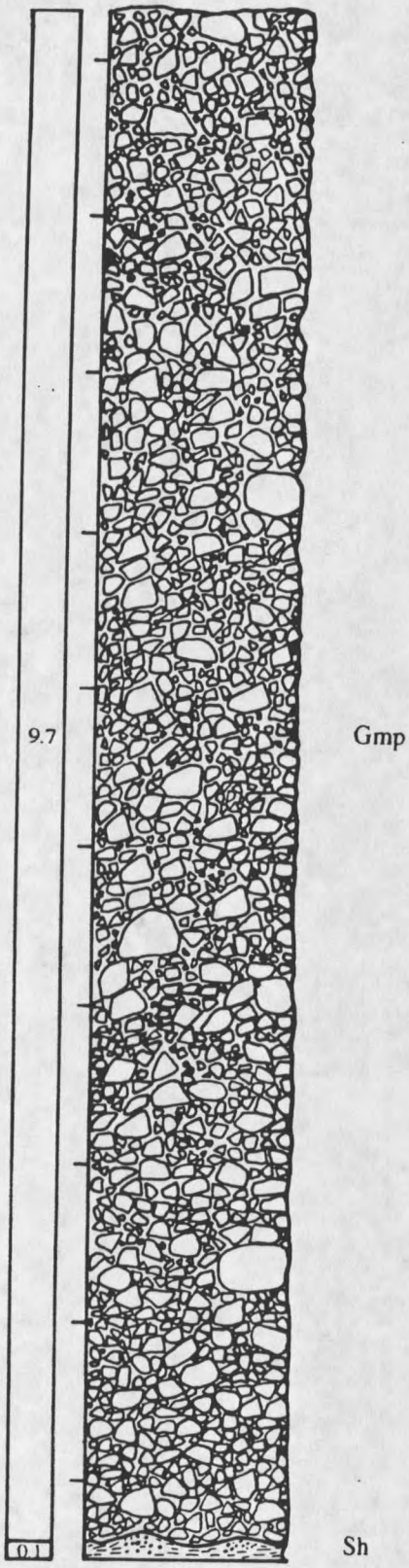
Antelope Butte Measured Section II

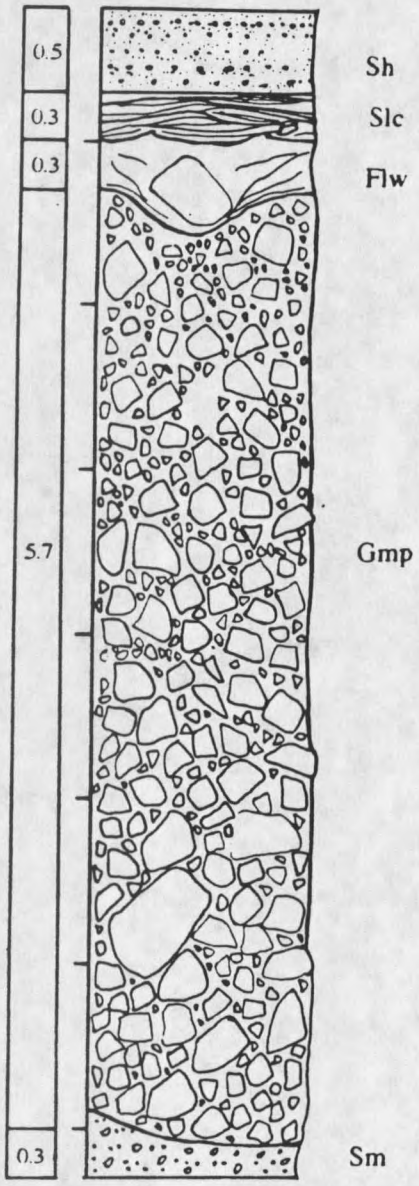
Location:
SW1/4, Sec 12, T4S, R7E

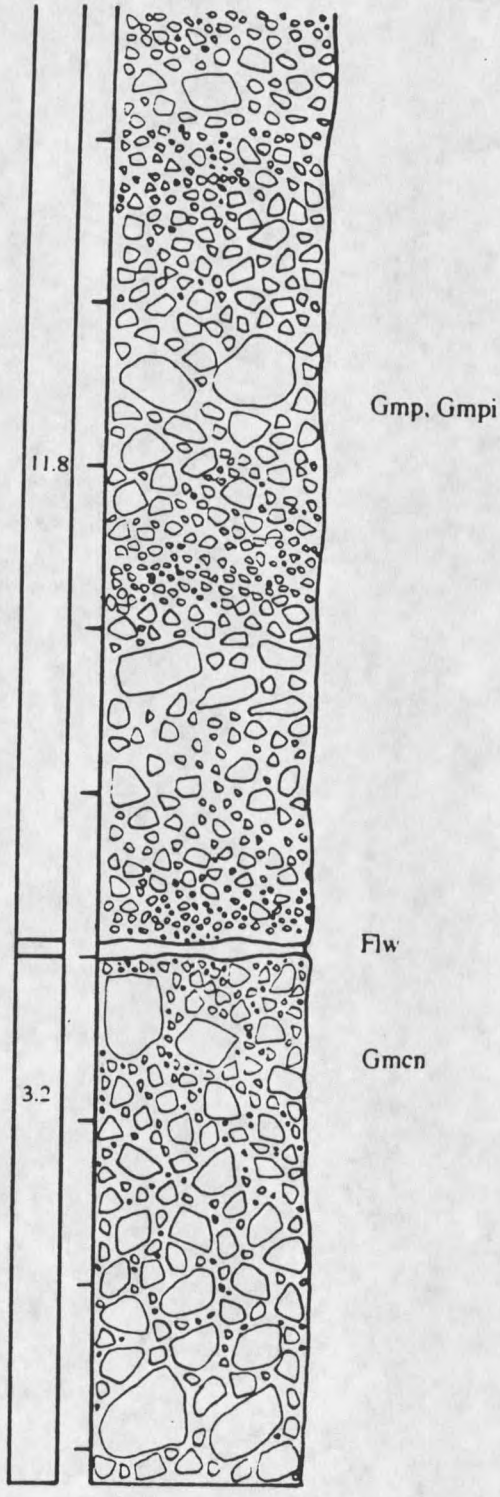


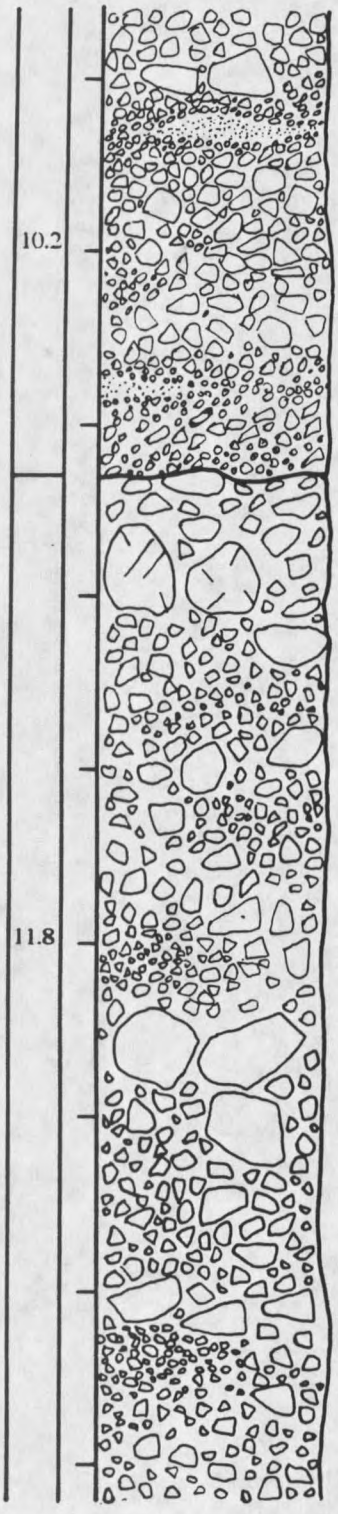



0.4
0.5
0.5
4.0
1.2
2.0
Gm
Gm, Sm
Gm
Gmp
Gmci
Sm
Gm


9.7
0.1
Gmp
Sh

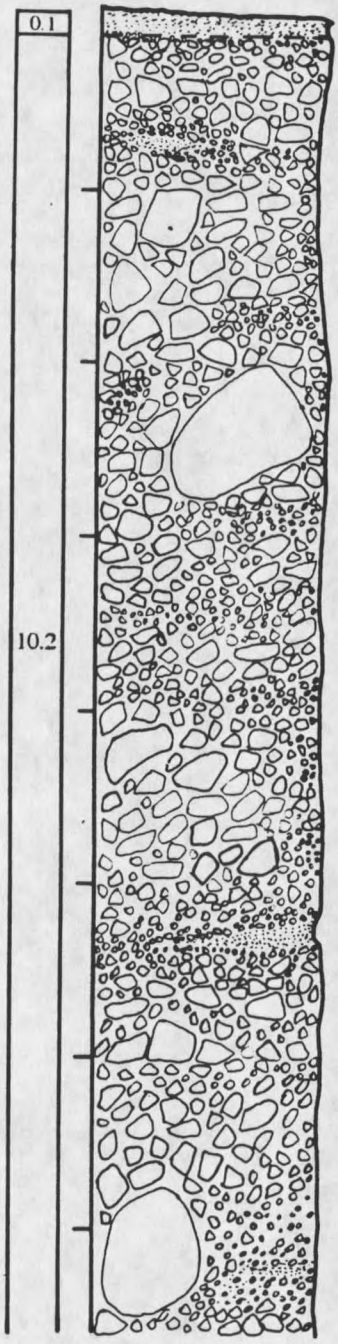

0.5
0.3
0.3
5.7
0.3
Sh
Slc
Flw
Gmp
Sm


11.8
3.2
Gmp, Gmpi
Flw
Gmcn



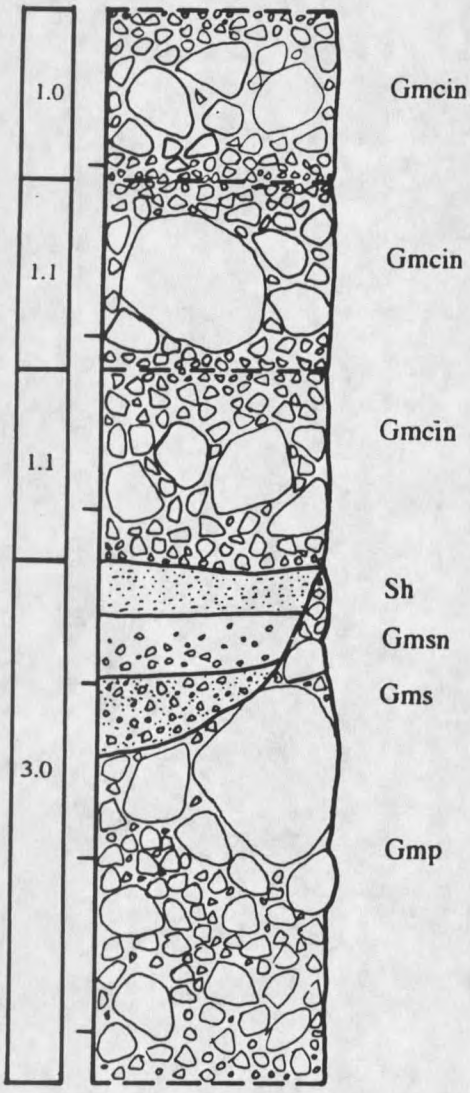
Gmpi, Se

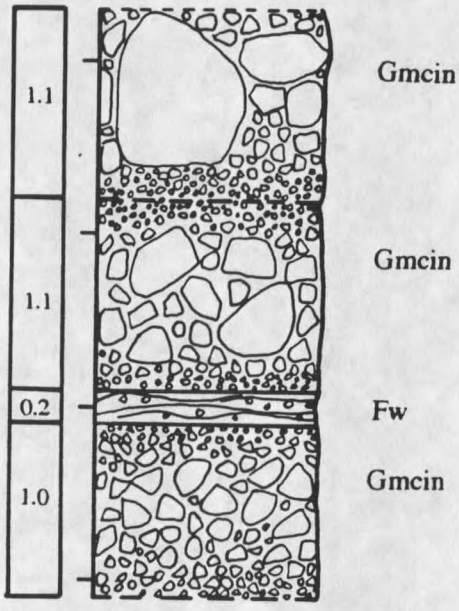
Gmp, Gmpi



Sm

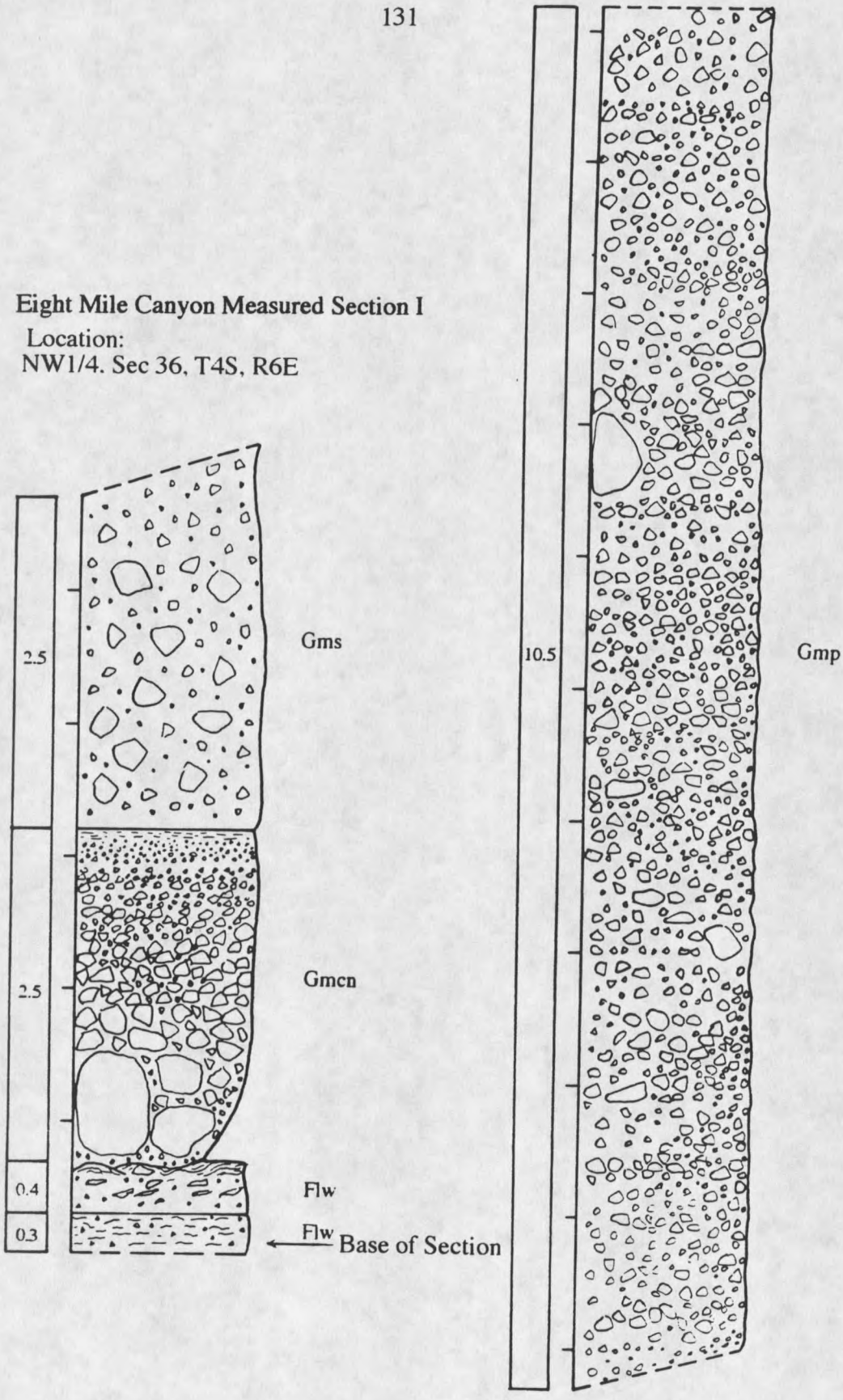
Gmpi, Se

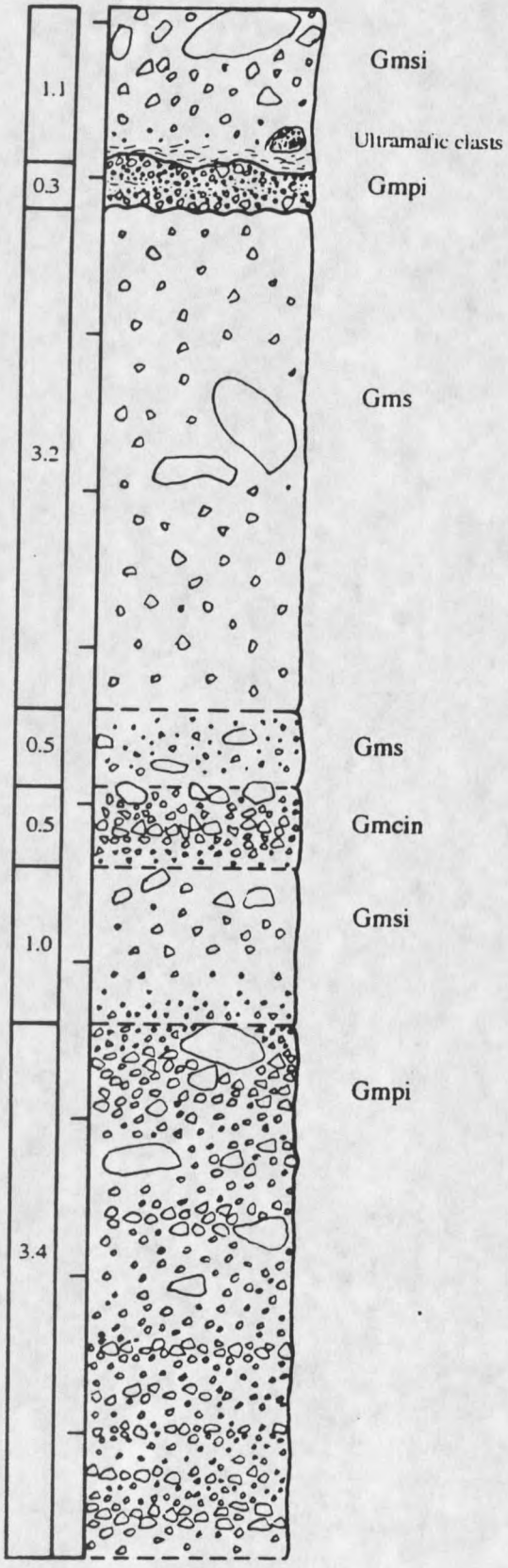

1.0
1.1
1.1
3.0
Gmcin
Gmcin
Gmcin
Sh
Gmsn
Gms
Gmp

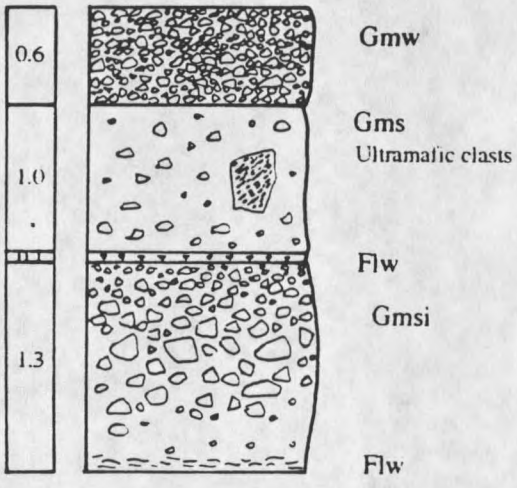

1.1
1.1
0.2
1.0
Gmcin
Gmcin
Fw
Gmcin

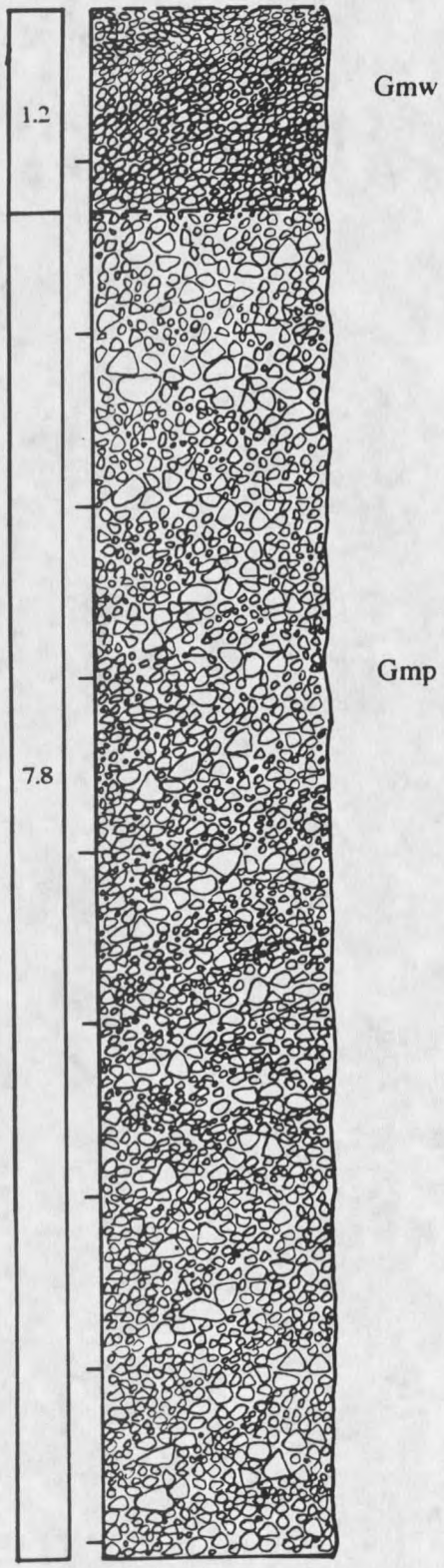
Eight Mile Canyon Measured Section I

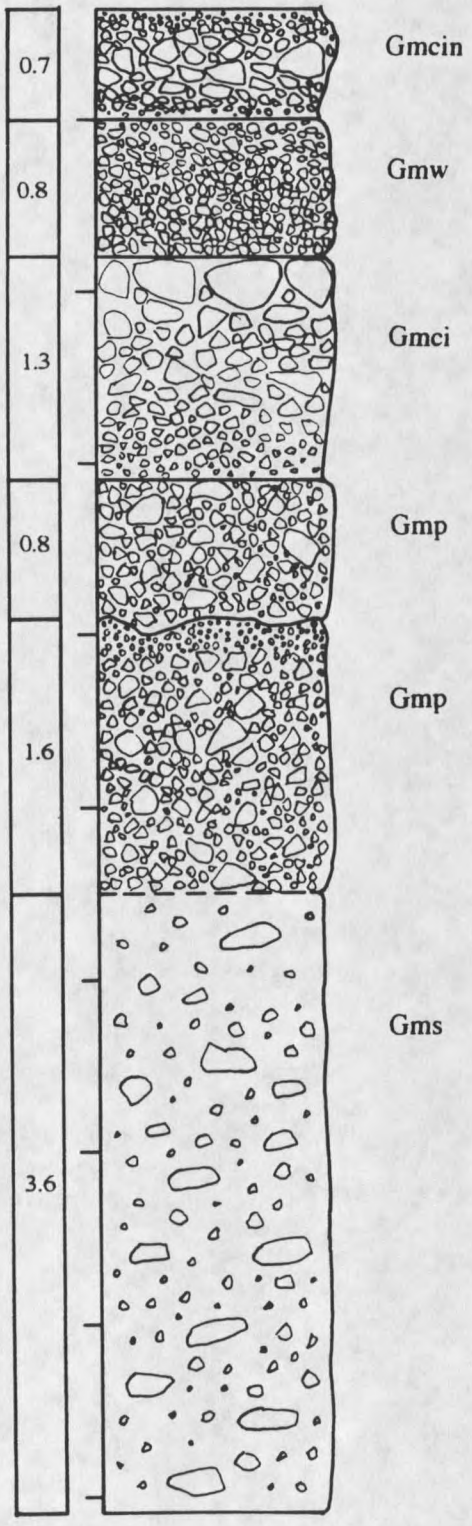
Location:
NW1/4. Sec 36, T4S, R6E

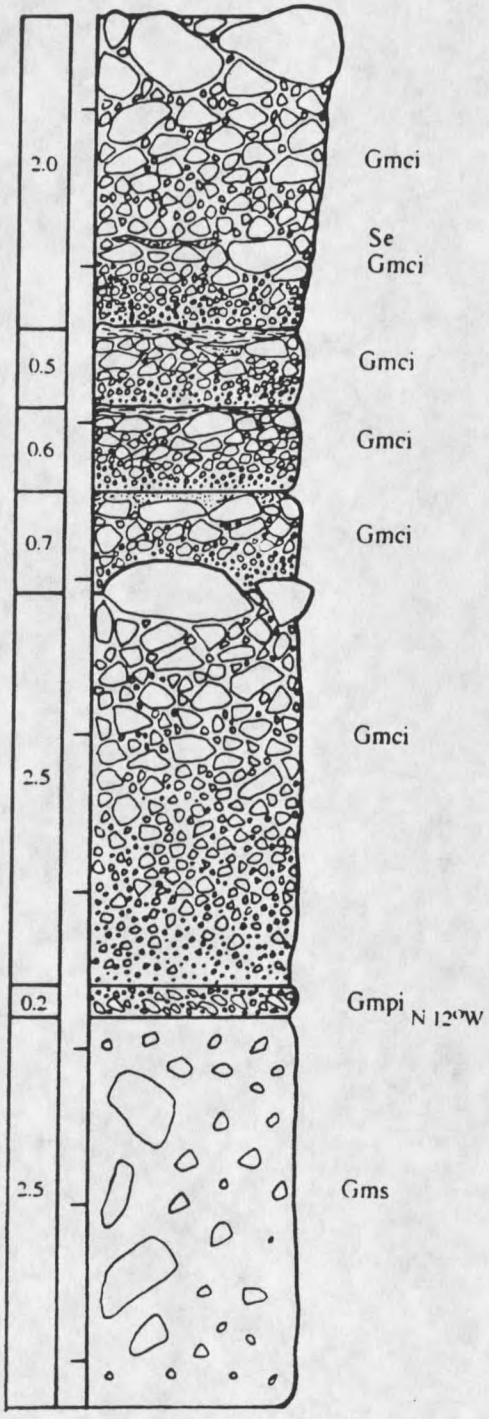


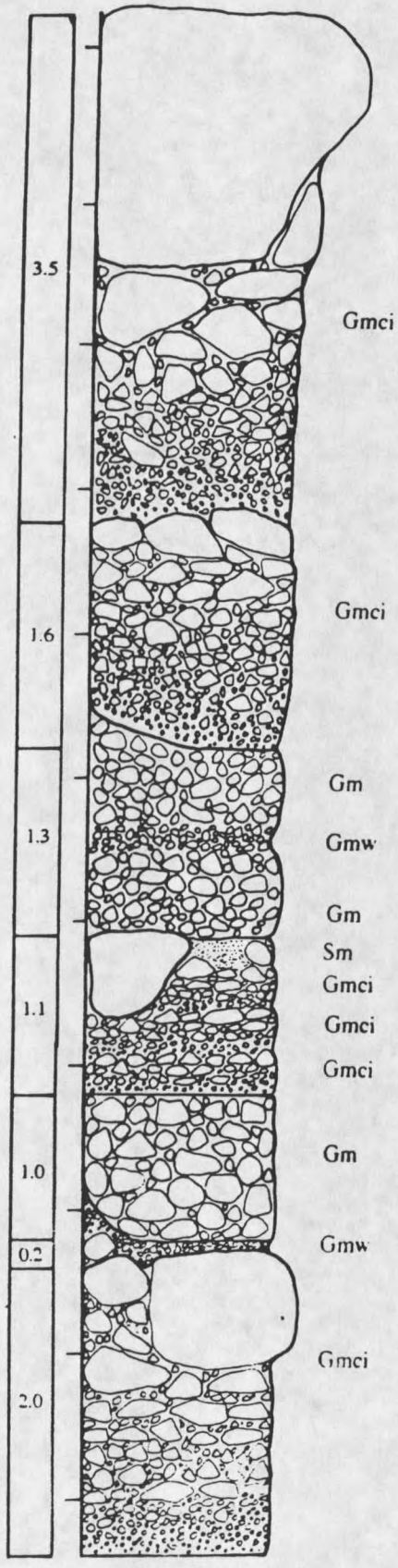

1.1
0.3
3.2
0.5
0.5
1.0
3.4
Gmsi
Ultramafic clasts
Gmpi
Gms
Gms
Gmcin
Gmsi
Gmpi

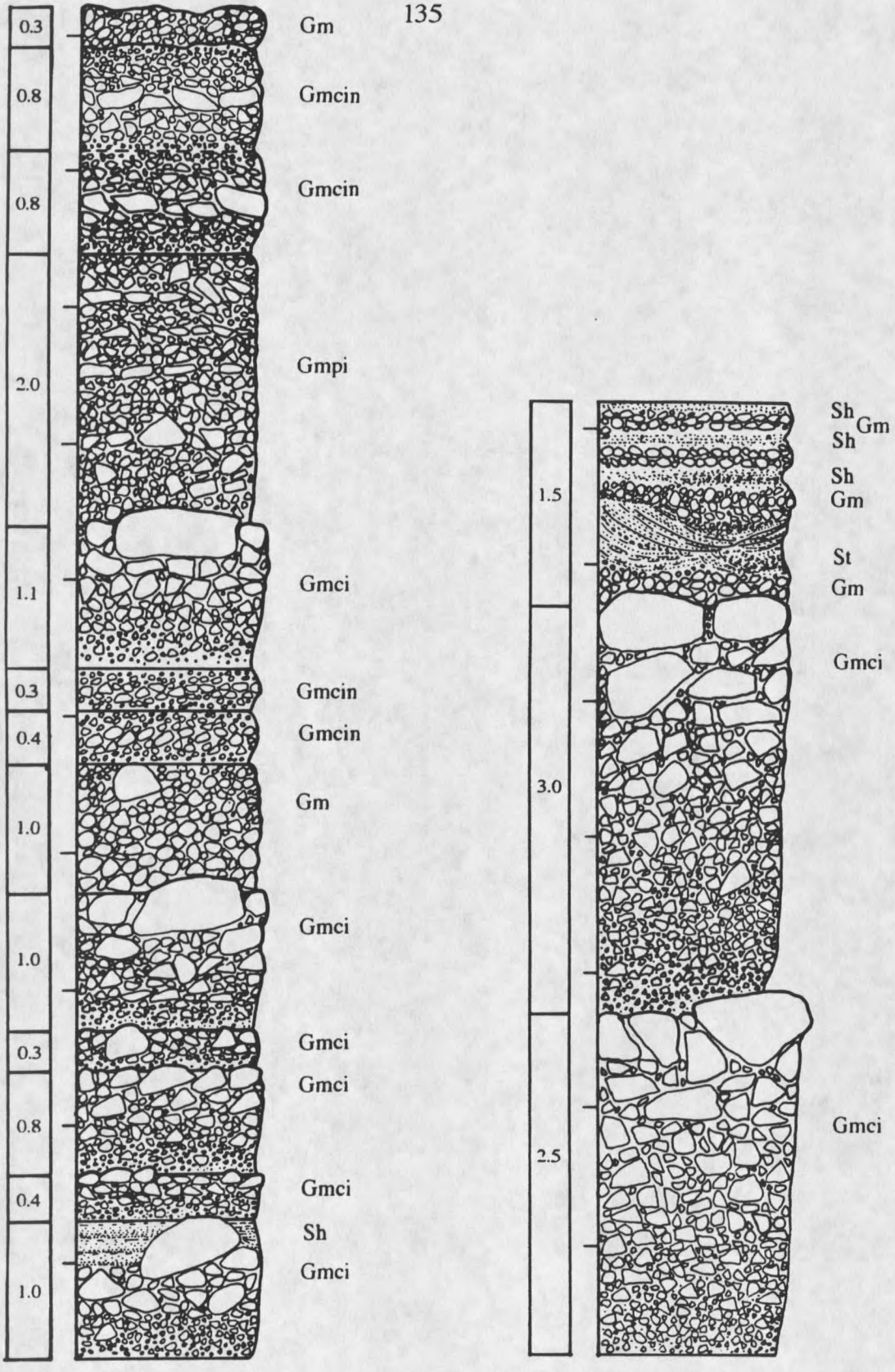

0.6
1.0
1.3
Gmw
Gms
Ultramafic clasts
Flw
Gmsi
Flw

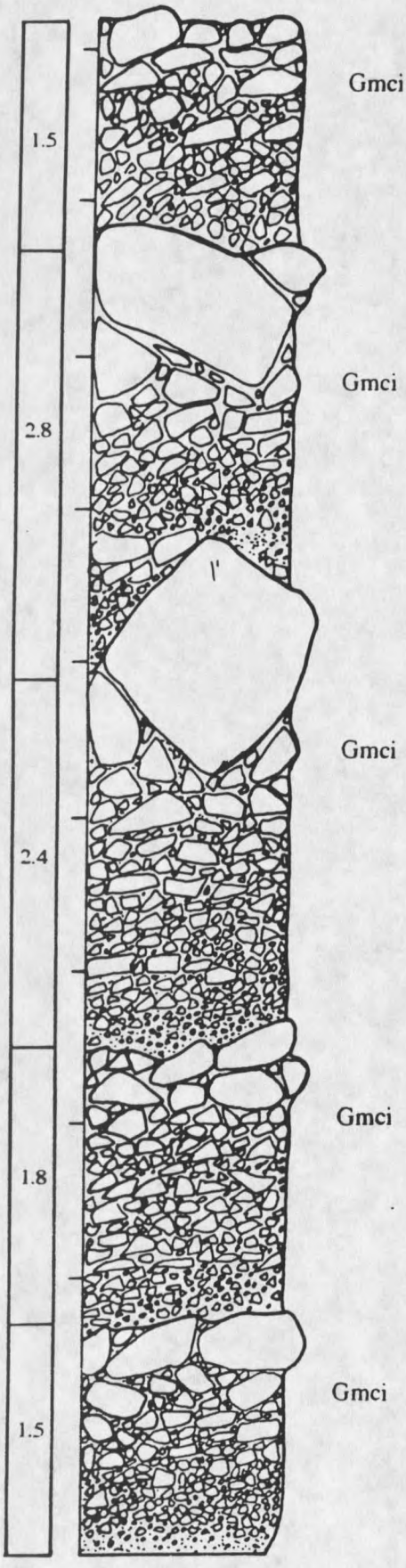

1.2
7.8
Gmw
Gmp

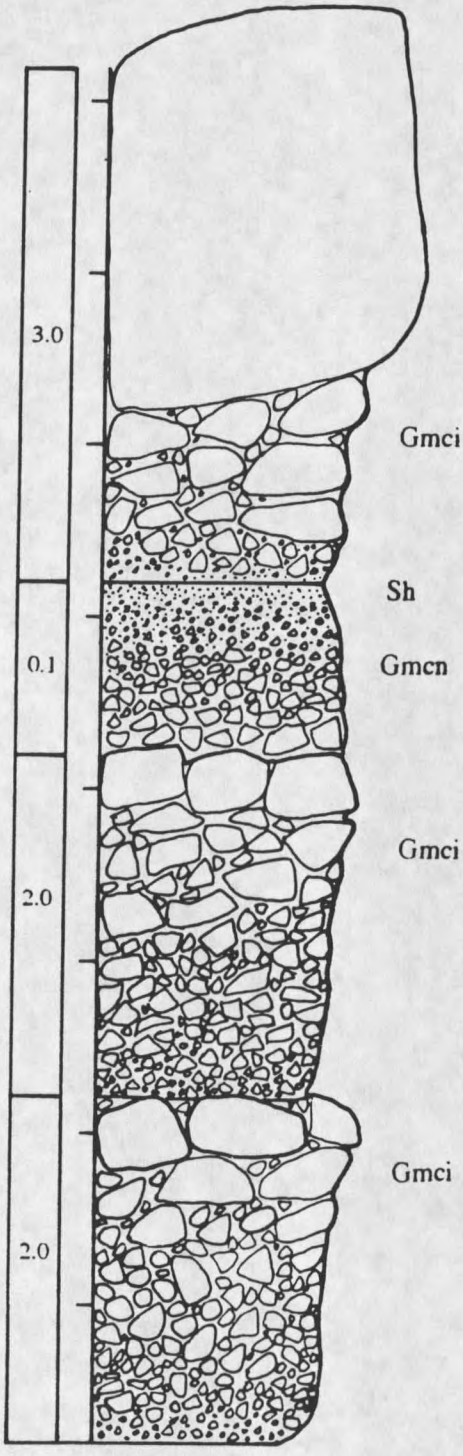

0.7
0.8
1.3
0.8
1.6
3.6
Gmcin
Gmw
Gmci
Gmp
Gmp
Gms

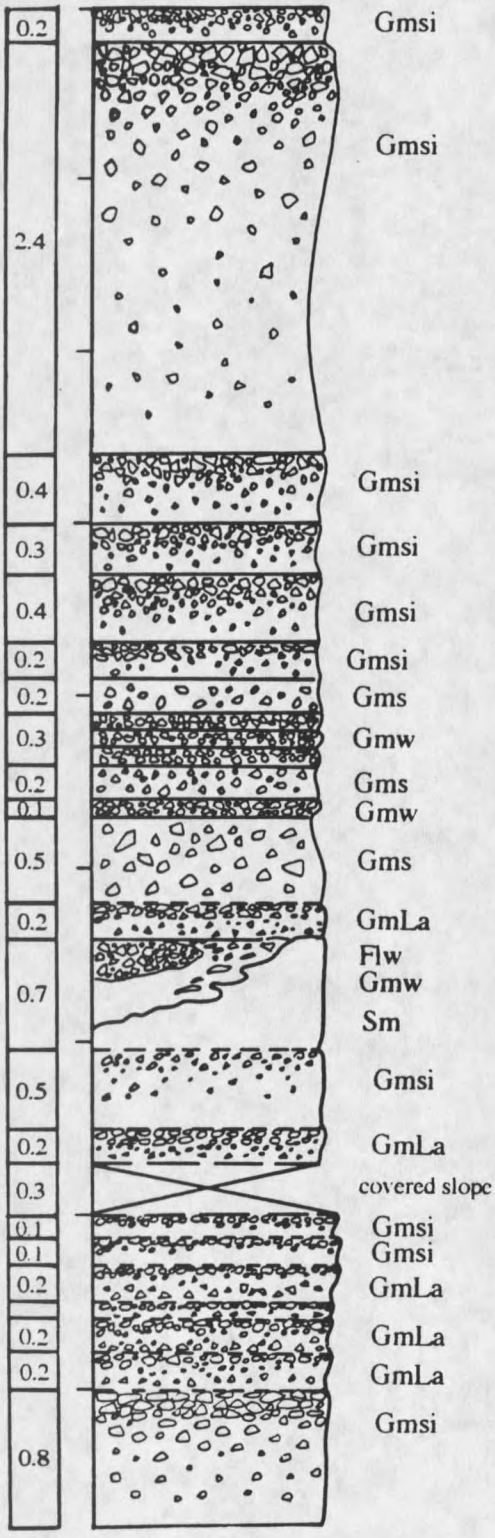

2.0
0.5
0.6
0.7
2.5
0.2
2.5
Gmci
Se
Gmci
Gmci
Gmci
Gmci
Gmci
Gmpi N 12°W
Gms

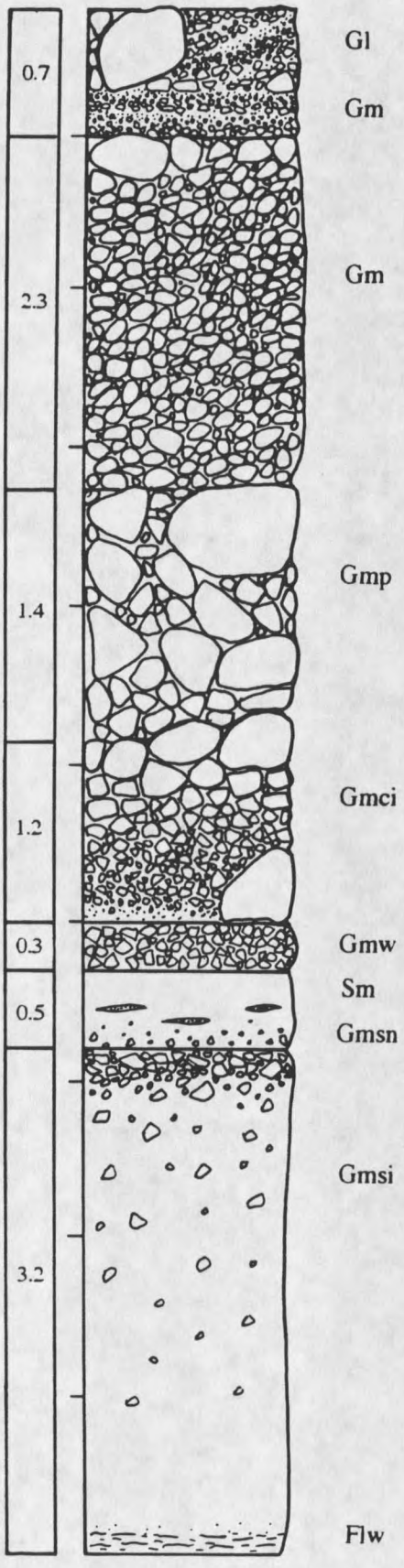

3.5
1.6
1.3
1.1
1.0
0.2
2.0
Gmci
Gmci
Gm
Gmw
Gm
Sm
Gmci
Gmci
Gmci
Gm
Gmw
Gmci

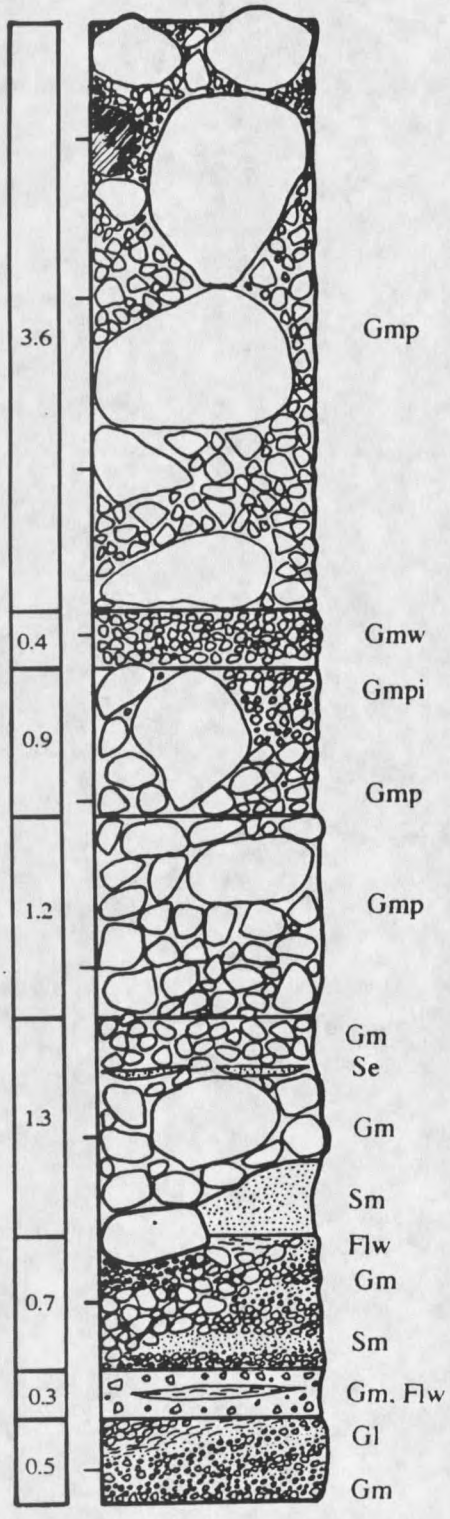

0.3
0.8
0.8
2.0
1.1
0.3
0.4
1.0
1.0
0.3
0.8
0.4
1.0
Gm
Gmcin
Gmcin
Gmpi
Gmci
Gmcin
Gmcin
Gm
Gmci
Gmci
Gmci
Gmci
Sh
Gmci
1.5
3.0
2.5
Sh
Sh
Gm
Sh
Gm
St
Gm
Gmci
Gmci

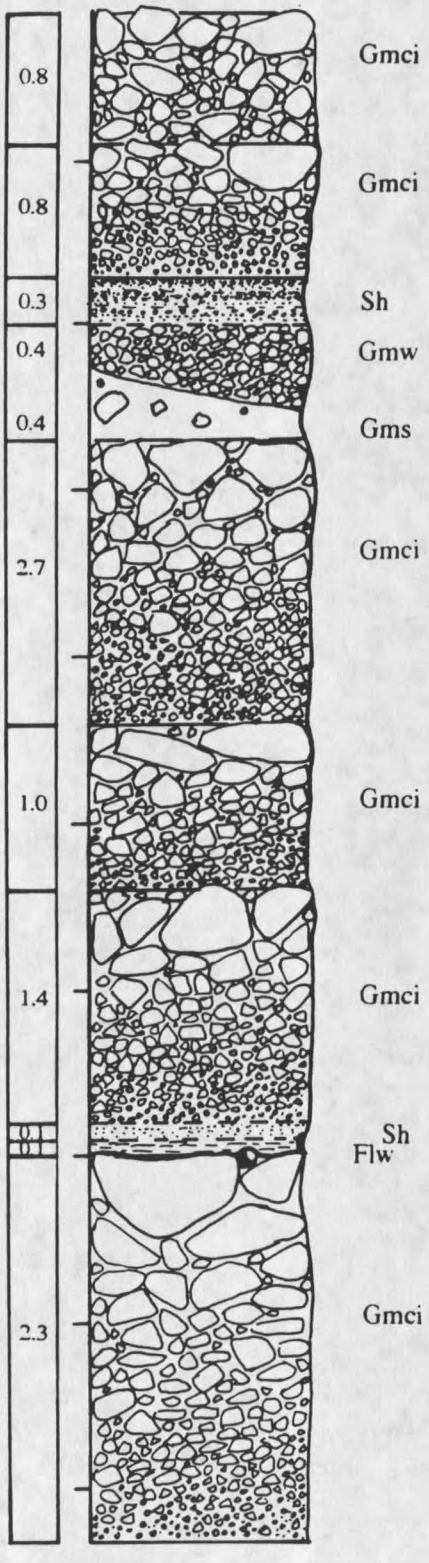

1.5
2.8
2.4
1.8
1.5
Gmci
Gmci
Gmci
Gmci
Gmci

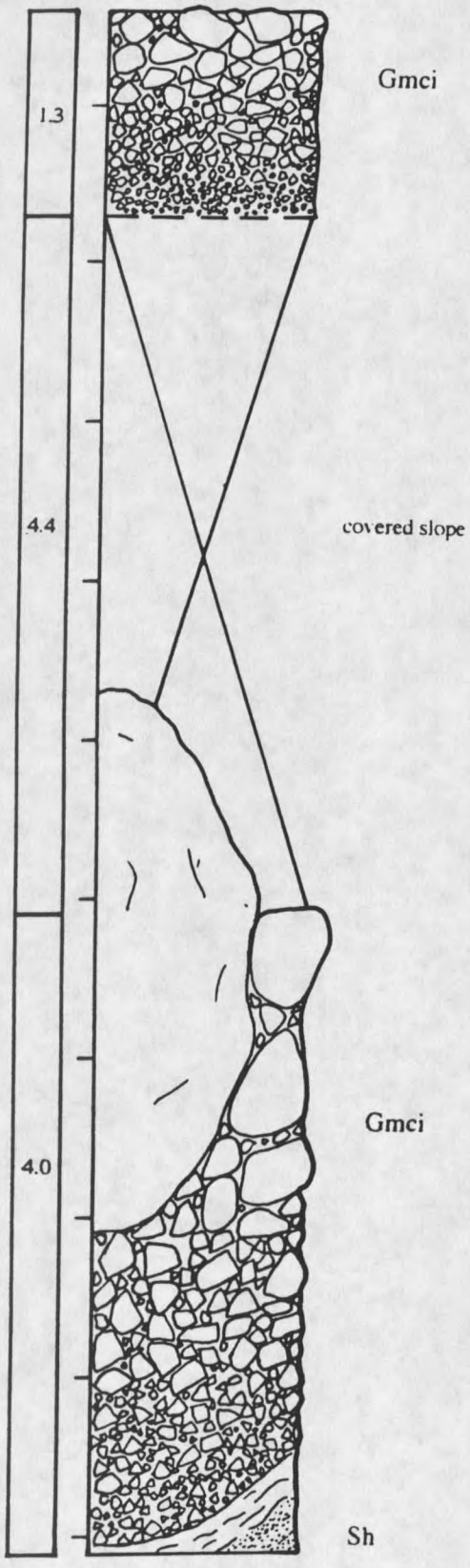

3.0
0.1
2.0
2.0
Gmci
Sh
Gmcn
Gmci
Gmci

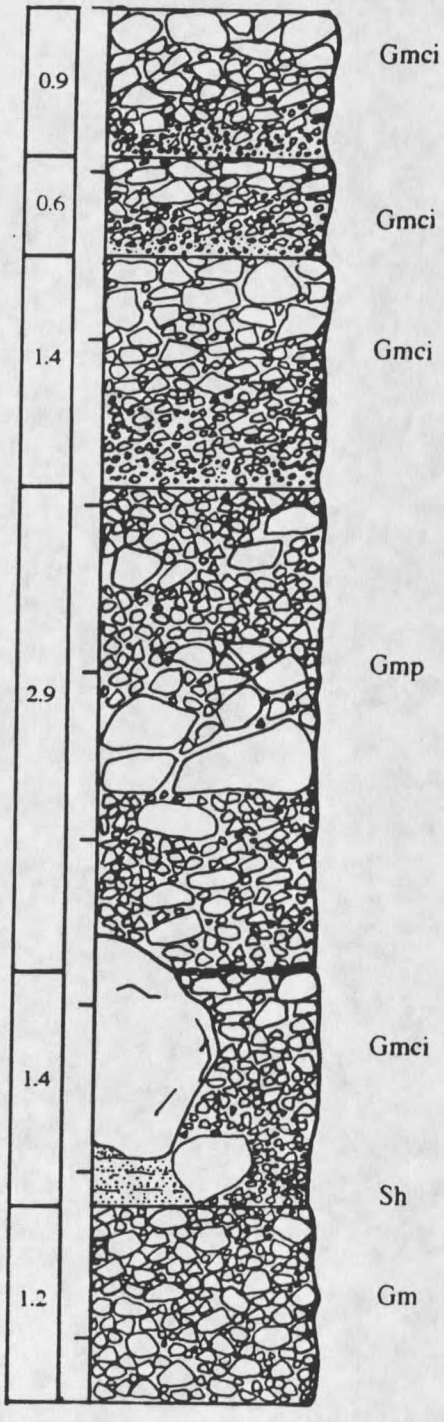

0.2
2.4
0.4
0.3
0.4
0.2
0.2
0.3
0.2
0.1
0.5
0.2
0.7
0.5
0.2
0.3
0.1
0.1
0.2
0.2
0.2
0.8
Gmsi
Gmsi
Gmsi
Gmsi
Gmsi
Gms
Gmw
Gms
Gmw
Gms
GmLa
Flw
Gmw
Sm
Gmsi
GmLa
covered slope
Gmsi
Gmsi
GmLa
GmLa
GmLa
Gmsi

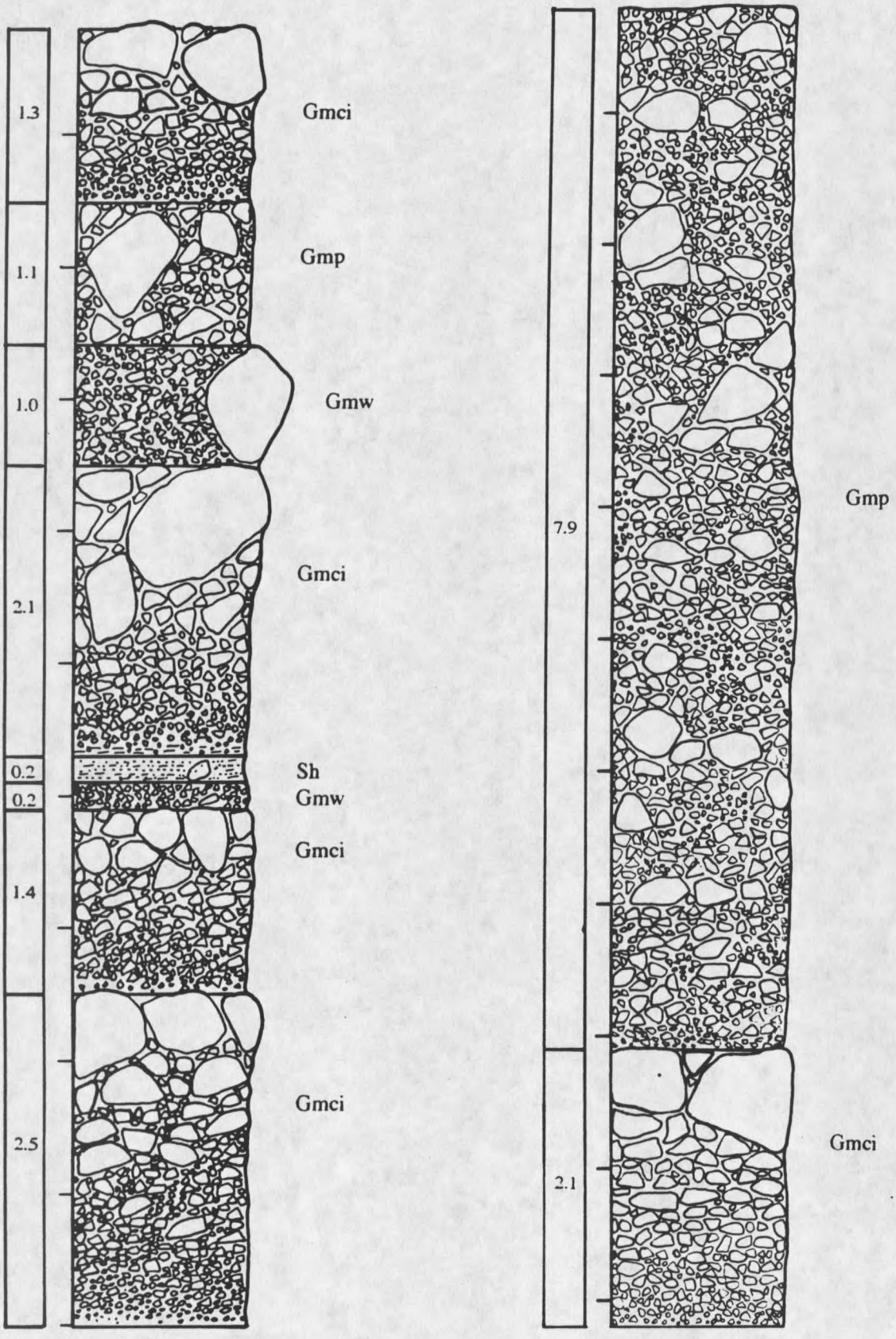

0.7
2.3
1.4
1.2
0.3
0.5
3.2
Gl
Gm
Gm
Gmp
Gmci
Gmw
Sm
Gmsn
Gmsi
Flw

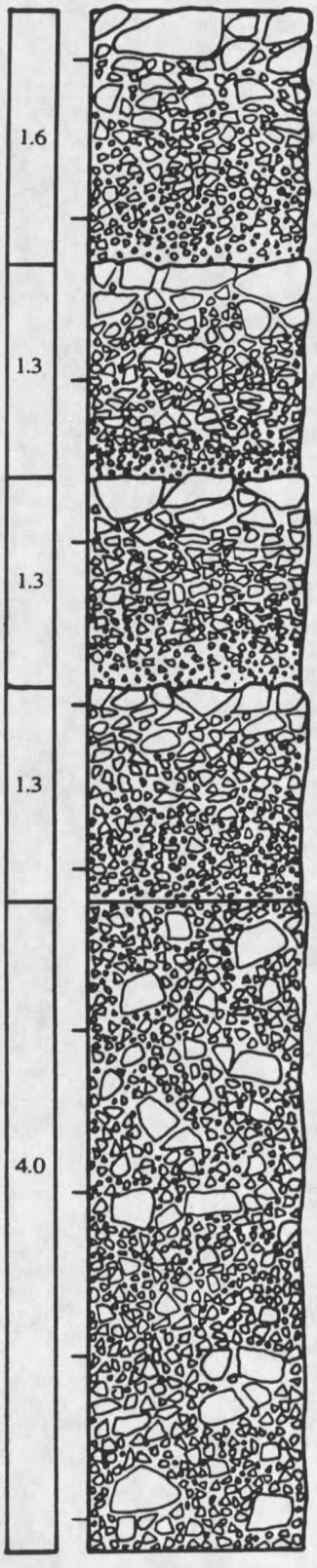

3.6
0.4
0.9
1.2
1.3
0.7
0.3
0.5
Gmp
Gmw
Gmpi
Gmp
Gmp
Gm
Se
Gm
Sm
Flw
Gm
Sm
Gm. Flw
Gl
Gm


0.8
0.8
0.3
0.4
0.4
2.7
1.0
1.4
0.1
2.3
Gmci
Gmci
Sh
Gmw
Gms
Gmci
Gmci
Gmci
Sh
Flw
Gmci


1.3
Gmci
4.4
covered slope
4.0
Gmci
Sh

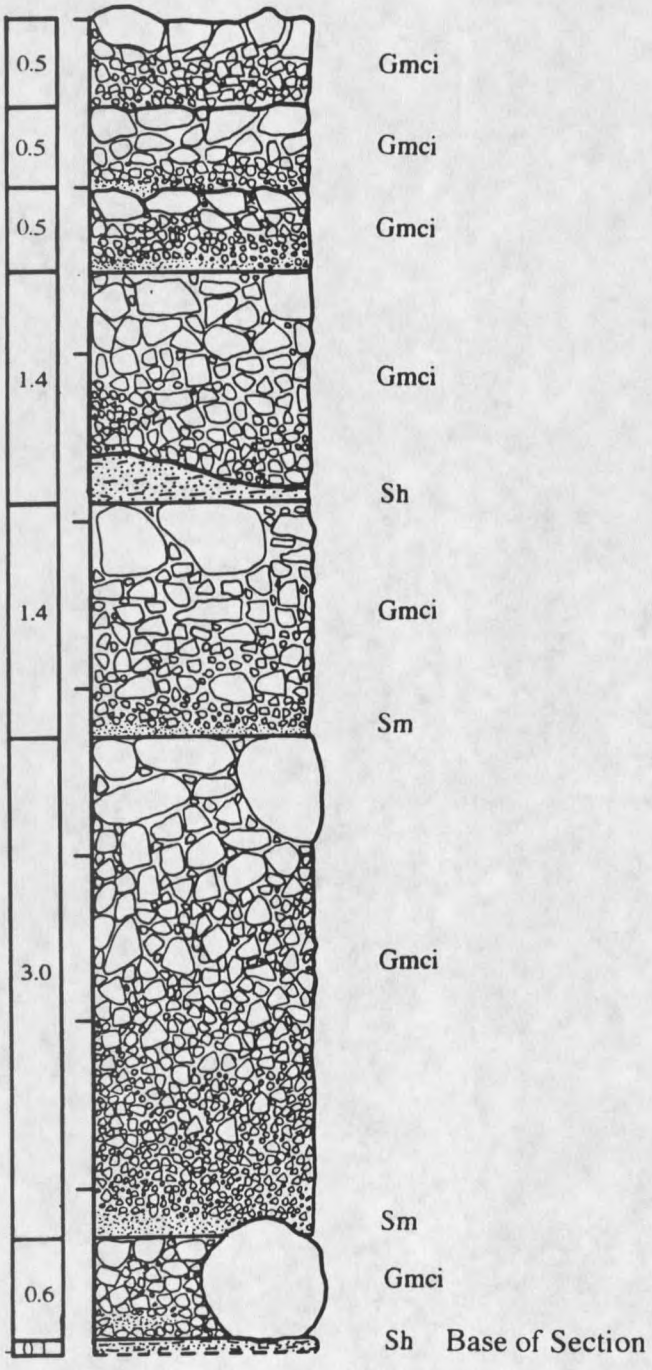

0.9
Gmci
0.6
Gmci
1.4
Gmci
2.9
Gmp
1.4
Gmci
Sh
1.2
Gm

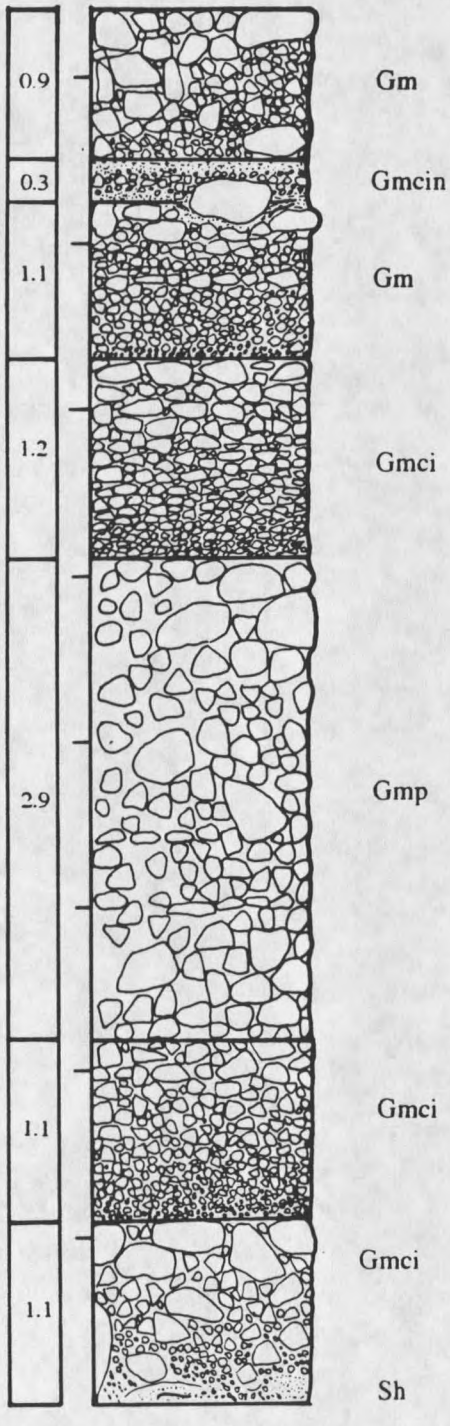

1.3
Gmci
1.1
Gmp
1.0
Gmw
2.1
Gmci
0.2
Sh
0.2
Gmw
1.4
Gmci
2.5
Gmci
7.9
Gmp
2.1
Gmci

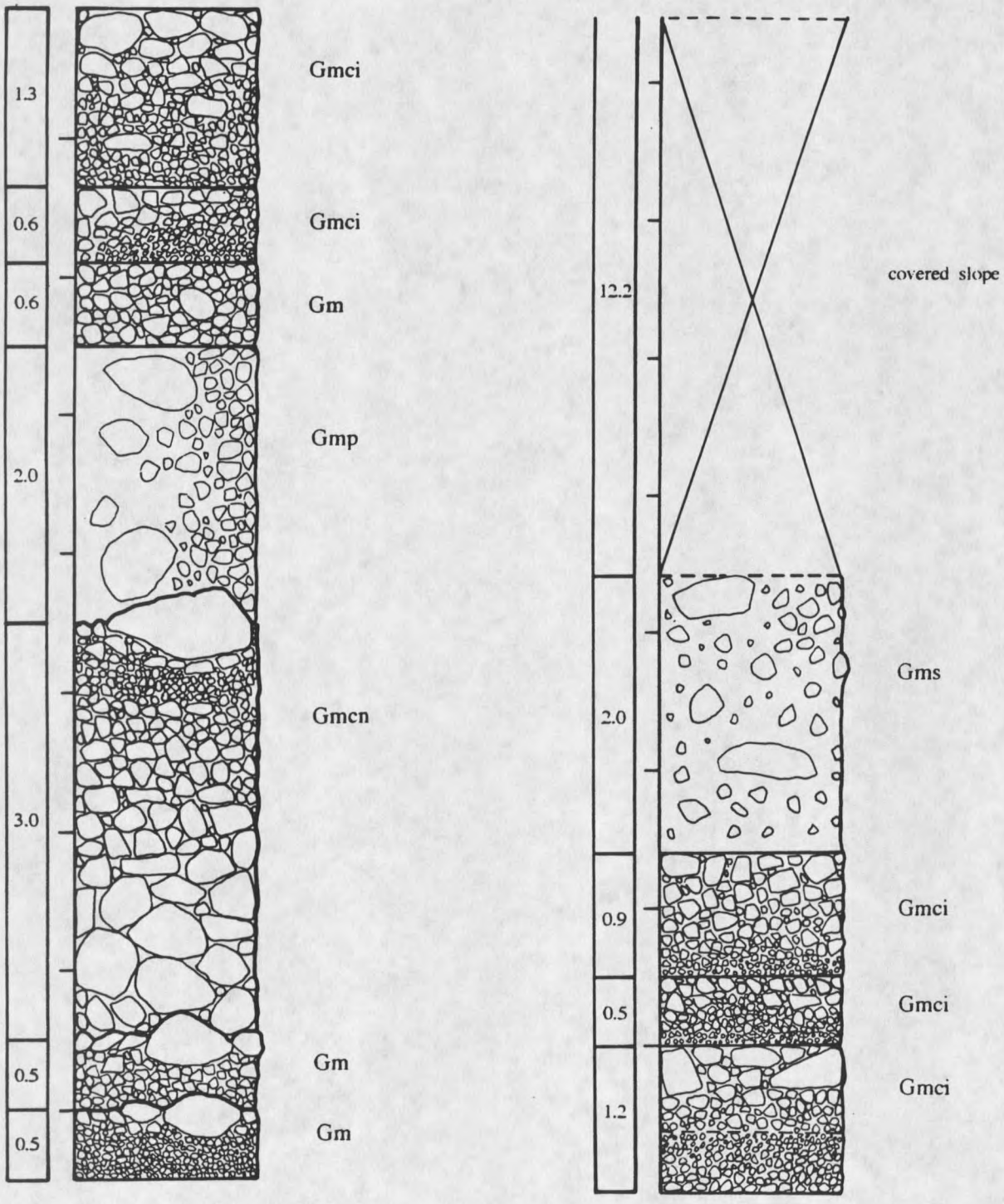

1.6
1.3
1.3
1.3
4.0
Gmci
Gmci
Gmci
Gmci
Gmp

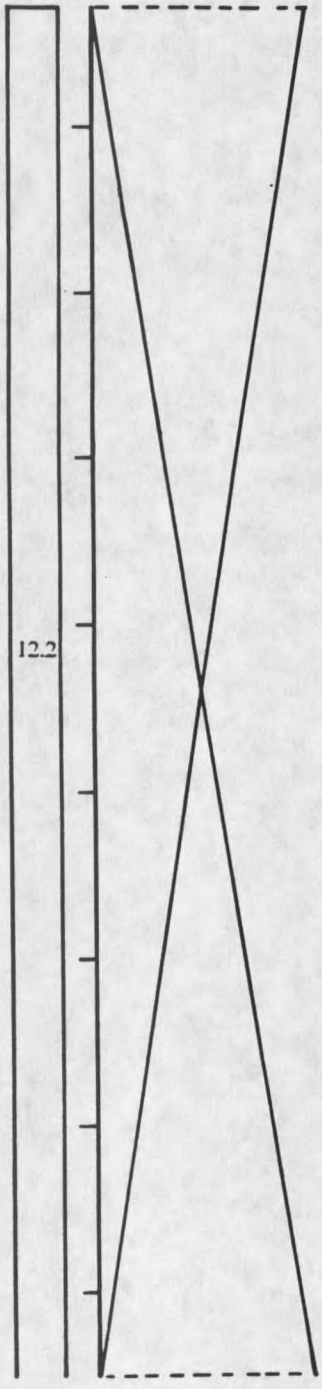
Eight Mile Canyon Measured Section II

Location:
SE1/4, Sec 31, T4S, R8E

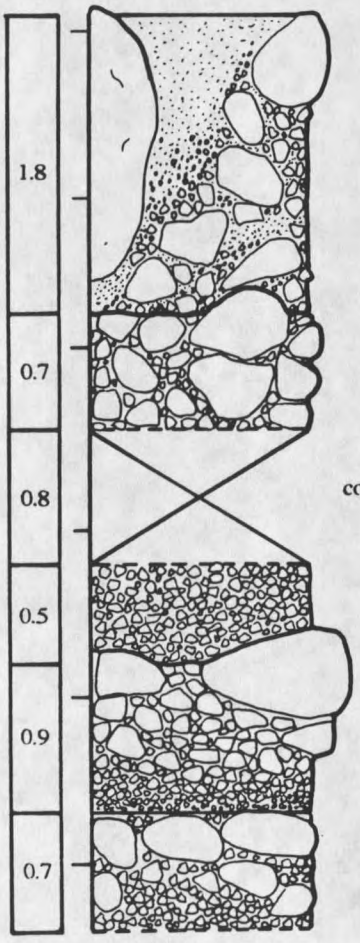





1.3
0.6
0.6
2.0
3.0
0.5
0.5
Gmci
Gmci
Gm
Gmp
Gmcn
Gm
Gm
12.2
2.0
0.9
0.5
1.2
covered slope
Gms
Gmci
Gmci
Gmci



covered slope



Gm, Sm

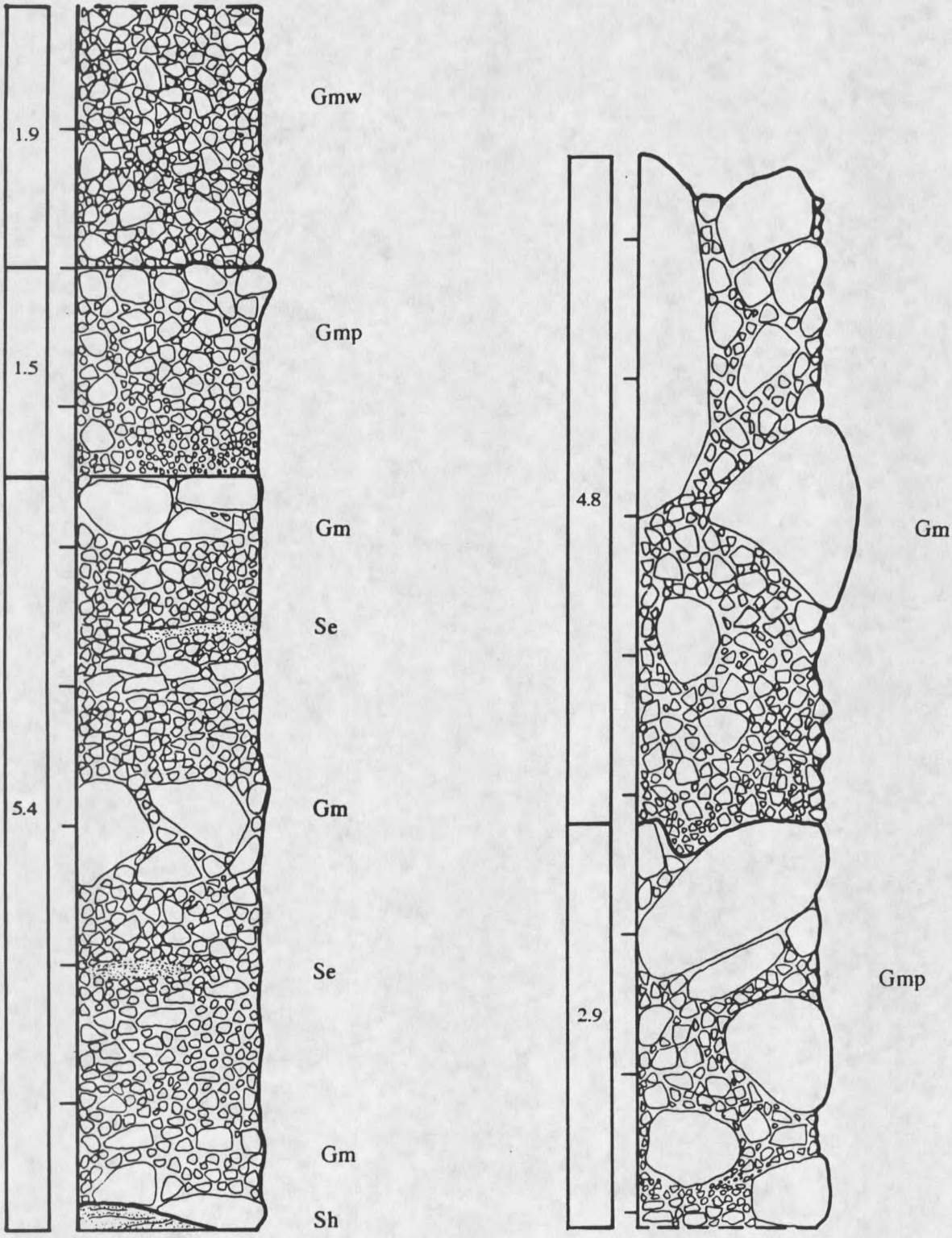
Gmp

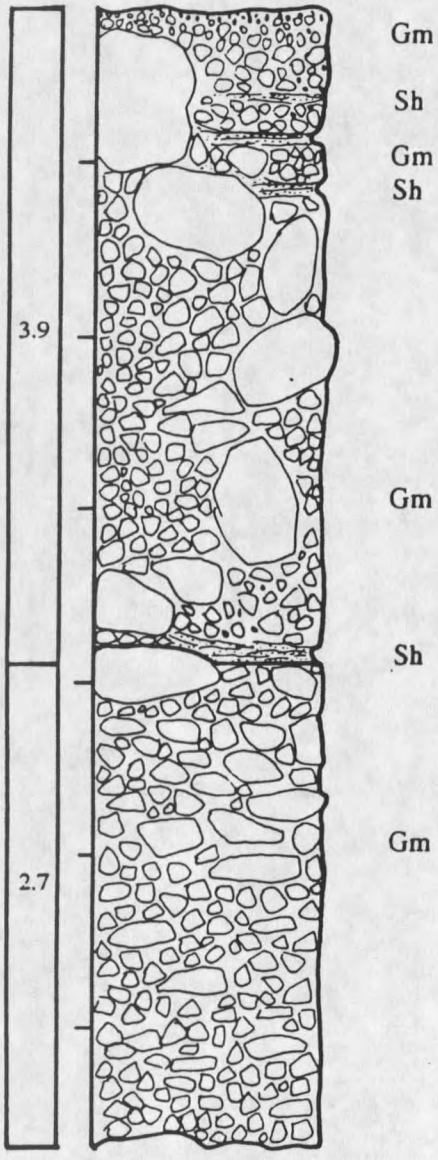
covered slope

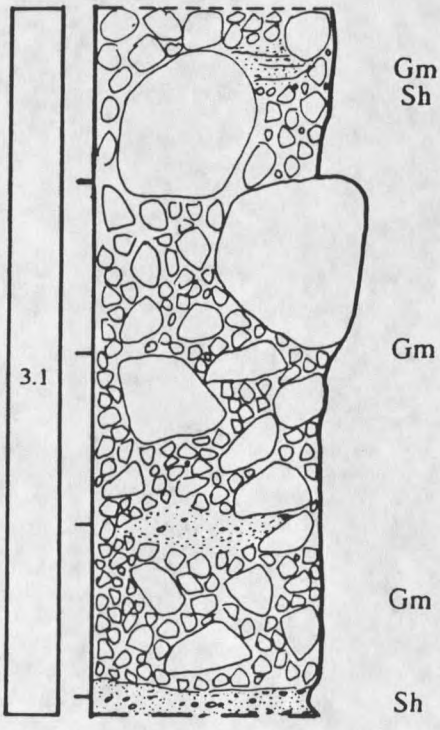
Gmw

Gmci

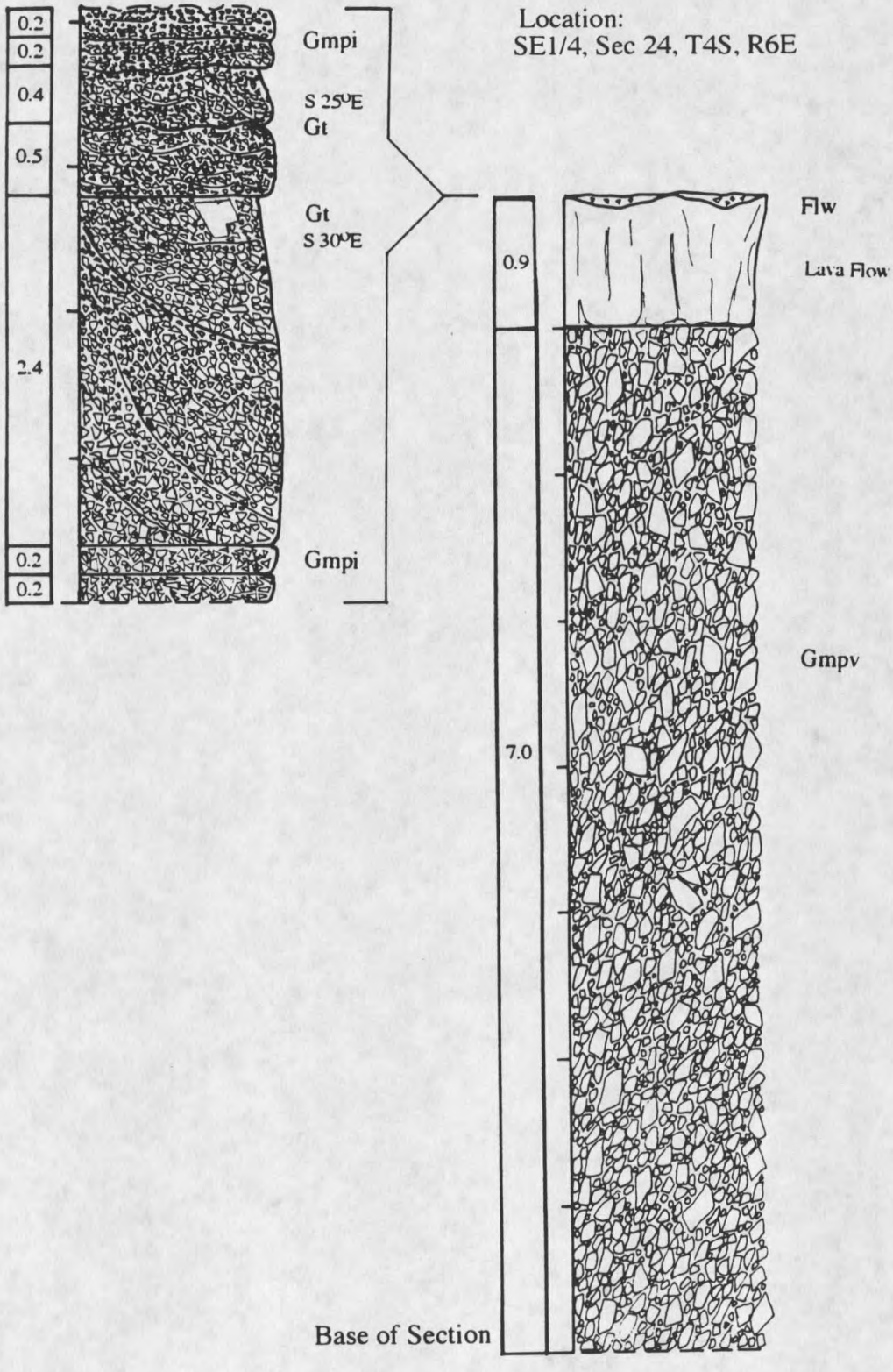
Gmp

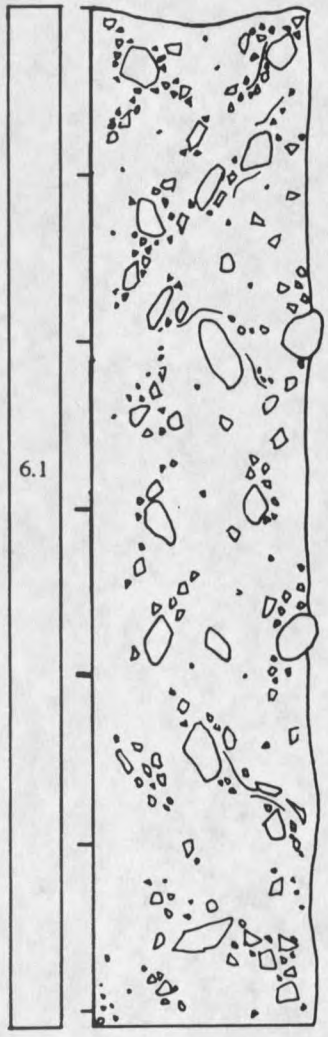

1.9
1.5
5.4
Gmw
Gmp
Gm
Se
Gm
Se
Gm
Sh
4.8
2.9
Gm
Gmp


3.9
2.7
Gm
Sh
Gm
Sh
Gm
Sh
Gm


3.1
Gm
Sh
Gm
Gm
Sh

Palisade Mountain Measured Section I

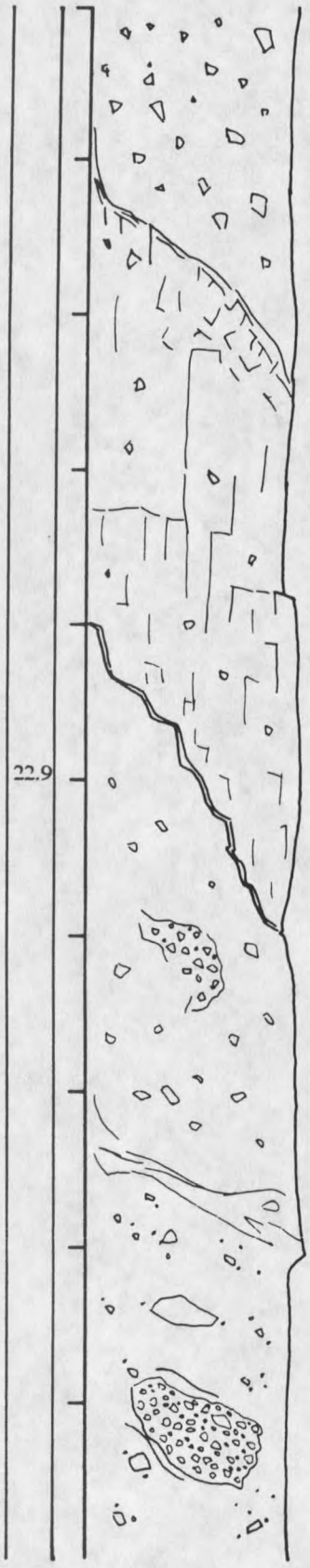


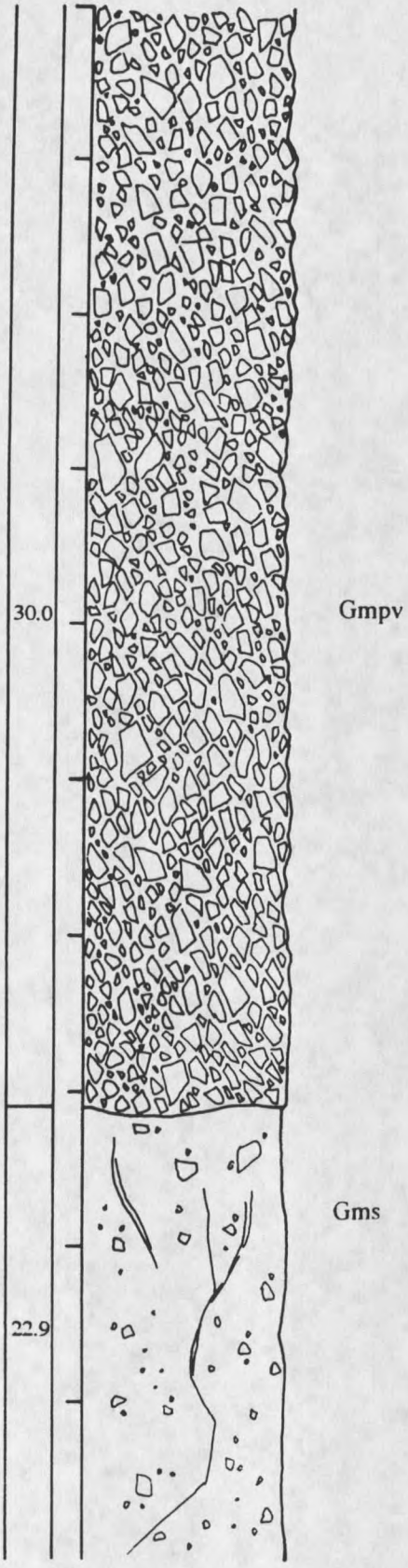


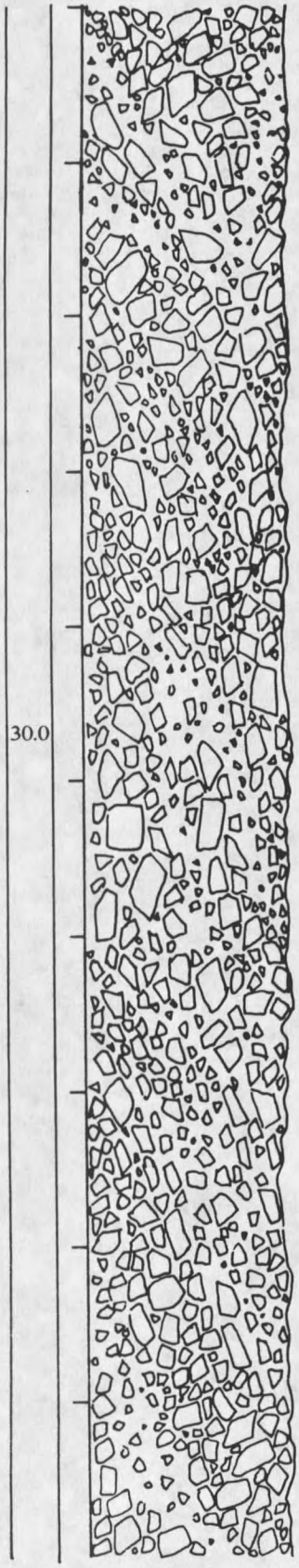
Gmpv

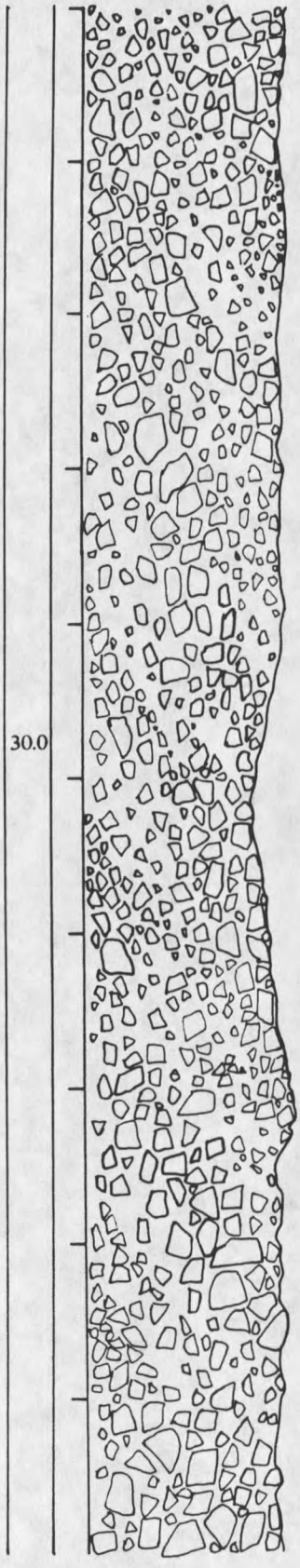


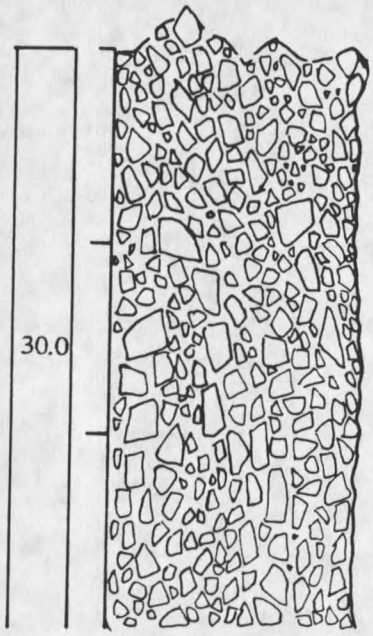
Gms


22.9
Gms

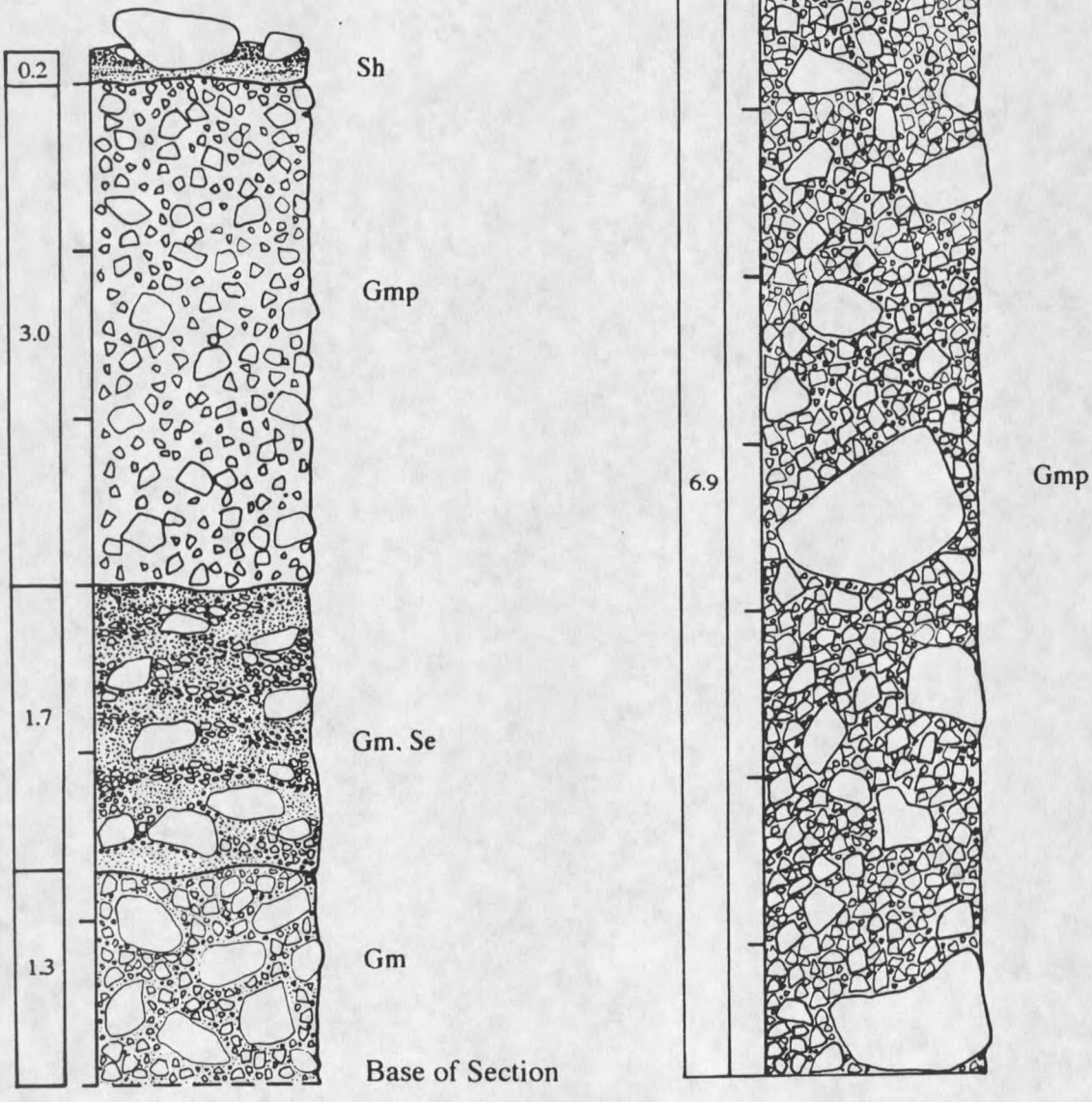

30.0
Gmpv
Gms
22.9

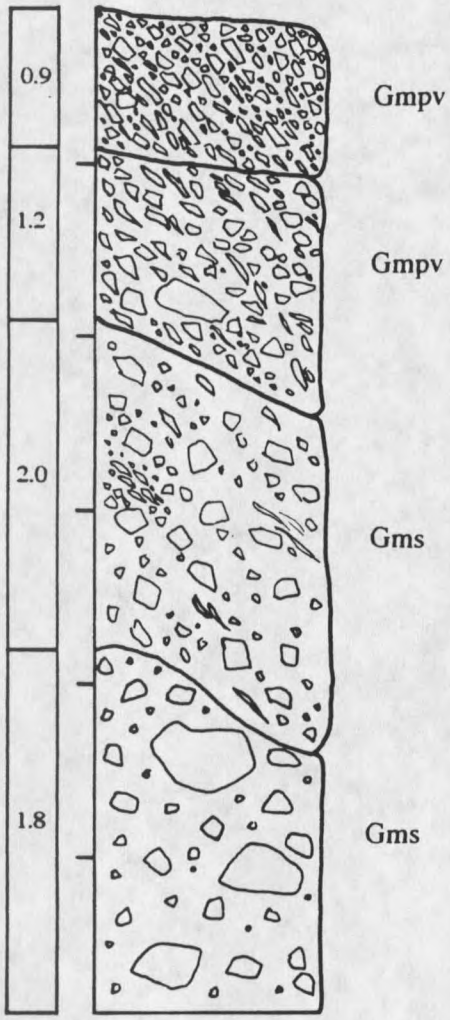

30.0
Gmpv

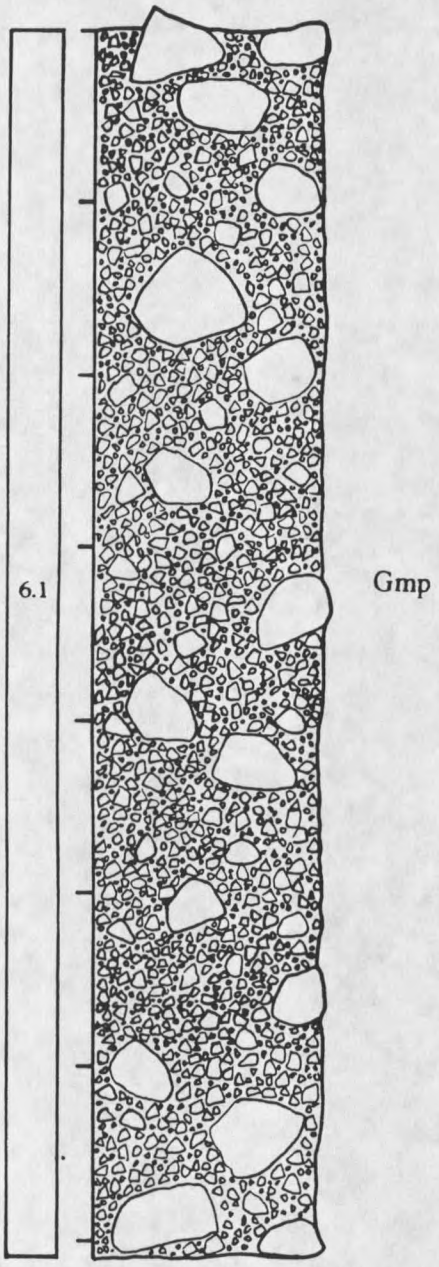

30.0
Gmpv

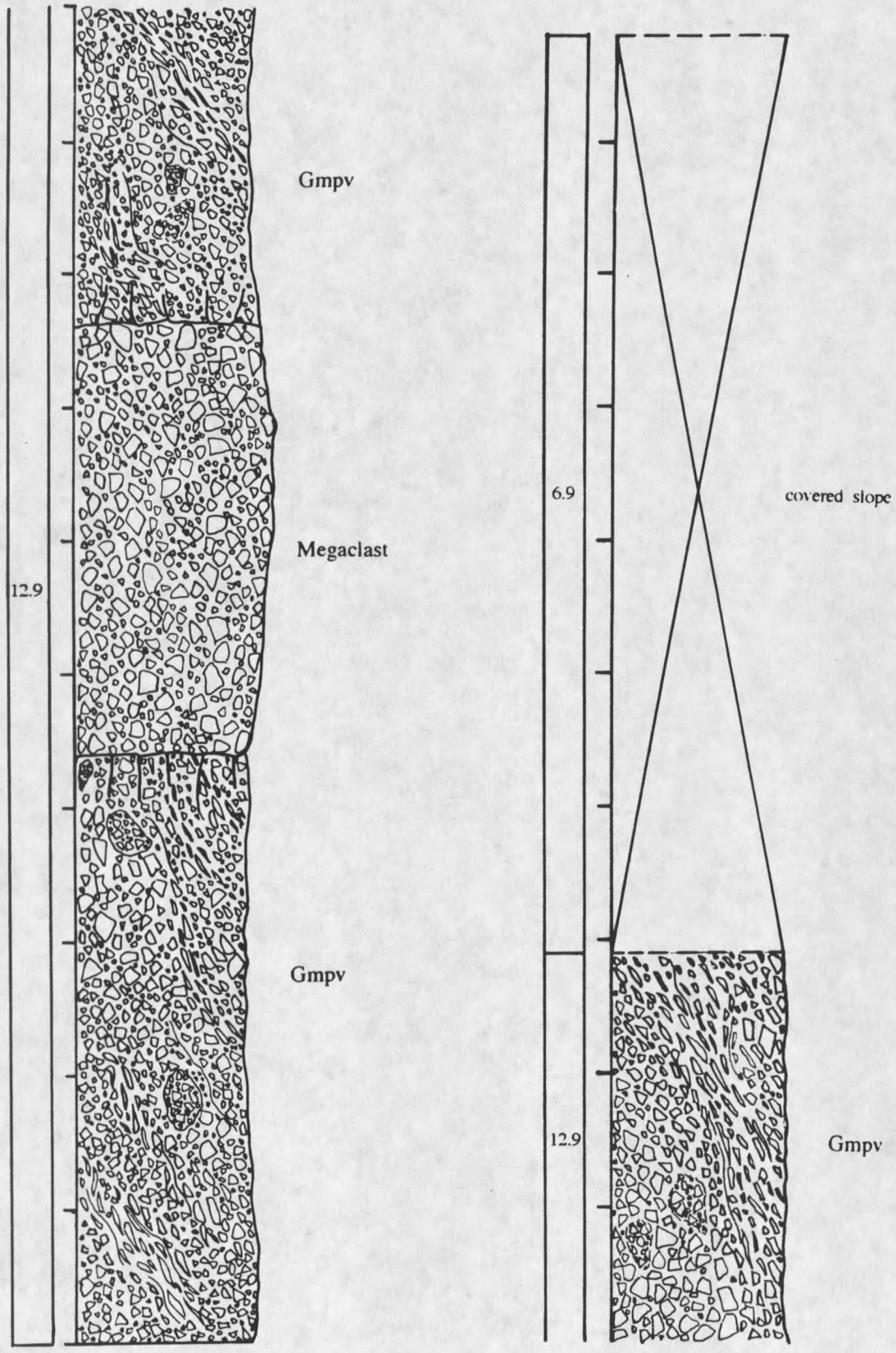

30.0
Gmpv

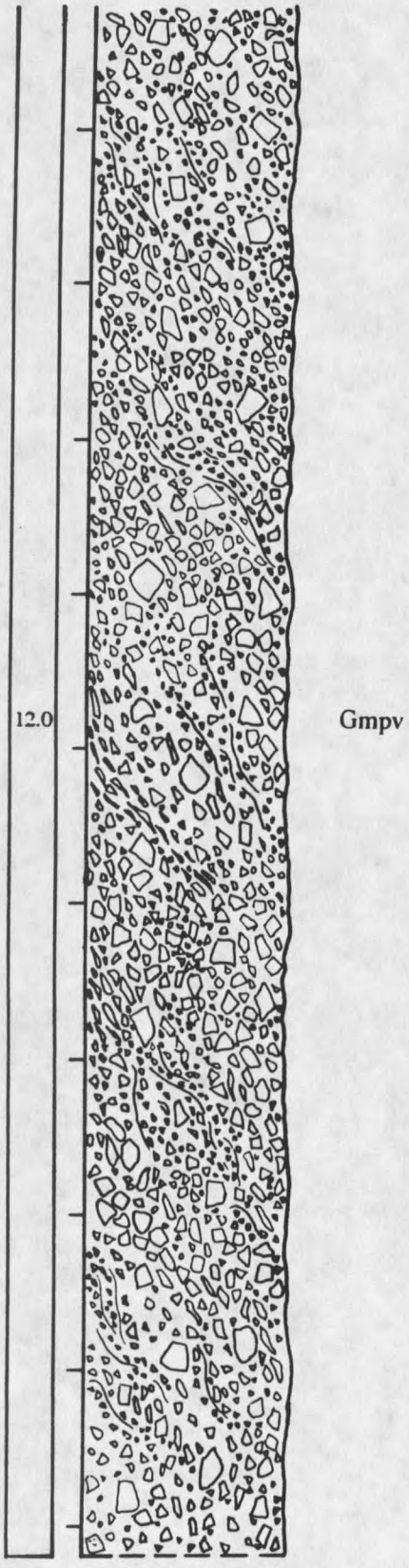
Palisade Mountain Measured Section II

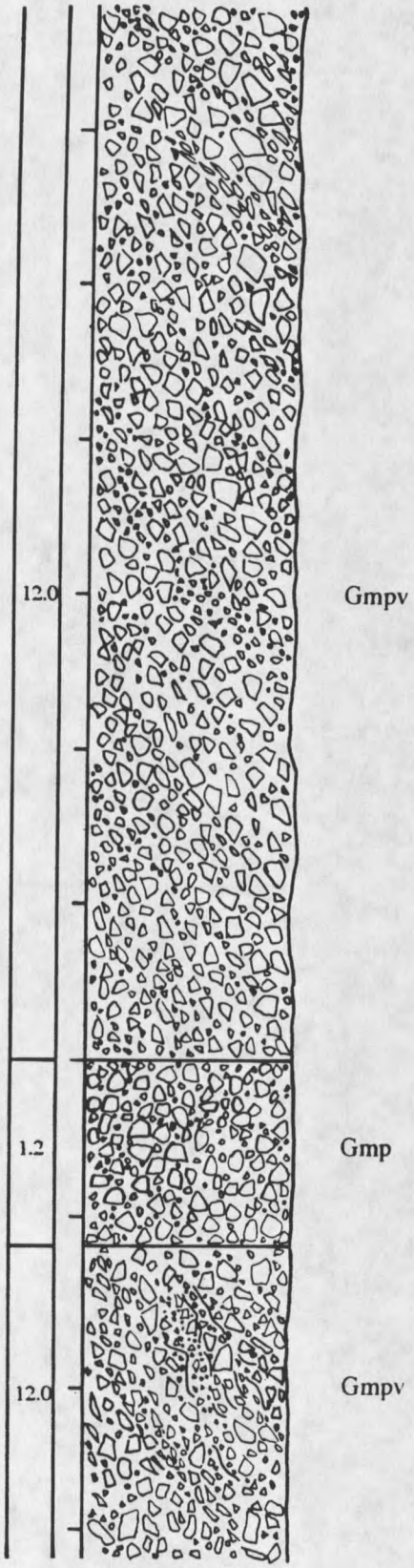


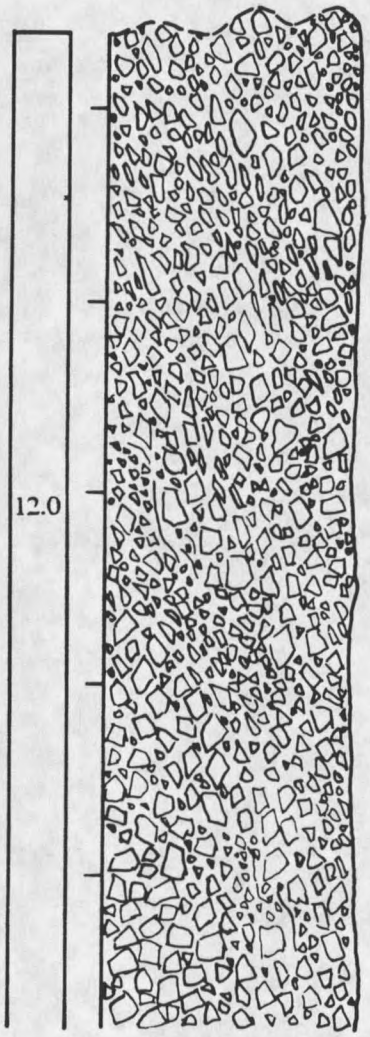

0.9
1.2
2.0
1.8
Gmpv
Gmpv
Gms
Gms


6.1
Gmp


12.9
Gmpv
Megaclast
Gmpv
6.9
covered slope
12.9
Gmpv

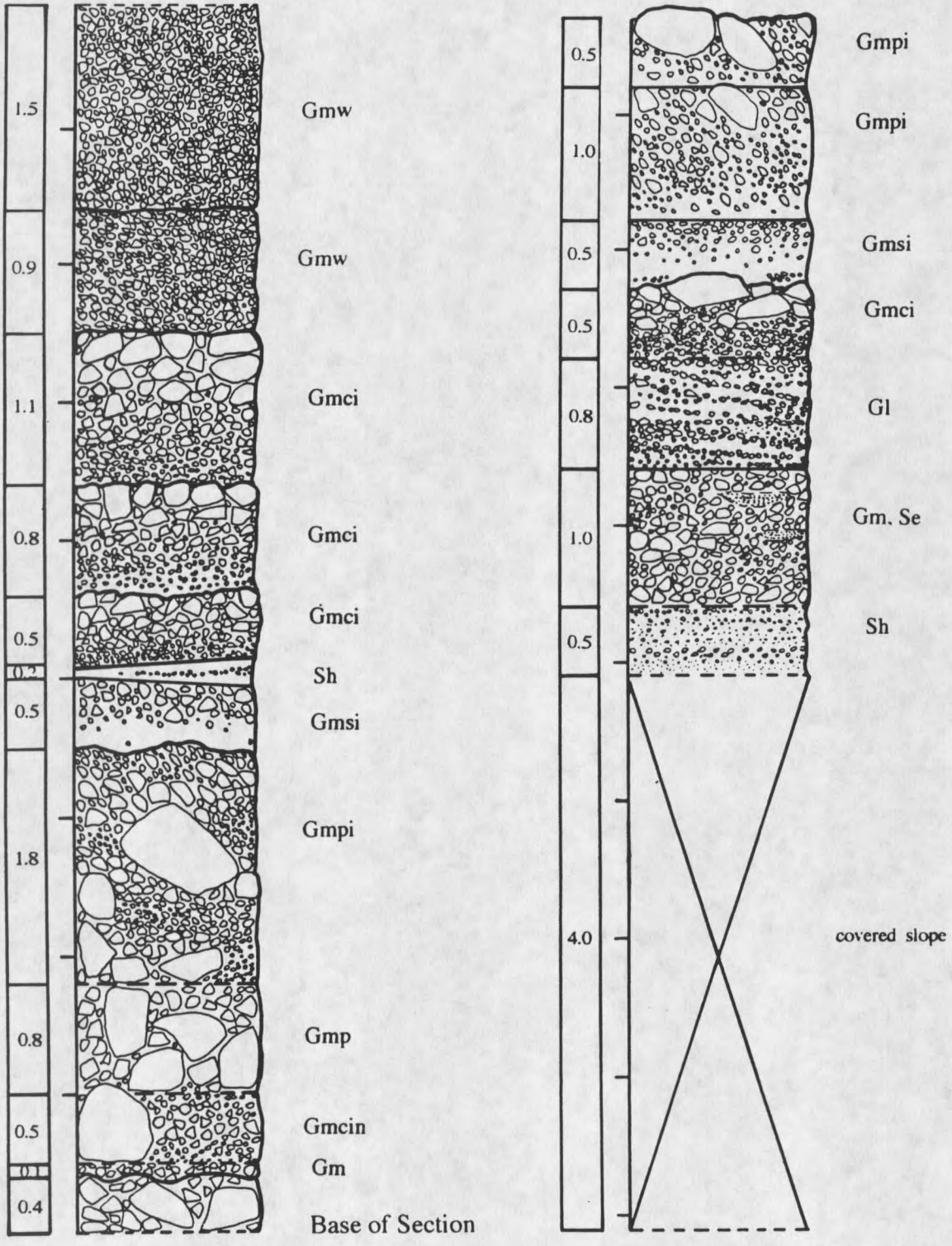

12.0
Gmpv

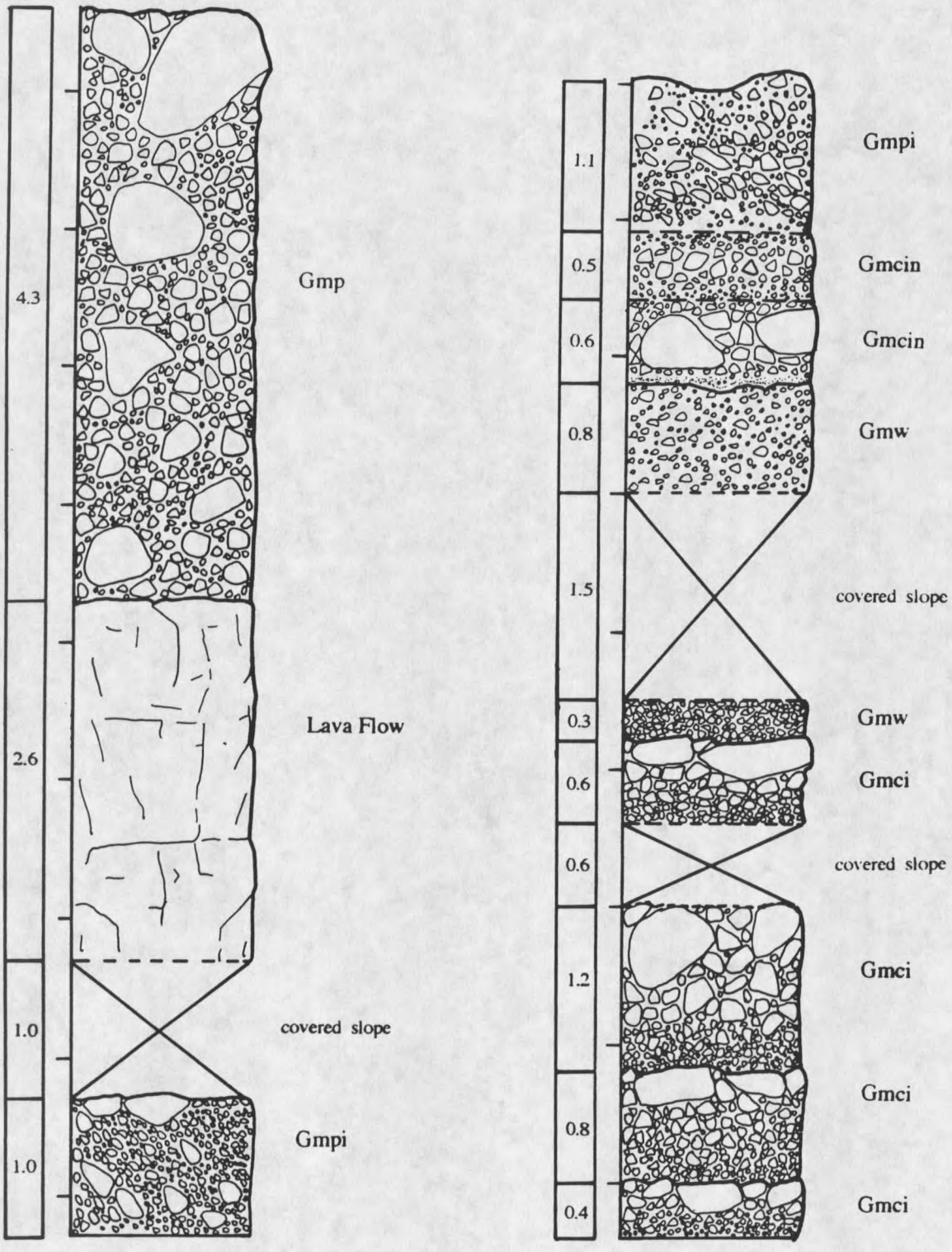

12.0
Gmpv
1.2
Gmp
12.0
Gmpv

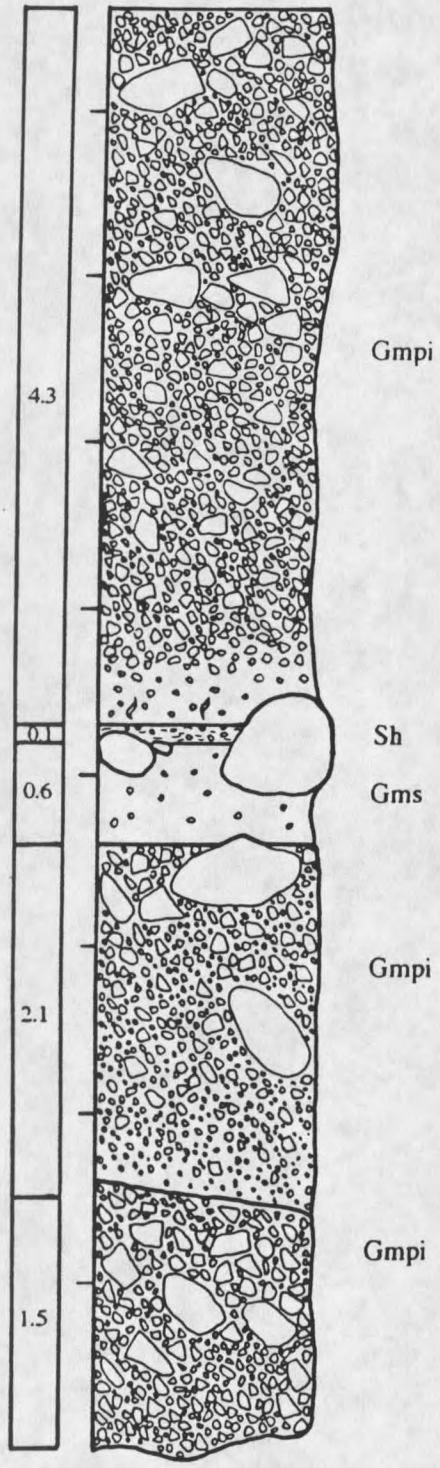

12.0
Gmpv

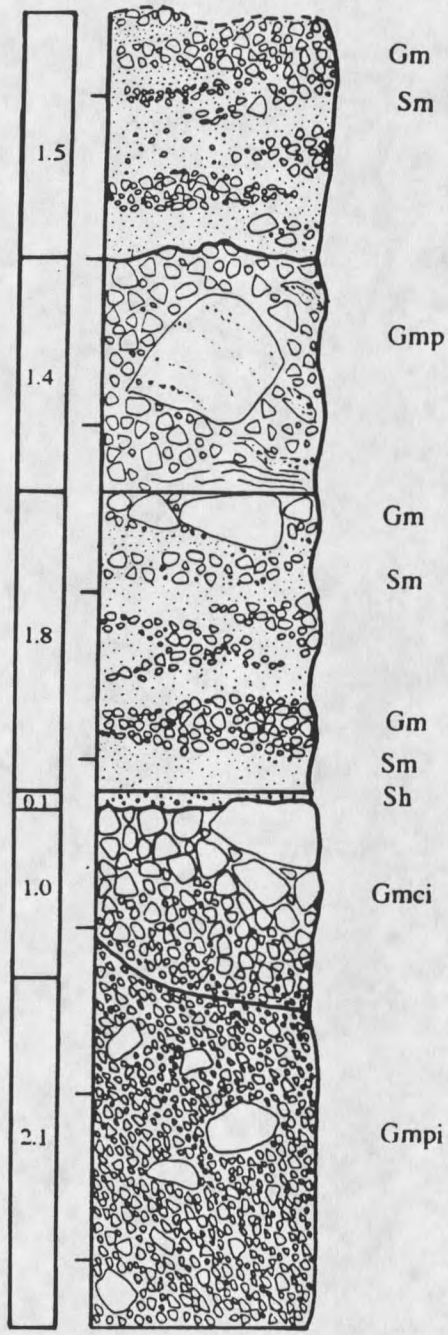
Silken Skein Falls Measured Section

Location:
SW1/4, Sec 2, T5S, R6E



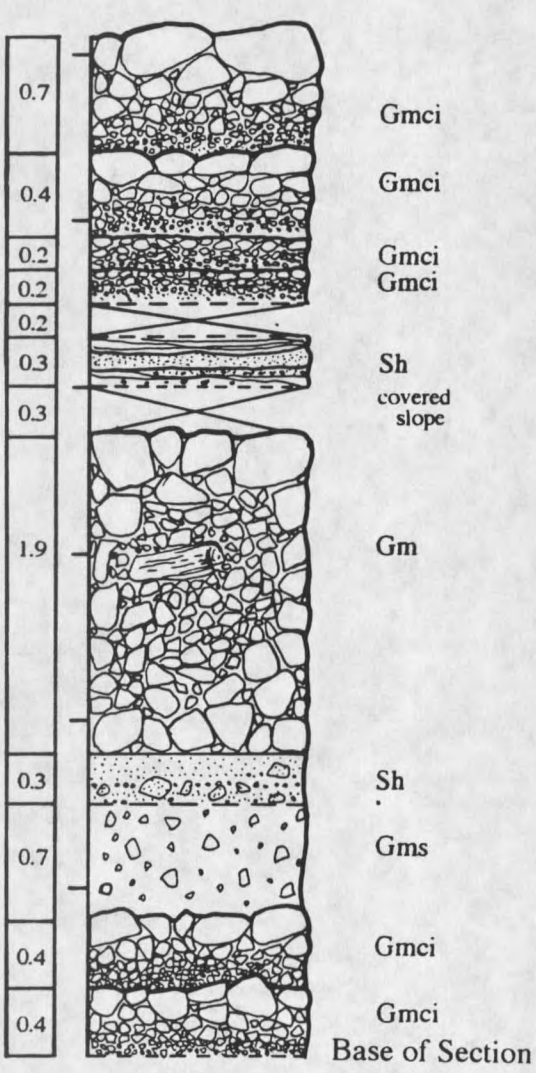

4.3
2.6
1.0
1.0
Gmp
Lava Flow
covered slope
Gmpi
1.1
0.5
0.6
0.8
1.5
0.3
0.6
0.6
1.2
0.8
0.4
Gmpi
Gmcin
Gmcin
Gmw
covered slope
Gmw
Gmci
covered slope
Gmci
Gmci
Gmci

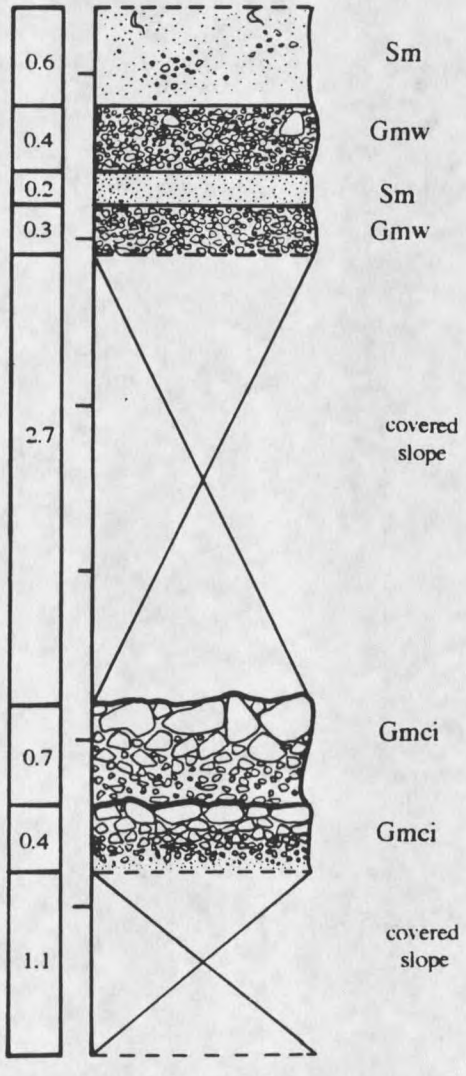

4.3
0.1
0.6
2.1
1.5
Gmpi
Sh
Gms
Gmpi
Gmpi

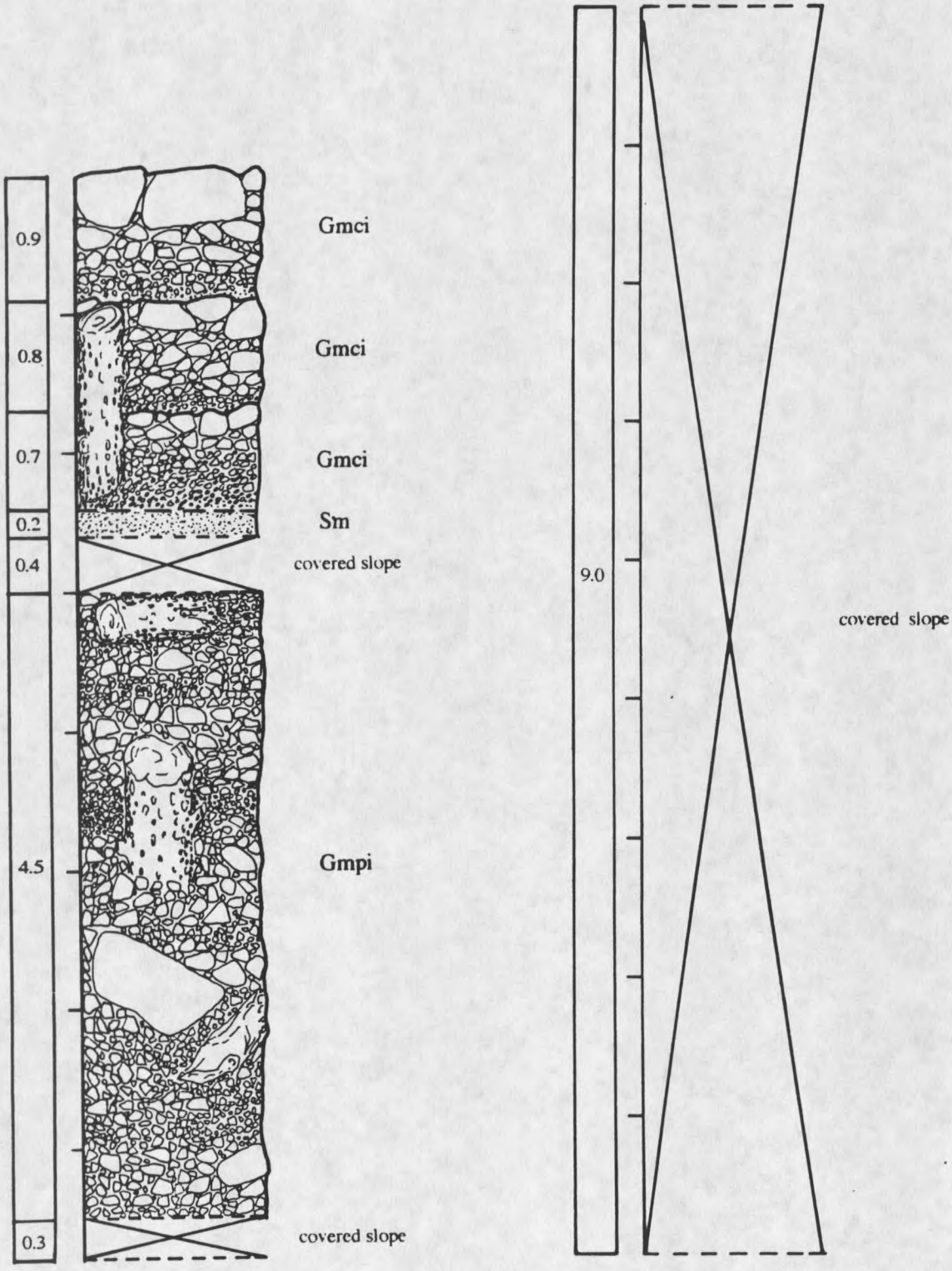

1.5
1.4
1.8
0.1
1.0
2.1
Gm
Sm
Gmp
Gm
Sm
Gm
Sm
Sh
Gmci
Gmpi

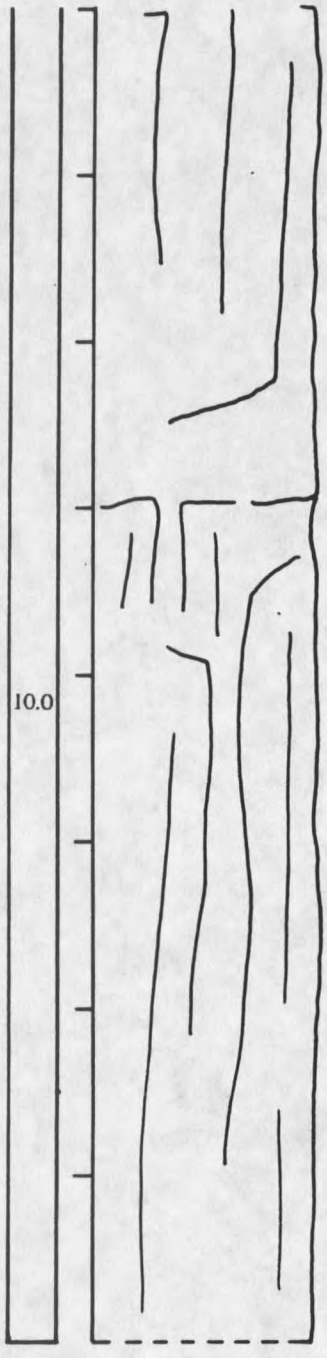
Flanders Mountain Measured Section

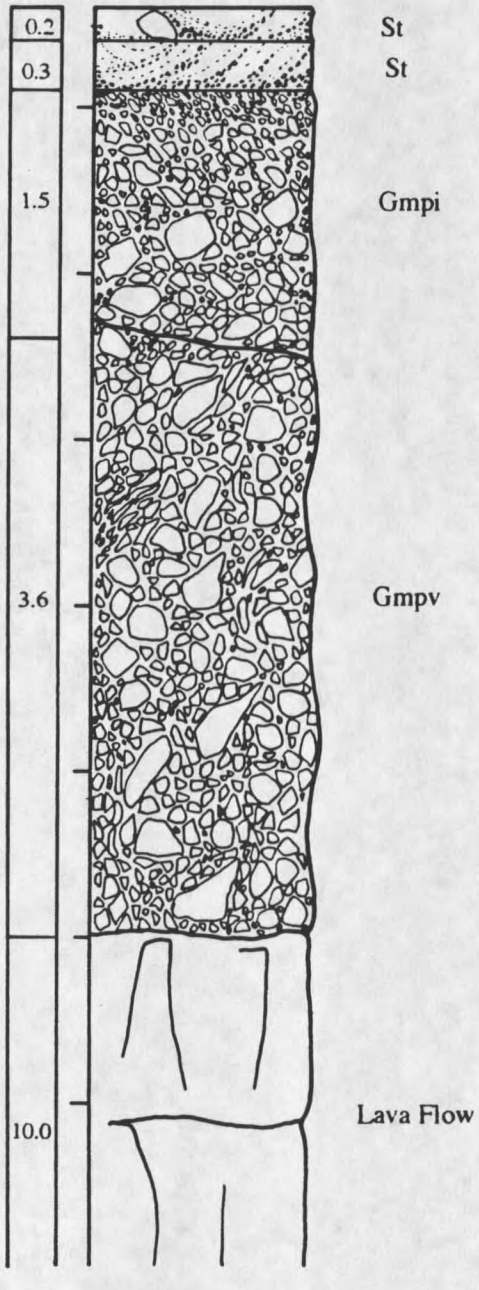
Location:
NW1/4, Sec 35, T4S, R6E

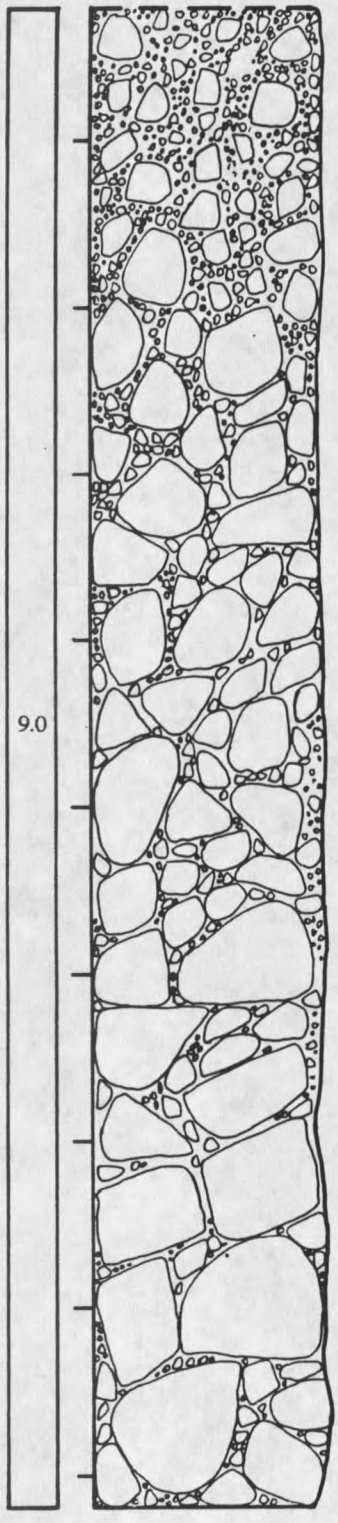


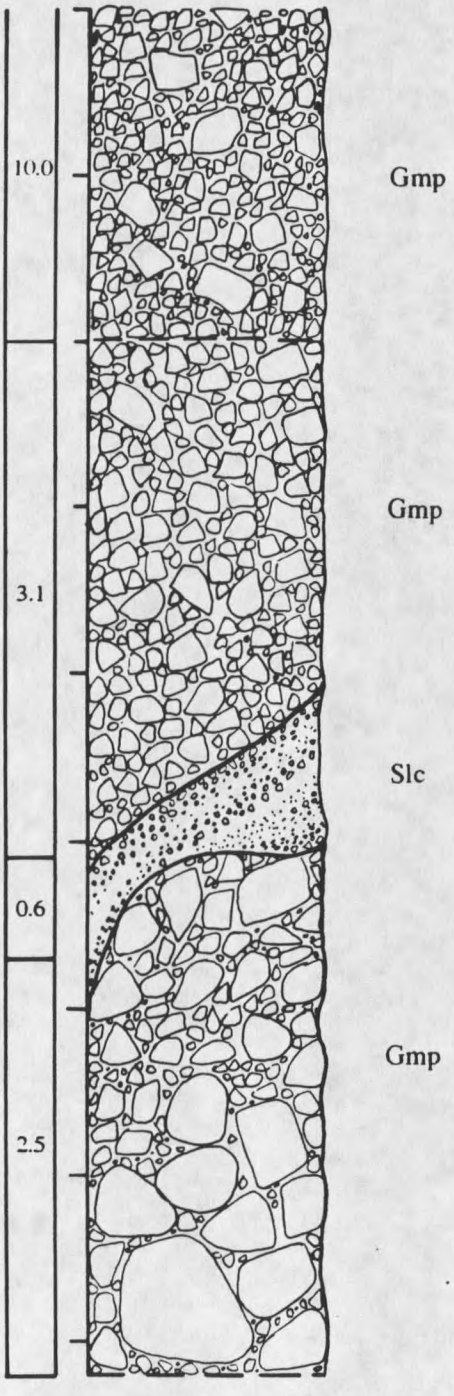


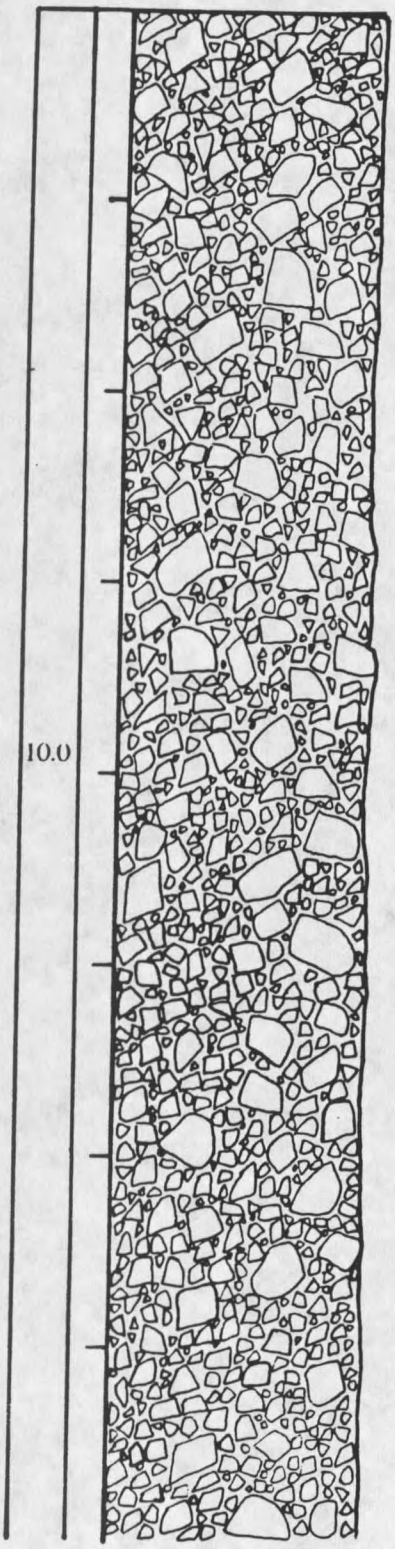

0.9
0.8
0.7
0.2
0.4
4.5
0.3
Gmci
Gmci
Gmci
Sm
covered slope
Gmpi
covered slope
9.0
covered slope


10.0
Lava Flow


0.2
0.3
1.5
3.6
10.0
St
St
Gmpi
Gmpv
Lava Flow

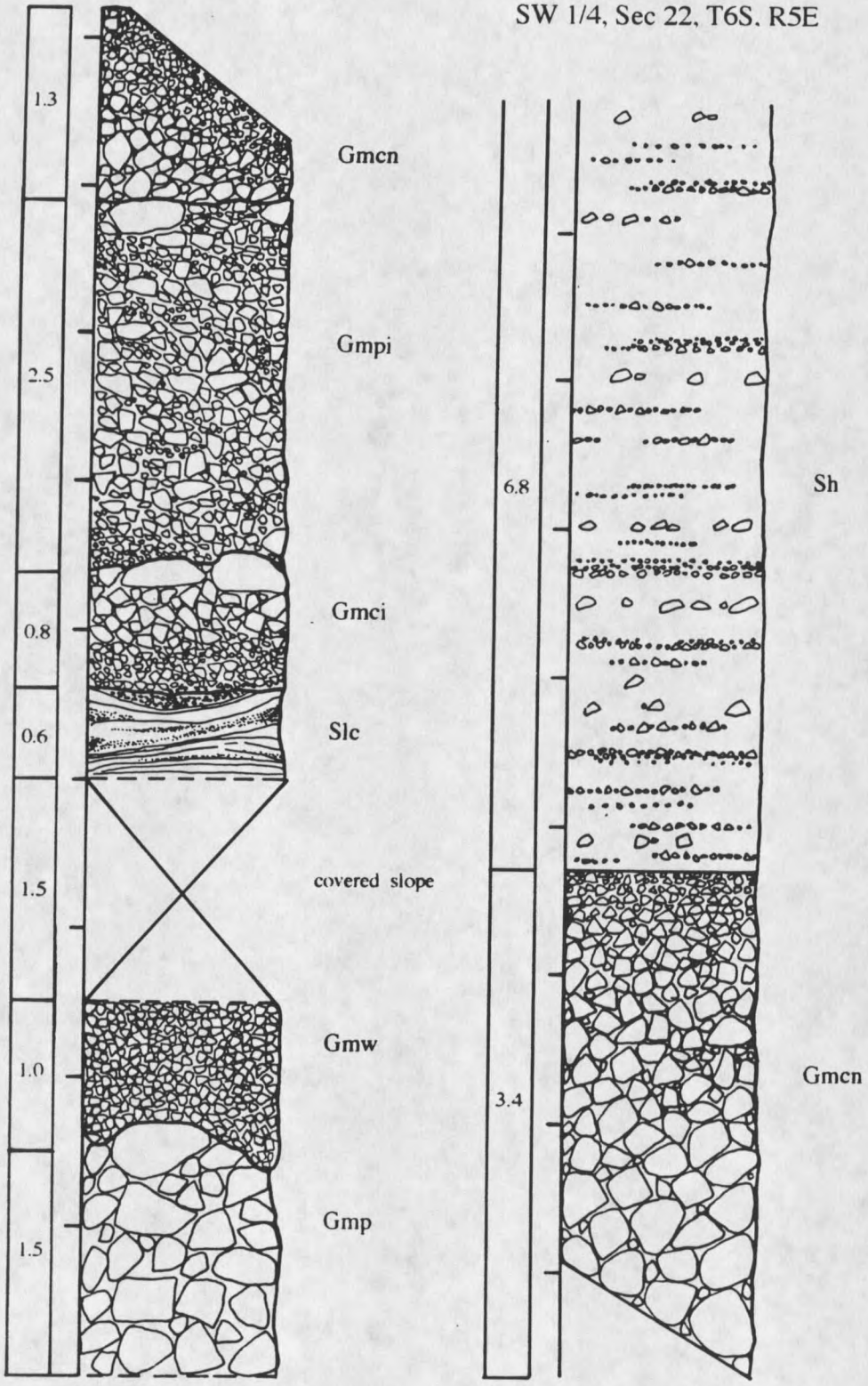

9.0
Gmcn

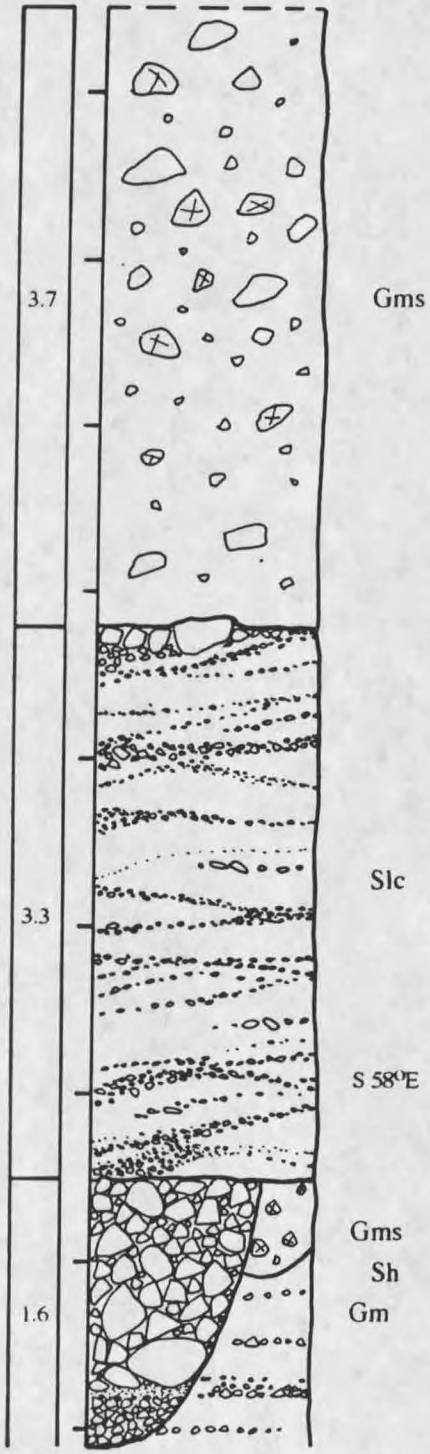

10.0
3.1
0.6
2.5
Gmp
Gmp
Slc
Gmp

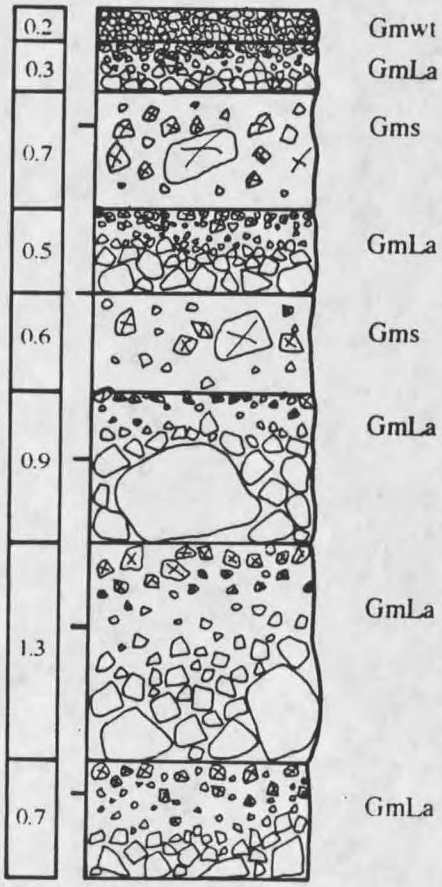

10.0
Gmp

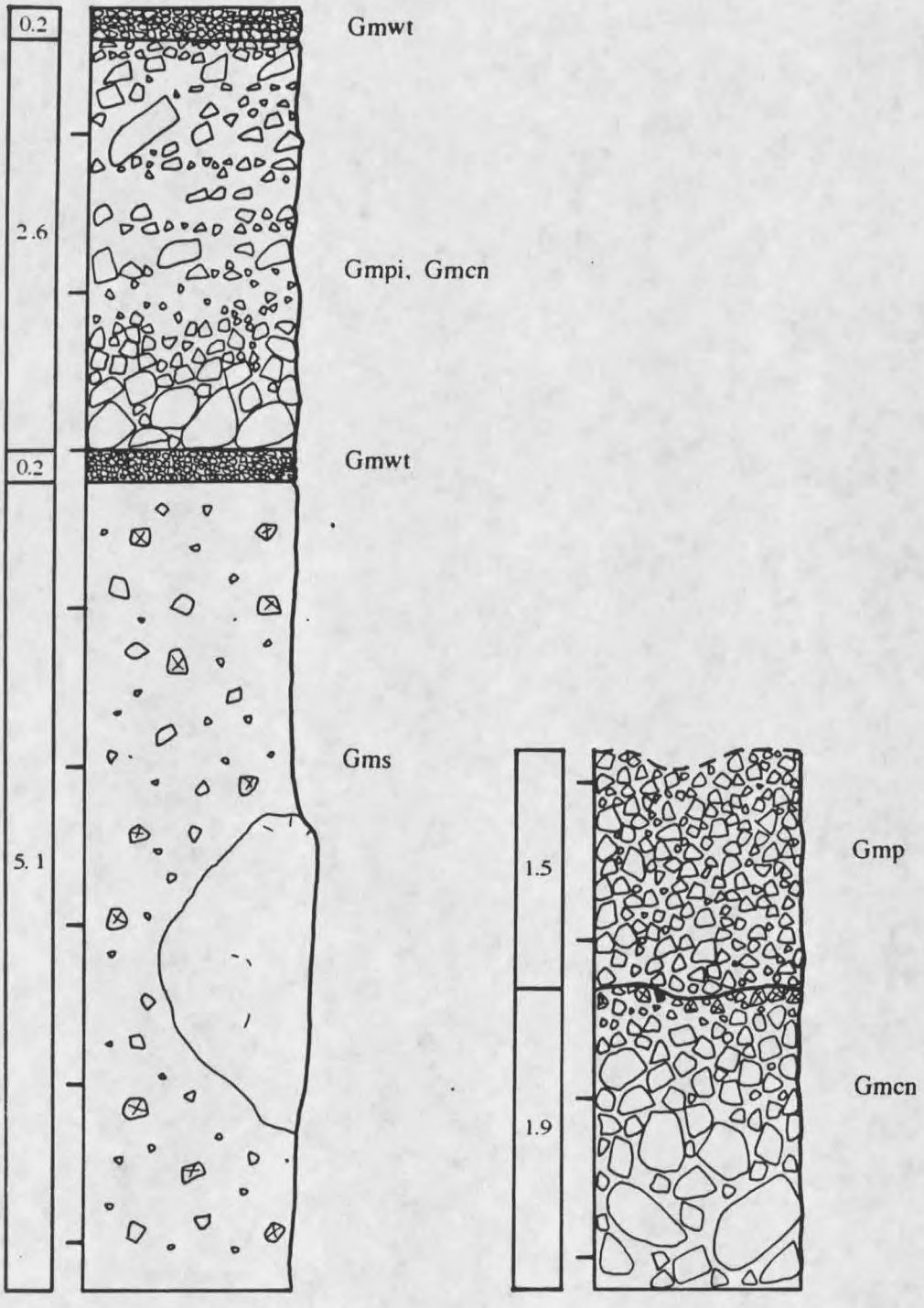
Windy Pass Measured Section

Location:
SW 1/4, Sec 22, T6S, R5E




3.7
3.3
1.6
Gms
Slc
S 58°E
Gms
Sh
Gm


0.2
0.3
0.7
0.5
0.6
0.9
1.3
0.7
Gmwt
GmLa
Gms
GmLa
Gms
GmLa
GmLa
GmLa


0.2
2.6
0.2
5.1
Gmwt
Gmpi, Gmcn
Gmwt
Gms
1.5
1.9
Gmp
Gmcn

MONTANA STATE UNIVERSITY LIBRARIES
3 1762 10254463 0